

# **Optical detection module for algae species used as early warning system**

Silvia Zieger

## **MASTER'S THESIS**

to achieve the university degree of

Master of Science (MSc)

in the Master's degree programme: Chemie

submitted to

**Graz University of Technology**

Supervisor:

Univ.-Prof. Dipl.-Chem. Dr.rer.nat. Ingo Klimant  
Institute of Analytical Chemistry and Food Chemistry

Graz, November, 2015



---

## Abstract

Algal blooms are sensitive to external environmental conditions. However, algal blooms may also pose a serious threat to marine and human life and have therefore an adverse effect on the ecosystem.

It is for this reason, that water monitoring tools have to recognise these harmful algal blooms at an early stage. The optical detection module, which was developed in the frame of the SChEMA project, will make an important contribution to this and support the long-term monitoring of the oceans on-site as a miniaturised and low-cost early warning system. As combination of a microflow cytometer and multi-channel fluorometer, it is designed and made out of robust components, such as LEDs, and requires little energy during the measurements. Algal cells, which are pumped through the system, are excited at certain wavelengths; their fluorescence is recorded and based on their characteristic absorbance behaviour a distinction of the algae is made. The miniaturised design of the detection module enables an improved sensitivity and therefore a detection of particular cell events is possible as well as a determination of the cell density.

In this work it is demonstrated that particular algal cells of medium size ( $22\ \mu\text{m}$ ) can be recorded on the device with a light intensity of  $300\ \text{pW}$ . The limit of detection is calculated to  $15\ \text{pW}$  over the background level. The power, which is required during the measurement, is  $180\ \text{mA} \cdot 5\ \text{V}$ .

Moreover, a comprehensive characterisation of 34 different algae species belonging to seven different phyla, is performed and it is demonstrated that a clearly distinction between cyanobacteria, which are known to produce cyanotoxins, and other algal phyla is possible by the means of this device.

As a result, this developed optical detection module can be considered as a valuable addition to existing technologies of early detection of algal blooms.



---

## Zusammenfassung

Algenblüten reagieren sensibel auf externe, sich ändernde Umweltfaktoren. Andererseits können auch Algenblüten eine Bedrohung für marines und menschliches Leben darstellen und einen negativen Effekt auf das Ökosystem ausüben.

Aus diesem Grund beschäftigt sich die Meerwasserüberwachung mit der frühzeitigen Erkennung dieser schädlichen Algenblüten. Das im Rahmen des SCHeMA-Projektes entwickelte optische Detektionsmodul soll hierbei einen wertvollen Beitrag leisten und als miniaturisiertes und kostengünstiges Frühwarnsystem die Langzeitüberwachung der Meere vor Ort unterstützen. Als Kombination aus Durchflussszytometer und Mehrkanal-Fluorimeter, ist es preiswert, aus robusten Komponenten aufgebaut und benötigt nur wenig Energie während den Messungen. Algenzellen, die durch das System gepumpt werden, werden bei verschiedenen Wellenlängen angeregt, deren emittierte Fluoreszenz gemessen und eine Unterscheidung der Algen basierend auf deren charakteristischem Anregungsverhalten durchgeführt. Gleichzeitig ermöglicht das miniaturisierte Design des Modules eine verbesserte Sensitivität um einzelne Zellen detektieren zu können, wodurch eine Bestimmung der Zelldichte ebenfalls ermöglicht wird.

Die durchgeführten Tests zeigen, dass einzelne Zellen mit einer durchschnittlichen Zellgröße von  $22\ \mu\text{m}$  mit einer Lichtintensität von  $300\ \text{pW}$  detektiert werden können. Die Nachweisgrenze liegt hierbei bei  $15\ \text{pW}$  über dem entsprechenden Kanalpegel. Gleichzeitig liegt der Stromverbrauch während der Messung bei  $180\ \text{mA} \cdot 5\ \text{V}$ .

Des Weiteren wurde eine umfassende Charakterisierung von 34 verschiedenen Algen aus sieben verschiedenen Stämmen durchgeführt und gezeigt, dass eine eindeutige Unterscheidung zwischen Cyanobakterien, welche für ihre Cyanotoxine bekannt sind, von anderen Algenstämmen durch das Modul möglich ist.

Infolgedessen kann das entwickelte Detektionsmodul als wertvolle Ergänzung zu bestehenden Technologien in der Früherkennung von Algenblüten betrachtet werden.



---

## STATUTORY DECLARATION

I declare that I have authored this thesis independently, that I have not used other than the declared sources/resources, and that I have explicitly indicated all material which has been quoted either literally or by content from the sources used. The text document uploaded to TUGRAZonline is identical to the present master's thesis/diploma thesis/doctoral dissertation.

## EIDESSTÄTTLICHE ERKLÄRUNG

Ich erkläre an Eides statt, dass ich die vorliegende Arbeit selbstständig verfasst, andere als die angegebenen Quellen/Hilfsmittel nicht benutzt, und die den benutzten Quellen wörtlich und inhaltlich entnommenen Stellen als solche kenntlich gemacht habe. Das in TUGRAZonline hochgeladene Textdokument ist mit der vorliegenden Masterarbeit identisch.

---

Datum/Date

---

Unterschrift/Signature



---

## Acknowledgement

I would like to take this opportunity to thank everyone, without whose professional and personal support the preparation of this work in its particular form would hardly have been possible.

First of all, I would like to say thank you to my supervisor, Prof. Ingo Klimant, who introduced me into a new and interesting theme, who always inspired and motivated me with his ideas and who was greatly helpful for the success of the thesis through his competent supervision. Furthermore, I have to thank Günter Mistlberger for the kind introduction in the team and the theme and giving me advices even after his job change. Thanks for the important development of the prototypes, without which the thesis would not have been successful. Thanks also for the trust. I want also thank Lukas and Alex for their technical assistance, without which the implementation of the project would not have been possible. My thanks go also to Alfred Burian from the Stockholm University, who acts as important algae supporter and enables the complex investigation of algae in this work.

Besides, I am grateful for my colleagues and friends. Heidi for some sunny and relaxing hours on the roof, which we could enjoy. Berni for being a kind of mentor and encouraging me, when the motivation was missing. Phips for the common lunch breaks and the feeling of belonging. Moreover, I want to thank Christopher, who not only supported me by proofreading my thesis, but who was kind and helpful and always up for a cup of coffee.

I am also grateful for my family, especially for my mom and my cousin Karin, who have always supported me in my decisions and have an open door for me. In particular, I would like to thank my boyfriend Korbinian, who is able to alleviate any of my worries by his warm smile and gives me the feeling of home.

Last but not least, I would like to take this opportunity to thank all staff members of the 1st ACFC and my friends in Munich, South Tyrol and Graz, who supported and motivated me during my years of study and who have accompanied me over the years.

Silvia Zieger

Graz, November, 2015



---

# Table of Contents

	Page
<b>1. Introduction</b>	3
<b>2. Theoretical background</b>	7
2.1. Diversity of algae . . . . .	7
2.2. Harmful algal blooms . . . . .	8
2.2.1. Definition and description . . . . .	8
2.2.2. Early warning and detection systems for algal blooms . . . . .	10
2.3. Photosynthesis and Chlorophyll-Fluorescence . . . . .	12
2.3.1. General overview of photosynthesis . . . . .	12
2.3.2. Light reaction and light-harvesting complex ( <i>LHC</i> ) . . . . .	13
2.3.3. Excitation and emission spectra of algae species . . . . .	16
2.3.4. Diagnostic pigments . . . . .	19
2.3.5. Chlorophyll fluorescence and induction kinetics . . . . .	24
2.4. Resume . . . . .	26
<b>3. Material and Methods</b>	29
3.1. Material . . . . .	29
3.1.1. Algae and bacteria cultures . . . . .	29
3.1.2. Culture medium . . . . .	31
3.2. Methods . . . . .	34
3.2.1. Cultivation . . . . .	34
3.2.2. Microscopy . . . . .	36
3.2.3. Spectral Characterisation . . . . .	37
3.2.4. Mathematical context – Principal component analysis (PCA) . . . . .	39
<b>4. Optical detection module for algae species</b>	47
4.1. 1 <sup>st</sup> generation prototype – Adapted optical oxygen meter . . . . .	48
4.2. 2 <sup>nd</sup> generation prototype – Small detection module . . . . .	49
4.3. 3 <sup>rd</sup> generation prototype – Multichannel measurement device . . . . .	50
4.4. Miniaturised optical detection module for algae species . . . . .	52
4.4.1. Optics part . . . . .	54
4.4.2. Electronic part . . . . .	55

---

<b>5. Results and Discussion</b>	57
5.1. General overview of the recorded time drive . . . . .	57
5.1.1. Conversion of the voltage signal into light intensity . . . . .	57
5.1.2. Time drive and influences of the signal level . . . . .	57
5.1.3. Different signal levels for water and air . . . . .	59
5.1.4. Aluminium or POM-C as device material . . . . .	60
5.2. Challenges to be solved . . . . .	61
5.2.1. Ambient light and optical density . . . . .	61
5.2.2. Electromagnetic interferences . . . . .	64
5.3. Performance characterisation of the optical detection module . . . . .	67
5.3.1. Calculation of the residence time . . . . .	67
5.3.2. Capturing particular cell events . . . . .	68
5.3.3. Linearity and sensitivity . . . . .	69
5.4. Data analysis . . . . .	72
5.4.1. Spectral differences between cyanobacteria and other algae species . . . . .	72
5.4.2. Data analysis using PCA . . . . .	73
<b>6. Conclusion and Outlook</b>	77
<b>A. Algae Fact Sheet</b>	81
A.1. Bacillariophyta . . . . .	83
A.2. Cryptophyta . . . . .	95
A.3. Dinophyta . . . . .	103
A.4. Haptophyta . . . . .	109
A.5. Orchophyta . . . . .	119
A.6. Chlorophyta . . . . .	129
A.7. Cyanophyta . . . . .	157
<b>B. List of Equipment</b>	165
<b>C. List of Figures</b>	169
<b>D. References</b>	176





---

# 1. Introduction

Although algae are a sensitive indicator for changing environmental conditions, they may have also an adverse impact on the ecosystem, when they form blooms during spring and summer. They may be harmful for marine as well as for human life. Therefore, within the frame of the SCHeMA project (integrated in-Situ Chemical MApping probes, grant agreement no: 614002), funded under the European research and innovation-funding programme FP7, a miniaturised, low-cost and multi-channel detection module has to be developed which enables a detection and identification of harmful algae species at an early stage. Furthermore, it should also feature low energy consumption and enables *in-situ* measurements as well as a long-term monitoring.

In order to implement this idea, we identified in a first step the algae classes, which may lead to harmful algal blooms and examined their characteristics. Therefore, a variety of different algae species belonging to different algal phyla were characterised to create an algae database. Besides a morphological description, all algae species were characterised spectrally and the differences in their absorbance and fluorescence behaviour were examined. These differences especially in their excitation spectra result from a different pigmentation of the photosynthetic apparatus. These differences in their pigment composition should then enable a distinction of different algal phyla. At this point the summarising book of Govindjee et al. has to be mentioned. [1] They worked on the optical characterisation of different algal phyla and determined the theoretical relations within the algal photosynthesis apparatus.

In the next step, a suitable concept, which combines a powerful flow cytometer on the one hand with a common compact and submersible fluorometer on the other hand, was designed. In this context, especially the microfluidic investigations of F. Ligler have to be highlighted, which enables a miniaturisation of a multi-channel device working in the flow-through mode. [12] To realise the underlying idea, several prototypes were built with which we gradually approach the final aim of a miniaturised, low-cost detection module featuring several excitation and emission channels, which enables a separation of algal phyla in the laboratory. Moreover, the results of the previous characterisation of the algae were used to achieve a differentiation of the algal phyla and enable a distinction of harmful cyanobacteria from other harmless algae. The final detection module might be a valuable addition to existing technologies, since it works modularly and its cell sensitivity is similar to a flow cytometer. Moreover, the module is built from robust components and due to its miniaturised design, the sensitivity is increased.

Related to its content, this work is structured as follows: First, the required relations and basic principles are presented in chapter 2 – *Theoretical background*. Besides a systematic introduction to the group of algae, the characteristics and features of harmful algal blooms were illustrated in the first two sections. Moreover, several possible methods for the detection of algae are presented as well as common early warning systems. For this purpose, the present thesis refers to the APEC’s report about *Monitoring and Management Strategies for Harmful Algal Blooms in Coastal Waters*, which offers a good introduction into the issue. Biochemical and photochemical principles, which are important for the understanding of the thesis, are presented subsequently in the following subsections. A brief overview of photosynthesis and its apparatus is given and also the principles of excitation and fluorescence in the light-harvesting complex of algae are described. Finally, possible applications of the developed device are described in the subsections 2.3.5 and 2.3.4, while this work focus primarily on the first application – the distinction of harmful cyanobacteria from other harmless algae.

Then in chapter 3 – *Material and Methods*, the cultivated algae species and their cultivation process are described briefly as well as the methods, which were used to characterise these algae species. The results of the characterisation are moved to the *appendix A*, since there are so many pages.

The prototypes and the miniaturised algae detection module are presented in chapter 4. Within this chapter, the conclusions, which we obtained from these first approaches, are explained and furthermore a description of the miniaturised device and its features is given. The realised experiments that we made with the miniaturised device, are explained and discussed in the next chapter 5.

Finally, chapter 6 – *Conclusion and Outlook* summarises the whole master’s thesis and the actual state of the miniaturised algae detection module considering its part in the SCHeMA project. Further investigations, that have to be done in order to obtain the goal of a miniaturised and low-cost algae detection module, which contributes as suitable early warning system to a marine monitoring programme, are also mentioned in the outlook of this chapter.





---

## 2. Theoretical background

This chapter provides an overview of all required fundamentals used. While the first two sections deal with the diversity within the huge group of algae and their potential negative environmental impacts, the third section – *Photosynthesis and Chlorophyll-Fluorescence* – presents the biochemical and photochemical principles.

### 2.1. Diversity of algae

Historically, biology consisted of only three different empires (plant, animals and minerals accordingly to Carl von Linné) and all known organisms were classified into the empires depending on their functional-ecological properties. Since algae and cyanobacteria, which were formerly known under the name "blue-green algae", are phototrophic organisms, they were included in the plant kingdom. With the development of the theory of evolution, however, biologists tried to examine genetic relationships between the organisms and to define monophyletic kingdoms. Phylogeny means the evolution of all living beings, belonging to a certain strain, and refers also to genetic relationships in all levels of the biological taxonomy. A kingdom should therefore combine organisms based on their similar phylogeny instead of their similar characteristics. Due to this effort and due to the fact that it is not yet possible to define monophyletic relationships between all algae species, the whole indefinite group of algae were divided into smaller phyla and classes and several algae classes were removed from the plant kingdom. Moreover, the blue-green algae were separated from the group of algae, since their inner structure differs from the rest; they lack of a nucleus and of chloroplasts. As a consequence, they were now classified, in the terms of biological systematics, as phototrophic cyanobacteria into the empire of prokaryotes. The other algae species, by contrast, remain in the eukaryotes empire and both empires are further divided into subordinate Taxa (kingdom, phylum, class, order, family, genus and species). The taxonomic classification is not yet completed and still under progress, but it is a first attempt to classify algae and bacteria species. Moreover, the indefinite term "algae" should be prevented in the context of biological systematics. In a functional-ecological context, however, the term "algae" is used to describe, in general, phototrophic organisms, that inhabits the water biotope. In this functional content, cyanobacteria and eukaryotic algae are not separated. [2]

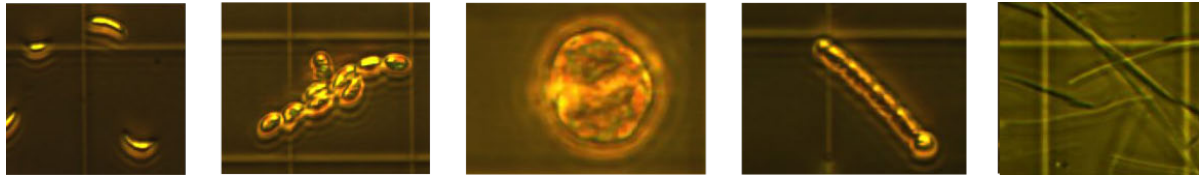


**Figure 2.1.:** Example of different cell shapes to demonstrate the diversity of algae.

As mentioned above, algae are an indefinite group that lacks of common characteristics and even of a common phylogeny. Therefore, the functional group of "algae" combines a huge diversity of species. They differ in their habitats, their size and morphology. Some algae species may live in freshwater areas, while other species prefer brackish water or even seawater. Their size and morphology may also vary between unicellular or filamentous, microscopically small cultures and multicellular, marine seaweed with a length of 80 m. Furthermore, some algae species have an armoured cell shape, whereas the cells of other species is integrated in a mucus matrix. Some species are (bi-) flagellated and motile, while other cultures are immobile. [3]

Several algae cultures may have a beneficial impact, since they can be used as a potential source in the biofuel production or may be used commercially in the pharmaceutical industry, when they are rich in lipids and proteins. Furthermore, several algae species can be used as nutritional supplements in human or animal feed or in ecotoxicological tests. On the other hand, some algae species may produce toxins and, therefore, may have adverse effects on marine animals and mammals, birds and humans. Nevertheless, algae, especially microalgae have an important impact on aquatic ecosystems, since they produce a huge amount of oxygen through their photosynthetic activities. [4]

## 2.2. Harmful algal blooms

Since the term "harmful algal blooms" is often used misleadingly to describe all phenomena of discoloured water surfaces caused by algae assemblages, the term "harmful algal blooms" is described first as it is used in accordance to the Asia-Pacific Economic Cooperation. In the second part, the methods, which can be used to detect algal blooms at an early stage, are described briefly.

### 2.2.1. Definition and description

In general, an algal bloom can be described as an overgrowth of micro-algae species, although a certain threshold level above, which an algae culture is recognised as algal bloom, is not officially defined. This results from the fact that not all algae species that might have an adverse effect on the ecosystem, lead to a discolouration of the water surface. These species may have

harmful impacts even when their cell concentration is not dense enough to change the colour of the water surface. On the other hand, not all algae species, that might form blooms, have a negative impact on the ecosystem. Besides, an algal bloom does not have to consist of only one single algae species. Therefore, the term "harmful algal bloom" has to be defined and it is used in accordance to Anderson et al.:

*"... [T]he term "harmful algal bloom " or HAB will be used in its most general or inclusive sense — it will refer to blooms of toxic and non-toxic algae which discolor the water, as well as to blooms which are not sufficiently dense to change water color but which are dangerous because of the algal toxins they contain or the physical damage they cause to other biota." [5]*



**Figure 2.2.:** Example of an algal bloom caused by cyanobacteria leading to a discolouration of the water surface. [6]

Over the last few years, harmful algal blooms have become a global problem that can affect each coastal region, since the algae cultures may occur in freshwater as well as in marine environments. In addition to the discolouration of the water surface mentioned above, some harmful algal blooms lead to a low oxygen condition, when they decay or may lead to a light attenuation caused by the dense biomass on the water surface. As a result of these unfavourable conditions, other marine organisms will be killed due to the lack of light and oxygen. Moreover, some algae species, whose cells are integrated in a mucus, can clog gills and thereby kill fish without producing toxins. However, some algae species can produce toxins and since algae are at the bottom of the food chain, they are eaten by other marine animals. The toxins accumulate in the tissue and, as a result, fishes, marine mammals and birds are then killed by biotoxins. Furthermore, after accumulation over the food chain, the produced toxins may lead to human disorders like gastrointestinal, neurological and cardiovascular disturbances or, when the toxins achieve levels which can be lethal to humans. Other marine toxins like saxitoxin, produced by dinoflagellates, lead to paralytic shellfish poisoning (PSP) — one of the five recognised human syndromes. PSP is a life threatening syndrome and saxitoxin itself has an acute intravenous  $LD_{50}$  of  $3.4 \mu\text{g STX kg}^{-1}$  body weight (mice). [7] Another important group of toxin producing marine organisms are cyanobacteria. These cyanotoxins

can also lead to gastrointestinal, liver disease, heart failure or even death after accumulation over the food chain. [8]

In addition to health effects listed above, harmful algal blooms constitute also a threat to the fish and oysters industry and the tourism sector by having tremendous economic impacts. Due to the algal contamination, the food products in the shell fish industry or even the shell fish itself gets poisoned and the tourism sector suffers heavy losses since they have to close their beaches. The estimated economic impacts of coastal HAB only in the US amount to 82 million \$ every year. [9]

The reasons for the expansion of harmful algal bloom are not secure and still under debate, although anthropogenic impacts and natural mechanisms of these species are discussed. [5] Nevertheless, the identification of harmful algae species at an early stage became more important over the last few years. Furthermore, monitoring tools to prevent, control and mitigate the occurrence of harmful algal blooms are needed.

### 2.2.2. Early warning and detection systems for algal blooms

Early warning systems for algal blooms should enable the observation of the algal distribution and, in a further step, their population dynamics. Furthermore, these systems should measure autonomously and continuously and should identify algae species which may produce toxins or have other harmful effects on the ecosystem, at an early stage. In the literature, there are several approaches for these early warning systems and long-term monitoring tools. The concepts range from the monitoring of some physical parameters of the water to complex methods which analyse the fluorescence and scatter properties of the phytoplankton, enabling the characterisation and quantification of the algal sample. Some concepts analyse the total content of chlorophyll *a* in a water sample by using fluorometric and photometric instruments, as it is an ubiquitous pigment which is present in all photosynthetic phytoplankton. Others try to analyse the pigment composition and the chlorophyll content by using the high performance liquid chromatography (HPLC). [5] These methods were generally used, when the phytoplankton samples can be collected and later be analysed in a laboratory.

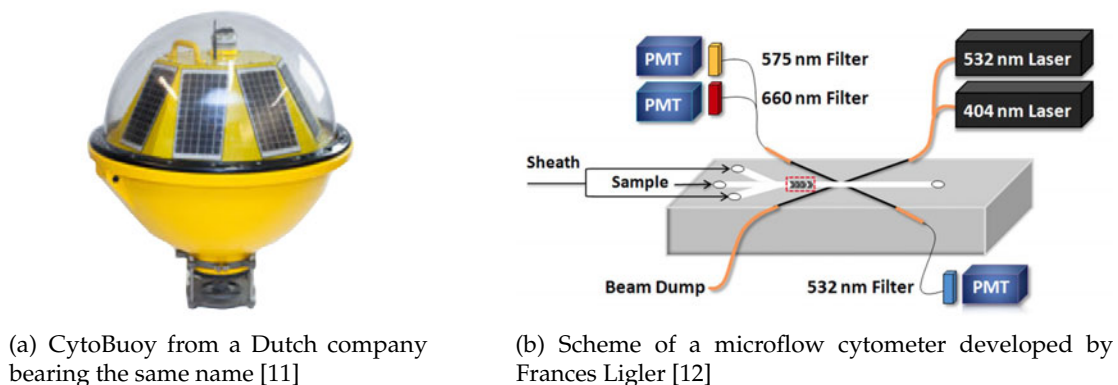
For *in situ* measurements and marine monitoring, however, ocean-colour methods can be used. Here, the reflected and fluoresced light as well as the scattering of light by algae, micro-organisms, particles and dissolved substances, is measured by satellites or radiometers installed on moorings or drifters. While these remote sensing methods were mainly used for wide-ranging or long-term comparisons, compact and submersible instruments were used for a real-time characterisation of the water conditions and *in situ* monitoring of marine life. For this purpose, fluorometers, which enable a fast identification of existing algae classes and – after a carefully calibration – a determination of the total chlorophyll *a* content, are useful. The multi-wavelength fluorometers from Chelsea Technologies Group are a good example for a



**Figure 2.3.:** *TriLux Fluorimeter from Chelsea Technologies as low-cost digital fluorometer for phycoerythrin, phycocyanin and chlorophyll a detection. [10]*

miniaturised and low-cost module, that enables these features as well as an environmental and cell culture monitoring. [10]

On the other hand, flow cytometry especially in combination with imaging technologies is a powerful method to characterise and classify algae species in a water sample. A cell solution is pumped rapidly through the system and the intrinsic light-harvesting pigments in the cells were excited separately by different laser-beams. The resulting fluorescence emitted by the cells as well as the scattering properties of the cells were analysed, providing detailed information on the cell morphology and pigment composition. Consequently, the flow cytometry is an effective instrument for the differentiation and quantification of different algae groups that can also be used for cell counting and cell sorting. The CytoBuoy from a Dutch company bearing the same name is a successful example where a bench-top flow cytometer is placed in a buoy and used as monitoring tool. [11] An example of the buoy is shown in Figure 2.4. However, these systems have some drawbacks. First, their fabrication is expensive, they are large in size and they require a lot of energy. Consequently, a more suitable system is of significant benefit. Especially due to the microfluidic studies of Frances S. Ligler and her working group, who have developed a microflow cytometer, it is now possible to fabricate a miniaturised and low-cost module for characterising of phytoplankton. [12]



(a) CytoBuoy from a Dutch company bearing the same name [11]

(b) Scheme of a microflow cytometer developed by Frances Ligler [12]

**Figure 2.4.:** *Comparison of a bench-top flow cytometer which is placed into a buoy and a microflow cytometer that exhibits a smaller footprint requiring only low power. Both systems can be used for marine monitoring*

## 2.3. Photosynthesis and Chlorophyll-Fluorescence

### 2.3.1. General overview of photosynthesis

All algae species and also cyanobacteria are phototrophic organisms, meaning that they are able to build up energy-rich compounds from low-energy substances by means of the sun's energy. If oxygen is produced during this process, the term *oxygenic photosynthesis* is also used, if not the photosynthesis is called *anoxygenic*. At the moment, there are only few cyanobacteria species known, which can switch optionally between the oxygenic and anoxygenic form. All other algae or cyanobacteria use the oxygenic form. [13]

As it is illustrated in Figure 2.5, the photosynthesis consists of two partial reactions; the first reaction is light dependent, whereas the other is not. During the light reaction, a part of the incident sun light is first absorbed by so-called light-harvesting complexes and then converted into chemical energy. The energy collected in the light-harvesting complexes is transferred to the reaction centre, where the chlorophyll initialises an oxidative photolysis.

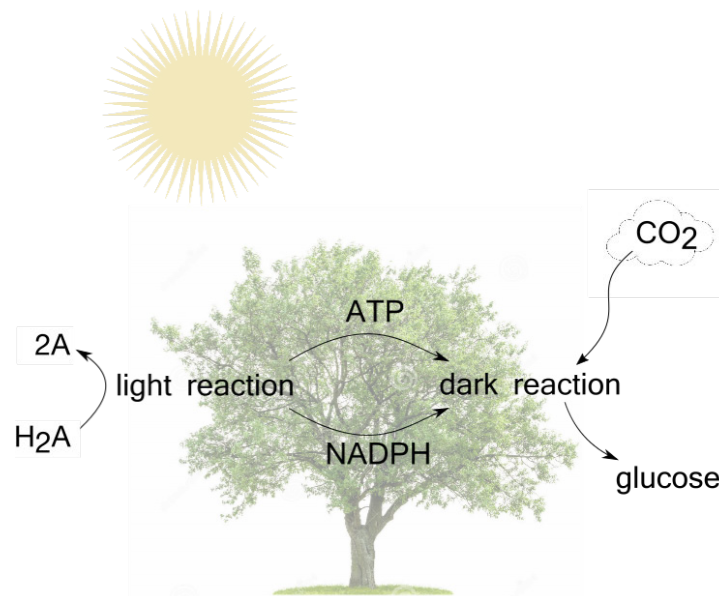


**Figure 2.5.:** Scheme of the photosynthesis. It consists of two partial reactions – the light reaction and the dark reaction, also called Calvin cycle. During the light reaction the energy of the sun is converted into chemical energy to synthesise organic compounds.

Water or other reducing agents (shown as  $H_2A$  in Figure 2.5) are oxidised, oxygen or another corresponding compound is produced and protons and electrons were transferred over a complex reaction cascade to built up energy-rich compounds, known as ATP and NADPH. During the following dark reaction, which is also called Calvin cycle, the energy-rich compounds are used to fix atmospheric carbon dioxide and synthesise carbohydrates. [1]

The whole photosynthesis is controlled by sensible control mechanisms to optimise the interaction of all partial reactions within the process and to adjust the photosynthesis to external environmental conditions. Since it depends on several changeable ecological factors, like the actual and elapsed irradiation or the nutritional state, a flexible adaptation of the photosynthesis apparatus must be possible to optimise the quantum yield. An essential part for this, are the light-harvesting complexes, which absorb the incident light during the light reaction. [5, 14]

### 2.3.2. Light reaction and light-harvesting complex (LHC)

The light reaction of higher plants and algae is located in the thylakoid-membrane of their chloroplasts. By contrast, since the cyanobacteria lack chloroplasts, their photosynthesis apparatus is spread out in the peripheral region of the cells. [14]

Furthermore, in all oxygenic organisms, the electron transport from the reduction agent to the coenzyme II (NADP<sup>+</sup>) is characterised by the interaction of three different protein complexes – the photosystem I and II and the cytochrome complex.

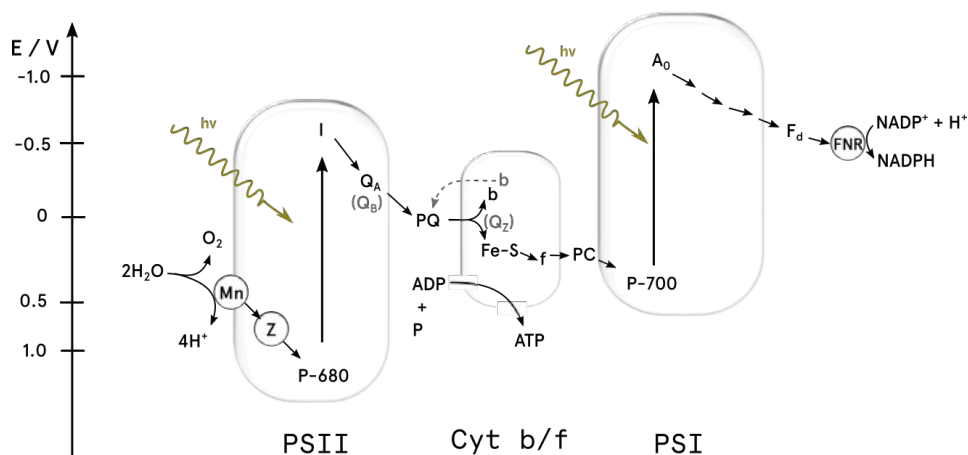


**Figure 2.6.:** Scheme of the electron transfer in the light reaction, when oxygen is evolved, based on the publication of Govindjee. The electrons are transported over several complex reaction cascades to the coenzyme II which is used during the Calvin cycle to synthesise carbohydrates. The redox potential is indicated on the left. [1]

In a first step, the chlorophyll-dimer which is the reactive part in the light-harvesting complex II (P-680, part of photosystem II), withdraw electrons from water and oxygen and four protons are evolved in the interior of the thylakoid-membrane. The resorbed electrons are then transferred to the first electron acceptor molecule in the photosystem II (pheophytin labelled as *I* in Figure 2.6) and, in the following, to plastoquinone molecules, which can move freely in the thylakoid-membrane. The electrons are transported to the cytochrome complex and to the third protein complex – the photosystem I (PSI). In the inside of the photosystem,

the second light-harvesting complex (P-700) continues to pump the electron, when it is excited by light. Finally, the electrons are transferred to the coenzyme II to synthesise NADPH and the energy that is accumulated during the transport of electrons and protons through the thylakoid-membrane is used for synthesis of ATP (phosphorylation). The light-harvesting complexes (*LHC*), P-680 and P-700, function as electron pumps in the whole system. [1]

Generally, the two main light-harvesting complexes (*LHC*) in higher plants and algae are assigned to the photosystems PSI and PSII. These complexes, working as a "light converter", consist of an antenna complex and a reaction centre at the bottom side. Within the antenna complex, several auxiliary pigments are tightly packed to a so-called "pigment collective". Auxiliary pigments are carotenoids, xanthophylls or chlorophylls which exhibit an extended conjugated  $\pi$ -electron system and absorb spectral light of a certain wavelength-range. The absorbed light is transferred by an energy transfer process to the reaction centre where a chlorophyll-dimer, known as *special pair*, initialises the light reaction and works as a electron pump in the whole electron transport process as it was mentioned above. The overall transmission process of the excitation energy to the reaction centre, is called *energy trapping*. Figure 2.7 illustrates a simplified model of an light-harvesting complex and demonstrates its role in the light reaction. The blue-green and red algae groups as well as the cryptophyta contain an additionally accessory complex, called phycobilisome. These peripheral antenna complexes consist of different phycobilins – the most important are phycoerythrin and phycocyanin. [14]

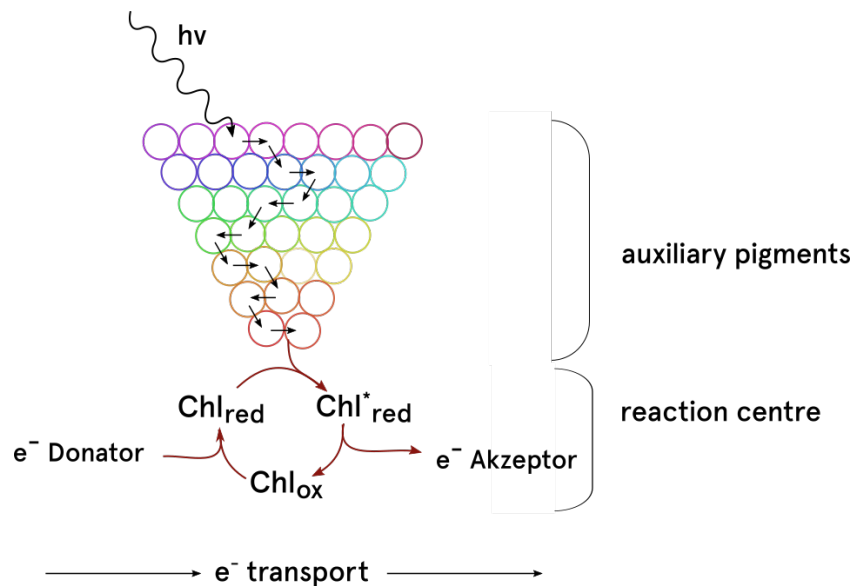


**Figure 2.7.:** Simplified model of the light-harvesting complex and its energy transport cascade, based on Schopfer, Brennicke, and Mohr. A part of the incident light is absorbed by the antenna pigments to increase the efficiency of light absorption. [14]

As a result, accessory pigments are used to enlarge the spectral range from which the energy is absorbed and, therefore, they are used to increase the efficiency of the light absorption.

Moreover, the internal conversion of the excitation energy to the reaction centre enables a reduction of the average reaction time. While a photochemical reaction needs only few femto- to pico-seconds ( $10^{-15}$  -  $10^{-12}$ s), a biochemical reaction generally needs few milliseconds or even seconds ( $10^{-3}$  - 1s). As a consequence, in order to use the light energy efficiently for the photosynthesis, the reaction time of the photosynthesis has to be reduced. [14]

Especially the carotenoids have an additional protective role in the light-harvesting complex. If there is excess of light that would damage the chlorophyll in the reaction centre, the carotenoids discharge the surplus light energy and convert it to harmless thermal energy. [14]

It should be noted that the pigmentation within the light-harvesting complex is not the same for all algae and higher plants, but may differ in the case of the antenna complexes. The reaction centre in higher plants, algae and cyanobacteria consists always of a chlorophyll-dimer which is known as *special pair*. Some algae groups have additionally phycobilins in their light-harvesting complex. These pigments enable a much broader absorption range and close the green gap where the other pigments do not absorb. Based on the pigmentation of the antenna complexes in cyanobacteria, algae and higher plants can be roughly combined into the following groups:

- **Orchophyta** contain only chlorophyll *a*
- **Greenalgae and higher plants** contain chlorophyll *a + b*
- **Diatoms, Dinophyta and Haptophyta** contain chlorophyll *a + c*
- **Cryptophyta** contain chlorophyll *a + c* and phycobilins
- **Rhodophyta** contain chlorophyll *a* and phycobilins
- **Blue-green algae** contain chlorophyll *a* and phycobilins
- **Prochlorophyta** contain chlorophyll *a + b*

Rhodophyta and cyanobacteria exhibit similar pigments in the peripheral antenna complex (phycobilins), but whereas the rhodophyta contain mainly phycoerythrin, phycocyanin is the dominant pigment in cyanobacteria.

Other bacteria, that conduct photosynthesis, but do not liberate oxygen, are called anoxygenic organisms. They contain bacteriochlorophyll instead of chlorophyll in their photosystems, which exhibit structural similarities, but absorb in different wavelength-ranges. [15]

### 2.3.3. Excitation and emission spectra of algae species

Excitation of pigments is the first step in the photosynthesis, when accessory pigments in the light-harvesting complexes absorb a part of the incident light and transfer the excitation energy through the antenna complex to the reaction centre. In general, excitation is the absorption of energy by a molecule and the stimulation of an electron in the highest energy level to higher levels. Besides, the pigment absorb only a part of the incident light that corresponds to the energy gap between the ground state ( $S_0$ ) and the excited state ( $S_1$  or  $S_2$ , labelled as  $S^*$ ). This relation is summarised in the following equation 2.1.

$$\Delta E = E_{S^*} - E_{S_0} = h\nu = \frac{h \cdot c}{\lambda} \quad (2.1)$$

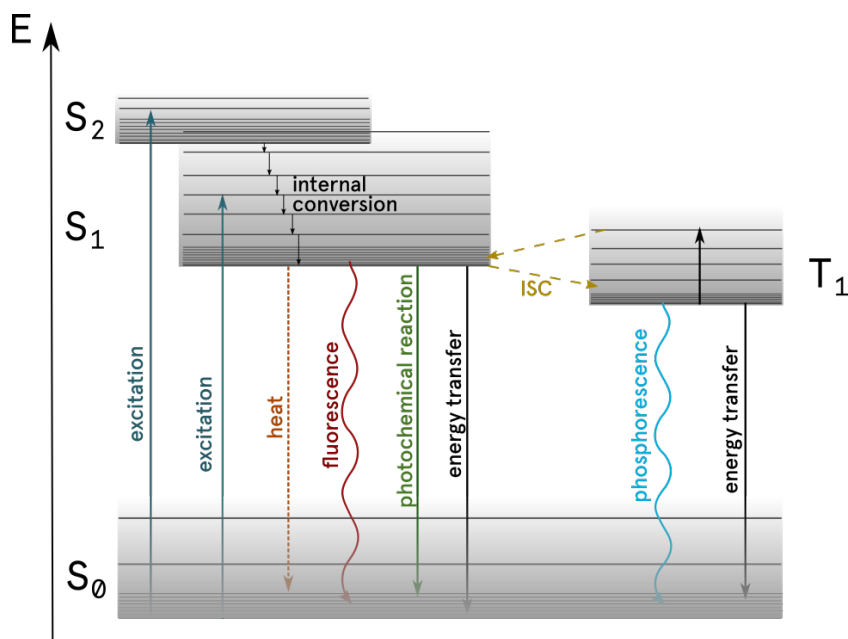


**Figure 2.8.:** A Jablonski diagram demonstrating the excitation of a pigment  $D$  to its excited states  $S_1$  or  $S_2$  followed by possible relaxation processes to reach the energetically favourable ground state  $S_0$ .

The remaining incident light that is not absorbed by the pigment but reflected, leads to the typical complementary colour of the pigment. Depending on the absorbed energy, the electron may be lifted from the ground state ( $S_0$ ) into the first or second excited state ( $S_1$  or  $S_2$ ). Since the excited state is energetically less stable than the ground state and the second excited state is even more unstable than the first, all excited electrons relax fast (1 ps) by an internal conversion to the first excited state and emit their surplus energy in form of heat. In order to reach the energetically most favourable ground state, the pigment has several possibilities of relaxation which compete among each other:

- Radiationless deactivation by an internal conversion and emission of heat ( $k_{IC}$ )
- Fluorescence ( $k_f$ )
- Intersystem crossing and phosphorescence ( $k_{ISC}$ )
- Photochemical reaction ( $k_p$ ) or energy transfer to a neighbouring molecule ( $k_t$ )

Nevertheless, the energy, which is transmitted or emitted from the first excited state, is always less than the initial excitation energy. Each energy level is overlaid with several vibration and rotation states and when a pigment is excited, it is mainly lifted up to one of those higher states. However, since all relaxation processes to the ground state  $S_0$  start from the ground state of an excited state  $S_1$ , the pigment has to emit surplus energy by internal conversion. Therefore the emitted energy is less than the initial excitation energy and the corresponding emission wavelength is higher than the excitation wavelength (Stokes shift).

The competition of relaxation processes can be seen during an experiment as an attenuation of the fluorescence quantum yield. Generally, the effective lifetime  $\tau^D$  of the first excited state ( $S_1$ ) and the fluorescence quantum yield  $\Phi_f$  after an excitation of the pigment, can be described as:

$$\tau^D = \frac{1}{k_{ges}^D} = \frac{1}{k_f^D + k_{ISC}^D + k_{IC}^D + k_p^D + k_t^D} \quad (2.2)$$

$$\Phi_f = \frac{k_f^D}{k_{ges}^D} \quad (2.3)$$

The *in-vitro* fluorescence quantum yield for a chlorophyll *a* solution can be determined as  $\Phi_f = 0.3$ , whereas the quantum yield in living cells is reduced to  $\Phi_f = 0.03$ , and phosphorescence does not occur in the cells under normal conditions ( $k_{ISC} = 0$ ). Therefore, the other relaxation processes compete for the excitation energy and the maximal fluorescence quantum yield is "quenched" to  $\Phi_f = 0.03$ . [14]

By comparison, the *in-vivo* fluorescence quantum yield of other light-harvesting pigments is even more reduced and thus other relaxation processes prevail. Although the mechanisms of energy transfer in the light-harvesting complex is not yet fully clarified in its complexity, Theodor Förster has developed a quantum mechanical model to describe the energy transfer between two pigments – the **Förster resonance energy transfer (FRET)**.

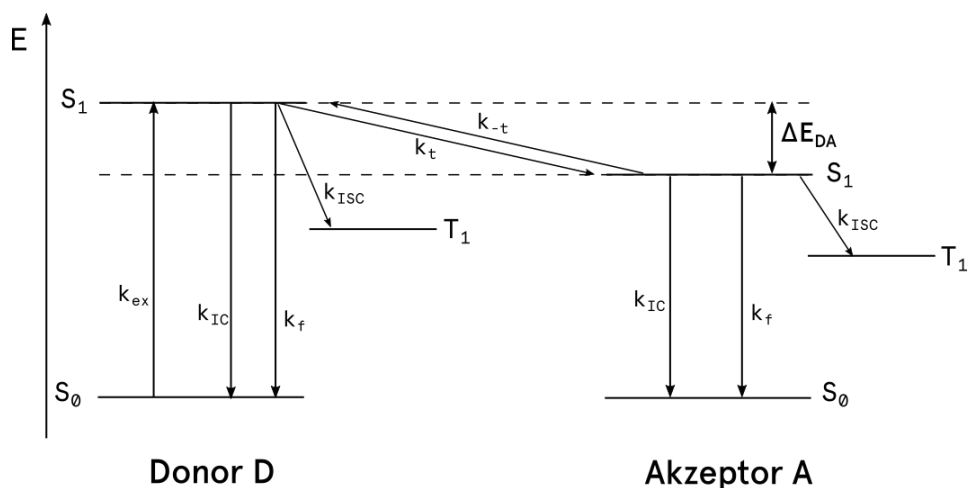


**Figure 2.9.:** A Jablonski diagram to describe the Förster resonance energy transfer (FRET). A pigment *D* is excited and besides the common relaxation processes of radiationless deactivation, phosphorescence or fluorescence, the pigment can transfer its excitation energy to an acceptor molecule *A*. The donor goes back radiationless to the ground state.

According to this theory, the donor pigment *D* which was excited to the first excited state, transfers its surplus energy to a neighbouring acceptor pigment *A*. While the donor pigment relaxes radiationless to the ground state, the electron of the acceptor pigment is lifted to the excited state. The excitation energy is transferred between these pigments over radiationless dipole-dipole interactions and, furthermore, the transfer occurs in general as a singlet-singlet transfer, while the total spin is maintained. The transmission takes place within few picoseconds ( $10^{-12}$  s) and the greater the energy difference between the excited states of the donor and acceptor, the more irreversible the transmission process is. Central conditions for this energy transfer are a physical proximity of the molecules and their compatible alignment, a coupling of the pigments (Coulomb interactions), and, furthermore, an overlap of the orbitals. Spectrally spoken, a possible interaction can be recognised by the fact that the emission spectra of the donor overlaps with the excitation spectra of the acceptor. According to Govindjee et al., the efficiency of the energy transfer process for accessory pigments exceeds, in the most cases, 90%. [1]

In addition to the FRET model, the Dexter mechanism is another theory for explaining the energy transfer between the pigments, when they are in close proximity. Here, instead of transmitting the excitation energy, electrons are exchanged between the donor and the acceptor molecules.

Finally, all excitation energy, absorbed by accessory pigments, is transferred to the reaction centre, where a chlorophyll-dimer is then excited, forming a radical pair (compare Figure 2.7). As it was shown in Figure 2.8, the excited radical pair has different possibilities to emit the surplus energy in order to go back to the ground state. Since the fluorescence quantum yield is reduced in living cells and chlorophyll phosphorescence does not take place in the thylakoid-

membrane under normal conditions, internal conversion, another energy transfer between these two radicals and a photochemical reaction remain as preferred relaxation processes. In order to maintain and drive the electron transport cascade in the light reaction, the excited chlorophyll-dimer transmits an electron to the acceptor molecule ( $Q_A$  in Figure 2.5) by an inner sphere electron transfer reaction and withdraws then an electron from the chlorophyll donor in the reaction centre. As underlying mechanism, a singlet-singlet annihilation between both chlorophyll radicals is assumed. [1, 16]

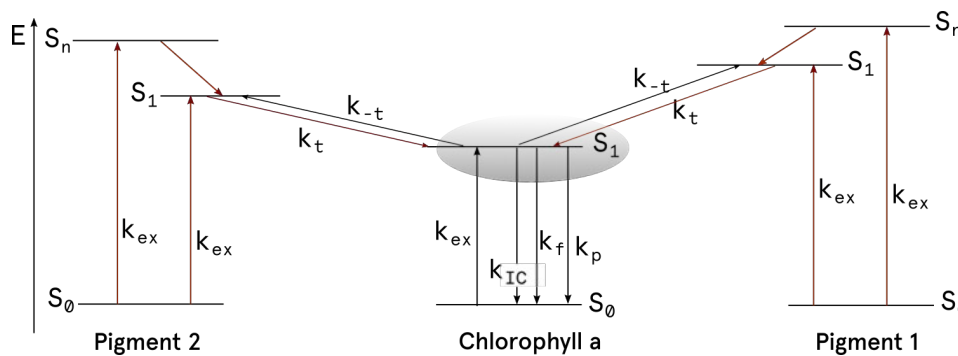


**Figure 2.10.:** A Jablonski diagram to give an overview of the energy trapping. All energy absorbed by the accessory pigments is transmitted to the chlorophyll-dimer in the reaction centre. The overall efficiency of the energy trapping exceeds 90%.

Since the energy trapping takes place with an overall efficiency of more than 90%, it is evident that the fluorescence spectrum of algae cells resembles that of chlorophyll. By contrast, the excitation spectra represent an overlay of all excitable pigments in the photosystem II and I. Surplus energy, which is absorbed by accessory pigments, but cannot be transferred to the reaction centre, is emitted by an internal conversion in form of heat or as fluorescence. This protective process is done by carotenoids in the antenna complexes.

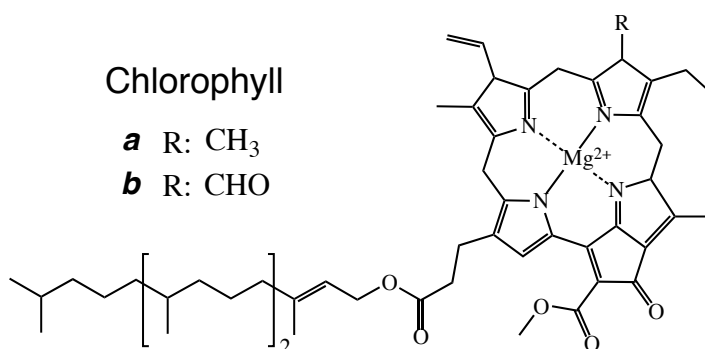
#### 2.3.4. Diagnostic pigments

As mentioned previously, the pigmentation of algae and cyanobacteria may differ in the presence of some light-harvesting pigments as well as in their relative composition. While chlorophyll *a* is an ubiquitous pigment that occurs in the antenna complex as well as in the reaction centre, other pigments are typical for a particular algal phylum or even class. These typical pigments are called "marker pigments" or "diagnostic pigments" and they absorb in a certain wavelength range. The interaction of all these special and ubiquitous pigments results in an overlapped excitation spectrum of a particular algae species. In order to enable a differentiation between different algal phyla based on their overall absorption behaviour, the differences in the excitation spectra and their marker pigments have to be worked out. The results are shown in the *appendix A*. Table 2.1 gives an overview of the diagnostic pigments and their absorption maxima, which were found in literature.

**Table 2.1.:** Marker pigments for different algae and cyanobacteria cultures and their absorption maxima

Phylum	Diagnostic pigments	Reference
Baciillariophyta / Diatoms	Fucoxanthin (450 nm, EtOH)	[17]
Cryptophyta	Alloxanthin (451 nm, acetone/hexane),	[17]
	Phycoerythrin (566 nm, phosphate buffer)	[18]
Dinophyta	Peridinin (454 nm, hexane)	[19]
Haptophyta	Fucoxanthin (450 nm, EtOH)	[17]
Orchophyta	Vaucheriaxanthin (418 nm, 441 nm, 470 nm, EtOH)	[20]
Chlorophyta	Lutein (446 nm),	[20]
	Chlorophyll b (472.2 nm, 655.5 nm, pyridine)	[21]
Cyanophyta	Zeaxanthin (450 nm, 475 nm, acetone/hexane),	[17]
	Allophycocyanin (655 nm, solvent unknown),	[22]
	Phycocyanin (621 nm, phosphate buffer), Phycoerythrin (566 nm, phosphate buffer)	[18] [18]

Moreover, the chemical structure and the excitation and emission spectra of few marker pigments are given below. Chlorophyll *a*, as ubiquitous pigment in all plants and algae phyla, is first shown in Figure 2.11. By contrast, chlorophyll *b* occurs as diagnostic pigment only in green algae. The structures are quite similar, they differ only in one substituent as it is illustrated in Figure 2.11. This substituent leads to a small bathochromic shift for chlorophyll *b* (Figure 2.12).

**Figure 2.11.:** Structures of chlorophyll *a* (left) and *b* (right), which differ only in one substituent.

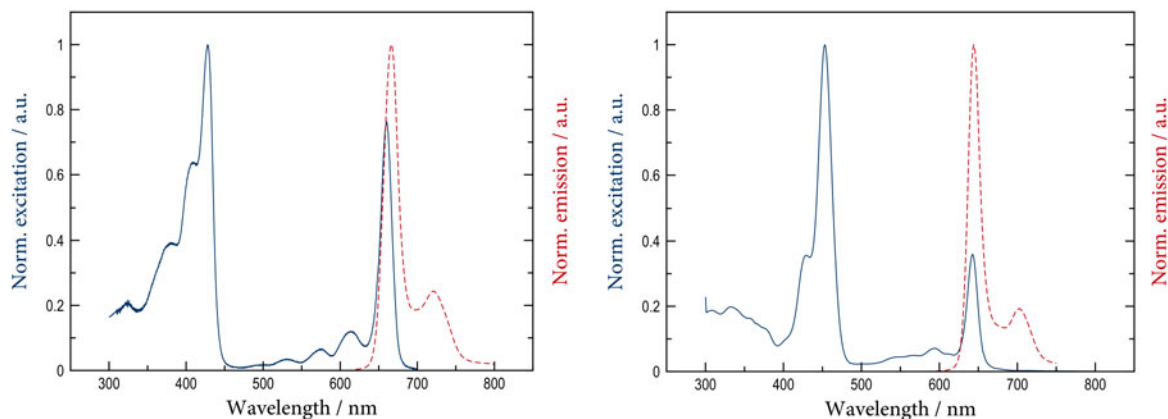


**Figure 2.12.:** Spectral characterisation of chlorophyll a and b based on [24]. The pigments were dissolved in diethylether. The excitation wavelength for the chlorophyll a emission was 614 nm and for chlorophyll b 435 nm.

A common representative of the carotenes, which is also part of the antenna complexes in the photosystems, is  $\beta$ -carotene. Especially  $\beta$ -carotene acts as protective agent in the light-harvesting complex and annihilate surplus energy. Its structure and its absorbance/emission behaviour are given in Figure 2.13.

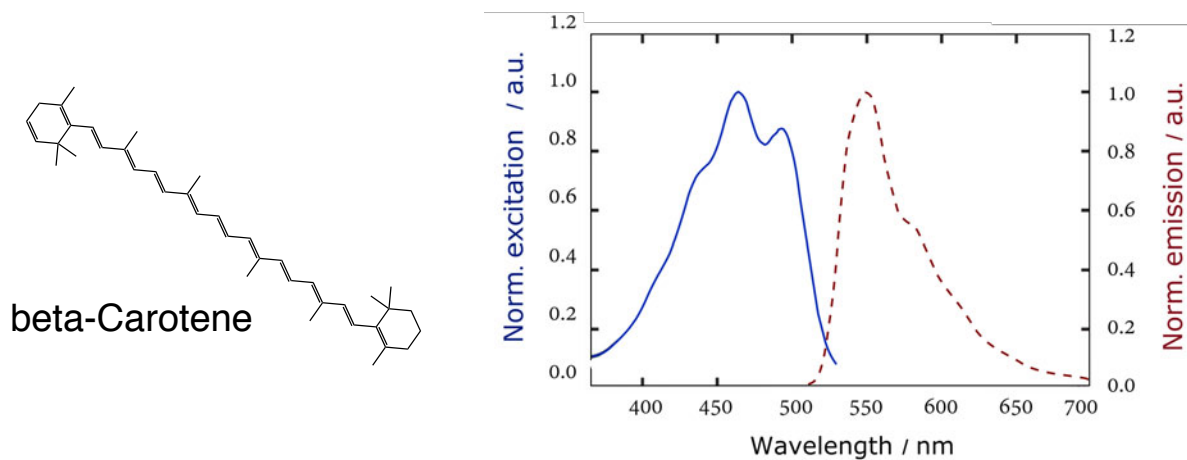


**Figure 2.13.:** Left: Structure of  $\beta$ -carotene as an example for the carotinoids. Right: Spectral characterisation of the pigment, which was dissolved in toluene; based on [25]. The excitation wavelength for the emission spectrum was 475 nm.

Besides the carotenes, there are also some xanthophylls, the second important class of the carotenoids, involved in the light-harvesting complex. Xanthophylls and carotenes exhibit a similar structure, but xanthophylls contain also oxygen, whereas carotenes do not.

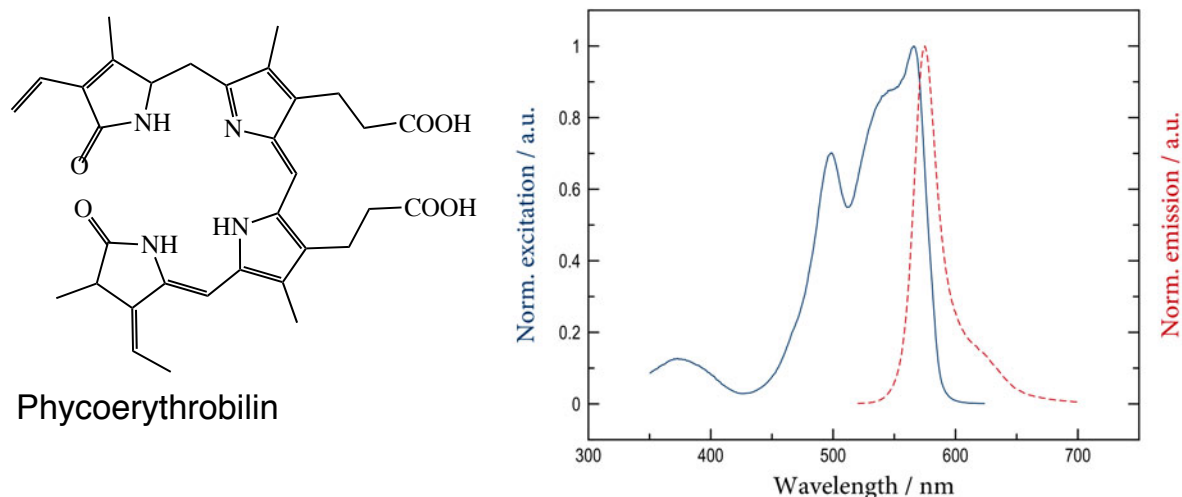
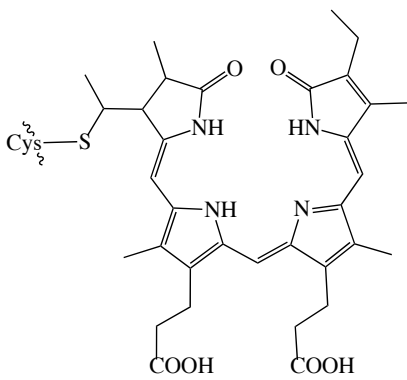


**Figure 2.14.:** Left: Structure of phycoerythrin, the chromophoric group of phycoerythrin, which is part of the peripheral antenna complexes in cyanobacteria and red algae. Right: Spectral characterisation of the phycobilin in sodium phosphate / EDTA / sodium azide; based on [23].

While the carotenoids and xanthophylls absorb in a quite similar wavelength-range, the absorption behaviour of the phycobilins – allophycocyanin, phycocyanin and phycoerythrin – differs obviously from other pigments. These phycobilins are arranged in line to form the peripheral antenna complex, instead of a cyclic arrangement such as the light-harvesting complex do, and transmit the excitation energy of the incident light to the reaction centre for photosynthesis. They occur in cyanobacteria, red algae and also partly in cryptophyta, which inhabit the great depths in the oceans and lead to a significantly different excitation spectra. Since light refracts in water and only light of high wavelengths penetrates further down, the cyanobacteria and cryptophyta need pigments which are able to absorb in this range. The following figures 2.14 and 2.15 illustrate the excitation and emission behaviour of phycoerythrin and phycocyanin as two examples of the peripheral antenna complex in cyanobacteria or red algae. The structures, which are given besides these spectra, show the chromophoric groups of the phycobilins. These groups exhibit structural similarities to the porphyrine-ring of the chlorophyll-molecule (compare Figure 2.11).

In order to distinguish cyanobacteria from other algal phyla, a sample has to be analysed, whether it absorbs in the typical wavelength-range of phycobilins. Furthermore it has to be checked, whether the absorbance of the sample is also increased in the range that is typical for other algal phyla. The ratio of the absorption in these two wavelengths allows a conclusion whether the sample contains cyanobacteria.



Phycocyanobilin

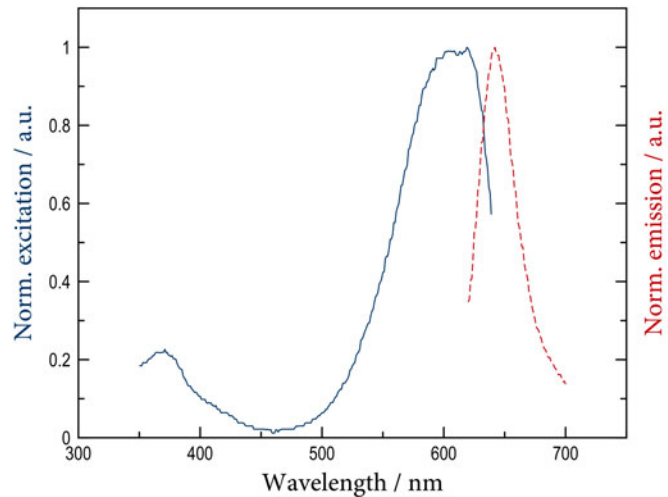


**Figure 2.15.:** Left: Structure of phycocyanobilin, the chromophoric group of phycocyanin, which is part of the peripheral antenna complex in cyanobacteria. Right: Spectral characterisation of the phycobilin in sodium phosphate / EDTA / sodium azide; based on [23].

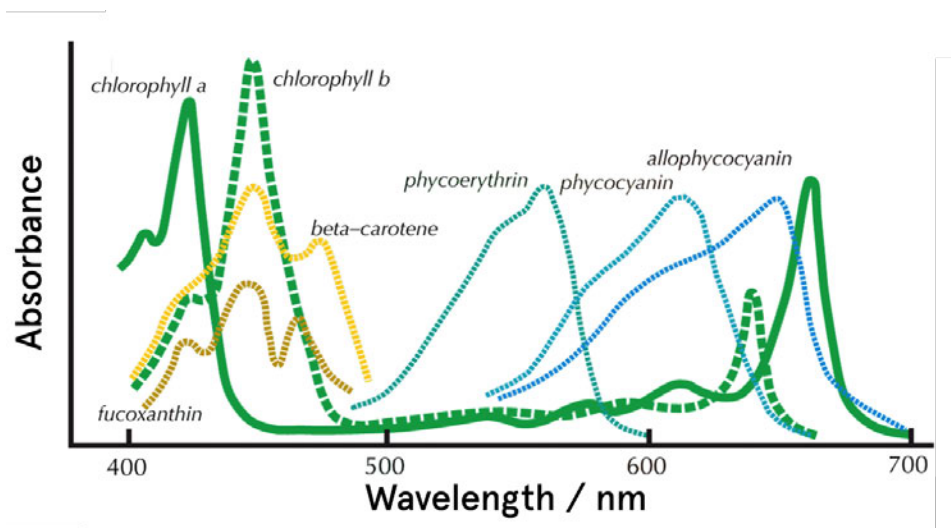


**Figure 2.16.:** Comparison of the absorption behaviour of different pigments. Phycobilins close the green gap where chlorophyll can not absorb light and enable a algal growth in the depth of the oceans. [26]

In a further step, when a separation of algal phyla with a similar absorption behaviour is preferred (e.g. dinoflagellates and diatoms), it is important to consider the overall shape of the spectra and to examine the differences in the effective absorption curve. If it is possible to determine characteristic wavelength-ranges, where only few phyla absorb strongly and others absorb less, then a separation of algal phyla in an unknown sample might be possible.

### 2.3.5. Chlorophyll fluorescence and induction kinetics

An important method for determining the photosynthesis activity of cells bases on the **Kautsky-effect**. This measurement method developed by Hans Kautsky, analyses the chlorophyll fluorescence of dark-adapted cells in a time resolved experiment. When cells, which were stored in the dark, are irradiated suddenly with light of moderate intensity, they emit a characteristic fluorescence signal over time as it can be seen in Figure 2.17. The differences in the fluorescence signal are strongly dependent on the integrity of the photosynthesis apparatus and their functionality. Thus, also the influence of different stress factors can be examined.

When the incident light is absorbed by the accessory pigments in the photosystems, it is further transmitted by energy transfer mechanisms to the chlorophyll-dimer in the reaction centre (compare Figure 2.10). The chlorophyll-dimer has several possibilities of relaxation and if it is possible, the dimer transfers the excitation energy to the electron acceptor molecule  $Q_A$ , in order to maintain the electron transport and the photosynthesis (*quenching reaction*). If the acceptor molecule, however, is fully reduced, as the electron transfer and the  $CO_2$ -fixation during the Calvin cycle is not possible, other relaxation processes, such as the emission of heat or fluorescence, are favoured. In accordance to Duysens and Sweers, an almost complementary relation between the chlorophyll fluorescence and the photosynthesis activity was noted. This means that the higher the chlorophyll fluorescence is, the lower the photosynthesis activity is and vice versa. Besides, the chlorophyll fluorescence is mainly observed from the chlorophyll in the photosystem II, where the energy of the light is converted into chemical energy. [1]

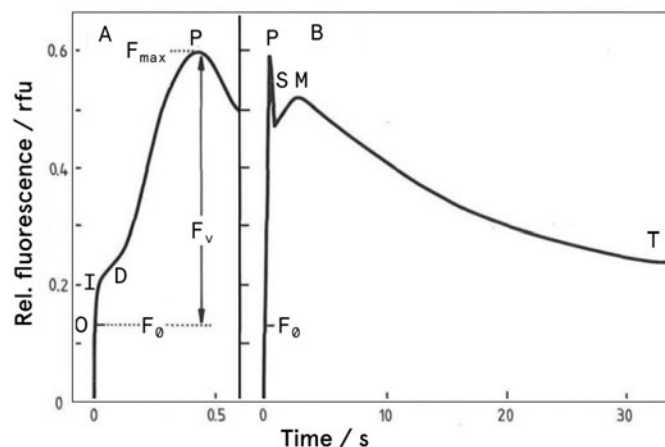


**Figure 2.17.:** A characteristic chlorophyll fluorescence induction curve of dark-adapted needles of *Pinus sylvestris* based on Bolhar-Nordenkampf, Long, and Lechner. The curve which can be divided into a fast phase (A) and a slow phase (B), was measured on a fluorometer with a photon flux of  $100 \mu\text{mol m}^{-2} \text{s}^{-1}$  at  $20^\circ\text{C}$ . The characteristic measurement points are marked. [27]

The characteristic Kautsky curve shown in Figure 2.17 can be divided into two parts: a first phase called *fast kinetics A*, followed by a phase of *slow kinetics B*. The essential measurement values for interpretation are the minimal and maximal fluorescence rate  $F_0$  and  $F_{max}$  and the

difference between both values, referred to as variable fluorescence rate  $F_v$ . Furthermore, the ratio between the variable and maximal fluorescence rate  $F_v / F_{max}$  is used as comparative value. The minimal fluorescence rate is obtained, when the primary quencher molecule  $Q_A$  is fully oxidised and a optimal benefit of photosynthesis is possible. By contrast, the fluorescence rate is maximal, when the quencher molecule is fully reduced and the electrons cannot be transferred to the Calvin cycle over the electron transport chain. In this case, as mentioned before, the emission of heat or fluorescence are the only possible relaxation processes. As a result, the ratio between the variable and maximal fluorescence rate contains information of the integrity of the photosynthesis apparatus and under normal conditions this ratio is between 0.75 - 0.85 .

The second part of the Kautsky-curve, by contrast, contains information on the  $CO_2$ -fixation activities of the cells.

Therefore, based on the information obtained from both phases, the efficiency and integrity of the photosynthesis can be described as well as the influence of several stress factors on the photosynthesis apparatus.

In order to excite the algae cells, which pass through the system, the optical detection module uses short and intensive light pulses. Therefore, the Kautsky-effect affects also the studied system. Due to the very short exposure time, the quantum yield of excitation and, as a result, the fluorescence quantum yield are not maximal. The effective quantum yield might be in the range between the inflection point  $I$  and the maximal fluorescence rate  $F_{max}$  (compare Figure 2.17). As a result, the fluorescence quantum yield might not be maximal or reproducible and therefore the quantification of the cells might be complicated. Thus, these effects have to be considered in further calculations. However, the induction kinetics provide an interesting opportunity to study the integrity of the photosynthesis apparatus and can be examined in further investigations.

## 2.4. Resume

To summarise, this chapter elucidates the diversity of algae. As it was mentioned in the first chapters, algae may vary widely and it is not possible to define a monophyletic relation between all algae species. They only share a common photosynthetic activity and that they inhabit water, oceans and seas. Moreover, they vary in their morphology, size and inner structure.

Algae are sensitive to external changing environmental factors and then again, some algae species, for their part, may have an adverse impact on the ecosystem, when they form blooms. In this context, especially cyanobacteria and dinoflagellates, which represent a serious threat for marine and human life, have to be mentioned. Therefore, monitoring and detection of harmful algal blooms at an early stage is an important part of marine monitoring. Since this master's thesis deals with the development of a low-cost and miniaturised early warning system, the possible methods for detecting and identifying photosynthetic phytoplankton and harmful algae blooms were presented briefly. Furthermore, it has to be emphasised that the underlying concept of the detection module represents a combination of the microflow cytometer based on the investigations of F. Ligler and a multi-channel fluorometer.

Furthermore, the required biochemical and photochemical principles were exhibited in the following sections. The light-harvesting complexes and their role in the entire process of photosynthesis were described as well as the photochemical relations of pigment excitation and chlorophyll fluorescence. The last two sections deal with possible applications and challenges of the algae detection module, whereas the special focus for the master's thesis was placed on the distinction of algal phyla based on their different excitation spectra. For this purpose, several algae species were cultivated and spectrally characterised during the thesis. Moreover, differences in their spectral behaviour were examined. For further information about this, please see *appendix A*. As mentioned before, the relative pigmentation in the light-harvesting complexes varies between different algal phyla; especially the excitation spectra of blue-green algae (cyanobacteria) are clearly distinguishable. During the development of the algae detection module, these evident differences have to be considered, in order to build a suitable early warning system for cyanobacteria which contributes to the detection of harmful algal blooms.





---

## 3. Material and Methods

The first part in this chapter lists the algae cultures used during the master's project. It lists also the culture media used for cultivating the algae and describes how they were made and stored.

The second part describes all methods needed in the project. First the cultivation method and all parameters that should be considered, are explained. The microscope technique, which was used for determining the cell density, for describing the morphology and also to check if the cultures are contaminated, is then presented. In the third section, the fluorometer and fluorescence spectrophotometer, which were used for the spectral characterisation of the algae species were described with focus on the parameters used during the measurement.

The last section deals with the mathematical algorithm used for data analysis. The algorithm is presented and described and the important interrelationships are explained. The results which algae classes and groups might be separated and which LEDs might be useful, are given in chapter 5 *Results and Discussion*.

### 3.1. Material

#### 3.1.1. Algae and bacteria cultures

Since the algal detection module should be able to differentiate and identify as much algae classes as possible, we cultivated 34 different algae species in order to achieve a broad distribution with respect to the spectral properties. The most relevant algae species which produce toxic products were identified by our project partners (University in Bordeaux and University of Genoa) and by our external collaborators Ifremer Nantes and the Stockholm University. The experts of the phycotoxins lab in Nantes provides us algae species which are most relevant for harmful algae blooms in fish farming as well as the most widespread, non-toxic background species during the blooms.

In Table 3.1 all algae species cultivated for this project, are listed and grouped by their phylum. The most important bloom-forming algae and bacteria phyla that might have serious effects on mammals, birds and humans, are marked in red.

Eight of the algae species are associated with adverse effects on their environment, when they bloom. They may cause discolouration of the water surface or kill marine organisms that take up algae as food. The toxicity status of these algae against humans, however, is unclear. Only for one algae species, the dinoflagellate *Alexandrium minutum*, it is clarified, that it is harmful by producing the neurotoxin Saxitoxin.

**Table 3.1.:** Cultivated algae species for spectral characterisation and data acquisition. The common bloom-forming algae cultures, on which we focus mainly, are marked in red.

Phylum	Algae species	Phylum	Algae species
<b>Diatom / Bacillariophyta</b>	Amphora	<b>Chlorophyta</b>	Tetraselmis suecica
	Phaeodactylum tricornutum		Chlamydomonas reinhardtii
	Ditylum brightwellii		Choricystis minor
	Skeletonema costatum		Dunaliella salina
	Cyclotella meneghiniana		Dunaliella tertiolecta
<b>Cryptophyta</b>	Hemiselmis sp rcc 659		Haematococcus pluvialis
	Rhodomonas minuta		Scenedesmus sp
	Rhodomonas salina		Monoraphidium
<b>Dinophyta</b>	Alexandrium minutum		Pseudokirchneriella subcapitata
	Heterocapsa triquetra		Selenastrum capricornutum
<b>Haptophyta</b>	Pleurochrysis elongata		Chlorella emersonii
	Isochrysis galbana		Chlorella vulgaris
	Ruttnera spectabilis		Unknown species
	Prymnesium saltans	<b>Cyanobacteria</b>	Cyanobakteriopsida
<b>Orchophyta</b>	Eustigmatos magnus		Anabaenopsis elenkinii
	Nannochloropsis salina		Synechocystis sp. PCC 6803
	Chloridella neglecta		
	Unknown species		

For more details about harmful effects of the algae species or their biology, please see chapter 2 *Theoretical background*. Moreover, a detailed description of each algal species analysed in this project, is given in the appendix under *Algae Fact Sheet*.

### 3.1.2. Culture medium

The growing media which were used for cultivating the algae species, are listed in the tables below. All media are prepared with autoclaved and filtered seawater, which is prepared from fresh Milli-Q water and a sea salt composition from our supplier AquaCare. The salinity of the seawater used to prepare the media may vary in some cases but usually a natural salinity of 30 to 33 ‰ is used. For the final media preparation the given volume of the stock solution and components has to be added to 1000 mL seawater. After the preparation, the media has to be stored at a cool place under low light intensity (15 to 18 °C). The media differ mainly in their trace metal composition, whereas the vitamins are similar. The most important nutrient elements are nitrate and phosphate, representing the bulk elements in all culture media.

Guillard's f/2 medium (compare Table 3.2) is used for the most diatoms and haptophyta. The original recipe was slightly modified by our external partner A. Burian from the Stockholm University. The salinity of the filtered and autoclaved seawater medium is either 18 ‰ or 30 ‰. The pH value has to be controlled and should be adjusted to 8.0 with 1 M *NaOH* or *HCl*.

**Table 3.2.:** Recipe for f/2 + Si medium according to Guillard [28] [29]

Substance	Concentration stock solution $c(\text{stock})$ [g L <sup>-1</sup> ]	Volume for nutrient solution $V(\text{nutrient})$ [mL]
<i>NaNO</i> <sub>3</sub>	75	1 mL
<i>NaH</i> <sub>2</sub> <i>PO</i> <sub>4</sub> · 2 <i>H</i> <sub>2</sub> <i>O</i>	5.65	1 mL
Trace metals stock solution (chelated)		1 mL
<i>Na</i> <sub>2</sub> <i>EDTA</i>	4.160	
<i>FeCl</i> <sub>3</sub> · 6 <i>H</i> <sub>2</sub> <i>O</i>	3.150	
<i>CuSO</i> <sub>4</sub> · 5 <i>H</i> <sub>2</sub> <i>O</i>	0.010	
<i>ZnSO</i> <sub>4</sub> · 7 <i>H</i> <sub>2</sub> <i>O</i>	0.022	
<i>CoCl</i> <sub>2</sub> · 6 <i>H</i> <sub>2</sub> <i>O</i>	0.010	
<i>MnCl</i> <sub>2</sub> · 4 <i>H</i> <sub>2</sub> <i>O</i>	0.180	
<i>Na</i> <sub>2</sub> <i>MoO</i> <sub>4</sub> · 2 <i>H</i> <sub>2</sub> <i>O</i>	0.006	
Vitamin mix stock solution		1 mL
<i>Cyanocobalamin</i> (Vitamin B <sub>12</sub> )	0.0005	
<i>Thiamine HCl</i> (Vitamin B <sub>1</sub> )	0.1	
<i>Biotin</i>	0.0005	
Sodium metasilicate stock solution		1 mL
<i>Na</i> <sub>2</sub> <i>SiO</i> <sub>3</sub> · 9 <i>H</i> <sub>2</sub> <i>O</i>	30	
De-ionised water		1000 mL

The L1 and the L1-Si media (compare Table 3.3) are a modification of the f/2 medium containing a wider variety of trace metals. According to our external partners, these media might be used as standard medium for marine diatoms. The L1 medium was prepared with an autoclaved and filtered seawater with a salinity of 33 ‰. The medium L1-Si is prepared without the sodium metasilicate stock solution and used for algae cultures without silicate requirement.

**Table 3.3.:** Recipe for L1 / L1-Si medium according to Guillard and Hargraves, Keller et al. [28] [30] [31]

Substance	Concentration stock solution $c(stock)$ [g/1000ml]	Volume for nutrient solution $V(nutrient)$ [ml]
$NaNO_3$	75	1 mL
$NaH_2PO_4 \cdot H_2O$	5.00	1 mL
Trace metals stock solution		1 mL
$MnCl_2 \cdot 4H_2O$	180.00	
$ZnSO_4 \cdot 7H_2O$	22.00	
$CoCl_2 \cdot 6H_2O$	10.00	
$CuSO_4 \cdot 5H_2O$	2.45	
$Na_2MoO_4 \cdot 2H_2O$	19.90	
$H_2SeO_3$	1.30	
$NiSO_4 \cdot 6H_2O$	2.70	
$Na_3VO_4$	1.84	
$K_2CrO_4$	1.94	
$Na_2EDTA \cdot 2H_2O$	4.36	
$FeCl_3 \cdot 6H_2O$	3.15	
Vitamin mix stock solution		0.5 mL
<i>Cyanocobalamin</i> (Vitamin B <sub>12</sub> )	0.001	
<i>Biotin</i>	0.001	
<i>Thiamine HCl</i> (Vitamin B <sub>1</sub> )	0.20	
Sodium metasilicate stock solution		0.5 mL
$Na_2SiO_3 \cdot 9H_2O$	100	
De-ionised water		1000 mL

This MWC medium is mainly used for chlorophyta and several freshwater algae. Its salinity is 0 ‰.

**Table 3.4.:** Recipe for MWC nutrient solution according to Guillard and Lorenzen [32]

Substance	Concentration stock solution $c(\text{stock})$ [g/1000ml]	Volume for nutrient solution $V(\text{nutrient})$ [ml]
$K_2HPO_4 \cdot 3H_2O$	11.4	1 mL
$NaNO_3$	85	1 ml
$CaCl_2 \cdot 2H_2O$	36.8	1 mL
$MgSO_4 \cdot 7H_2O$	37	1 mL
$NaHCO_3$	12.6	1 ml
$Na_2SiO_3 \cdot 9H_2O$	21.2	1 mL
Micro-nutrient solution		1 mL
$Na_2EDTA$	4.36	
$FeCl_3 \cdot 6H_2O$	3.15	
$CuSO_4 \cdot 5H_2O$	0.01	
$ZnSO_4 \cdot 7H_2O$	0.022	
$CoCl_2 \cdot 6H_2O$	0.01	
$MnCl_2 \cdot 4H_2O$	0.18	
$Na_2MoO_4 \cdot 2H_2O$	0.006	
$H_3BO_3$	1	
Vitamin solution		1 mL
<i>Thiamine HCl</i> (Vitamin B <sub>1</sub> )	0.1	
<i>Biotin</i>	0.0005	
TES buffer		0.115 g
De-ionised water		1000 mL

## 3.2. Methods

### 3.2.1. Cultivation

To cultivate the algae several parameters have to be considered. In addition to a sterile environment, the growing medium, the right amount of light and also a defined temperature are important. Unfortunately, all these parameters depend on the algae species and may vary widely. Since we are limited in space and possibilities, we tried to find optimal conditions under which all species might grow. For detailed information about the growing conditions, please see Appendix A. In this chapter, the relevant parameters are presented and discussed, so you might get an overview of the techniques. [33] [34]

For the most species we used sterile Erlenmeyer flasks, which were closed with Steristopfen<sup>®</sup> based on cellulose (Figure 3.1, left). These plugs are air-permeable to permit gas exchange. The carbon dioxide ( $CO_2$ ), which is necessary for the photosynthesis of the algae, can pass through the plugs and furthermore, ensures a constant pH value.

Initially, the algae flasks were placed in a rotary shaker with a defined growth temperature. Moreover, we installed a timer controlled lighting installation in the rotary shaker. Thereby, all algal cells were equally exposed to light and air and therefore a homogeneous growing of the algae species was ensured. Since the temperature monitoring of the rotary shaker got damaged, we tried to cultivate our algae without a shaker. We placed the flasks in a small, unused dark laboratory, installed the timer controlled lighting installation above the algae and cooled the whole room to 18 °C (Figure 3.1, right).



**Figure 3.1.:** Example of the algal cultivation in sterile Erlenmeyer flasks with cellulose plug (left). Right: Final storage of the algae species under the timer controlled lighting installation in a dark and temperature-controlled laboratory.

For the cyanobacteria, we built a small size algae cultivation tube with controlled illumination and constant aeration as it is shown in Figure 3.2. Due to the fact, that they are robust, less demanding regarding their growing conditions but prefer warmer temperatures and since

they have contaminated other algae species several times, we separated them physically from the rest.



**Figure 3.2.:** *Algae cultivation tubes with a timer controlled illumination. Each tube fits 3 litres of algae culture and the aeration can be adjusted for each tube.*

### **Sterile materials – autoclaving**

Since the contamination of algae cultures with other species is a serious problem that has to be avoided, all used Erlenmeyer flasks, bottles and plugs have to be autoclaved. Moreover, the seawater for the culture media has to be sterilised.

For the autoclaving process the Erlenmeyer flasks and bottles containing a small amount of water, are closed with the plugs and marked with a sterilization tape. When using a screw cap for the bottle, do not close it quite, so the steam may escape. Then, the flasks and bottles are placed into the autoclave and sterilised 35 min at 135 °C.

### **Culture medium and salinity**

The culture medium provides the important elements and nutrients for the algae and bacteria, so that they can grow in high cell densities. Normally, the media are rich in nitrate and phosphate and contain a smaller amount of vitamins and several trace elements. In addition to the nutrients the salinity of the culture media is another parameter to consider. In general the algae species are tolerant to fluctuations of salinity, but nevertheless, there is an optimal salinity at which the algae species grow best. Furthermore, every 2 to 3 weeks, all algae cultures were fed with a fresh growing medium to regulate their growth and to hold them in the exponential growth phase. This step is important to have the relevant species available for the spectral characterisation on a daily basis.

The recipes of the culture media and the used salinity are given in subsection 3.1.2 Culture medium. Moreover, the medium used for a certain species as well as the salinity is listed in the fact sheets.

### Light and Temperature

As algae and bacteria are photosynthetic organisms, they need light as a source of energy to drive their photosynthesis and convert inorganic carbon dioxide and build up organic matter. Moreover, the light intensity needed depends on the species and also on the cell density, but should not exceed a certain range, because too much light leads to an overheating of the cells. [34]

To ensure a natural growth of the cells and a natural formation of the pigments, we used a fluorescence tube with a daylight spectrum from Osram (Sylvania T8 F18W/865 G13 LuxLine Plus). The fluorescence tubes were installed right above the flasks or behind the cultivation tubes and the illumination times is controlled by a clock timer. The duration of the artificial illumination for the algae is set to 10 hours per day. By contrast, the *green sulphur cyanobacteria* and the bacteria *Synechocystis sp.* are illuminated only 4 hours per day, since they grow rapidly.

The most microalgae have an optimal growing temperature around 19 to 24 °C and are tolerant to a certain temperature fluctuation. However, a too high temperature is worse than a too low temperature. If the temperature is too high, it might have lethal consequences for some species, whereas a too low temperature only reduces the growth rate. Taking this into account, we cultivate the algae species under an effective temperature of 19 °C. The bacteria, by contrast, are cultivated under 23 °C.

#### 3.2.2. Microscopy

To describe the algal morphology and also for cell counting, the algae culture is placed on a counting chamber and observed under the microscope Axiovert 25 from Carl Zeiss which is an inverted transmitted light microscope. [35]

The algal cells were placed on a counting chamber from ThomaNeu, which is shown in Figure 3.3. The chamber contains 16 group squares and each group square is divided into 16 least squares. The least squares have an area of 0.05 mm × 0.05 mm and a height of 0.1 mm, so that the volume of these squares is defined as 0.000 25 mm<sup>3</sup>.

Furthermore, the motile algae cells were fixed by using the red to brown Lugol's solution (*J<sub>2</sub>/KJ*). By using this, the algae were fixed which makes it easier to take a photo and count the cells. Moreover, the contrast is increased. Moreover, the algae cells get a homogeneous brown to yellow colour and the fixing agent annihilates the autofluorescence of the pigments of the light-harvesting complex. Therefore, a preliminary selection of the different algae cells is no longer possible. Since we work with pure algae cultures, a selection is not necessary and so this disadvantage is negligible. [36]

The prepared counting chamber can then be placed under the microscope. The photo of the cells is taken by our GenICam RGB-camera. During the microscopic investigations, not only the cell shape can be described, but also the cell density can be determined. Besides this, the algae cultures are checked for contamination.

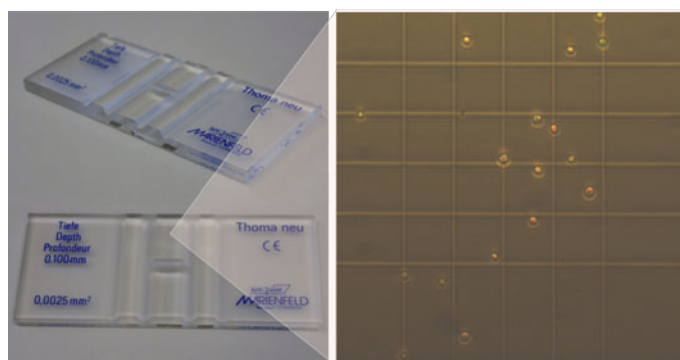


**Figure 3.3.:** ThomaNeu counting chamber for microscopic investigations. The picture on the right shows one group square divided into 16 least squares.

### 3.2.3. Spectral Characterisation

For the description of the spectral behaviour of each algae species, an excitation spectrum as well as an emission spectrum was measured using either the Fluorolog<sup>®</sup> - Spectrofluorometer with a photomultiplier tube from Horiba or the Fluorescence Spectrophotometer F-7000 with the IR-sensitive photomultiplier of Hitachi.

To obtain a first overview, a 3D spectrum (fluorescence emission/excitation) of each phylum was acquired in suspensions diluted with glycerine to avoid sedimentation of the cells during lengthy measurements. These spectra were obtained by using the Fluorolog<sup>®</sup> - Spectrofluorometer. They do not contain more information about the spectral behaviour as the excitation and emission spectrum. However, they visualise the differences between the phyla with more clarity.

After this initial characterisation, emission and especially excitation spectra were collected for the most distinctive emission peaks. While 3D spectra provide an overview of the spectral behaviour of the algae culture, the excitation spectra are the basis for the selection of the most suitable excitation / emission wavelengths for classifying and identifying different algae species.

The parameters for the Fluorolog<sup>®</sup> used for the spectral characterisation are listed in the table below (compare Table 3.5). They were set to the same values for all algal measurements. Only the excitation wavelength used to record the emission spectra was changed for the bacterial measurements to excite the phycobilins in the bacterial light-harvesting complex. The experiment was repeated ten times for each type of spectrum. Then, the spectra were averaged and normalised separately. The emission spectrum was normalised to the maximal fluorescence signal. For the most algae cultures, this maximum was recorded at approximately 680 nm, which corresponds to the chlorophyll fluorescence. The bacterial emission spectra, however, was normalised to the maximal fluorescence of the contained phycobilins ( 650 - 664 nm). By contrast, the excitation spectrum was normalised to the maximal absorption of the pigments. Usually, the maximal excitation is around 435 nm. At this wavelength, which is called the Soret

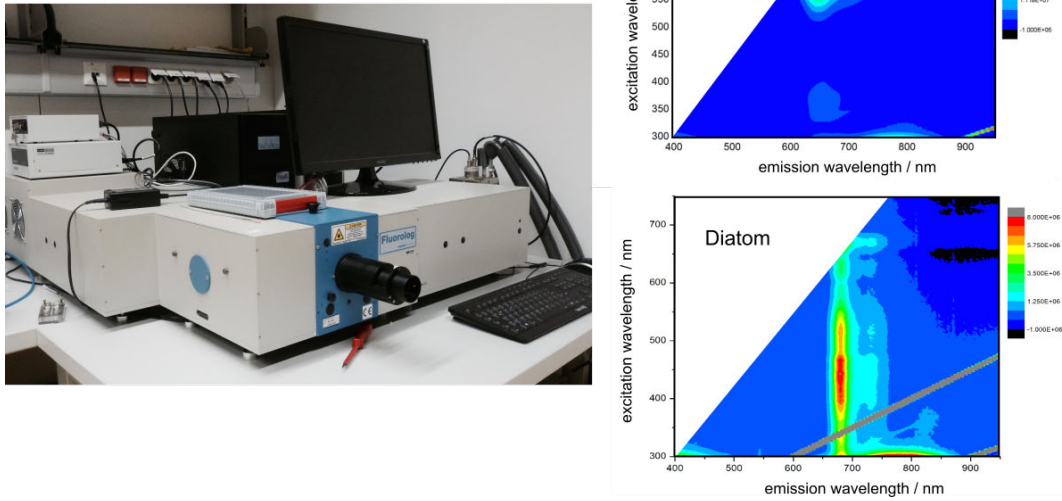


**Figure 3.4.:** Picture of Horiba’s Fluorolog<sup>®</sup> - Spectrofluorometer on the left. Examples of 3D spectra of different phyla to demonstrate the spectral differences. The spectra are shown for cyanobacteria and brown algae (right).

peak, chlorophyll *a* is excited. For the cyanobacteria, in contrast, the maximal excitation is around 640 nm. In this range, the excitation of bacteriochlorophylls and phycocyanin takes place.

When the signal intensity exceeded the dynamic range, a transmission filter was used. The filter was placed between the excitation light and the sample cuvette to reduce the intensity of the excitation light.

**Table 3.5.:** Parameters used on the spectrofluorometer for spectral characterisation

spectrum	slit width [nm]	fixed emission or excitation wavelength
emission spectrum	em-slit = 7 nm	excitation wavelength = 440 nm (algae)
	ex-slit = 14 nm	excitation wavelength = 595 nm (cyanobacteria)
excitation spectrum	em-slit = 14 nm ex-slit = 7 nm	emission wavelength = 750 nm

Since the Fluorolog broke down during the project, some algae species were characterised by using the spectrophotometer from Hitachi. Compared to the spectrofluorometer, the sensitivity of the photometer is worse but good enough for the spectral characterisation of the algae and bacteria cultures. The parameters used on this fluorescence spectrophotometer, are listed in Table 3.6. The measurement process was similar to the method used for the Fluorolog, but after

the measurement, the obtained emission spectra had to be corrected, as there is no internal correction. The excitation spectra, however, were corrected directly during the measurement by an internal quantum counter.

To optimise the signal intensity and the signal to noise ratio, the voltage of the photomultiplier could be adjusted.

**Table 3.6.:** *Parameters used on the spectrophotometer for spectral characterisation*

spectrum	slit width [nm]	fixed emission or excitation wavelength
emission spectrum	em-slit = 5 nm	excitation wavelength = 440 nm (algae)
	ex-slit = 5 nm	excitation wavelength = 595 nm (cyanobacteria)
excitation spectrum	em-slit = 20 nm ex-slit = 5 nm	emission wavelength = 750 nm

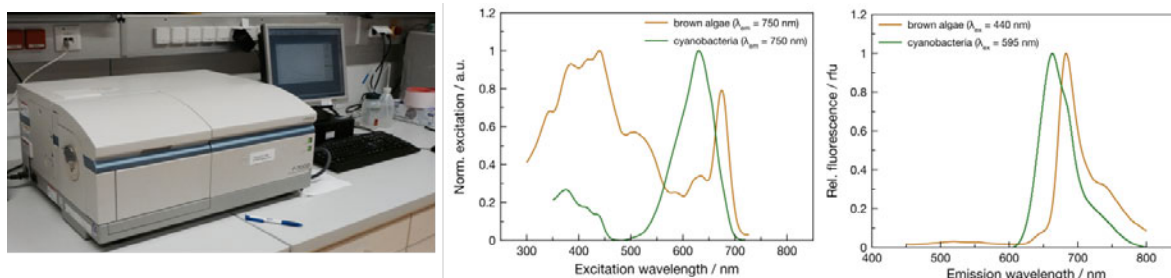


**Figure 3.5.:** *Left: Picture of Hitachi's fluorescence spectrophotometer. The excitation spectra illustrate different absorption behaviour due to a different pigmentation in algae belonging to different phyla (middle). By contrast, the emission spectra on the right is quite similar as chlorophyll a is the principal molecule in the reaction centre.*

### 3.2.4. Mathematical context – Principal component analysis (PCA)

The data, we record with our detection module, are averaged fluorescence intensity over the time at different wavelengths. Since each algae species is excited with 12 different LEDs, we collect a comprehensive data set for each measurement. The detection module, however, has only 8 excitation channels, so we have to reduce the number of LEDs. On the other hand, the data analysis should cluster algae species, which are quite similar and separate those with different pigment pattern. In addition to the principal component analysis, we might use either a factor analysis or a correspondence analysis, as they are all methods to discover a hidden structure. Since the principal component analysis does not lose information while it reduces the overall structure, we thought it might be the best reference method. Furthermore, we hope to reduce the number of LEDs which are needed to distinguish between harmful and harmless algae to a minimum by using the principle component analysis.

The mathematical background of the principal component analysis is described on the following pages.

### Principle of PCA

The principal component analysis, also called singular value decomposition, is a statistical method to analyse comprehensive data sets and extracts, visualise and simplify the underlying structure. The aim of this method is to express a complex and comprehensive data set through a minimal number of linear combinations. The solutions of these linear combinations are called principal components.

The crucial step in this process is a coordinate transformation to a low dimensional (sub-) space. By means of this step, the correlations of the original data are merged without losing valuable sample information. The overall structure is simplified and simultaneously extracted. In other words, it projects the data along the direction where the data varies the most.

### Mathematical derivation

The principal component analysis starts with a comprehensive data set that contains the averaged excitation intensity  $a_{ij}$  of different algae species at a certain excitation wavelength. If we analyse seven different algae cultures and 12 different excitation wavelength (LEDs) for demonstration purposes, we get a  $7 \times 12$  data set as it is shown in Table 3.1.

$$\begin{array}{l}
 \text{Cyano} \\
 \text{Diatom} \\
 \text{Salina} \\
 \text{Dinoflagellat} \\
 \text{Pleurochrysis} \\
 \text{Alexandrium} \\
 \text{Hemiselmis}
 \end{array}
 \begin{pmatrix}
 \text{LED1} & \text{LED2} & \text{LED3} & \dots & \text{LED11} & \text{LED12} \\
 a_{11} & a_{12} & a_{13} & \dots & a_{111} & a_{112} \\
 a_{21} & a_{22} & a_{23} & \dots & a_{211} & a_{212} \\
 a_{31} & a_{32} & a_{33} & \dots & a_{311} & a_{312} \\
 a_{41} & a_{42} & a_{43} & \dots & a_{411} & a_{412} \\
 a_{51} & a_{52} & a_{53} & \dots & a_{511} & a_{512} \\
 a_{61} & a_{62} & a_{63} & \dots & a_{611} & a_{612} \\
 a_{71} & a_{72} & a_{73} & \dots & a_{711} & a_{712}
 \end{pmatrix}
 \quad (3.1)$$

The order of the species in the matrix can be chosen randomly. The LEDs, by contrast, are arranged by their peak wavelength. Nevertheless, the order of the LEDs is not determining for the evaluation. The data matrix 3.1 contains the mean values of the original measured fluorescence intensities over time and the correlation is unknown at that time.

One mandatory precondition for the PCA is that a (unknown) correlation between the matrix entries exists. If the data do not correlate, it is impossible to determine an underlying structure. Furthermore, the principal component analysis is only useful for Gaussian distributed data sets since only in this case a decorrelation of the original data and also statistical independent data are guaranteed after the application of the PCA. If the matrix entries are correlated or not

could be checked by means of Pearson's correlation coefficient shown in equation 3.2. [37]

$$r = \frac{s_{xy}}{s_x \cdot s_y} = \frac{\sum_{i=1}^n (x_i - \bar{x})(y_i - \bar{y})}{\sqrt{\sum_{i=1}^n (x_i - \bar{x})^2 \sum_{i=1}^n (y_i - \bar{y})^2}} \quad (3.2)$$

The parameter  $s_{xy}$  in the equation above is the empirical covariance of the variables  $X$  and  $Y$ , whereas the parameter  $s_x$  and  $s_y$  are the corresponding standard deviations. The mean values of the correlating variables  $X$  and  $Y$  are represented by  $\bar{x}$  and  $\bar{y}$  and  $n$  is the number of value pairs  $(x_i, y_i)$ . The sign of the correlation coefficient indicates if the linear relationship is positive or negative. When the coefficient is zero, however, no linear relationship is determinable. Is the value of the correlation coefficient  $|r|$  higher than 0.2, a (weak) linear relation is assumed and, consequently, the higher the value of the coefficient, the clearer the relationship.

Since we want to determine the underlying structure of a given data set and separate the data pairs as much as possible, we have to find first a linear approximation, which fits best to the given and standardised data set. To standardise the original values, the data were centred by subtracting each entry of the data matrix  $a_{ij}$  (3.2) from column mean value  $\bar{a}_j$ . The resulting data matrix is called centred data matrix  $\tilde{A}$ .

$$\tilde{A} = \sum_{i=1}^7 \sum_{j=1}^{12} (a_{ij} - \bar{a}_j) \quad (3.3)$$

Starting from this centred data set, the best linear approximation is determined. The best approximation, on the one side, is achieved when the sum of the euclidean distance between the single data points and an assumed straight line becomes minimal. On the other hand, the variance of the data, which is a measure for the content of information of the original data, has to become maximal. If the variance is maximal, we do not lose information by separating the characters. To visualise this part, please have a look at Figure 3.6.

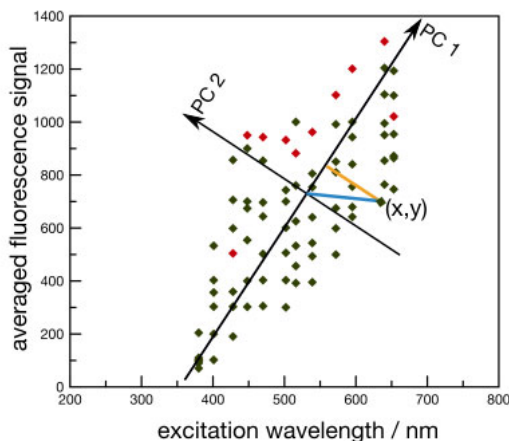


**Figure 3.6:** Principle of PCA – Original data set were the data points of one species, which should be separated are marked in red. Blue marked is the distance between the data centre and a single data point, whereas the euclidean distance which is the distance between an assumed straight line ( $PC_1$ ) and the data point, is marked in orange. The best approximation is achieved, when the euclidean distance is minimal.

In accordance to the Pythagorean theorem, shown in equation 3.4, the squared distance between the data centre and a data point  $d^2$  is equal to the sum of the squares of the euclidean distance  $x^2$  and the variance of the data in one direction  $y^2$ .

$$d^2 = x^2 + y^2 \quad (3.4)$$

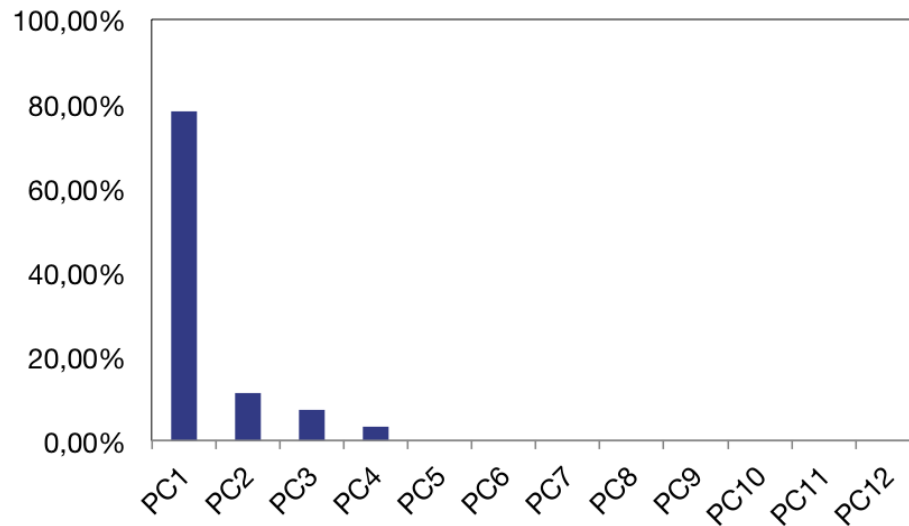


**Figure 3.7.:** Histogram showing the proportion of the total data variance for different principal components as an example. The number of components used for the data analysis depends on the desired content of information of the original data.

Since we are looking for the best linear approximation, the sum of the euclidean distance between the assumed line and a data point  $x^2$  has to become minimal. Following the equation 3.4, the variance of data in one direction  $y^2$ , therefore, becomes maximal. The distance between data centre and data point  $d$  remains constant. By solving this problem, we obtain the straight lines, we are looking for, which are then called principal components **PC**. The number of principal components is equal to the number of features in the original data set – in our case the number of LEDs used for analysis. Besides, the first principal component (**PC1**) has the major proportion of the total data variance and the second principal component (**PC2**), which is orthogonally to the first, has the second largest proportion and so on. Figure 3.7 illustrates the proportions of the total data variance for different principal components exemplarily. We do not have to use all principal components in our data analysis. The effective number of those used for the analysis should be minimal but sufficient so that we obtain a good separation of the important algae and bacteria cultures.

Practically seen, the principal components are obtained from the covariance matrix, shown in equation 3.5, whereby the covariance  $Cov(X,Y)$  is a measure for the "common" variance between two variables  $X$  and  $Y$ . [38]

$$Cov(X, Y) := E[(X - E(X)) \cdot (Y - E(Y))] = \frac{1}{n} \sum_{i=1}^n (x_i - \bar{x}) \cdot (y_i - \bar{y}) \quad (3.5)$$

The covariance is a matrix containing all paired covariances of each components  $Cov(X_i, X_j)$ . Thus, for the given 7 x 12 data set (compare matrix shown under 3.1), we obtain a square and symmetric covariance matrix:

$$Cov(X_i, X_j) = \begin{pmatrix} Cov(X_1, X_1) & \cdots & Cov(X_1, X_{12}) \\ : & \ddots & : \\ Cov(X_{12}, X_1) & \cdots & Cov(X_{12}, X_{12}) \end{pmatrix} \quad (3.6)$$

mit  $Cov(X_i, X_j) = Cov(X_j, X_i)$  und  $Cov(X_i, X_i) = Var(X_i)$

The principal components correspond to the **eigenvalues of this covariance matrix (3.6)**. As a result, the corresponding eigenvalue problem that is generally described in equation 3.7, has to be solved to determine the principal components *PCs*.

$$A \cdot \vec{x} = \lambda \cdot \vec{x} \leftrightarrow (A - \lambda \cdot E) \cdot \vec{x} = 0 \quad (3.7)$$

Here,  $A$  is a 12 x 12 matrix corresponding to the symmetric covariance matrix, shown under 3.6. The eigenvalue  $\vec{x}$ , which corresponds to the principal component  $PC_i$ , is a 12-dimensional column vector and generates an eigenspace. The eigenvalue  $\lambda$  to a given eigenvector  $\vec{x}$  ( $\lambda \neq 0$ ), by contrast, is a real or complex number and corresponds to the proportion of the total data variance which is explained by the principal component.

After solving the eigenvalue problem and determining the eigenvalues and -vectors, the eigenvectors  $\vec{x}$  might be combined to form a matrix as it is shown under 3.8.

$$\begin{array}{c} LED1 \\ LED2 \\ : \\ LED12 \end{array} \begin{pmatrix} PC1 & PC2 & \cdots & PC12 \\ x_{11} & x_{12} & \cdots & x_{112} \\ x_{21} & x_{22} & \cdots & x_{212} \\ : & : & \ddots & : \\ x_{121} & x_{122} & \cdots & x_{1212} \end{pmatrix} \quad (3.8)$$

The principal component  $PC_i$  in the matrix above is a linear combination of the entries of a particular eigenvector  $\vec{x}_i$ . If we use the values of the centred data matrix  $\tilde{a}_{ij}$  in the linear combination of individual components  $PC_i$ , we obtain the so-called *scores* (3.9). These scores are the new coordinates of the data points after a succeeded transformation of coordinates to the space of the principal components.

$$Score_{ki} = PC_i(\text{algae}_k) = \tilde{a}_{k1} \cdot x_{i1} + \tilde{a}_{k2} \cdot x_{i2} + \cdots + \tilde{a}_{k12} \cdot x_{i12} \quad (3.9)$$

Based on these scores, we can verify if and how well the different algae cultures were separated from each other. We can also examine if some algae species cluster due to their similar pigment pattern, which we then cannot separate and differentiate. Figure 3.8 visualises the process of the principal component analysis.

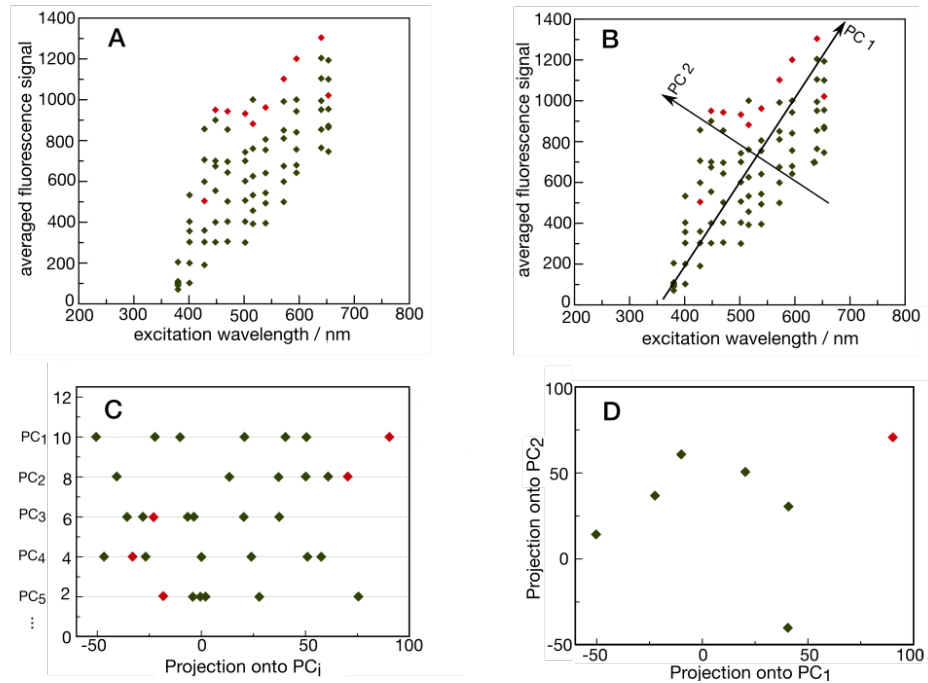


**Figure 3.8.:** A: Original data set where the red marked data point represent the sample that should be separated. B: Principle of the PCA and data after coordinate transformation and projection onto a specific principal component (C). D: Score plot with two PCs to visualise the resulting separation of the original data set.

### Resume and comments

The principal component analysis is a powerful statistical method for reducing large data sets and for separating of data by means of a linear coordinates transformation.

With regard to our miniaturised algae detection device, we have 12 different LED light sources, which might excite the algae cultures in the range between 380 nm and 653 nm. Since we have only 8 channels in our device, we have to reduce the number of LEDs (ideally reduced to 4 or 6 LEDs) and choose the best LED combination so that we are able to distinguish between the harmful cyanobacteria and harmless algae cultures.

It must be noted, however, that we should not use the raw data recorded with our device as they reflect the absolute fluorescence intensity of the analysed algae cells. These data are not standardised and since the intensity is strongly influenced by the cell density of the algae, the

data are weighted. Then, we are not able to analyse the relative pigment pattern of different algae cultures. Therefore, we have to prepare the data first and standardise them.

For this master's thesis, an analysis algorithm was developed using the *Matlab* program based on the principal component analysis after standardising the raw data first. The algorithm was adjusted to the given situation of the device and is used for the selection of the best-suited LED combination by reducing the dimension of the variables.



---

## 4. Optical detection module for algae species

In this chapter, the three prototypes designed and realised by G. Mistlberger and C. Holly to proof the concept and to gain information about the basic idea of a miniaturised and multi-wavelength device are presented (unpublished work).

Starting with a commercially available and slightly adapted phase fluorometer from Pyro-Science, they designed first a new software which enables a faster sampling rate. This second prototype was able to detect cell events passing through the measurement volume, although the time resolution had to be accelerated since an adequate distinction of cell events and electronic noise was hardly possible. The third prototype was then the first attempt of building a multi-wavelength device. Although it was not a miniaturised device, we were able to study potentially cross-interference effects by using more than one LED for excitation.

In the last step, based on the previous experiences, we designed a miniaturised optical detection module containing 8 different excitation light sources. In the last subsection 4.4, this device and its specifications are described. The characterisation of what could be measured using this optical detection module is described by contrast, in the next chapter 5 – *Results and Discussion*.

### 4.1. 1<sup>st</sup> generation prototype – Adapted optical oxygen meter

Since the miniaturisation of an existing device is a complicate step where new challenges like cross-interferences may occur, we decided to proof a reasonable concept first on a larger scale. Then, in the next steps after optimising the concept, the dimensions of the detection module should be reduced to obtain a miniaturised device.

Following this idea, a commercially available phase fluorometer with an optics block from PyroScience GmbH was used and slightly modified. As it is shown in the Figure below 4.1, one LED combined with an excitation filter was placed in the measurement channel, whereas the other side of this optics block – the reference channel – was blocked optically. Below this block on the emission side, an emission filter was placed in front of the photodiode used as detector. The installed LED was exchanged with a coupler to allow the application of different LEDs. Apart from that, the electronics were not changed so that the commercial software for data acquisition on this module could be used.

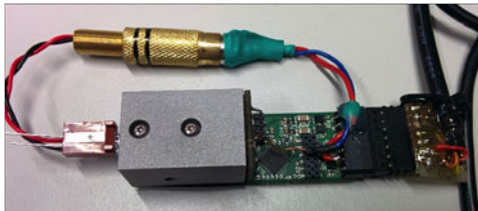


**Figure 4.1:** 1<sup>st</sup> generation prototype. Adapted optical oxygen meter from PyroScience with one exchangeable LED.

Using this device the first data were recorded. Measuring with a sampling rate of 20 Hz, we obtained a good signal to noise ratio as it is shown in Figure 4.2. Moreover, this device was able to capture signals down to a concentration of approximately 2 cells in 10  $\mu$ L. However, this prototype had two disadvantages. First, the sampling rate of this device is limited to 20 Hz due to the time-consuming phase modulation techniques. As

the final detection module should be capable of counting particular cell events, the sampling rate should be accelerated. Furthermore, the final version of the device should be a miniaturised module featuring eight different excitation channels. Using four other modules of this adapted oxygen meter, the geometric dimensions of the device might be around 67 x 100 mm, which does not correspond to the desired miniaturisation of the detection module.

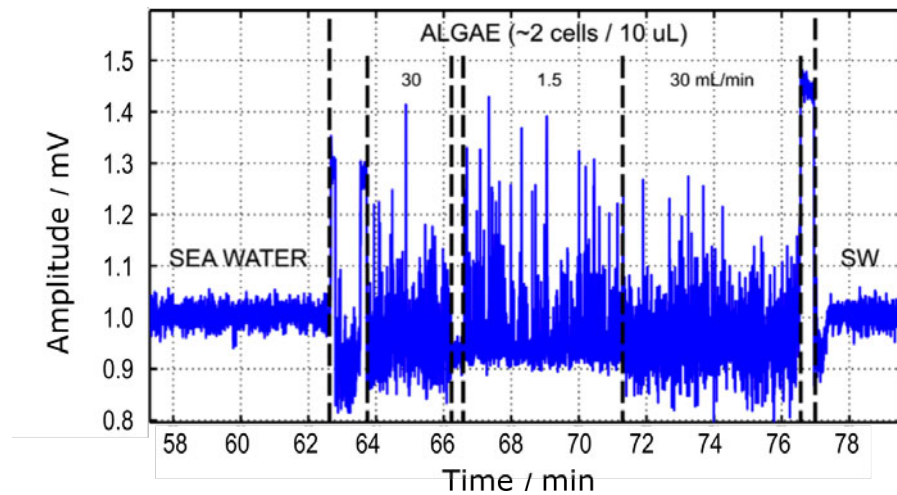


**Figure 4.2.:** The time drive shows that by using the modified fluorometer a signal change could be recorded down to a concentration of approximately 2 cells in 10  $\mu\text{l}$  – the measurement volume of the flow channel.

## 4.2. 2<sup>nd</sup> generation prototype – Small detection module

Due to the drawbacks mentioned above, a new device which is more adjusted to the actual purpose of the device was designed. The next prototype, shown in Figure 4.3, exhibits one excitation and emission channel using the same optic block as before in the modified device. To accelerate the sampling rate, a new software was designed. As a result, the new electronics enable a simple constant illumination and also a high speed data acquisition. The second prototype was then able to measure with a sampling rate of 760 Hz. Furthermore, also the footprint of the whole device was reduced. The analogue-digital-converter, however, was not yet able to achieve the same resolution as the one of the first prototype.

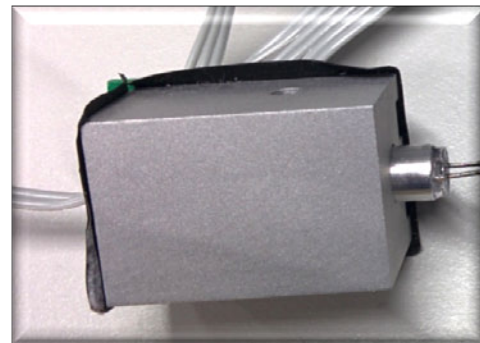


**Figure 4.3.:** 2<sup>nd</sup> generation prototype with electronics which enables high speed sampling and a smaller footprint.

Figure 4.5, showing a successive zoom level of the measured time drive, illustrates the high sampling rate which enables the differentiation of single cell events from the random noise signal.

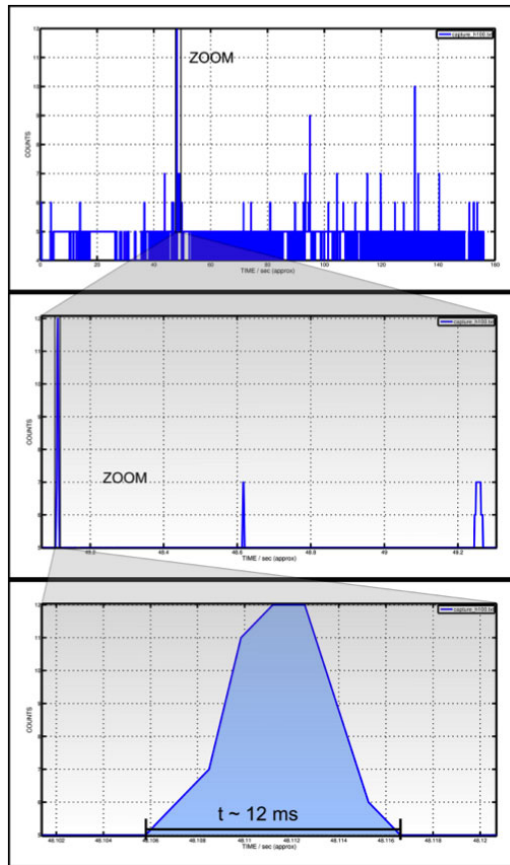


**Figure 4.4:** The intensity vs. time data recorded with the 2<sup>nd</sup> generation prototype show that the sharp spikes shown in the first plot is in fact not an electronic spike but a real particles luminescing while passing the measurement volume. Consequently a higher time resolution is needed to identify these signal peaks as sample peaks rather than random electronic noise. The duration of one peak corresponds to the residence time of a particle in the measurement chamber calculated from the diameter of the capillary and the pump speed.

### 4.3. 3<sup>rd</sup> generation prototype – Multichannel measurement device

Among enabling a high-speed sampling, the final detection module should also feature more than one excitation channel. Therefore, the third generation prototype – the first multichannel device shown in Figure 4.5 – was designed containing four excitation and two emission channels. To achieve this, the optics block was slightly changed and a second excitation source is inserted in the device. A fast sequential measurement of the LEDs was adjusted in order to prevent potential cross-interference of the four different LEDs. Furthermore, it was checked that only one LED is on at a certain time. Moreover, the readout process and the electronics were optimised to enable a data acquisition of 460 Hz per LED, meaning approximately 1840 values

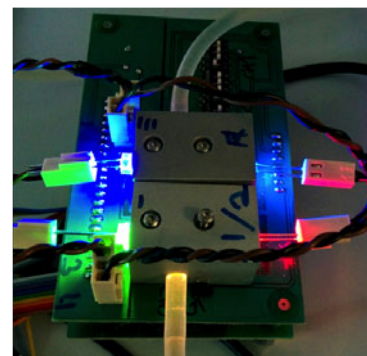


**Figure 4.5.:** 3<sup>rd</sup> generation prototype. 4 LEDs can be used together with a sampling frequency of 460 Hz per channel.

per second at a resolution of 22 bit. The results of this device were promising collecting the first time data with sufficient reproducibility. Finally, this device was the first prototype that was used for the primarily evaluation of real samples in order to develop an algorithm required to distinguish the algae cultures.

An example of the data plot that obtained from the multichannel measurement device is shown in Figure 4.6. Due to the different spectral behaviour of the emission filters, the intensity of the signal for each channel differs significantly.

Based on the results of this device first decisions on what LED/filter combination shall be used for further investigations were made. On the other hand, there are some challenges that have to be met. Instead of the desired 8 channels, this device features only 4 channels and the system is still too big. While miniaturising the system, we have to be careful to prevent optical crosstalk or a higher background signal. Furthermore, the designed module is not yet ready to be integrated in the host system since the storage of raw data and the development of simple data processing on the chip is not finished.

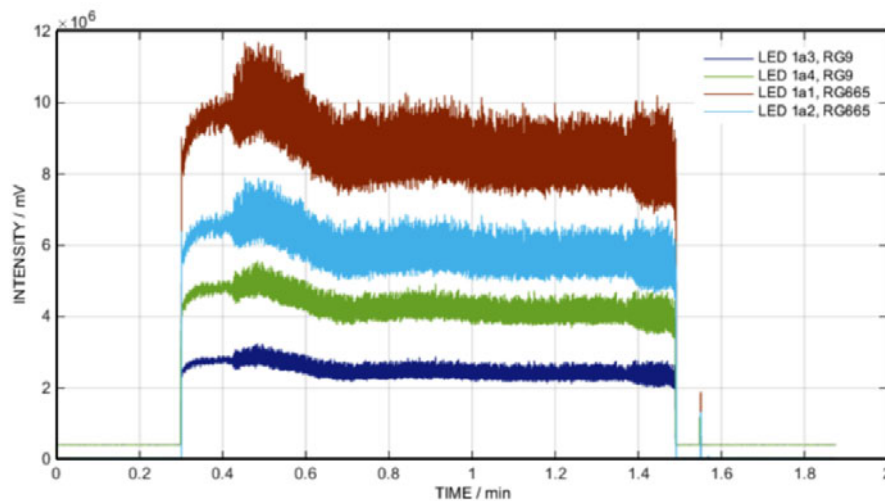


**Figure 4.6.:** Example of the time data recorded with the 3<sup>rd</sup> generation prototype. The differences in the signal intensity result from the different spectral behaviour of the emission filter and also from the different excitation potential of the chosen LED.

#### 4.4. Miniaturised optical detection module for algae species

Based on the previous experiences of the three prototypes, the first miniaturised optical detection module for algae species was designed. This device features eight excitation channels as it was desired and four different emission channels. For the realisation of this device, several challenges had to be considered. First, the design of a miniaturised optical block had to be constructed in such a way that the performance is not lost due to optical crosstalk or background signal. The final miniaturised optics block has a geometrical dimension of  $28 \times 34.8 \times 15.8 \text{ mm}^3$ . A rendered picture of the device is shown in Figure 4.7. The optical block by itself is either made out of aluminium or of polyoxymethylene (POM-C), a thermoplastic containing a quartz capillary with an inner diameter of 1.94 mm. The POM-C device is cheaper, but since not yet all tests have been done, a conclusive decision, whether it is an adequate alternative for the aluminium device, can not be made. The active side of the photodiode is 2 mm and the resulting measurement volume of one channel is therefore  $5.91 \mu\text{L}$ . The whole system is connected to a peristaltic pump using an averaged flow rate of  $10 \text{ mL min}^{-1}$ .

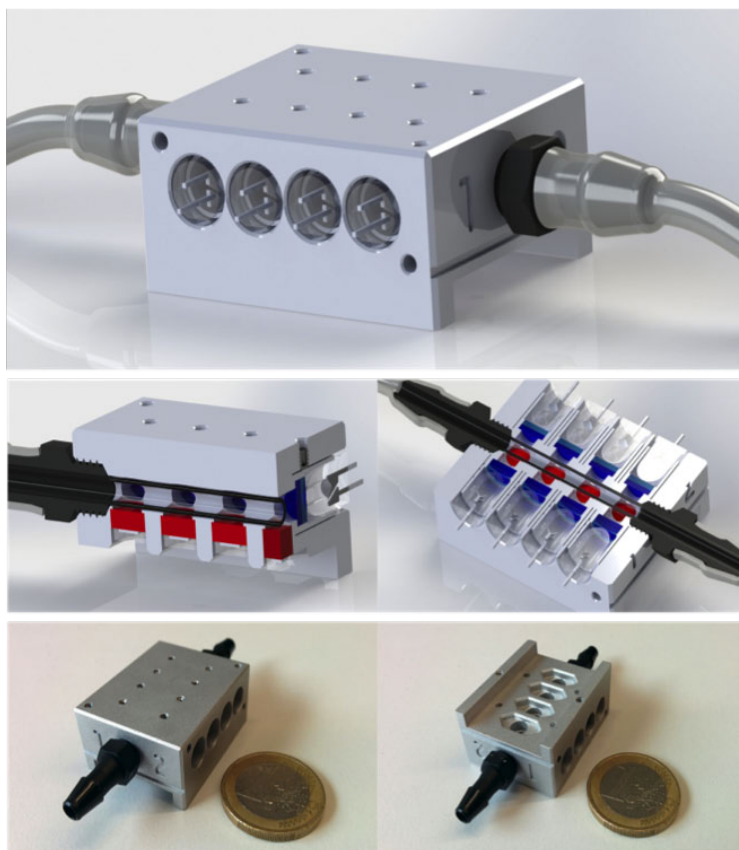


**Figure 4.7:** Rendered picture of our low-cost prototype featuring 8 channels in an optics block with minimized dimensions. The upper three figures show rendered representations of the assembled device without the electronics. The lower 2 figures show photographs of the machined optics block with standard barbed fluidic connectors.

The excitation of the algae cells passing through the capillary is done by exchangeable LED light sources, which are described below. The maximal sampling frequency used in this device is 380 Hz but normally the sampling rate is set to 125 Hz. The emitted fluorescence signal

is recorded on four different silicon pin photodiode (BPW34) used as detectors which are sensitive to visible and near infrared radiation. Hence, each photodetector has to read out the emitted fluorescence intensity of two excitation channels. The raw and processed data might be stored on a SD card. A general description of the device specifications is given in Table 4.1. For more information about the optics and electronics, please see the following pages.

For application in the laboratory, the data were transferred via an USB-Port to the measurement laptop. The data evaluation may then be done by the principal component analysis. For the application in the host system, by contrast, a simpler and autonomous working mathematical algorithm has to be developed in further investigations.

**Table 4.1.:** *Specification of the miniaturised multi-wavelength detection module for algae species*

Specification	
<b>Mechanical and Dimensions</b>	
Material	polyoxymethylene (POM-C) or aluminium
Size	28 x 34.8 x 15.8 mm <sup>3</sup>
Capillary	quartz, ID = 1.94 mm, OD = 3 mm
Measurement volume	5.91 µL
<b>Further components</b>	
Excitation light source	LEDs 380 - 653 nm
Detector	silicon pin photodiode (BPW34, Vishay) sensitive detection area 2 mm
<b>Performance</b>	
Sampling rate	< 380 Hz
Resolution	15 bit
Flow rate	10 mL min <sup>-1</sup>
<b>Electrical</b>	
Energy consumption	5 V @ 180 mA measurement mode 12 mA standby mode
Data storage	SD card
Communication protocol	RS-485

Since the detection module shows a sensitivity to the ambient light and to other electromagnetic interferences, we placed the whole system in a dark metal box and shielded the plastic tubes which were used for the connection to the peristaltic pump. By using this metal box and the shielded tubes, we reduced the influence of the ambient light, but we prevented also electromagnetic interferences from the peristaltic pump. Furthermore, the material of the box enables a grounding of the detection module.

#### 4.4.1. Optics part

Since the excitation of the algae cells should be done by different and, in particular, only low-cost light sources, we decided to use exchangeable LEDs as light sources. They are constructed with narrow emission angles, which do not require additional lenses for focusing the light onto the sample stream. In the first step, we decided to use 12 different LEDs in the range between 380 - 653 nm to excite the most important algal pigments in the light-harvesting complex (= *diagnostic pigments*). The LEDs were combined with optical glass and interference filters. The spectra in Figure 4.8 show the good cover throughout the visible range with more LEDs in the violet-blue range, where most pigments absorb.

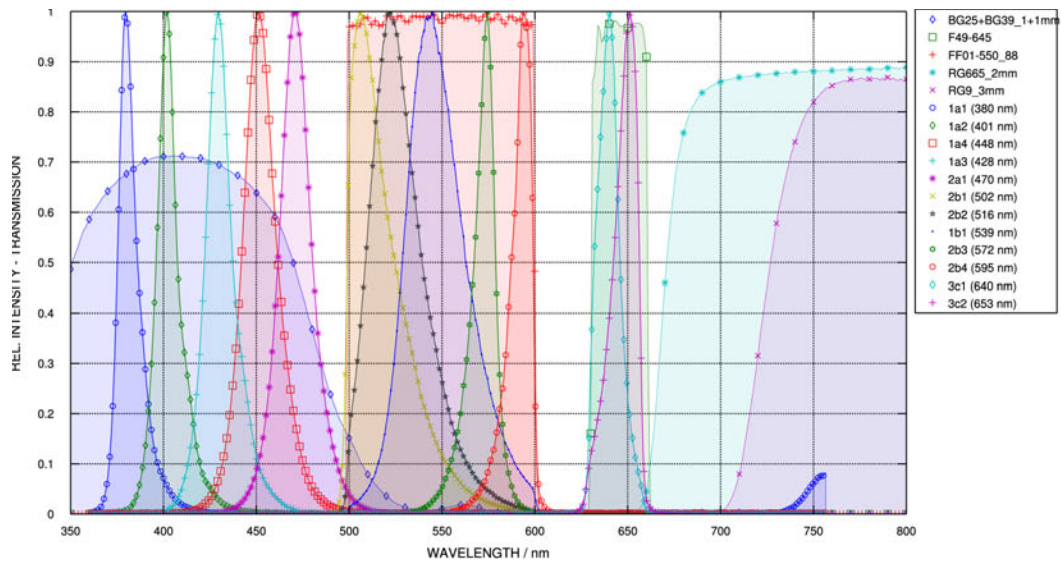


**Figure 4.8.:** Emission/Transmission spectra of the LED and filters, used for the algae detection module.

We characterised our LEDs, since a small deviation from the given set point might have an influence on the effective excitation of the different algae species. Moreover, we were interested in the half width of each LED as they do not emit monochromatic light. In Table 4.2 the peak wavelength of all LEDs used in the system and their half width are listed.

Furthermore, we constructed a housing for the LEDs, where we can combine the light sources with the optical glass and interference filters. The resulting LED module, illustrated in Figure 4.9, makes the whole detection module more flexible.

Additionally, to enhance the sensitivity, the photodiodes are covered with a longpass filter, either RG665 or RG9. The first emission filter, RG665, opens at 665 nm and let the signal pass through, whereas the second filter has a transmission of 50% at 720 nm. Therefore, the RG9 longpass filter only transmits the second chlorophyll fluorescence peak (720-740 nm, [40]). Since these filters have a different sensitivity and a different transmission behaviour (compare Figure 4.8), they are not suitable for all LEDs and thus, the optimal combination of excitation and emission has to be defined.

**Table 4.2.:** Spectral characterisation of the implemented LED light sources. [39]

LED	Peak wavelength $\lambda_p$ [nm]	Half width $\Delta\lambda$ [nm]	Viewing half angle $\Theta_{1/2}$ [°]	Forward current $I_F$ [mA]	Radiated power $I_R$ [mW]
1a1	380	10	$\pm 4$	20	2.5
1a2	401	15	$\pm 4$	20	15
1a3	429	20	$\pm 5$	20	22
1a4	452	25	$\pm 4$	20	20
2a1	470	20	$\pm 7.5$	50	370
2b1	506	30	$\pm 4$	20	41
2b2	522	30	$\pm 4$	20	42
1b1	545	30	$\pm 3$	20	5
2b3	575	25	$\pm 4$	20	17
2b4	594	10	$\pm 7.5$	70	641
3c1	640	20	$\pm 4$	20	51
3c2	651	25	$\pm 4$	20	13

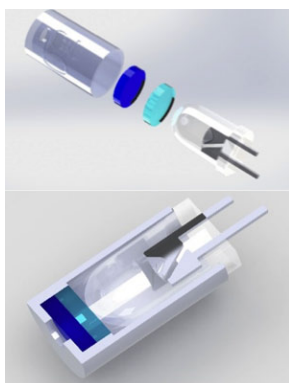


**Figure 4.9:** LED module showing the composition above and a cross section through the module below. This housing for the LEDs allows an easy replacement of the light source on demand.

#### 4.4.2. Electronic part

As mentioned above, the emitted fluorescence signal is recorded on a silicon pin photodiode as detector. For each of the four emission channels the photodiode is placed on the bottom side and covered with a longpass filter.

For the electronics we use a professionally manufactured printed circuit board (PCB) for the installation of the LEDs, photodiodes and amplifiers. The readout of the measured data is done by the 15 bit analog-digital-converter (ADC) from MAZeT. The storage of raw data will be on an SD card while a PIC32-PINGUINO-MICRO board with 80 MHz and a 32 bit microcontroller is used for instrument control. The adjustment of the LED intensity and amplification is regulated analogously. Besides, in a further step, the microprocessor will also be used for data transfer via an USB-Port. Furthermore, we used surface-mounted-device components (*smd components*) to enable a fully miniaturised design.



---

## 5. Results and Discussion

### 5.1. General overview of the recorded time drive

In this section, a general overview is given about what we measure when an algal or bacterial sample is pumped through the system and what can be extracted from the time drive recorded on the detection module. Moreover, a short section will focus on the differences in the measurement signal, when the capillary is filled with water or with air. In the last part, the two different materials that were used for the optics block are presented and shortly described.

#### 5.1.1. Conversion of the voltage signal into light intensity

During a measurement cycle we are recording the fluorescence signal of an algal or bacterial sample over time when cells, passing through the device, are excited. The fluorescence signal is detected with the silicon pin photodiodes and therefore the resulting measurement values are given in volts. The measured voltage in  $V$ , however, can be converted into light intensity with the unit Watt ( $W$ ) as follows:

$$1 \text{ V} \cdot \frac{1}{20 \text{ M}\Omega \cdot 0.5 \text{ A W}^{-1}} = 100 \text{ nW} \quad (5.1)$$

The measurement values outputted by the device as voltage can be converted back into the current if we take the internal resistor of the amplifier ( $R = 20 \text{ M}\Omega$ ) into account. Moreover, the spectral sensitivity of the photodiodes with approximately  $0.5 \text{ W A}^{-1}$  at  $700 \text{ nm}$  should also be considered. [41] When we consider both factors, we may count the outputted voltage back into the light intensity generated from the excited biomass.

For the following measurements and time drives, the measured voltage is converted into light intensity by using the equation above (Eq. 5.1).

#### 5.1.2. Time drive and influences of the signal level

The average signal level recorded at a particular channel depends on the excitation efficiency of the cells passing through the system. Apart from that, the more cells are in the measurement channel, the higher is the biomass in the optical path and, as a consequent, the more rises the average signal level. In addition to the rising signal intensity, the overall signal of the sample

gets compressed as it is demonstrated in Figure 5.1. Otherwise, if we reduce the average cell density, the fluorescence signal is disbanded and we are able to identify single spikes resulting from particular cells passing through the excitation channel.

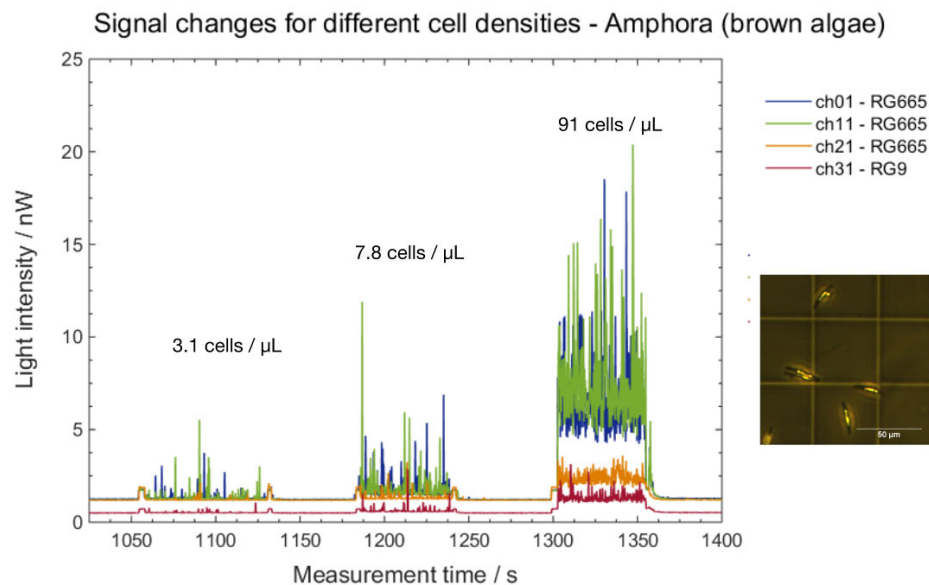


**Figure 5.1.:** Time drive of amphora samples with different cell densities: The average signal level depends on the average biomass within the optical path. The higher the biomass, the higher and more compressed are the fluorescence signals emitted from the algal sample.

Furthermore, having a closer look on the time drive at a certain cell density (compare Figure 5.1, right), we see a few signals with much higher signal intensity than the average level. These spikes originate from cell agglomerates that have been formed during the cultivation process in the Erlenmeyer flasks, as we do not shake the algae cultures on a rotary shaker.

It should further be noted that the average signal level of the two last channels (ch3\_1 and ch3\_2) is lower than for the other channels since the last photodiode is covered with the RG9 longpass emission filter instead of the RG665 emission filter as it is done for the other channels. The RG665 filter starts to transmit at 665 nm and therefore is able to detect the maximal chlorophyll fluorescence at 680 nm. The RG9 filter, by contrast, starts to transmit at higher wavelength than the RG665 and only detects the second emission band of chlorophyll, which is far less intense.

Moreover, the signal intensity measured on each channel derives also from the efficiency of excitation. The better the algal cell is excited the higher is the fluorescence emission of the cell.

### 5.1.3. Different signal levels for water and air

During the measurements, differences in the average signal level of water and air were observed. When the whole capillary was filled with air instead of water or if a few air bubbles entered the system, we recorded an average signal level twice higher than for water.

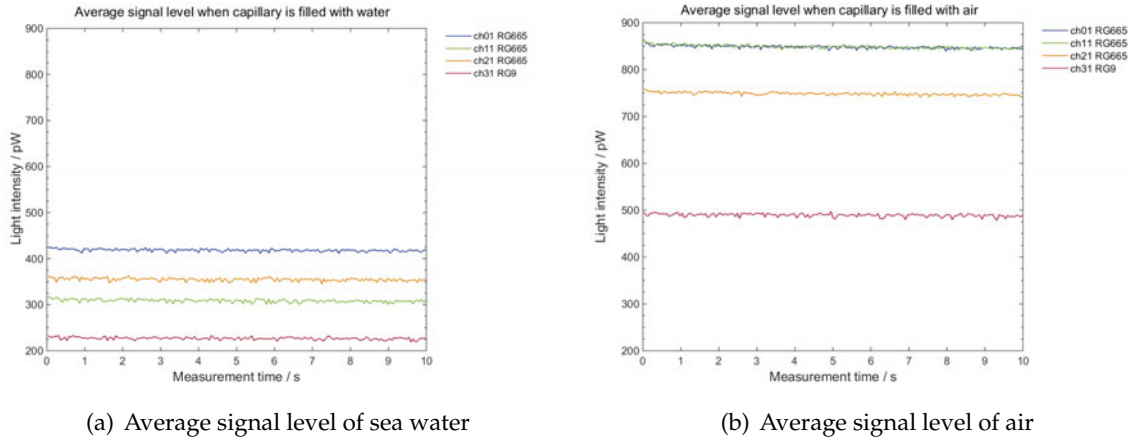


**Figure 5.2.:** Comparison between the different signal levels for seawater (left) and air (right). The signal level for air is twice higher than for water due to the better refraction conditions within the capillary.

This increase in the signal level for the air measurement compared to the water results from the differences in the refractive index of the media. The refractive index of the air is  $\eta(\text{air}) = 1$ , whereas water has a higher refractive index of  $\eta(\text{water}) = 1.33$ . This higher refractive index of water results in a deflection of the excitation light, when it enters the water in the capillary and leaves the air of the excitation channel. Furthermore, due to the refraction on the capillary, the optical path of the excitation light changes within the capillary. These differences in the refraction conditions between air and water lead then to a different signal level that is recorded in the photodiode.

For this purpose, air bubbles that might be formed during the measurements on connections between two PVC tubes should be avoided since they might lead to a different blank signal or might even be recognised as signal-peaks. Furthermore, in order to prevent an air bubble is retained in the capillary, the whole detection module is placed upright. Air bubbles, however, might not be an issue for our project as the buoy is always in water. When we place the detection module upright in the buoy, we should not have a problem with air bubbles in our system.

#### 5.1.4. Aluminium or POM-C as device material

In the first attempt, we decided to build the detection module out of aluminium, since the aluminium might be helpful for the improvement of low signals. The degree of reflectance for aluminium is for the entire visible spectrum very high. That means, aluminium reflects the incoming light from the LEDs in the light path in this way that the efficiency of the algal or bacterial excitation is accelerated. Furthermore, the emission intensity that is recorded on the photodiodes might also be enhanced. As a consequence, these multiple reflectance of the light might be helpful to detect particular cells, especially even when the signal of these single cells is low.

On the other hand, aluminium as housing material is expensive and since the device should be as cheap as possible, we considered to build the device out of polyoxymethylene (POM-C). If the detection module made out of POM-C is sensitive enough, this copolymer might be a good alternative to aluminium, since it is much cheaper than the metal. However, we have to shield the copolymer, which was not necessary for the previous device and prevent electromagnetic irradiations. The first tests, however, were promising that we do not need the multiple reflections of the aluminium and might obtain similar results as for the previous device version. Nevertheless a final verification if the performance of the POM-C device is similar to the aluminium block has to be done in further investigations.

## 5.2. Challenges to be solved

After defining the general characteristics of the device, we had also some challenges to solve, which are described in the next subsection. The first deals with the influence of ambient light on our POM-C device and how we solved this problem. The second subsection, by contrast, is about the significant influences of electromagnetic interferences.

### 5.2.1. Ambient light and optical density

First, we noticed a significant influence of the ambient light on our measurement signal. When measuring distilled water in the laboratory at dimmed ambient light and repeating the same measurement when the ambient light was switched on, we recognised a doubling of the signal. We decided then to store the device during the measurements in a metal box (compare Figure 5.3) and improve therefore the optical density of our detection module. In addition to the improved optical density, the device could also be grounded on the metal box and divert electro-magnetic currents into the ground.



**Figure 5.3.:** Device made out of POM-C installed on a cardboard to store it in the metal box during the measurements. Besides, the device is grounded on the metal box.

In the next step, after reducing the influence of the ambient light, we recognised a LED back radiation in the metal box with is recorded on the diodes as artefact. The backside of the housing built for exchangeable LED modules as it is shown in Figure 4.9, is not closed and when the LED is on, they also emit light on the backside. This light, emitted on the backside, is then detected on the PIN photodiode, as these diodes do not fit tightly on the printed circuit board (PCB). Therefore, we constructed a support for the LEDs, that is optically dense on the backside and shielded the diodes against optical interferences by the means of a bicycle tube. A small layer of the tube was installed around the photodiodes to prevent the unintentional irradiation caused from the LED back radiation. The bicycle tube, however, contains graphite for blackening and when the samples were measured, the current flows on our circuit board support the layer formation of the graphite. As a result, the bicycle tube becomes a parallel resistor to the diodes and the measurement results becomes incomprehensibly.

ing and when the samples were measured, the current flows on our circuit board support the layer formation of the graphite. As a result, the bicycle tube becomes a parallel resistor to the diodes and the measurement results becomes incomprehensibly.

To demonstrate the effect of the bicycle tubes, please have a look at the diagrams below (Figure 5.5). We carried out a linearity and sensitivity test on our device by using Sulforhodamine 101 in different concentrations. The standard solutions were enclosed in capillaries that might be replaced easily in the device. The solutions were excited at 460 nm and their emission was recorded on the photodiodes covered with the RG665 longpass filter. Therefore, only the emission of Sulforhodamine 101 at higher wavelengths than 665 nm was detected. For the spectral characterisation of the standard solution, compare Figure 5.4.

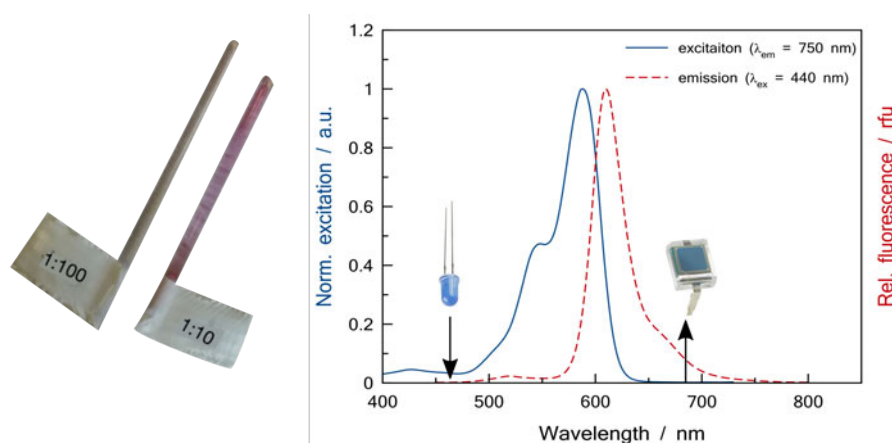
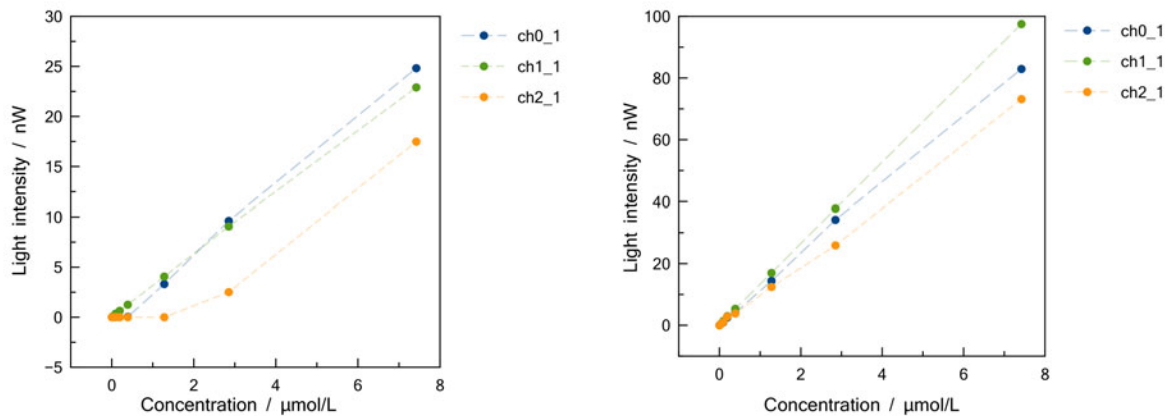


**Figure 5.4.:** *Left: Example of the standard solutions enclosed in capillaries for an easy replacement. Right: Spectral behaviour of Sulforhodamine 101. The excitation and emission wavelengths used for the linearity test are marked. The molar attenuation coefficient is  $139.000 \text{ L cm}^{-1} \text{ mol}^{-1}$ .*

We placed the standard solutions with different concentrations, one after the other, in the detection module and measured the emission signal of Sulforhodamine 101 on three different channels. As you may see in the left diagram of Figure 5.5, the channels did not behave linear and even the sensitivity of the channels were bad since we were not able to record a Sulforhodamine concentration of  $1.25 \mu\text{mol L}^{-1}$  on each of the three channels (compare the diagram on the left in Figure 5.6). Due to these results, we decided to remove the bicycle tube that surrounds the PIN photodiodes and to repeat the measurements. The overall results of the measurements are shown in Figure 5.5 in the right diagram. A zoomed in diagram that shows the lower concentrations is also given in Figure 5.6. Please be aware that the scales for the y-axis are different.

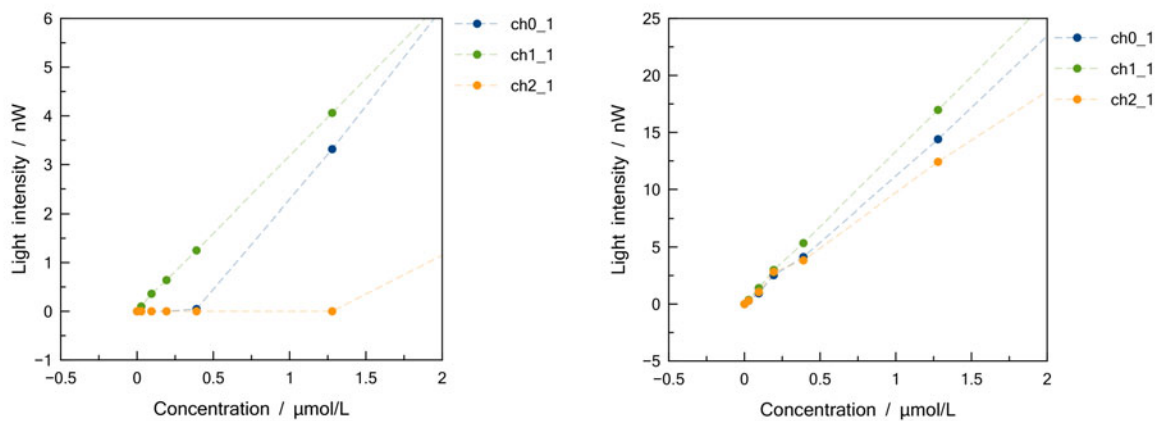
Since we obtain such promising results when we remove the bicycle tube, we decided to remove the tube completely from our detection module. The complete characterisation for the linear behaviour of each channel of the detection module is shown in the next section 5.3 under *Performance characterisation of the optical detection module*.



(a) Linearity test with a bicycle tube used for optical isolation.

(b) Linearity test after removing the optical isolator.

**Figure 5.5.:** Linearity test with Sulforhodamine 101. The coefficient of determination ( $R^2$ ) is lower when the bicycle tube is used as optical isolator in the system (left). When the isolator is removed, the linearity increase (right). The scaling of the y-axis is varying due to a better presentation of the linearity.



(a) Less sensitivity for all channels when the bicycle tube is used for optical isolation.

(b) The sensitivity is improved for all channels when the tube is removed.

**Figure 5.6.:** Linearity test with Sulforhodamine 101 showing the same results as above but with the focus on the lower concentrations. The bicycle tube leads to a loss of the sensitivity (left), whereas after removing the tube, all channels exhibit a good sensitivity (right). The scaling of the y-axis is varying due to a better presentation of the linearity.

### 5.2.2. Electromagnetic interferences

After sealing the detection module optically, we connected the POM-C device with the peristaltic pump by using PVC tubes and tried to repeat the previous measurements in air and water. For this, we filled the capillary with air and used four LEDs with an emission maximum at 460 nm. Although the device was linked to the peristaltic pump, we did not use the pump during the measurement – the flow rate was set to 0 mL min<sup>-1</sup>. The results were promising that the noise amplitude is small with an average deviation of the amplitude of 13 pW. The average signal of the three channels was between 680 - 1300 pW. The resulting time drive is shown in Figure 5.7.

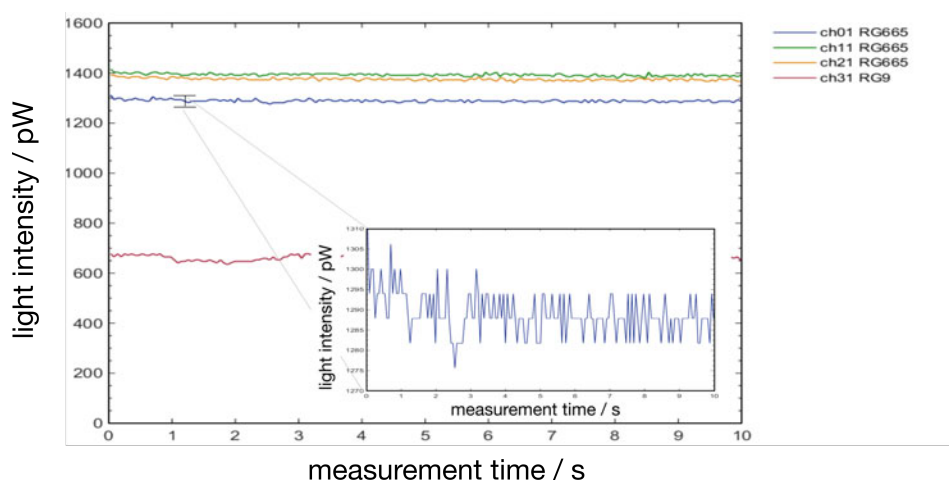


**Figure 5.7.:** Average noise level of four different channels when the capillary is filled with air. The device is connected with the peristaltic pump over PCV tubes. The average noise level is 700 - 1400 pW and the deviation of the noise amplitude is 13 pW.

In the next step, we filled the capillary with water and repeated the measurement under the same conditions. Instead of an average signal level that is half of the previous level and a smaller deviation of the amplitude as we expected, we obtained a homogeneous sinusoidal signal. In addition to that, the signal level was similar to the previous signal level when we measured with an air-filled capillary. Figure 5.8 exhibits the resulting sinusoidal signal that was recorded on three different channels. The average signal level was between 300 - 825 pW and the average deviation of the amplitude was 300 pW.

Furthermore, there was no difference, if the pump was on or not. The sinusoidal signal was recorded in both situations.

We decided therefore to shield the PVC tubes, which connect the device in the box with the peristaltic pump placed outside of the metal box. Since we assumed that the sinusoidal signal might be an effect of the electro-magnetic background radiation which couples over the water into the detection module, the noise signal must be more statistically after the shielding. Therefore, we coated the plastic tubes with steel as it is shown in Figure 5.9.

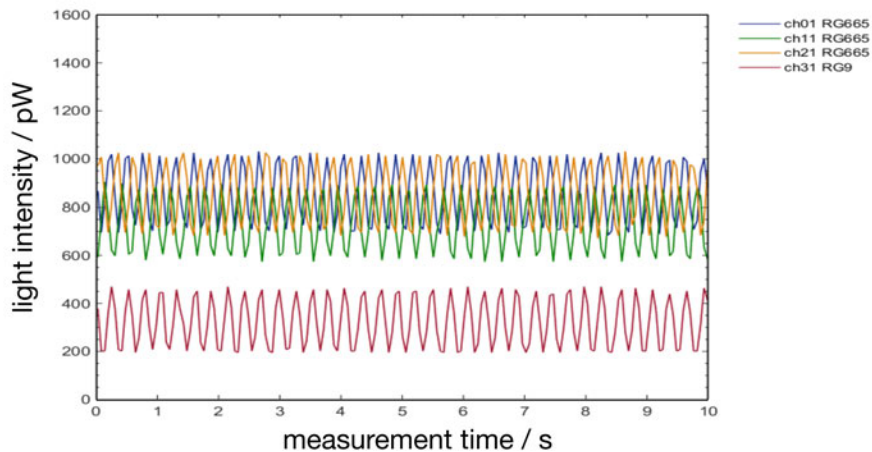


**Figure 5.8.:** Average noise level of four different channels, when the capillary is filled with water. The sinusoidal signal results from the surrounding electro-magnetic irradiation. The average background level is 300 - 825 pW and the deviation of the noise is 300 pW.



**Figure 5.9:** One end of a PVC tube that connects the peristaltic pump with the detection module; coated with steel to prevent electro-magnetic interferences.

The measurements were repeated with shielded tubes when the capillary was filled with water and connected to the pump. The average noise level was lower for both measurements and the signal of the water measurement was more statistical than before. The results for the water measurement are shown in Figure 5.10. The baseline is now between 225 and 420 pW, which means approximately a reduction of the baseline level by half. The average deviation of the noise amplitude is 5 pW. As a result, the limit of detection for the algal detection module (POM-C) can be calculated to 15 pW.

Figure 5.11 illustrates the results for the air-filled measurement. The average signal level was in this case between 490 - 850 pW and the average deviation of the noise amplitude was 8 pW. Compared to the previous measurement with the air-filled capillary, the average signal level is reduced by 1.6 and, moreover, the average deviation of the noise amplitude is also reduced.

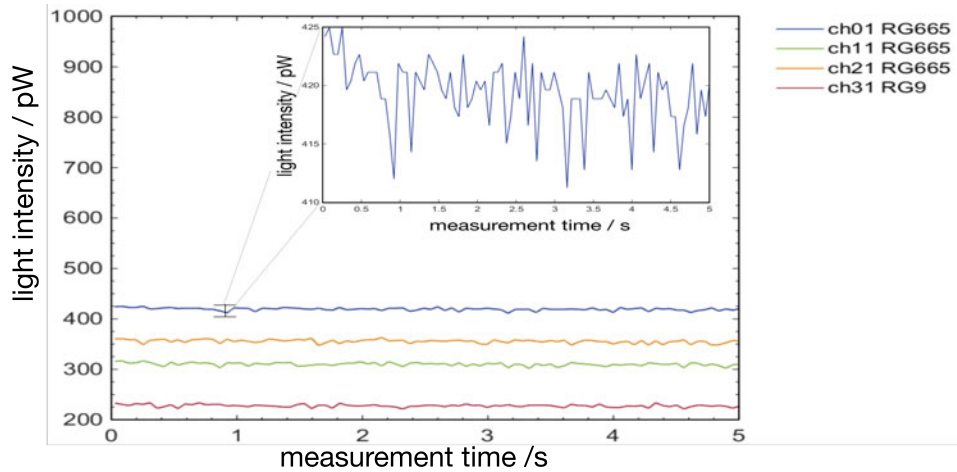


**Figure 5.10.:** Average noise level of four different channels, when the capillary is filled with water and the PVC tubes are shielded. The average noise level is more statistical than before and furthermore reduced by half compared to the previous measurement. The baseline is here 225 - 420 pW and the deviation of the noise is now 5 pW.

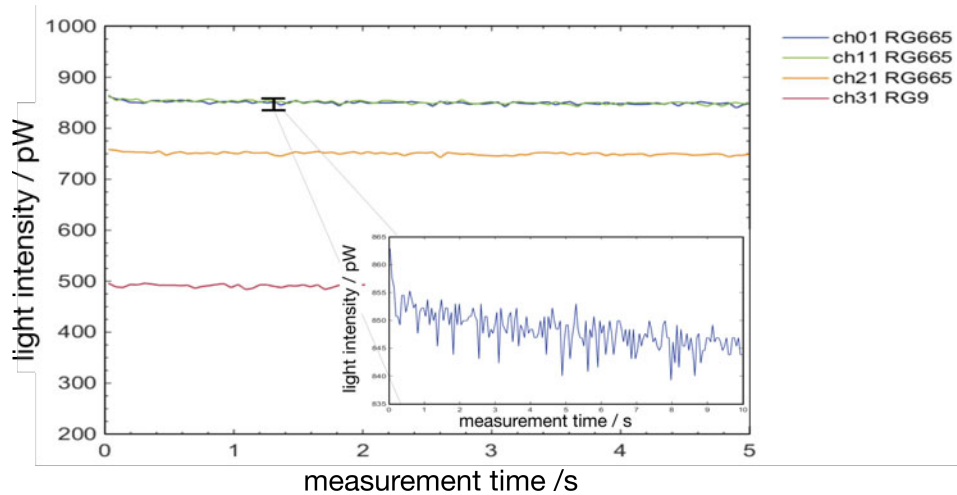


**Figure 5.11.:** Average noise level of four different channels, when the capillary is filled with air and the PVC tubes are shielded. The noise level and also the deviation of the noise amplitude is reduced by 1.6. Now the average background level is 490 - 850 pW and the noise is approximately 8 pW.

Summarising the above, it can be said that the detection module is highly sensitive to electromagnetic background radiation as it was shown in Figure 5.8 and therefore it has to be shielded. Even the tubing connections between the peristaltic pump and the metal box, where the detection module is stored, have to be shielded, since the electro-magnetic irradiation would couple over the water into the system and lead to a higher and sinusoidal noise level (compare Figure 5.8). The best would be to prevent the electro-magnetic background interferences as far as possible and work in a laboratory with fewer instruments and sockets. These interferences have also to be taken into account, when the detection module is placed into the buoy.

### 5.3. Performance characterisation of the optical detection module

In the final version, the detection module should be able to work autonomously as an early warning system and therefore detect algae phyla and especially identify harmful algae at an early stage. In order to achieve this goal, the device should be able to record algae and bacterial cells at the lowest possible density. At best, one particular cell in the measurement volume should be detectable with a sufficient signal-to-noise-ratio. Moreover, the linear behaviour of the device should be checked, since only a linear behaviour of the channels permits reliable statement about the cell density in a water sample.

It should be mentioned that the first tests, if the device is able to track cells and to capture particular cells passing through the system, were done with the aluminium device. The linearity and sensitivity tests, by contrast, were done with the POM-C device.

#### 5.3.1. Calculation of the residence time

In order to detect single cell events in one channel of the device, we have first to calculate the residence time of a particular cell in the measurement volume. Furthermore, the parameters, which influence the residence time, should also be identified.

The measurement volume corresponds to a cylinder whose volumetric capacity derives from the inner diameter of the capillary  $ID_{capillary}$  and the active area of the photodiode  $h$ . Taking these into account, the measurement volume of one channel can be calculated to 5.91  $\mu\text{L}$  (compare equation 5.2).

$$V_{measurement} = \left(\frac{1}{2} \cdot ID_{capillary}\right)^2 \cdot \pi \cdot h = \left(\frac{1}{2} \cdot 1.94 \text{ mm}\right)^2 \cdot \pi \cdot 2 \text{ mm} = 5.91 \mu\text{L} \quad (5.2)$$

Moreover, the cells can be recorded on the diodes as long as the cell resides in the illuminated volume. As a consequence, also the flow rate  $\vec{v}_{pump}$  affects the residence time of the cell.

$$\vec{v}_{pump} = \frac{\Delta V_{transported}}{\Delta t} \Leftrightarrow \Delta t = \frac{\Delta V_{measurement}}{\vec{v}_{pump}} \quad (5.3)$$

Since the flow rate describes which volume is transported in one minute, we can calculate the time that is needed to transport the measurement volume along the capillary. This time  $\Delta t$ , calculated in accordance to equation 5.3, corresponds then to the residence time of one cell in the measurement volume.

### 5.3.2. Capturing particular cell events

As a first step to characterise the performance of the detection module, we tried to adjust the device so that we were able to track cells, passing through the system. For this experiment we used the *Amphora* algae, a common bloom-forming diatom, with an average cell density of 3 cells / measurement volume (5.91  $\mu\text{L}$ ). For this experiment we used only four excitation channels along the capillary instead of eight. The sampling rate for these four LEDs was 125 Hz and the flow rate was set to 30  $\text{mL min}^{-1}$ . The resolution was 15 bit. The residence time of a particular cell, which can be calculated from the geometric dimensions of the capillary and the adjusted flow rate, was 12 ms. As it is shown in Figure 5.12, with this configurations, we were able to track cells which were pumped through the device, and record them on each channel. The signal intensity measured on each channel derives, as it was mentioned before, from the efficiency of excitation and depends also on the emission filter that was used to cover the photodiodes.

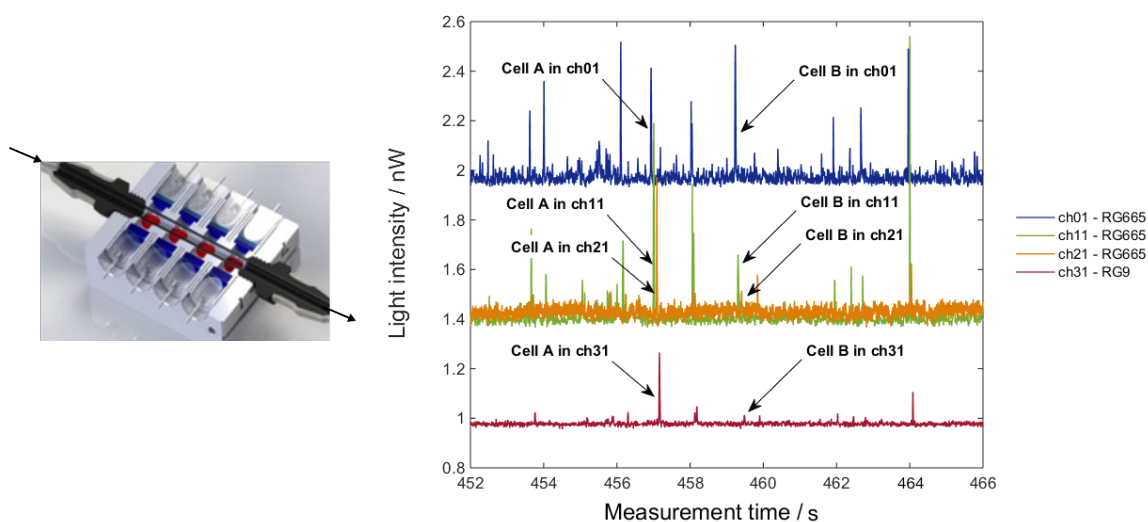


**Figure 5.12.:** Left: Rendered picture of the detection module to demonstrate the direction of the flow. Right: The high resolution of the aluminium device enables the capturing of cells passing through the system. The experiment was done with *Amphora* algae at a cell density of 3 cells / measurement volume (5.91  $\mu\text{L}$ ).

In a further step, we tried to record particular cell events with a sufficient signal-to-noise-ratio. Again, we used for this experiment the *Amphora* algae, which has an average cell length of 21.9  $\mu\text{m}$ . Thus, the size of these algal cells is in the middle range compared to other micro-algae and therefore these cells should be recorded on the detection module. Here, the average cell density of the algae sample was 2 cells / measurement volume (5.91  $\mu\text{L}$ ). We reduced the flow rate to 2.5  $\text{mL min}^{-1}$  and increased the sampling rate to 240 Hz, since we wanted to observe the entrance and passage of the cell with a resolution as good as possible. Furthermore, we used only one excitation channel for this experiment. For the excitation of the cell we used the

460 nm LED and the diode was covered with the RG665 emission filter. The residence time of a particular cell was calculated, in accordance to equation 5.3, to 141 ms. Figure 5.13 illustrates the passage of a particular cell through one channel. The entrance and even the whole passing through of the cell can be recorded clearly. The measured residence time of the cell agrees well with the calculated time.

As a result, it can be noted, that the detection module made out of aluminium should be able to count particular cell events, as it was preferred.

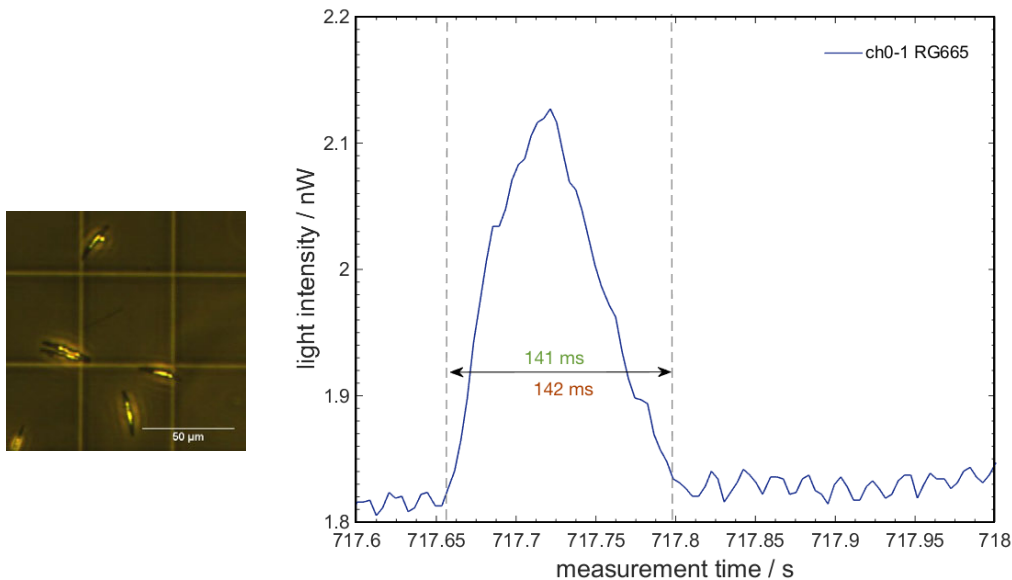


**Figure 5.13.:** The *measured* residence time of a particular algae cell matches well with the *calculated* time (right). Furthermore, the signal-to-noise-ratio can be calculated in this case to  $SNR \approx 10.3$ . The microscopic image on the left illustrates the average cell length of the *Amphora* cells.

Moreover, the signal-to-noise-ratio for the aluminium device can be calculated in this experiment. The average signal intensity of one particular cell was approximately 310 pW and the average amplitude of the noise was 30 pW. As a result, the signal-to-noise-ratio for the aluminium device is in this case  $SNR \approx 10.3$ .

### 5.3.3. Linearity and sensitivity

As mentioned in the previous section 5.2.1 we tested the linearity and sensitivity of the whole POM-C device after removing the bicycle tube from the printed circuit board (PCB). For the tests we used Sulforhodamine 101 in different concentrations between 0.03 - 19.7  $\mu\text{mol L}^{-1}$ . On all channels the excitation was done with a 460 nm LED and the emission was detected on the photodiodes covered with the RG665 or – for the last channel – the RG9 emission filter. The standard solutions were enclosed into a capillary for an easy replacement and, furthermore, to

ensure that the concentration of the standards is not changed during the measurements. The signals are blank corrected. The overall behaviour of the channels is shown in Figure 5.14.

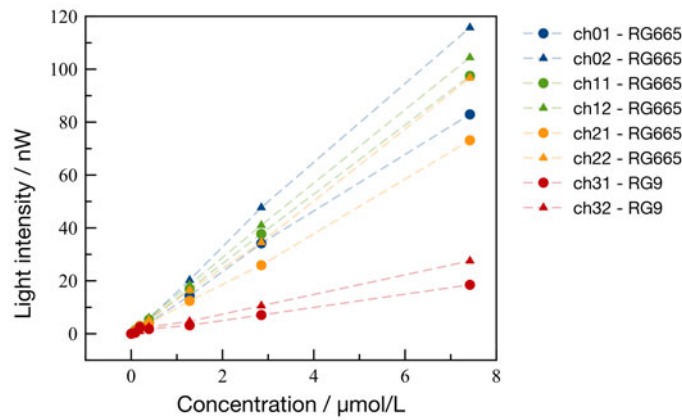


**Figure 5.14.:** Linearity test for the whole POM-C device by using Sulforhodamine 101 as standard solution. The signals are blank corrected. All channels behave linearly.

The diagram suggests a linear behaviour for all channels and also the coefficient of determination  $R^2$ , which was calculated for all channels, confirm this assumption. For the first three channels, the coefficient was better than 99.9%. Only for the last channel, which was covered with the RG9 emission filter, the coefficient was slightly worse.

**Table 5.1.:** Coefficient of determination for all channels to confirm the linear behaviour. Only the last channel exhibits a slightly worse linearity.

channel	coefficient of determination $R^2$
channel 01	0.9992
channel 02	0.9992
channel 11	1.0
channel 12	0.9999
channel 21	0.9991
channel 22	0.9992
channel 31	0.9981
channel 32	0.9985

The sensitivity of the channels could also be described in this experiment, when we focus on the lower concentrations of Sulforhodamine 101 (compare Figure 5.15). All channels of the POM-C device were able to detect even the least concentrated standard solution with a concentration of  $30 \text{ nmol L}^{-1}$ . For this standard the detection module records on the first three channels, after the blank correction, a light intensity of 250 - 400 pW. The last channel records a light intensity of 140 - 200 pW.

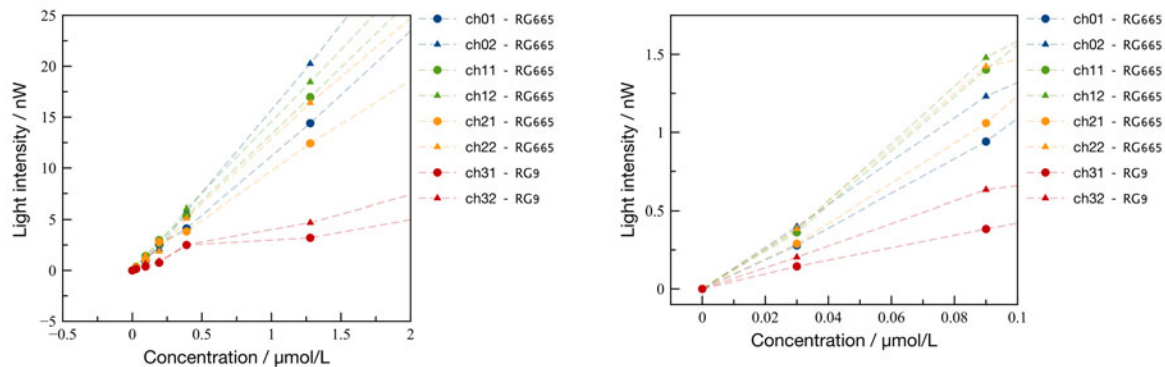


**Figure 5.15.:** Sensitivity test with Sulforhodamine 101 for the whole detection module. All eight channels exhibit a high sensitivity, since they are able to detect the lowest concentrated standard on an average light intensity of 270 pW. The signals are blank corrected.

To summarise the results presented in these sections, it can be said that all eight channels of the POM-C device behave linearly in the range between 0 - 120 nW, as the coefficient of determination is almost 1. Furthermore, the POM-C detection module exhibits a good sensitivity, since it is able to distinguish a light intensity of approximately 300 pW from the blank signal. Furthermore, the limit of detection for the POM-C device can be calculated to 15 pW over the blank signal.

On the other hand, the aluminium device was able to detect single cell events, passing through the measurement volume, and track them along the capillary. Furthermore, the average signal intensity for one single cell on the aluminium device was calculated to 310 pW and the signal-to-noise-ratio was in this case  $\approx 10.3$ . Under the condition that the signal intensity of one single cell measured on the aluminium module can be transferred to the POM-C device, and also under the condition that the limit of detection adheres to approximately 15 pW as it was measured before, we might be able to detect and count single cell events even with the cheaper detection module. Nevertheless, this presumption has to be checked in further investigations.

## 5.4. Data analysis

In the last experiment, we tried a separation of different algae and bacterial samples on the POM-C device based on their spectral differences. For the separation of the species, we used the principal component analysis which was described in a previous chapter 3.2.4 – *Mathematical context – Principal component analysis (PCA)*. In the first attempt, we focus on the separation of the harmful cyanobacteria, since these bacteria might produce toxins, when they bloom. Therefore these bacteria should be identified at an early stage and their blooming should be prevented. It is further to be noted that this experiment can be seen as a proof of concept. This experiment should demonstrate if a reasonable separation of the relevant species would be possible.

### 5.4.1. Spectral differences between cyanobacteria and other algae species

The characterisation of the algae and bacteria cultures, which were cultivated in the laboratory, was done by recording the excitation and emission spectra of each sample. The whole characterisation is attached in the appendix A *Algae Fact Sheet*. At this point, a short overview of the differences in the spectral behaviour of the cyanobacteria and the algae should be presented. The emission spectra of a cyanobacteria species and a diatom species, shown in Figure 5.16 on the right, are quite similar. Since both species contain chlorophyll in their reaction centre, their resulting emission spectra are only slightly different.

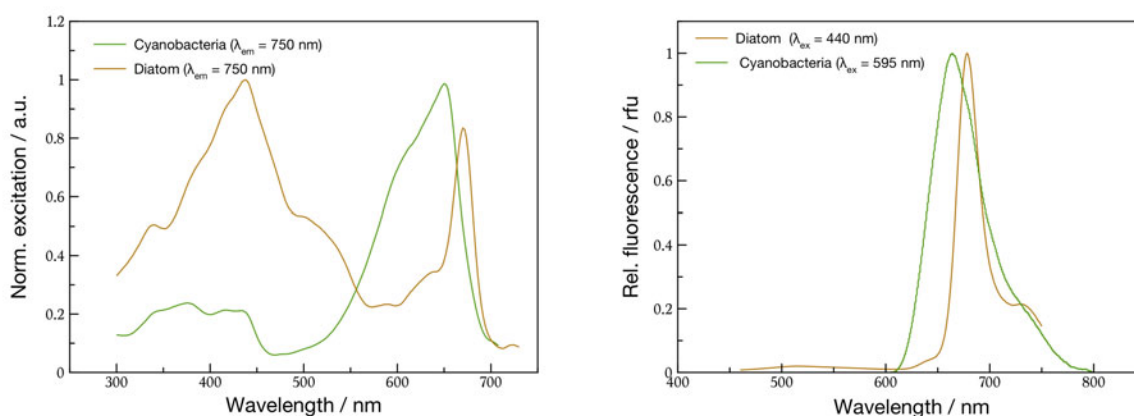


**Figure 5.16.:** Example of the spectral differences between a diatom and a bacterial species. While the emission spectra seem to be quite similar, the excitation spectra are clearly different. Therefore the excitation of the samples has to be done in these spectral ranges that lead to a maximal variance in the excitation intensities.

On the other side, the bacterial excitation spectrum is clearly different from the algal excitation spectrum due to the differences in their light-harvesting complexes (Figure 5.16, left). The

maximal excitation of the algal species is done around 430 nm, whereas the bacteria species is mainly excited between 600 - 660 nm. Therefore, for a clear differentiation of the bacteria and algae cultures, we have to use LEDs in these two spectral ranges. In addition to that, it should be considered that LEDs do not emit monochromatic light and due to their spectral width they would not excite only a particular pigment in the light-harvesting complex. The emission signal of an algal or bacterial species measured on the detection module results rather from the excitation of several pigments.

Further information on the spectra differences between the cultures are given in the appendix and can be used for additional separation experiments.

#### 5.4.2. Data analysis using PCA

For the proof of concept, we measured six different algal and bacterial samples with eight different LEDs in our device. The selection of LEDs based on the spectral differences of the samples. Since we want to separate cyanobacteria from other algae species, we used LEDs in the range between 380 - 640 nm. One emission channel was covered with the longpass filter RG9, the rest was covered with the RG665 emission filter. After the measurement, we calculated, in a first step, the actual pigment pattern of the samples as it is illustrated in Figure 5.17. The resulting pattern illustrates the efficiency of excitation at a particular LED in combination with a particular emission filter. It represents the actual pigment composition of the samples how it could be measured on the device.

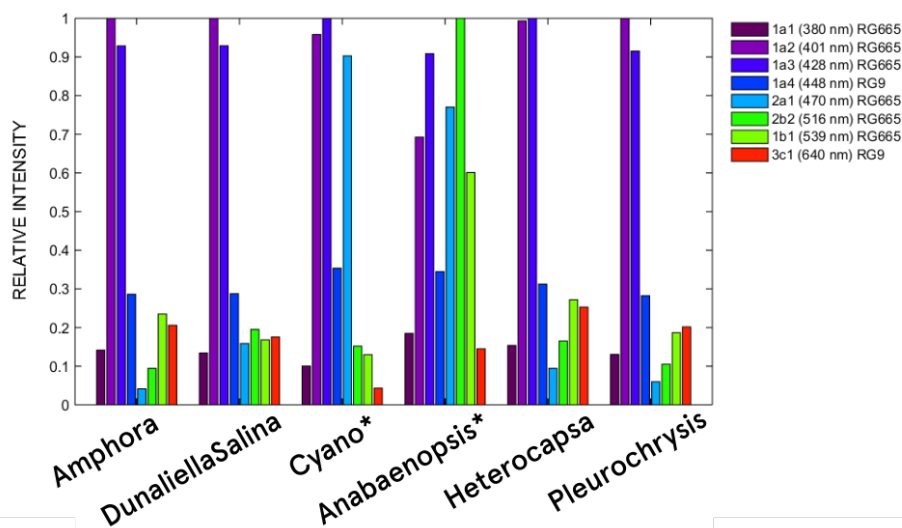


**Figure 5.17.:** Example of the pigment patterns of four different algae species and two bacterial species (marked with \*). These patterns exhibit the efficiency of excitation and illustrate therefore the actual pigment composition how it could be measured on the detection module. The LEDs and emission filters used in this experiment are listed on the right.

The pigment composition of both cyanobacteria – the nameless cyanobacteria and the anabaenopsis – differs clearly from the other four algae species. Both bacteria were well excited by the LED 1a2 (401 nm), but also by the LEDs 1a3 (428 nm), 2a1 (470 nm) and 1b1 (539 nm). Although the algae species were also well excited in the purple range by the LEDs 1a2 (401 nm) and 1a3 (428 nm), the relative excitation by these LEDs, however, differs between all species. Moreover, having a closer look at the green to red range, the cyanobacteria were mainly excited by the LEDs 1b1 (539 nm), whereas the algae were hardly excited in this region.

Consequently, both diagrams in Figure 5.16 and 5.17 lead to similar results and describe the relative pigment composition of the algal and bacterial species. Nevertheless, it has to be noted that these diagrams are similar but not equal, since the pigment composition of the light-harvesting-complex is variable and may depend on the effective light intensity which is used during the cultivation process. The relative pigment composition depends furthermore on the available nutrient supply in the samples. The algal and bacterial species may change their natural colour as a result of nutrient deficiency. On the other hand, the methods used to obtain these diagrams were different. While the fluorometer used to characterise the cultures, has a monochromatic excitation light, excitation on the detection module is done with LEDs that have a spectral width of approximately 20 nm. This spectral width of the LEDs leads to an excitation of more than one specific pigment in the light-harvesting-complex.

As a first proof of concept we analysed then the samples by using the principal component analysis. Since the whole evaluation was done in Matlab, a code based on the mathematical principles of the principal component analysis (PCA) was written in Matlab. The code is not given in this work, since it is a first outline and has to be optimised and adjusted in further steps. Figure 5.18 demonstrates the resulting separation of the samples. Both cyanobacteria could be distinguished clearly from the algae species by using only two principal components.

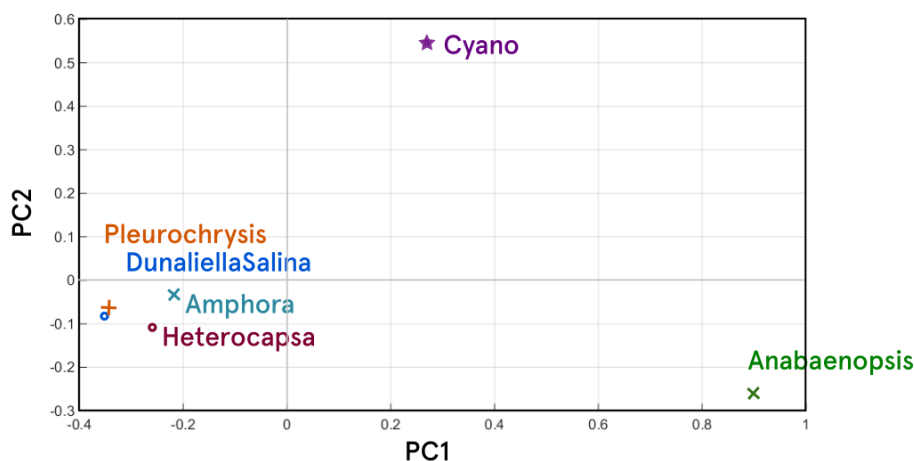


**Figure 5.18.:** Resulting score plot after analysing the data by the means of the principal component analysis. Both cyanobacteria – the unknown bacteria and the anabaenopsis species were separated clearly from the rest.

To summarise this section, it can be noted that we were able to analyse the actual pigment composition of several algal and bacterial species, by using all eight excitation channels for this proof of concept. The resulting pigment compositions recorded on the detection module fit to the spectral characterisation of the sample (with only few restrictions). In further investigations, it should be checked whether a separation of the bacteria is also possible with only two LEDs.



---

## 6. Conclusion and Outlook

In order to come to an end and summarise the present master's thesis, all important results and findings are presented briefly in this chapter.

A multitude of different algae species was cultivated and described morphologically concerning their outer structure and average cell size. Furthermore, all 34 different species were characterised spectrally and the differences between different algal phyla were examined with special respect to their absorbance behaviour. These differences in the excitation spectra were assigned, by the means of the literature, to marker pigments, which are typical for a particular algal phylum. These variable pigmentations of different algal phyla are presented at the beginning of each phylum (compare *appendix A*). It is to be mentioned that the cyanobacteria are clearly distinctive from other algal phyla, since their excitation spectrum is mainly influenced by additional peripheral antenna complexes – the phycobilisomes. Since these pigments absorb in the spectral range between 566 - 655 nm, the phycobilisomes close the green gap, where chlorophyll and other light-harvesting pigments are not able to absorb. Other algae and higher plants, by contrast, absorb mainly in the blue-green range (380 - 550 nm) as well as in the red range (Q band of chlorophyll *a*) featuring the typical green gap.

For further investigations and attempts to distinguish more algae phyla, the shape of the absorption spectra has to be analysed in the blue-green spectral range (380 - 550 nm). In this range, the pigmentation of the light-harvesting complexes and photosystems lead to a characteristic curve, since the resulting shape of the curve represents an overlay of the absorptions characteristics of several pigments. Therefore, the relative differences at certain wavelengths have to be examined and analysed.

Concerning the miniaturised algae detection module, which should be feasible to work as a early warning system in the marine monitoring, it has to be mentioned that the three prototypes were important and necessary in order to reach the desired goals and adapt the optical detection module subsequently. The last two versions of the detection module – the aluminium based and the device made out of POM-C – have shown in several tests that they are able to detect particular algae cells of medium size. However, since these devices are very sensitive, they have to be shielded against ambient light and electro-magnetic interferences. We had problems, especially with the POM-C device, to shield the module, make it optically dense in order to reduce the average noise to a reasonable level. Since the signals, which we want to detect, are small with approximately 300 pW, we have to ensure that a too high noise level does not prevent the detection of particular cells. It is for this reason that we invested a

lot of time and energy in this part of shielding the detection module. By a complete shielding of the device, we prevent electro-magnetic coupling from surrounding sources into our device and reduced the background level from 300 - 825 pW to 225 - 440 pW. The different levels were measured on different channels. The deviation of the noise amplitude was 5 pW. Consequently, we obtain a detection limit of 15 pW with an average signal of 300 pW for a particular cell. According to that a particular cells with an average cell size of 22  $\mu\text{m}$  are detectable. Most of the cyanobacteria exhibit an average filament length of 60  $\mu\text{m}$ , although few cyanobacteria, which have cells instead of filaments, such as the cultivated *Synechocystis sp.*, grow only to 10  $\mu\text{m}$  in size. Nevertheless, it is important that the average noise level is low as much as possible and the resulting limit of detection is smaller than 300 pW. Furthermore, the detection module has to ensure a linear behaviour in this area, which we tested successfully by the means of a Sulforhodamine 101 calibrations.

However, it has to be noted that the POM-C device has to be tested, whether all available and relevant LEDs could be used for separation and whether the whole system is optically dense in order to prevent scattering effects and interferences, which may lead to undesirable signals or raise the average noise level.

The data analysis, by contrast, has proven that a distinction of cyanobacteria from other algal phyla is possible by the means of the multivariate data analysis. Although the experiment was just a proof of concept in order to demonstrate that it may be possible to differentiate between blue-green algae and other phyla with our device, since we used all eight excitation channels for the separation. Further investigations with the available optic elements have to demonstrate, which LED/filter combination might be optimal for a distinction of cyanobacteria with only two LEDs. Moreover, it has to be checked, whether all LEDs can be used on this detection module or whether they lead to undesirable signal interferences.

As a consequence, it has to be mentioned as a final outlook that the optical detection module has to be optimised in further tests. Several experiments have to be done with respect to the robustness and long-term stability of the module concerning the pressure and the temperature drift. The energy consumption in the stand-by mode, which is very high so far, has to be reduced, if possible and an autonomously working measurement record for an optimal application in the SCHeMA project and also for other field trips has to be designed. Therefore, the measurement time and the pump velocity have to be coordinated as well as the LED-modulation frequency and the read out of the photodiodes. Furthermore, a simple mathematical algorithm, which may achieve adequate separation results as the multivariate data analysis, has to be developed. Instead of a complex eigenvalue problem, the data should be analysed with mathematical operations as simple as possible.

All further investigations should always be done with the aim of developing a valuable addition to existing technologies in marine monitoring in order to detect and identify harmful algae blooms at an early stage.





---

## A. Algae Fact Sheet

On the following pages, all analysed algae species are presented. Their characteristic attributes, their morphology meaning their cell shape and average cell diameter, and also their spectral behaviour based on their pigmentation are presented on two sides. For each algae species the typical habitat is described and also, if available in the literature, further information about harmful effects or their commercial application. Since the algae species are classified into phyla, there is as general introduction for each chapter containing the main features of the phylum. In addition to that, a 3D spectrum illustrates the general absorption and fluorescence behaviour of the phylum. Based on this 3D spectrum, the diagnostic pigments as well as other relevant pigments, which are important for an adequate differentiation, are deduced for each phylum. Besides these diagnostic pigments, the overall shape of the absorption curve is important for a suitable differentiation of the algal phyla. It has to be noted that it was not possible to record a 3D spectrum for the chlorophyta, since the fluorometer was defective. Therefore, an overlapped excitation and emission spectrum was presented to examine the typical pigments of the phylum.

For the morphological description, a microscopic picture of each algae species was made using the light microscope *Axiocvert 25* of Carl Zeiss in combination with the GenICam camera, which takes the photo in the infrared range. Moreover, the algae cells were fixed by means of Lugol's solution. Based on this picture, the cell shape as well as the approximate cell diameter could be characterised. Additionally, since the colour of an algae sample is the first visual and catchy feature of an algae, a photograph showing the species in its cultivation flask, was taken. The individual cultivation conditions, under which the algae species were grown, are listed furthermore.

Concerning the absorption and fluorescence behaviour of the algae, an excitation spectrum as well as an emission spectrum was recorded with the aid of the fluorometer. The typical pigment composition within the photosynthetic apparatus, which leads to the resulting spectral behaviour, is also described by the means of the literature. The basic idea how the algae could be distinguished in an unknown water sample is described in chapter 2 *Theoretical background*. In addition to the diagnostic pigments, the overall shape of the excitation spectra and their differences have to be examined in a further step in order to optimise the separation algorithm.

For more details about the individual methods used in this appendix, please see chapter 3 *Material and Methods*.



## A.1. Bacillariophyta

Bacillariophyta, also called *diatoms* or *brown alga*, form one of twelve phyla in the kingdom *Chromista*. It is a widespread algal group with more than 13.000 different species listed in the algae-database [42]. As a result, the phylum contains a variety of morphological types – oval, fusiform or even cylindrical cells forming chains or staying solitary. Common to all of them, however, is their siliceous frustule.

Moreover, diatoms can occur in any habitat: in freshwater, marine or brackish zones all over the world, in benthic or planktonic water areas. In addition to their flexible habitat, they are well-known bloom-forming organisms. [43]

It is also reported in the literature, that few of the diatoms might accumulate metabolites such as poly-unsaturated aldehydes, fatty acids or unhealthy biotoxins. Besides, some algae species belonging to this phylum may also produce harmful domoic acids by itself. [43]

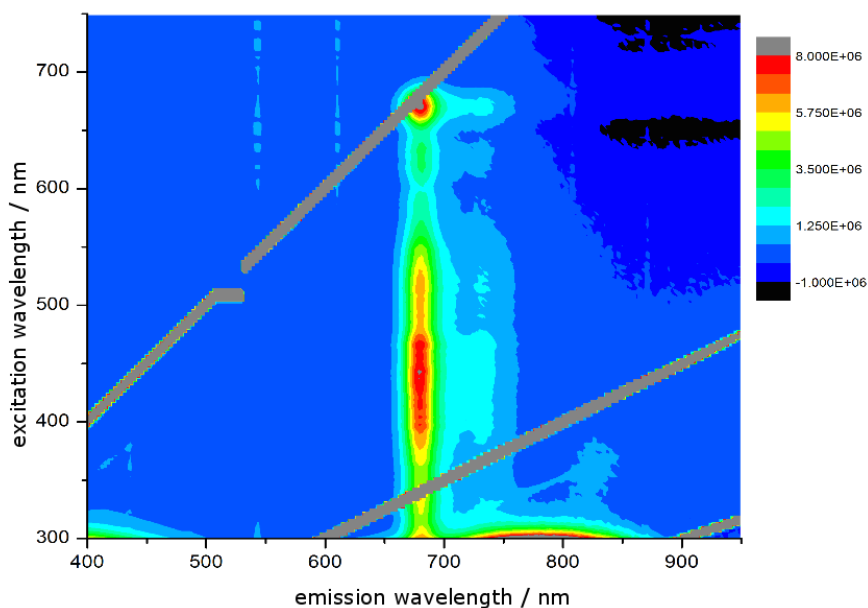


**Figure A.1.:** 3D spectrum of *Skeletonema Costatum* belonging to the phylum *Bacillariophyta*. Excitation between 300 - 750 nm, slitwidth = 2.5 nm; Emission between 400 - 950 nm, slitwidth = 2.5 nm.

Since Bacillariophyta are photoautotrophic microorganisms that often appear with harmful *Dinophyta*, it is important that they are studied. Typical pigments, which are present in all *Diatoms*, are *fucoxanthin*, *chlorophyll a* and *chlorophyll c*. Considering the fact, that chlorophyll *a* is an ubiquitous photosynthetic pigment and chlorophyll *c* is typical for all algae species belonging to the kingdom *Chromista*, only fucoxanthin could be used as "marker" pigment. Comparing the 3D spectrum of *S. costatum* (cf. Figure A.1), a representative of this phylum, all photosynthetic pigments named above could be found in this spectrum. The significant emission of these algae takes place around 680 nm resulting from the fluorescence of chlorophyll *a*. On the other side, the maximal excitation appears in the region of 400 - 500 nm, resulting from fucoxanthin (450 nm, EtOH), the Soret peak of chlorophyll *a* (432 nm, acetone) and chlorophyll *c* (444 nm, acetone). The intensive excitation around 650 nm results from the excitation of both chlorophyll molecules. [44]

## **Amphora – C.G.Ehrenberg ex F.T.Kützing**

This yellow-brown diatom is mainly found in benthic zones, but can also occur in brackish or fresh water areas. Some species of the genus *Amphora* may produce domoic acid, which is a neurotoxin that causes amnesic shellfish poisoning (ASP), if it is accumulated over the food chain. [43]

Since the species is not known, the detailed pigmentation of the algae could not be determined. Consequently, only the major pigments of the phylum *Bacillariophyta*, to which the alga belongs, are listed below.

### **Characterisation**

Taxonomy [42]

<b>Empire</b>	Eukaryota
<b>Kingdom</b>	Chromista
<b>Phylum</b>	Bacillariophyta
<b>Class</b>	Bacillariophyceae
<b>Order</b>	Thalassiosiphales
<b>Family</b>	Catenulaceae
<b>Genus</b>	<i>Amphora</i>

Pigments of the light-harvesting complex

#### **accessory pigments**

major Fucoxanthin,  
Chlorophyll *a*, *c*<sub>1</sub> + *c*<sub>2</sub>

#### **reaction centre**

Chlorophyll *a*

Morphology

**Cell length** 21.9  $\mu\text{m}$   
**Cell shape** convex dorsal and straight ventral margin; clear raphe with radial dorsal striae [43]

### **Cultivation**

Culture medium	L1
Light intensity	0.277 $\text{W m}^{-2}$
Light/dark cycles	10 h / 14 h
Growth temperature	19 °C

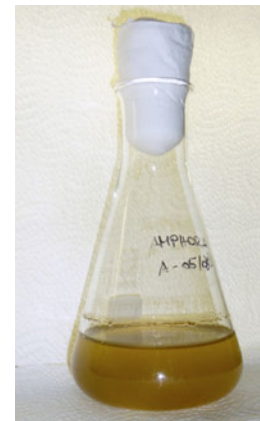


**Figure A.2.:** Cultivation of the alga belonging to the genus *Amphora*

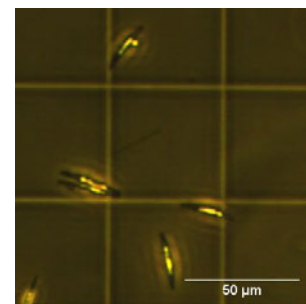


**Figure A.3.:** Fusiformed *Amphora* cells under the light microscope; Lugol's solution ( $I_2/KI$ ) as fixing agent

For the spectral characterisation of the *Amphora* algae, as it is shown in Figure A.4, the algal sample was diluted in glycerine to avoid sedimentation effects of the algae cells. An emission spectrum with an excitation wavelength of 440 nm as well as an excitation spectrum with an emission at 750 nm were measured using the spectrofluorometer. Each measurement was repeated ten times and the resulting excitation and emission spectra were averaged. After the measurement, the emission spectrum was normalised to the maximal chlorophyll fluorescence (678 nm), whereas the excitation spectrum was normalised to the Soret peak of chlorophyll *a* (438 nm).

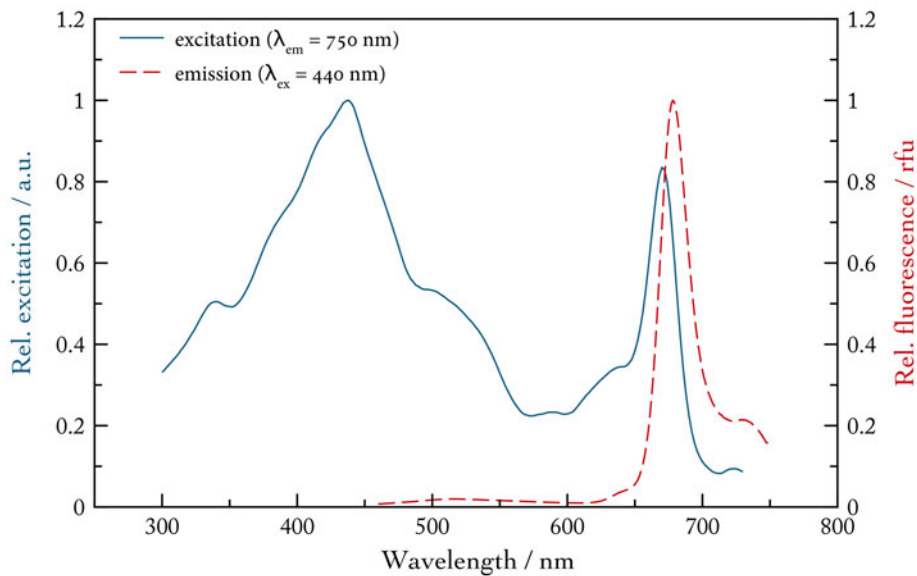


**Figure A.4.:** Normalised emission and excitation spectrum of the alga *Amphora* for spectral characterisation. Excitation at 440 nm, slitwidth = 14 nm, emission slitwidth = 7 nm. Emission at 750 nm, slitwidth = 14 nm, excitation slitwidth = 7 nm. Averaged spectra after 10 measurements.

## **Phaeodactylum tricornutum – Bohlin**

*P. tricornutum* is a widely distributed brown alga, which can be found in coastal or marine regions, but also in freshwater zones. Harmful effects of this algal species itself or of its blooms are not known.

The morphology of this microalgae is greatly influenced by its environmental conditions and may arise in three different morphological types (oval, fusiform or triradiate). [45]

### **Characterisation**

Taxonomy [42]

<b>Empire</b>	Eukaryota
<b>Kingdom</b>	Chromista
<b>Phylum</b>	Bacillariophyta
<b>Class</b>	Bacillariophyta incertae sedis
<b>Order</b>	Bacillariophyta incertae sedis
<b>Family</b>	Phaeodactylaceae
<b>Genus</b>	Phaeodactylum

Pigments of the light-harvesting complex [46]

#### **accessory pigments**

major	Fucoxanthin, Chlorophyll <i>a</i> , <i>c</i> <sub>1</sub> + <i>c</i> <sub>2</sub>
minor	Diadinoxanthin, Diatoxanthin, $\beta$ -Carotene

#### **reaction centre**

Chlorophyll *a*

Morphology

<b>Cell length</b>	17.5 $\mu\text{m}$
<b>Cell shape</b>	fusiform

### **Cultivation**

Culture medium	F <sub>2</sub> / 30%
Light intensity	0.277 W m <sup>-2</sup>
Light/dark cycles	10 h / 14 h
Growth temperature	19 °C

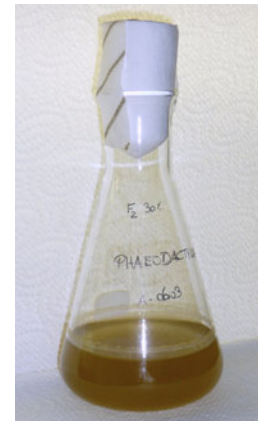


**Figure A.5.:** Cultivation of the microalga *Phaeodactylum tricornutum*

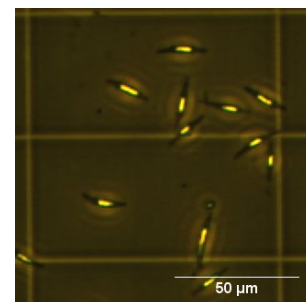


**Figure A.6.:** Image of *Phaeodactylum tricornutum* under the light microscope with Lugol's solution ( $I_2/KI$ ) as fixing agent

The spectra in A.7 illustrate the spectral characterisation of *P. tricornutum*. The algal sample was diluted in glycerine to avoid sedimentation effects of the cells. An emission spectrum with an excitation at 440 nm as well as an excitation spectrum with an emission wavelength of 750 nm were measured using the fluorometer. The sample was measured ten times and then, the excitation and emission spectra were averaged. Afterwards, the emission spectrum was normalised to the maximal chlorophyll fluorescence (676 nm), whereas the excitation spectrum was normalised to the Soret band of chlorophyll *a* (434 nm).

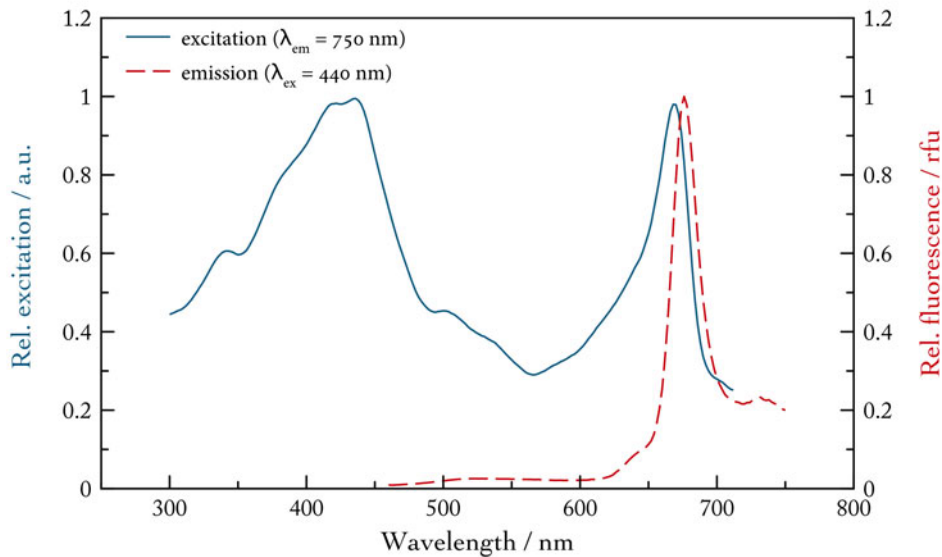


**Figure A.7.:** Normalised emission and excitation spectrum of the microalgae *Phaeodactylum tricornutum*. Excitation at 440 nm, slitwidth = 14 nm, emission slitwidth = 7 nm. Emission at 750 nm, slitwidth = 14 nm, excitation slitwidth = 7 nm. Averaged spectra after 10 measurements.

## Ditylum brightwellii – (T.West) Grunow

This yellow-brown microalga occurs in shallow near-shore or marine areas and may bloom especially during spring, consisting of genetically different populations. Harmful effects of this centric diatom are not known. [47]

### Characterisation

Taxonomy [42]

<b>Empire</b>	Eukaryota
<b>Kingdom</b>	Chromista
<b>Phylum</b>	Bacillariophyta
<b>Class</b>	Mediophyceae
<b>Order</b>	Lithodesmiales
<b>Family</b>	Lithodesmiaceae
<b>Genus</b>	Ditylum

Pigments of the light-harvesting complex [48]

#### **accessory pigments**

major	Fucoxanthin, Chlorophyll <i>a</i> , <i>c</i> <sub>1</sub> + <i>c</i> <sub>2</sub>
-------	--

#### **reaction centre**

Chlorophyll *a*

Morphology [47]

<b>Cell length</b>	40 - 300 $\mu\text{m}$
<b>Cell shape</b>	triangular prism connection through central spine

### Cultivation

Culture medium	F <sub>2</sub> / 18%
Light intensity	0.277 W m <sup>-2</sup>
Light/dark cycles	10 h / 14 h
Growth temperature	19 °C

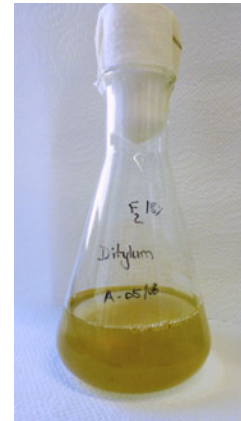


**Figure A.8.:** Cultivation of the microalga *Ditylum brightwellii*

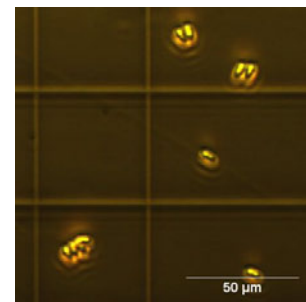


**Figure A.9.:** Small chains of the microalgae *Ditylum brightwellii* under the microscope; Lugol's solution (*I*<sub>2</sub>/*KI*) as fixing agent

The spectra A.10 illustrate the spectral behaviour of the algae *D. brightwellii*. The algal sample was diluted in glycerine to avoid sedimentation of the algae cells. An emission spectrum with an excitation at 440 nm and an excitation spectrum with an emission wavelength of 750 nm were measured using the spectrophotometer. Each measurement was repeated ten times and then the excitation and emission spectra were averaged. Afterwards, the emission spectrum was normalised to the maximum of the chlorophyll fluorescence (692 nm) and the excitation spectrum was normalised to the Soret band of chlorophyll *a* (439 nm).

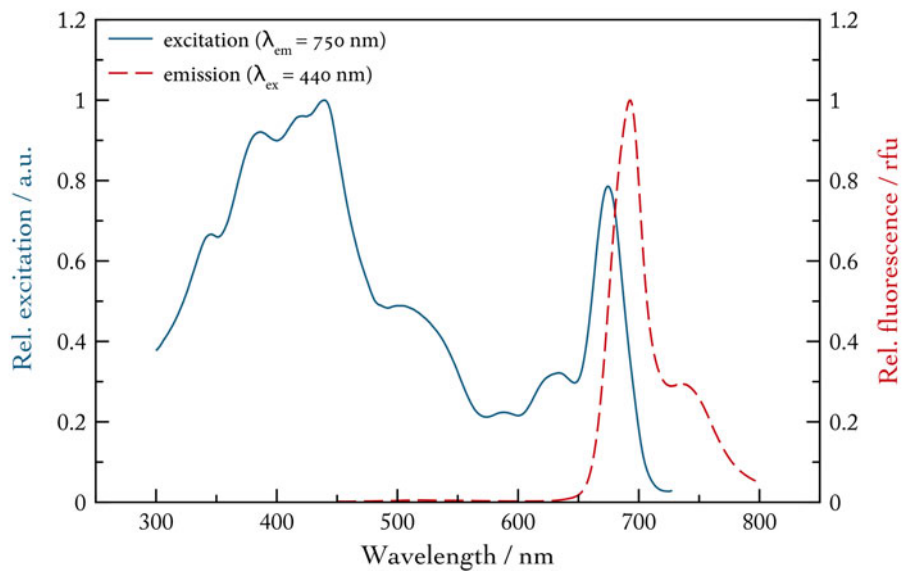


**Figure A.10.:** Normalised emission and excitation spectra of *Ditylum brightwellii*. Excitation at 440 nm, slitwidth = 5 nm, emission slitwidth = 5 nm. Emission at 750 nm, slitwidth = 20 nm, excitation slitwidth = 5 nm. Averaged spectra after 10 measurements.

## **Skeletonema costatum – (Greville) Cleve**

*S. costatum* is a centric, yellow-brown diatom, which appears in coastal regions all over the world, preferring the shallow parts of the oceans. When the microalgae blooms, it causes water discolourations and reduces the oxygen content in the water systems (= *anoxic water*). [47]

### **Characterisation**

Taxonomy [42]

<b>Empire</b>	Eukaryota
<b>Kingdom</b>	Chromista
<b>Phylum</b>	Bacillariophyta
<b>Class</b>	Mediophyceae
<b>Order</b>	Thalassiosirales
<b>Family</b>	Skeletonemataceae
<b>Genus</b>	Skeletonema

Pigments of the light-harvesting complex [49]

#### **accessory pigments**

major Fucoxanthin, Diadinoxanthin  
Chlorophyll *a*, *c*<sub>1</sub> + *c*<sub>2</sub>

minor Diatoxanthin,  $\beta$ -Carotene

#### **reaction centre**

Chlorophyll *a*

Morphology

**Cell length** 6.4  $\mu\text{m}$

**Cell shape** cylindrical cells forming  
marginal ring of spines [47]

### **Cultivation**

Culture medium	L1
Light intensity	0.277 W m <sup>-2</sup>
Light/dark cycles	10 h / 14 h
Growth temperature	19 °C

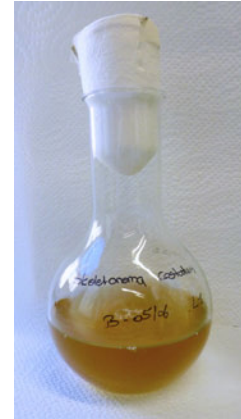


**Figure A.11.:** Cultivation of the microalgae *Skeletonema Costatum*

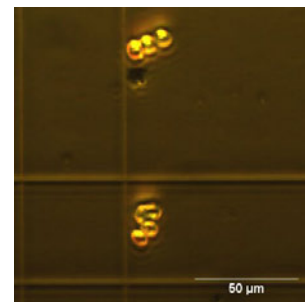


**Figure A.12.:** Small chains of *Skeletonema costatum* under the microscope with Lugol's solution ( $I_2/KI$ ) as fixing agent

For the spectral characterisation of *S. costatum* (compare Figure A.13), an algal sample was diluted in glycerine and an emission spectrum as well as an excitation spectrum were recorded using the spectrophotometer. For the measurement of the algal emission, an excitation of 440 nm was used. The spectrum was normalised to the maximal chlorophyll fluorescence at 682 nm. Furthermore, the excitation spectrum was measured using an emission wavelength of 750 nm. Afterwards the spectrum was normalised to the maximal excitation peak at 416 nm. The measurement for each spectrum was repeated ten times and then the spectra were averaged.

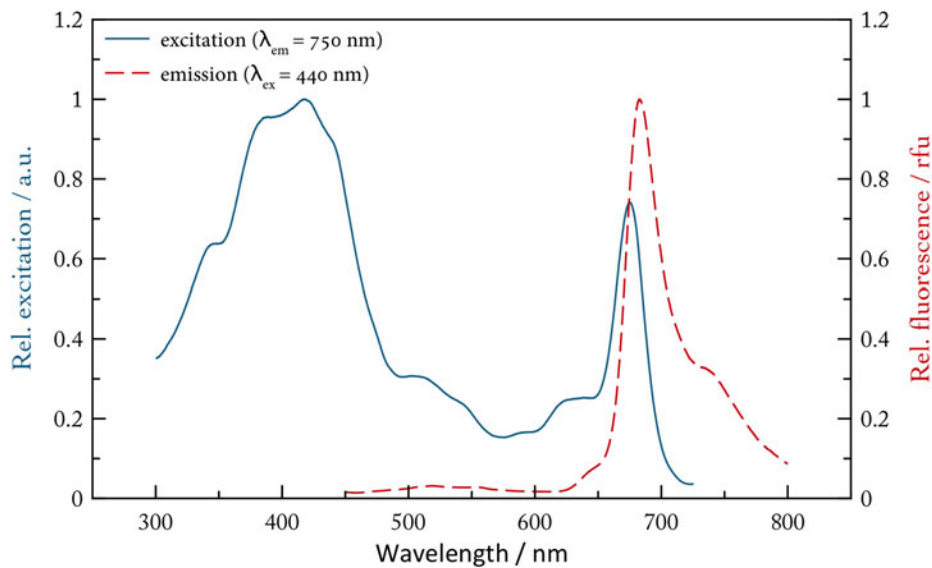


**Figure A.13.:** Normalised emission and excitation spectrum of *Skeletonema costatum* for spectral characterisation. Excitation at 440 nm, slitwidth = 5 nm, emission slitwidth = 5 nm. Emission at 750 nm, slitwidth = 20 nm, excitation slitwidth = 5 nm. Averaged spectra after 10 measurements.

## **Cyclotella meneghiniana – Kützing**

The algal species *C. meneghiniana* is a yellow-brown diatom which is widely distributed in freshwater areas all over the world. It is one of the most common diatom species. Harmful effects are not known, but this microalga is highly salt-tolerant and has morphological varieties. [50]

Since the detailed pigment composition of this algal species is not known in the literature, the description of the pigmentation is carried out by the genetically very similar alga *Cyclotella. sp.*, which belongs to the same genus as *C. meneghiniana*.

### **Characterisation**

Taxonomy [42]

<b>Empire</b>	Eukaryota
<b>Kingdom</b>	Chromista
<b>Phylum</b>	Bacillariophyta
<b>Class</b>	Mediophyceae
<b>Order</b>	Thalassiosirales
<b>Family</b>	Stephanodiscaceae
<b>Genus</b>	Cyclotella

Pigments of the light-harvesting complex [51]

#### **accessory pigments**

major	Fucoxanthin, Diadinoxanthin, Chlorophyll <i>a</i> , $c_1 + c_2$
minor	Diatoxanthin, $\beta$ -Carotene

#### **reaction centre**

Chlorophyll *a*

Morphology

<b>Cell diameter</b>	10 - 35 $\mu\text{m}$
<b>Cell shape</b>	complex and therefore not clearly defined [50]; here cylindrical cells forming small chains

### **Cultivation**

Culture medium	F <sub>2</sub> / 18%
Light intensity	0.277 W m <sup>-2</sup>
Light/dark cycles	10 h / 14 h
Growth temperature	19 °C

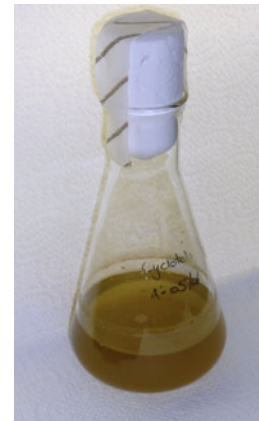


**Figure A.14.:** Cultivation of the microalga *Cyclotella meneghiniana*

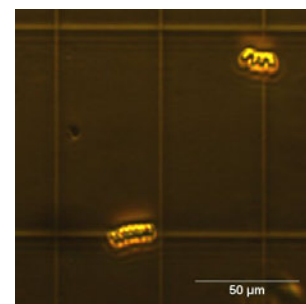


**Figure A.15.:** Small chains of *Cyclotella meneghiniana* under the microscope; Lugol's solution ( $I_2/KI$ ) as fixing agent

For the spectral characterisation of *C. meneghiniana*, an algal sample was diluted in glycerine to hold the algae cells in suspension. An emission spectrum and an excitation spectrum were measured using the spectrophotometer. The excitation wavelength for the emission spectrum was set to 440 nm, whereas the emission wavelength for the excitation spectrum was set to 750 nm. The measurement for each spectrum was repeated ten times and afterwards the spectra were averaged and normalised. The resulting emission spectrum was normalised to the maximal chlorophyll fluorescence at 688 nm and the excitation spectrum was normalised to the Soret band of chlorophyll *a* at 440 nm.

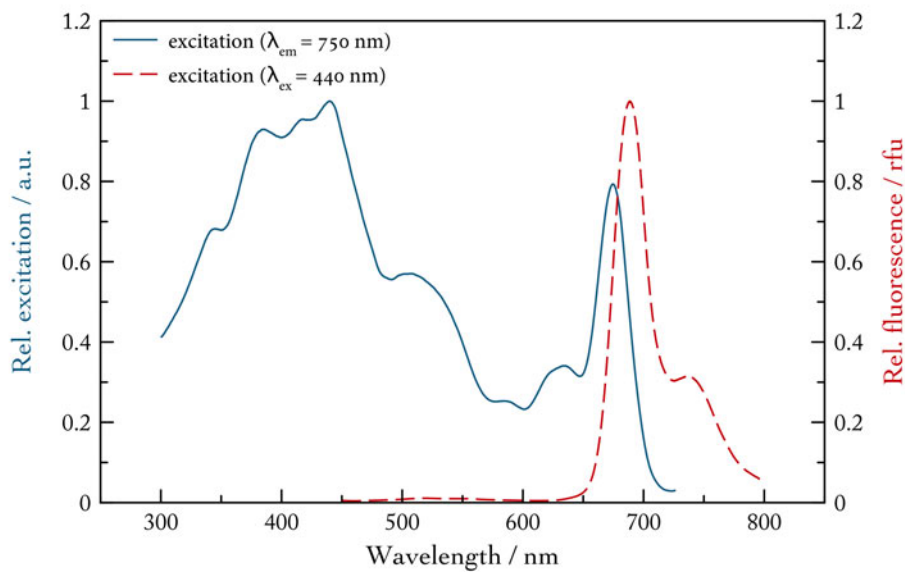


**Figure A.16.:** Normalised emission and excitation spectrum of *Cyclotella meneghiniana*. Excitation at 440 nm, slitwidth = 5 nm, emission slitwidth = 5 nm. Emission at 750 nm, slitwidth = 20 nm, excitation slitwidth = 5 nm. Averaged spectra after 10 measurements.



## A.2. Cryptophyta

*Cryptophyta* are the photosynthetic cells of the whole phylum *Cryptista*, which belongs to the kingdom *Chromista*. In the literature, they are mainly called *Cryptista*, although the accepted scientific name of the algal phylum is *Cryptophyta*. [52] At the moment, there are more than 200 different species of the phylum *Cryptophyta* listed in the algae-database. [42] These microalgae inhabit freshwater as well as marine areas, but all of the investigated algae species in this thesis prefer the brackish water.

Moreover, these non-toxic algae species are very consistent in their morphology. All of the organisms have an asymmetrical cell shape that can be described as an unicellular spherical drop with two flagella.

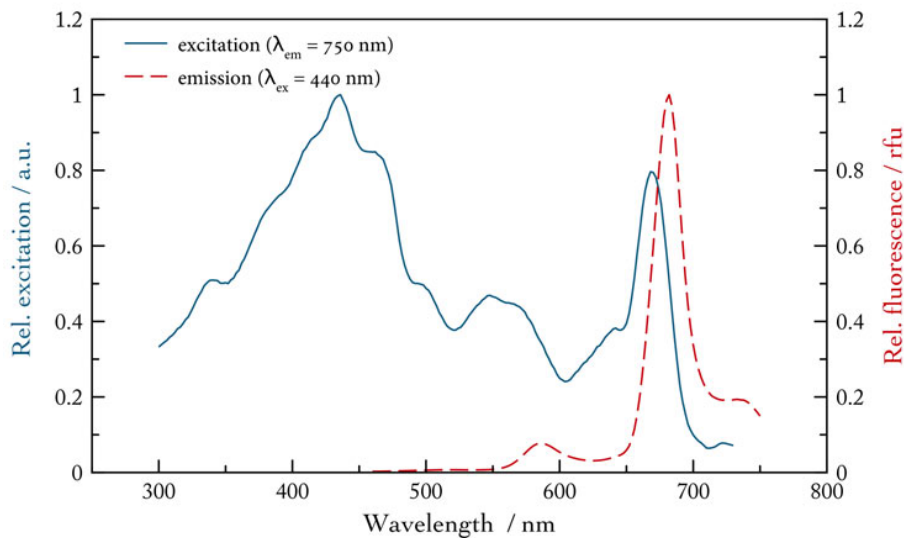


**Figure A.17.:** 2D spectrum of the microalgae *Rhodomonas minuta* belonging to the phylum *Cryptophyta*. Normalised emission and excitation spectrum of *Rhodomonas minuta* for spectral characterisation. Excitation at 440 nm, slitwidth = 14 nm, emission slitwidth = 7 nm. Emission at 750 nm, slitwidth = 14 nm, excitation slitwidth = 7 nm.

In previous articles, it was reported that *Cryptophyta* are risen from red algae and therefore, they contain additionally phycobilins as accessory pigments. As a result, *Cryptophyta* are able to absorb the incident light in a broader wavelength-range. It is furthermore suggested that phycobilins are used to optimise the photosynthesis under reduced light conditions. [53] By using these phycobilins, *Cryptophyta* close the green gap where chlorophyll cannot absorb. As it is indicated from their ancestors, *Cryptophyta* contain a modified form of phycoerythrin in the thylakoidal space. [54]

A typical pigment of *Cryptophyta*, additionally to *chlorophyll a*, *chlorophyll c* and the modified *biliprotein* mentioned above, is *alloxanthin*. Since *alloxanthin* only occurs in *Cryptophyta*, it might be used as "marker" pigment. In the 2D spectrum of *Rhodomonas minuta*, a representative of the *Cryptophyta* (cf. Figure A.17), all typical pigments of this phylum could be found. The absorbance around 560 nm results from the modified biliprotein. Moreover, the excitation of *alloxanthin* is seen in the shoulder around 450 nm (451 nm acetone/hexane). [17] Also *chlorophyll a* and *chlorophyll c* are excited in this region (chl *a* at 432 nm, chl *c* at 432 nm, acetone). [44] The emission peak results from the *chlorophyll a* fluorescence.

## **Hemiselmis sp. rcc 659**

This algal species appears commonly in freshwater and marine, brackish and coastal regions. It is a flagellate, unicellular *Cryptophyta* and its cells are one of the smallest ones in this phylum. [55] Harmful effects of *H. sp.* are not known in the literature.

### **Characterisation**

Taxonomy [42]

<b>Empire</b>	Eukaryota
<b>Kingdom</b>	Chromista
<b>Phylum</b>	Cryptophyta
<b>Class</b>	Cryptophyceae
<b>Order</b>	Pyrenomonadales
<b>Family</b>	Chroomonadaceae
<b>Genus</b>	Hemiselmis

Pigments of the light-harvesting complex [51]

#### **accessory pigments**

major Alloxanthin, Chlorophyll *a* + *c*<sub>2</sub>

#### **reaction centre**

Chlorophyll *a*

Morphology

**Cell diameter** 12.0  $\mu\text{m}$

**Cell shape** cone with half sphere [56]  
flagellated [55]

### **Cultivation**

Culture medium	L1-Si
Light intensity	0.277 W m <sup>-2</sup>
Light/dark cycles	10 h / 14 h
Growth temperature	19 °C

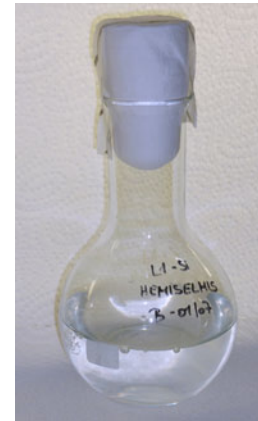


**Figure A.18.:** Clear to bluish culture of the microalga *Hemiselmis sp.*

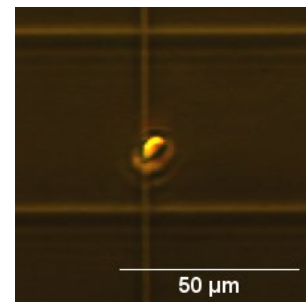


**Figure A.19.:** Drop shaped *Hemiselmis sp.* under the light microscope with Lugol's solution ( $I_2/KI$ ) as fixing agent

For the spectral characterisation of *Hemiselmis sp. rcc 659*, an excitation spectrum and an emission spectrum of this alga were measured using the fluorometer. The sample was diluted in glycerine to avoid sedimentation of the algae cells. The excitation wavelength for the emission spectrum was set to 440 nm and the emission wavelength for the excitation spectrum was set to 750 nm. The measurement for each type of spectrum was repeated ten times. Afterwards the spectra were averaged and normalised. The emission spectrum was normalised to the maximal chlorophyll fluorescence at 678 nm, whereas the excitation spectrum was normalised to the Soret peak of chlorophyll *a* at 436 nm.

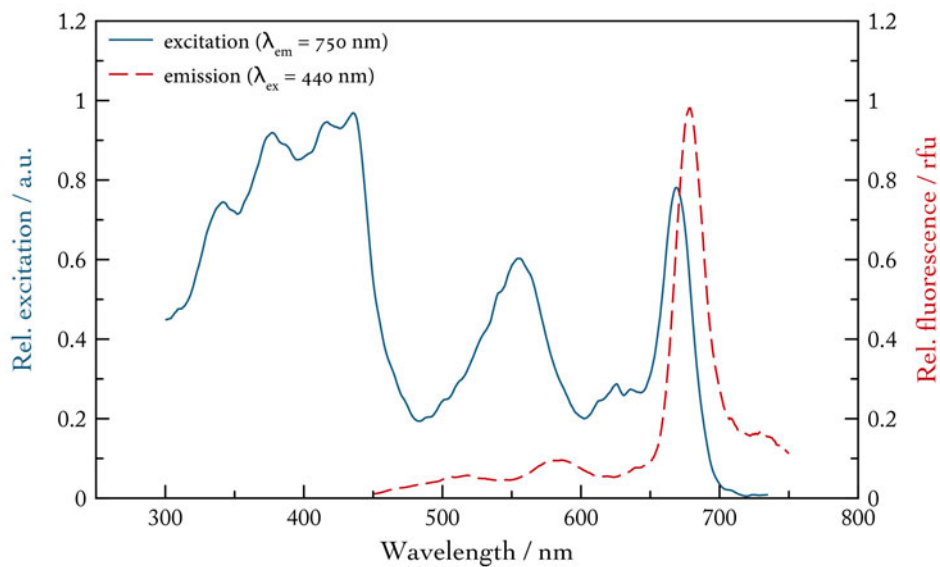


**Figure A.20.:** Normalised emission and excitation spectrum of *Hemiselmis sp.*. Excitation at 440 nm, slitwidth = 14 nm, emission slitwidth = 7 nm. Emission at 750 nm, slitwidth = 14 nm, excitation slitwidth = 7 nm. Averaged spectra after 10 measurements.

## **Rhodomonas minuta – Skuja**

*Rh. minuta* is a cosmopolitan *Cryptophyta* that occurs in freshwater areas, marine and brackish water. [57] Harmful effects of this alga are not known in the literature. [58]

According to the algae database the currently accepted name of this species is *Rhodomonas lacustris* var. *nannoplanctica* (Skuja) Javornicky. [42]

### **Characterisation**

Taxonomy [42]

<b>Empire</b>	Eukaryota
<b>Kingdom</b>	Chromista
<b>Phylum</b>	Cryptophyta
<b>Class</b>	Cryptophyceae
<b>Order</b>	Pyrenomonadales
<b>Family</b>	Pyrenomonadaceae
<b>Genus</b>	Rhodomonas

Pigments of the light-harvesting complex [59]

#### **accessory pigments**

major Alloxanthin, Chlorophyll *a* + *c*<sub>2</sub>  
 minor  $\beta$ -Carotene

#### **reaction centre**

Chlorophyll *a*

Morphology

**Cell diameter** 13.0  $\mu\text{m}$   
**Cell shape** cone with half sphere [56]

### **Cultivation**

Culture medium MWC 0%  
 Light intensity 0.277  $\text{W m}^{-2}$   
 Light/dark cycles 10 h / 14 h  
 Growth temperature 19 °C

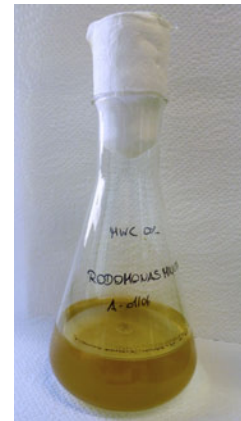


**Figure A.21.:** Cultivation of the microalga *Rhodomonas minuta*

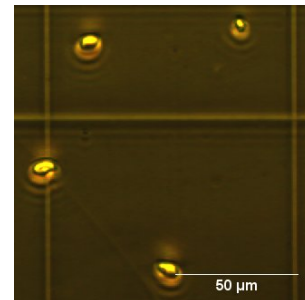


**Figure A.22.:** Drop shaped cells of *Rhodomonas minuta* under the light microscope with Lugol's solution ( $I_2/KI$ ) as fixing agent

To describe the spectral behaviour of *Rh. minuta*, the algal sample was diluted in glycerine and an emission spectrum and an excitation spectrum were recorded using the spectrofluorometer. For the emission spectrum, the excitation wavelength was set to 440 nm, whereas the emission wavelength for the excitation spectrum was set to 750 nm. The measurements for both spectra were repeated ten times and then the spectra were averaged and normalised separately. The emission spectrum was normalised to the maximum of the chlorophyll fluorescence at 682 nm and, by contrast, the excitation spectrum was normalised to the Soret band of chlorophyll *a* at 436 nm. The resulting spectra are given in Figure A.23.

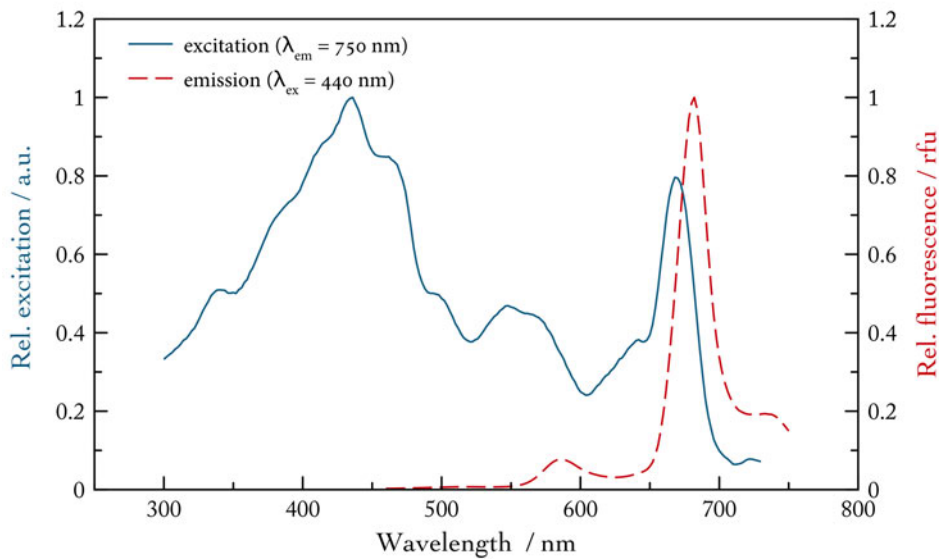


**Figure A.23.:** Normalised emission and excitation spectrum of *Rhodomonas minuta* for spectral characterisation. Excitation at 440 nm, slitwidth = 14 nm, emission slitwidth = 7 nm. Emission at 750 nm, slitwidth = 14 nm, excitation slitwidth = 7 nm. Averaged spectra after 10 measurements.

**Rhodomonas salina – (Wislouch) D.R.A.Hill & R.Wetherbee**

The microalga *Rh. salina* is a red to brown alga that occurs mainly in marine or brackish areas. Only few species were found in freshwater regions. [57] Moreover, this alga is a non-toxic *Cryptophyta*. [60]

**Characterisation**

Taxonomy [42]

<b>Empire</b>	Eukaryota
<b>Kingdom</b>	Chromista
<b>Phylum</b>	Cryptophyta
<b>Class</b>	Cryptophyceae
<b>Order</b>	Pyrenomonadales
<b>Family</b>	Pyrenomonadaceae
<b>Genus</b>	Rhodomonas

Pigments of the light-harvesting complex [46]

**accessory pigments**

major	Alloxanthin, Chlorophyll <i>a</i> + <i>c</i> <sub>2</sub>
minor	$\alpha$ -Carotene, Crocoxanthin, Monadoxanthin

**reaction centre**

Chlorophyll *a*

Morphology

<b>Cell diameter</b>	17.0 $\mu m$
<b>Cell shape</b>	cone with half sphere [56]

**Cultivation**

Culture medium	F <sub>2</sub> / 18%
Light intensity	0.277 W m <sup>-2</sup>
Light/dark cycles	10 h / 14 h
Growth temperature	19 °C

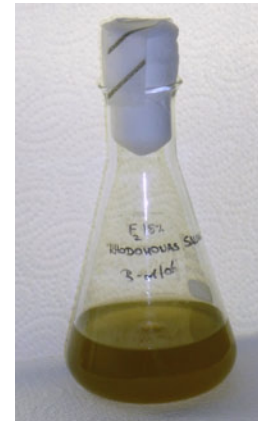


**Figure A.24.:** Cultivation of the microalga *Rhodomonas salina*

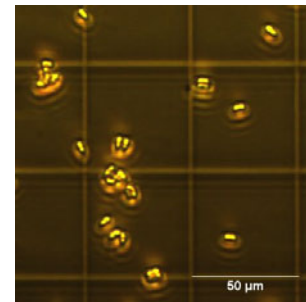


**Figure A.25.:** Drop shaped cells of *Rhodomonas salina* under the microscope. Lugol's solution (I<sub>2</sub>/KI) used as fixing agent

For the spectral characterisation of *Rh. salina* the algal sample was diluted in glycerine to avoid sedimentation of algae cells and an emission as well as an excitation spectrum were measured using the spectrofluorometer. For the emission spectrum the excitation wavelength was set to 440 nm and for the excitation spectrum the emission wavelength was set to 750 nm. The measurements for both spectra were repeated ten times and then the spectra were averaged and normalised separately. The emission spectrum was normalised to the maximum of the chlorophyll fluorescence at 683 nm whereas the excitation spectrum was normalised to the Soret peak of chlorophyll *a* at 434 nm. The results are given in Figure A.26.

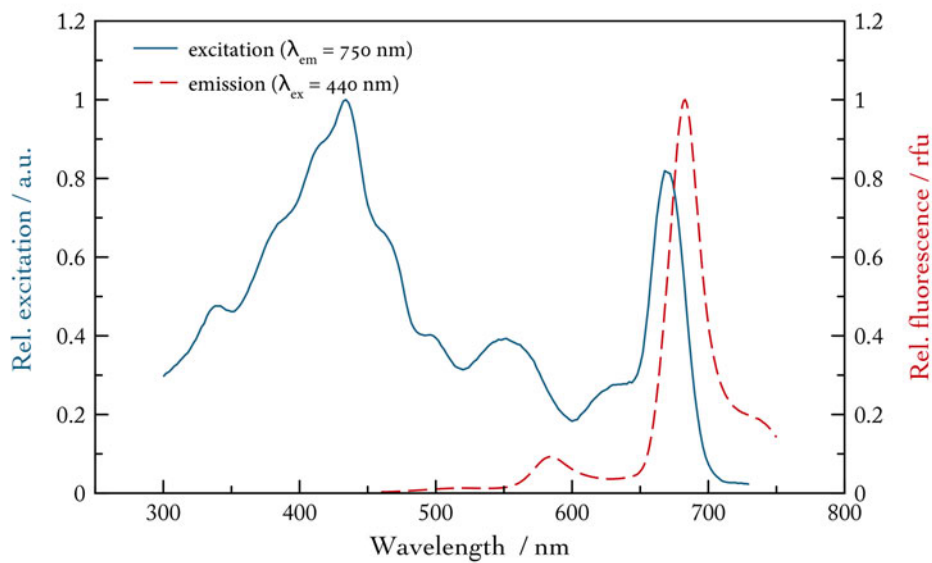


**Figure A.26.:** Normalised emission and excitation spectrum of *Rhodomonas salina* for spectral characterisation. Excitation at 440 nm, slitwidth = 14 nm, emission slitwidth = 7 nm. Emission at 750 nm, slitwidth = 14 nm, excitation slitwidth = 7 nm. Averaged spectra after 10 measurements.



### A.3. *Dinophyta*

*Dinophyta* is a phylum of the kingdom *Chromista* that contains more than 3.000 algae species according to the algal database AlgaeBase [42]. These algae group mainly occurs in coastal and estuarine regions all over the world and it is a well-known bloom-forming group. [61]

Furthermore, several algae species in this phylum produce biotoxins, which cause gastrointestinal disturbances like the ciguatera fish poisoning (CFP) or the diarrhetic shellfish poisoning (DSP) syndrome. Other syndromes like the paralytic shellfish poisoning (PSP), which is caused by *A. minutum* or the neurotoxic shellfish poisoning (NSP), induce neurological disorders. [62]

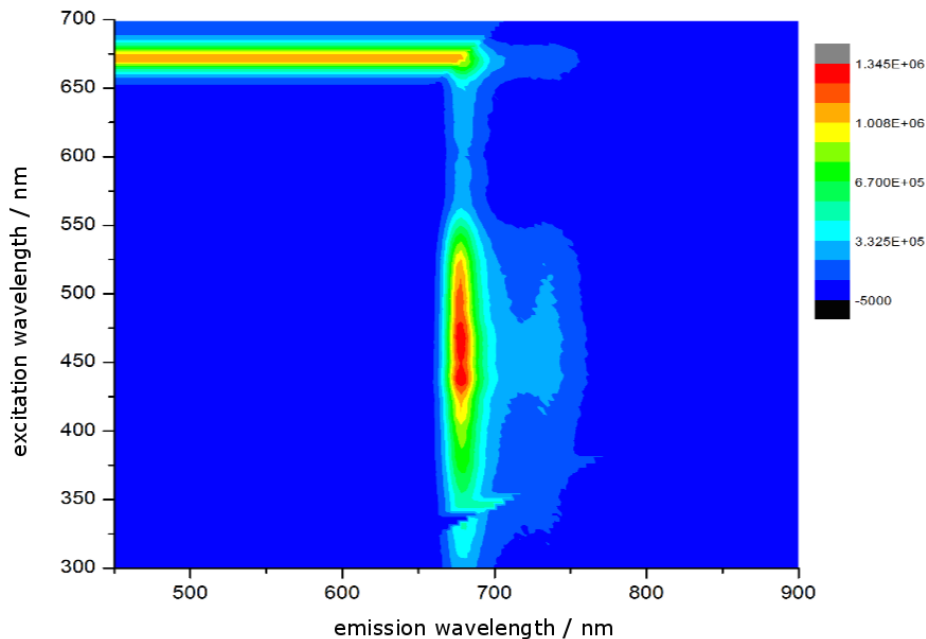


**Figure A.27.:** 3D spectrum of the algae *Alexandrium minutum* belonging to the phylum *Dinophyta*. Excitation between 300 - 700 nm, slitwidth = 5 nm; Emission between 450 - 900 nm, slitwidth = 5 nm.

Since this phylum contains several toxin-producing algae, it is of high interest to analyse these algae and determine their pigmentation to prevent further disturbances caused by the consumption of contaminated seafood.

Typical pigments, which are present in all *Dinoflagellates*, are *peridinin*, *diatoxanthin*, *diadinoxanthin* and *chlorophyll a + c* as accessory pigments in the light-harvesting complex (LHC) and *chlorophyll a* as dimer in the reaction centre. Since both xanthophylls are only a minor part in the LHC, and both chlorophylls are present in other algae, peridinin is the most suitable molecule used as "marker" pigment.

The excitation and emission properties of these pigments are shown in the 3D spectrum of *Alexandrium minutum* (compare Figure A.27), a toxic alga belonging to the phylum *Dinophyta*. The maximal emission at 680 nm results from the fluorescence of the chlorophyll *a* molecule. The intensive excitation band between 425 - 500 nm, by contrast, results from peridinin, as major accessory pigment (454 nm, hexane), the Soret band of chlorophyll *a* (432 nm, acetone) and chlorophyll *c* (444 nm, acetone). Also the minor pigments are excited in this region. [19, 44] The intensive excitation around 650 nm results from the excitation of both chlorophylls.

## Alexandrium minutum – Halim

The alga *A. minutum* is found in coastal regions all over the world and occurs as dense red tides, when it blooms. As algae bloom, *A. minutum* can produce the neurotoxin Saxitoxin (STX), which threatens marine organisms and, after accumulation over the food chain, leads to paralytic shellfish poisoning (PSP). [61]

### Characterisation

Taxonomy [42]

<b>Empire</b>	Eukaryota
<b>Kingdom</b>	Chromista
<b>Phylum</b>	Dinophyta
<b>Class</b>	Dinophyceae
<b>Order</b>	Gonyaulacales
<b>Family</b>	Goniodomataceae
<b>Genus</b>	Alexandrium

Pigments of the light-harvesting complex [63]

#### **accessory pigments**

major	Peridinin, Chlorophyll <i>a</i> + <i>c</i>
minor	Dinoxanthin, Diadinoxanthin, Diatoxanthin

#### **reaction centre**

Chlorophyll *a*

Morphology

<b>Cell diameter</b>	32.0 $\mu\text{m}$
<b>Cell shape</b>	spherical to ellipsoidal, armoured [61]

### Cultivation

Culture medium	L1-Si
Light intensity	0.277 $\text{W m}^{-2}$
Light/dark cycles	10 h / 14 h
Growth temperature	19 °C

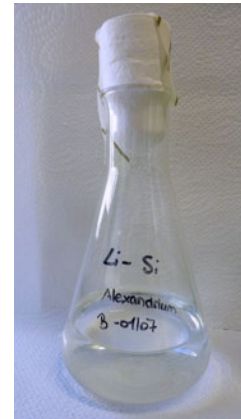


**Figure A.28.:** Cultivation of the microalga *Alexandrium minutum*

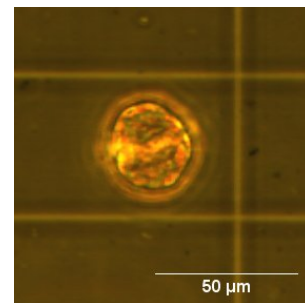


**Figure A.29.:** Spherical cell of *Alexandrium minutum* under the light microscope using Lugol's solution ( $I_2/KI$ ) as fixing agent

For the spectral characterisation of *A. minutum*, the alga was diluted in glycerine and an excitation as well as an emission spectrum were measured using the spectrofluorometer. The excitation wavelength for the emission spectrum was set to 440 nm, whereas the emission wavelength for the excitation spectrum was set to 750 nm. The measurement for each spectrum was repeated ten times and, afterwards, the resulting spectra were averaged and normalised. The emission spectrum was normalised to the maximal chlorophyll fluorescence at 680 nm and the excitation spectrum was normalised to the Soret peak of chlorophyll *a* at 430 nm.

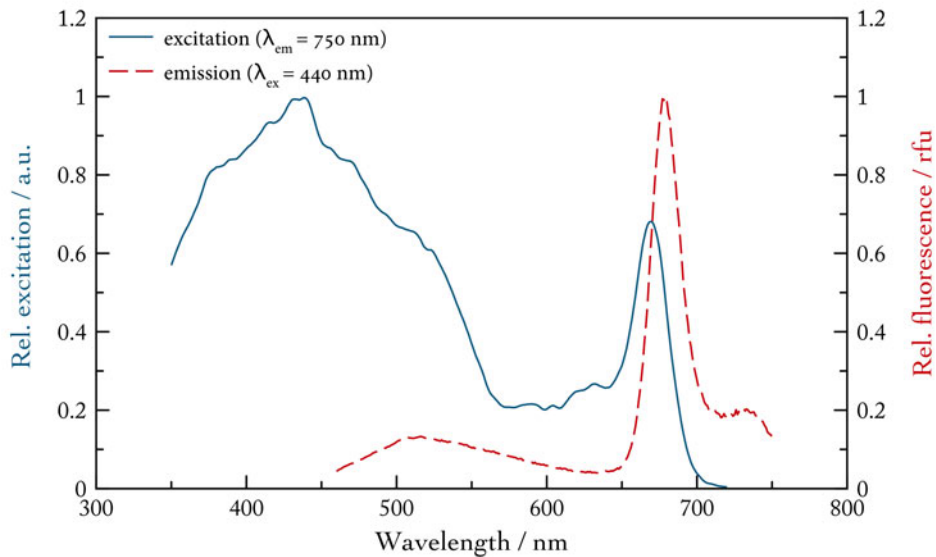


**Figure A.30.:** Normalised emission and excitation spectrum of *Alexandrium minutum*. Excitation at 440 nm, slitwidth = 14 nm, emission slitwidth = 7 nm. Emission at 750 nm, slitwidth = 14 nm, excitation slitwidth = 7 nm. Averaged spectra after 10 measurements.

## **Heterocapsa triquetra – (Ehrenberg) Stein**

The golden *Dinophyta H. triquetra* occurs in neritic and estuarine zones and may form blooms during summer. Harmful effects of this microalga are not known in the literature, but rather, it is considered to be a quality food for other marine organisms. [47]

### **Characterisation**

Taxonomy [42]

<b>Empire</b>	Eukaryota
<b>Kingdom</b>	Chromista
<b>Phylum</b>	Dinophyta
<b>Class</b>	Dinophyceae
<b>Order</b>	Peridinales
<b>Family</b>	Heterocapsaceae
<b>Genus</b>	Heterocapsa

Pigments of the light-harvesting complex [51]

#### **accessory pigments**

major Peridinin, Diadinoxanthin,  
Chlorophyll *a* + *c*<sub>2</sub>

minor Alloxanthin, Diatoxanthin,  
 $\beta$ -Carotene

#### **reaction centre**

Chlorophyll *a*

Morphology

**Cell length** 21.0  $\mu\text{m}$

**Cell shape** two joined cones,  
with unilateral protrusion [47]

### **Cultivation**

Culture medium	L1-Si
Light intensity	0.277 W m <sup>-2</sup>
Light/dark cycles	10 h / 14 h
Growth temperature	19 °C



**Figure A.31.:** Cultivation of the microalga *Heterocapsa triquetra*

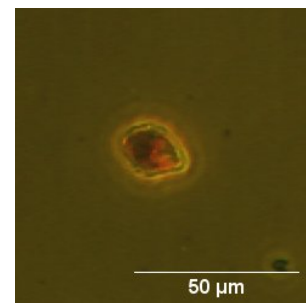


**Figure A.32.:** Microscopic image of *Heterocapsa triquetra*. Lugol's solution ( $I_2/KI$ ) used as fixing agent

The spectral characterisation of *H. triquetra* is shown in Figure A.33. The algal sample was diluted in glycerine and both spectra – the emission as well as the excitation spectrum – were recorded using the spectrofluorometer. For the emission spectrum an excitation of 440 nm was used, whereas the excitation spectrum was measured with an emission of 750 nm. The measurement for each spectrum was repeated ten times and then the resulting excitation and emission spectra were averaged and normalised separately. The emission spectrum was normalised to the maximum of the chlorophyll fluorescence at 679 nm and, by contrast, the excitation spectrum was normalised to the maximal excitation at 456 nm.

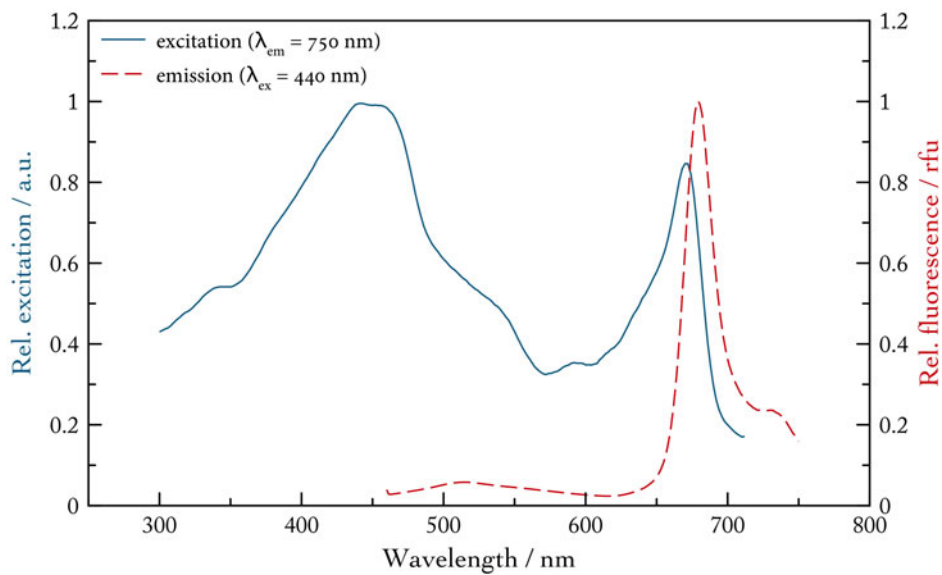


**Figure A.33.:** Normalised emission and excitation spectrum of *Heterocapsa triquetra*. Excitation at 440 nm, slitwidth = 14 nm, emission slitwidth = 7 nm. Emission at 750 nm, slitwidth = 14 nm, excitation slitwidth = 7 nm. Averaged spectra after 10 measurements.



## A.4. Haptophyta

The phylum *Haptophyta* belongs to the kingdom *Chromista* and includes more than 600 algae species – according to the database *AlgaeBase*. [42]

These algae species mainly occur in marine water, but could also be found in terrestrial and brackish areas. Furthermore, few microalgae of this phylum are reported to be harmful for marine animals, however, adverse effects for humans are not known in the literature.

Moreover, this algal group is not very important for the industry. Some might be used as feed in aquacultures, but apart from that, a commercial use is not reported.

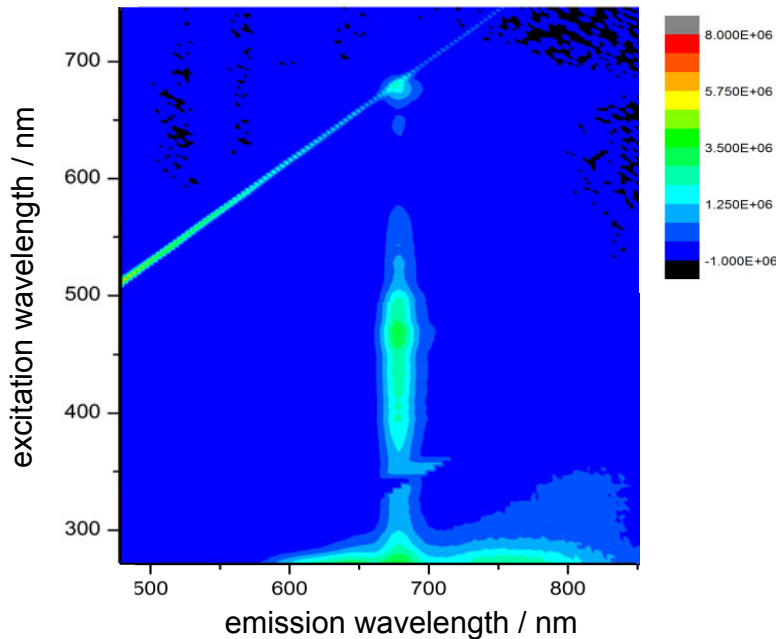


**Figure A.34.:** 3D spectrum of the algae species *Pleurochrysis elongata* belonging to the phylum *Haptophyta*. Excitation between 300 - 750 nm, slitwidth = 3 nm; Emission between 400 - 850 nm, slitwidth = 6 nm.

Normally *Haptophyta* are golden to brown and have a similar pigmentation as the algae belonging to the phylum *Bacillariophyta* / *Diatoms*. Pigments, that are present in all algae species of the *Haptophyta*, are *fucoxanthin*, *chlorophyll a* and *chlorophyll c<sub>1</sub>*. Since the major pigmentation is quite similar, a differentiation of *Diatoms* and *Haptophyta* might not be easy and depends primarily on the minor pigments of the photosystem.

Nevertheless, the 3D spectrum of *Pleurochrysis elongata* (cf. Figure A.34), a representative alga of the phylum *Haptophyta*, illustrates the excitation and emission behaviour of the photosynthetic pigments in this phylum. The significant emission around 680 nm results from the fluorescence of *chlorophyll a*. By contrast, the most intensive excitation in the range of 450 - 500 nm results from *fucoxanthin* (450 nm, EtOH), from the excitation of the Soret band of *chlorophyll a* (432 nm, acetone) and also from the excitation of *chlorophyll c* (444 nm, acetone). [44]

**Pleurochrysis elongata – (Droop) R. W. Jordan, L. Cros & J. R. Young**

This golden-brown alga appears in marine and coastal regions. According to Houdan et al. *P. elongata* was found to be toxic against the shrimp *Artemia salina*, but harmful effects against humans are not known in the literature. [64]

Since a detailed pigment composition of *P. elongata* is not known in the literature, the description of the pigmentation is done by the genetically very similar alga *P. roscoffensis*, which also belongs to the genus *Pleurochrysis*.

**Characterisation**

Taxonomy [42]

<b>Empire</b>	Eukaryota
<b>Kingdom</b>	Chromista
<b>Phylum</b>	Haptophyta
<b>Class</b>	Coccolithophyceae
<b>Order</b>	Coccolithales
<b>Family</b>	Pleurochrysidaceae
<b>Genus</b>	Pleurochrysis

Pigments of the light-harvesting complex [65]

**accessory pigments**

major Fucoxanthin,  
Chlorophyll *a* + *c*<sub>1</sub> + *c*<sub>2</sub>

**reaction centre**

Chlorophyll *a*

Morphology

**Cell length** 18.0  $\mu\text{m}$   
**Cell shape** spherical to drop-shaped

**Cultivation**

Culture medium L1-Si  
Light intensity 0.277  $\text{W m}^{-2}$   
Light/dark cycles 10 h / 14 h  
Growth temperature 19 °C

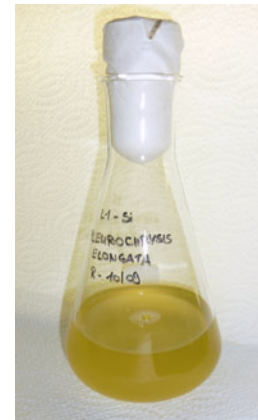


**Figure A.35.:** Cultivation of the microalga *Pleurochrysis elongata*

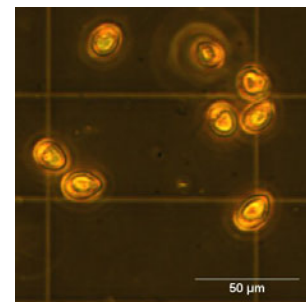


**Figure A.36.:** Microscopic photograph of drop shaped cells of *Pleurochrysis elongata* with Lugol's solution ( $I_2/KI$ ) as fixing agent

For the spectral characterisation, which is illustrated in Figure A.37, the algal sample was diluted in glycerine to avoid sedimentation of algae cells. An emission and an excitation spectrum were measured using the spectrofluorometer. For the emission spectrum the excitation wavelength was set to 440 nm, whereas the emission wavelength of 750 nm was used for the excitation spectrum. The measurement for each spectrum was repeated ten times and then the resulting excitation and emission spectra were averaged. After that, both spectra were normalised separately. The excitation spectrum was normalised to the Soret peak of chlorophyll *a* at 436 nm and the emission spectrum was normalised to the maximal chlorophyll fluorescence at 681 nm.

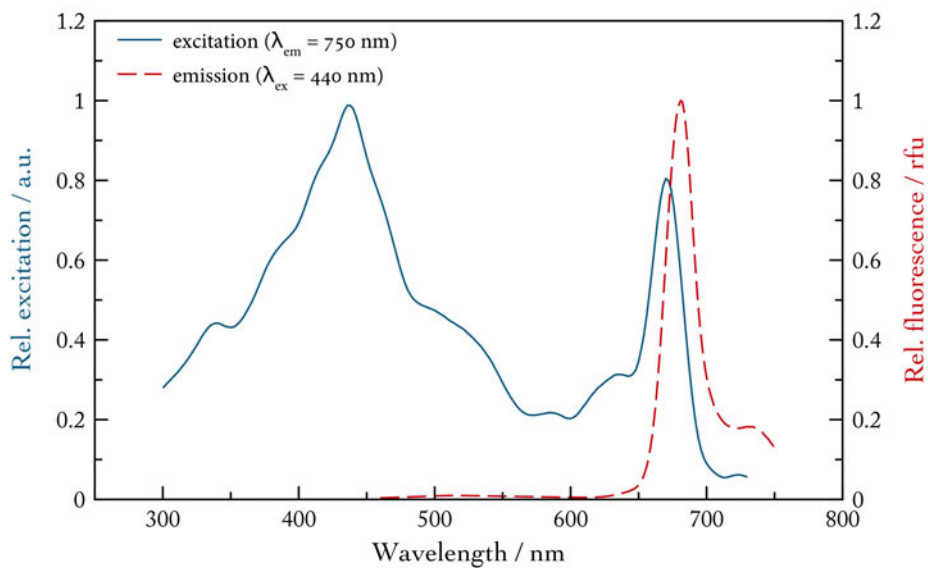


**Figure A.37.:** Normalised emission and excitation spectrum of *Pleurochrysis elongata* for spectral characterisation. Excitation at 440 nm, slitwidth = 14 nm, emission slitwidth = 7 nm. Emission at 750 nm, slitwidth = 14 nm, excitation slitwidth = 7 nm. Averaged spectra after 10 measurements.

## Isochrysis galbana – Parke

The golden-brown alga occurs in marine water systems and their cells are motile and stay solitary. Harmful effects are not known in the literature.

Moreover, *I. galbana* is used in aquacultures as feed for marine animals. [66]

### Characterisation

Taxonomy [42]

<b>Empire</b>	Eukaryota
<b>Kingdom</b>	Chromista
<b>Phylum</b>	Haptophyta
<b>Class</b>	Coccolithophyceae
<b>Order</b>	Isochrysidales
<b>Family</b>	Isochrysidaceae
<b>Genus</b>	Isochrysis

Pigments of the light-harvesting complex [51]

#### accessory pigments

major	Fucoxanthin, Diadinoxanthin, Chlorophyll <i>a</i> + <i>c</i> <sub>1</sub> + <i>c</i> <sub>2</sub>
minor	Diatoxanthin, $\beta$ -Carotene

#### reaction centre

Chlorophyll *a*

Morphology

<b>Cell diameter</b>	10.0 $\mu\text{m}$
<b>Cell shape</b>	ellipsoid, bi-flagellate [66]

### Cultivation

Culture medium	F <sub>2</sub> / 30%
Light intensity	0.277 W m <sup>-2</sup>
Light/dark cycles	10 h / 14 h
Growth temperature	19 °C



**Figure A.38.:** Cultivation of the microalga *Isochrysis galbana*

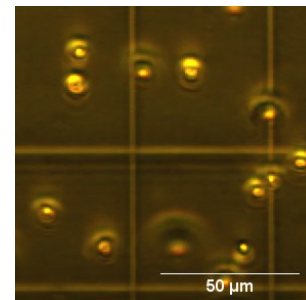


**Figure A.39.:** Solitary cells of *Isochrysis galbana* under the light microscope with Lugol's solution (*I*<sub>2</sub>/*KI*) as fixing agent

For the spectral characterisation of *I. galbana* as it is shown in Figure A.40, an algal sample was diluted in glycerine. An emission and an excitation spectrum were recorded using the spectrofluorometer. For the excitation spectrum, the emission wavelength was set to 750 nm and for the emission spectrum, the excitation was set to 440 nm. The measurement for each spectrum was repeated ten times and the resulting excitation and emission spectra were averaged and normalised separately. The excitation spectrum was normalised to the Soret band of chlorophyll *a* at 436 nm and the emission spectrum was normalised to the maximum of chlorophyll fluorescence at 682 nm.

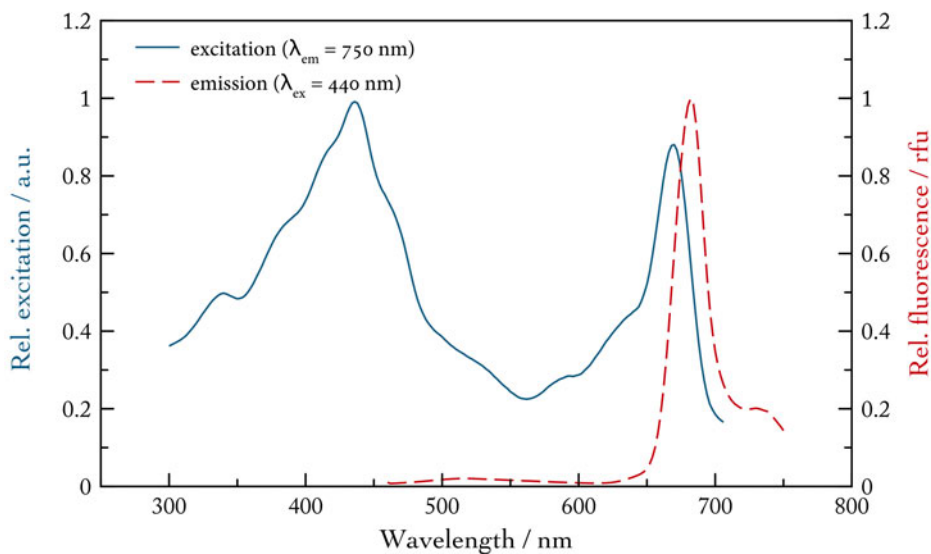


**Figure A.40.:** Normalised emission and excitation spectrum of *Isochrysis galbana* for spectral characterisation. Excitation at 440 nm, slitwidth = 14 nm, emission slitwidth = 7 nm. Emission at 750 nm, slitwidth = 14 nm, excitation slitwidth = 7 nm. Averaged spectra after 10 measurements.

## **Ruttnera spectabilis – Geitler**

*R. spectabilis* is a golden-brown microalga, which is distributed in freshwater, terrestrial and coastal regions. Harmful effects are not known in the literature. [58]

Besides, this microalga is more common under its taxonomic synonym *Chrysothila lamellosa*. [42]

### **Characterisation**

Taxonomy [42]

<b>Empire</b>	Eukaryota
<b>Kingdom</b>	Chromista
<b>Phylum</b>	Haptophyta
<b>Class</b>	Coccolithophyceae
<b>Order</b>	Isochrysidales
<b>Family</b>	Isochrysidaceae
<b>Genus</b>	Ruttnera

Pigments of the light-harvesting complex [65]

#### **accessory pigments**

major	Fucoxanthin, Chlorophyll <i>a</i> + <i>c</i> <sub>1</sub> + <i>c</i> <sub>2</sub>
-------	--

#### **reaction centre**

Chlorophyll *a*

Morphology

<b>Cell diameter</b>	9.0 $\mu\text{m}$
<b>Cell shape</b>	spherical to laminar [58]

### **Cultivation**

Culture medium	F <sub>2</sub> / 18%
Light intensity	0.277 W m <sup>-2</sup>
Light/dark cycles	10 h / 14 h
Growth temperature	19 °C

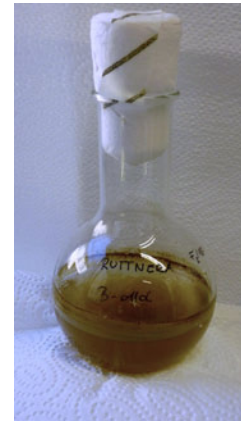


**Figure A.41.:** Cultivation of the microalga *Ruttnera spectabilis*

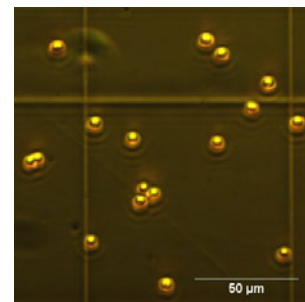


**Figure A.42.:** *Ruttnera spectabilis* under the microscope. Lugol's solution (*I*<sub>2</sub>/*KI*) used as fixing agent

Figure A.43 illustrates the averaged and normalised emission and excitation spectra of *R. spectabilis* to describe its spectral properties. The algal sample was diluted in glycerine to avoid sedimentation effects of the cells and measured using the spectrofluorometer. For the excitation spectrum, the emission wavelength was 750 nm and for the emission spectrum, the excitation wavelength was set to 440 nm. Each measurement was repeated ten times and the resulting excitation and emission spectra were averaged. Afterwards, the excitation spectrum was normalised to the Soret peak of chlorophyll *a* at 442 nm, but the emission spectrum was normalised to the maximal chlorophyll fluorescence at 678 nm.

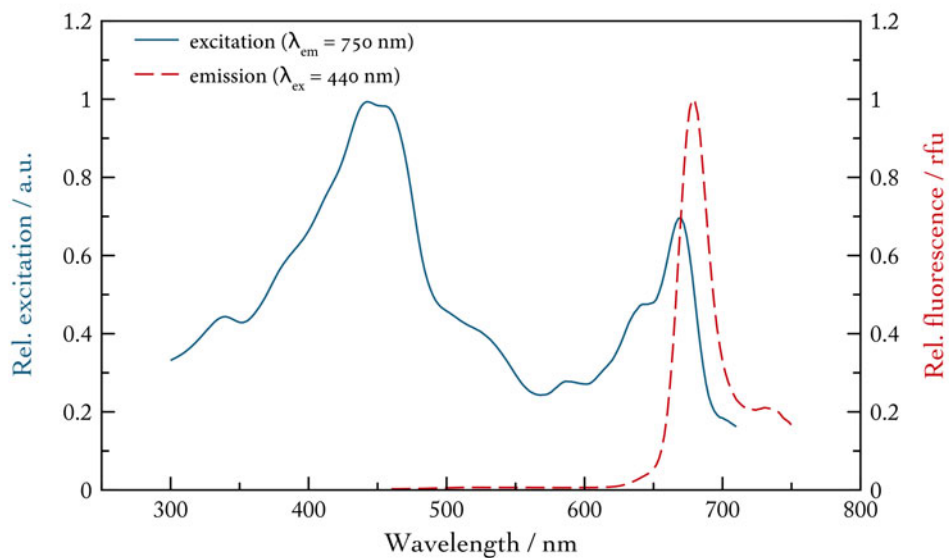


**Figure A.43.:** Normalised emission and excitation spectrum of *Ruttnera spectabilis* for spectral characterisation. Excitation at 440 nm, slitwidth = 14 nm, emission slitwidth = 7 nm. Emission at 750 nm, slitwidth = 14 nm, excitation slitwidth = 7 nm. Averaged spectra after 10 measurements.

## Prymnesium saltans – Massart

*P. saltans* is an unicellular, golden-brown microalga that could be found in marine water. [42, 67] It is a rare species and for some time, *P. saltans* was suggested to be of the same species as *P. parvum*. Hence, both marine algae were reported to form harmful algae blooms. In fact, unhealthy impacts are determined for *P. parvum*, however, the status of *P. saltans* remains unclear. [67]

Since a detailed pigmentation is not yet known in the literature, the description of the pigment composition is done by the genetically very similar alga *P. parvum*.

### Characterisation

Taxonomy [42]

<b>Empire</b>	Eukaryota
<b>Kingdom</b>	Chromista
<b>Phylum</b>	Haptophyta
<b>Class</b>	Coccolithophyceae
<b>Order</b>	Prymnesiales
<b>Family</b>	Prymnesiaceae
<b>Genus</b>	Prymnesium

Pigments of the light-harvesting complex [51]

#### **accessory pigments**

major Fucoxanthin, Diadinoxanthin, Diatoxanthin, Chlorophyll *a* + *c*<sub>3</sub> + *c*<sub>1</sub> [49]

minor  $\beta$ -Carotene

#### **reaction centre**

Chlorophyll *a*

Morphology

**Cell length** 14.0  $\mu\text{m}$

**Cell shape** oblong and irregular [67]

### Cultivation

Culture medium	F <sub>2</sub> / 18‰
Light intensity	0.277 W m <sup>-2</sup>
Light/dark cycles	10 h / 14 h
Growth temperature	19 °C



**Figure A.44.:** Cultivation of the microalga *Prymnesium saltans*

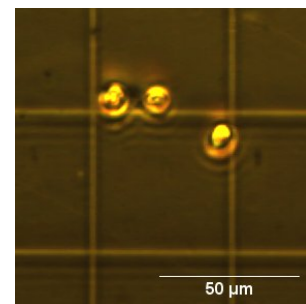


**Figure A.45.:** Microscopic photograph of *Prymnesium saltans* with Lugol's solution ( $I_2/KI$ ) as fixing agent

An emission spectrum and an excitation spectrum of the alga *P. saltans* were measured using the spectrofluorometer for spectral characterisation. The algal sample was diluted in glycerine and the emission wavelength for the excitation spectrum was set to 750 nm, whereas the excitation wavelength for the emission spectrum was 440 nm. The measurement for each spectrum was repeated ten times and then the resulting excitation and emission spectra were averaged. Both spectra were normalised separately as it is illustrated in Figure A.46. The excitation spectrum was normalised to the Soret peak of chlorophyll *a* at 440 nm and the emission spectrum was normalised to the maximal chlorophyll fluorescence at 680 nm.

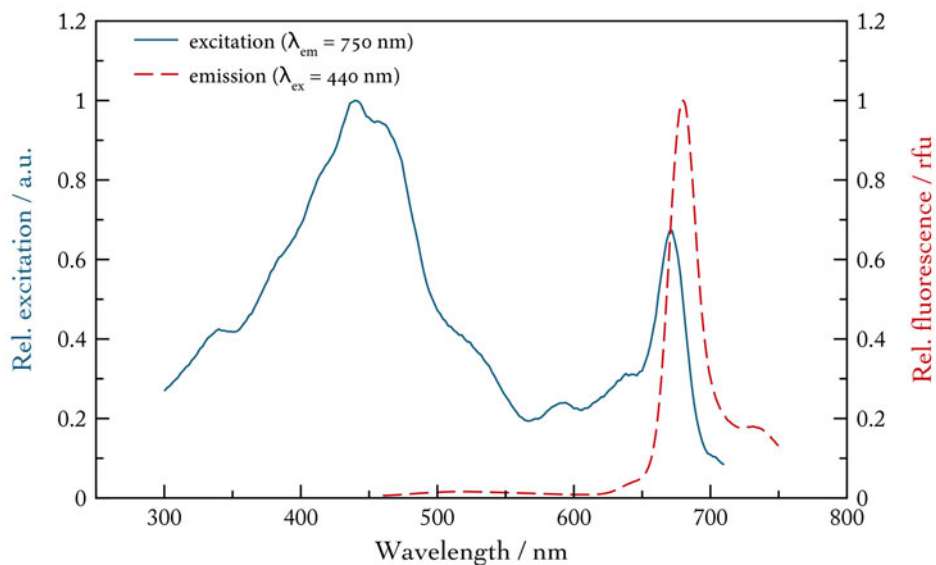


**Figure A.46.:** Normalised emission and excitation spectrum of *Prymnesium saltans* for spectral characterisation. Excitation at 440 nm, slitwidth = 14 nm, emission slitwidth = 7 nm. Emission at 750 nm, slitwidth = 14 nm, excitation slitwidth = 7 nm. Averaged spectra after 10 measurements.



## A.5. *Orchophyta*

The *Orchophyta* is a phylum belonging to the kingdom *Chromista*. In accordance to the algal database AlgaeBase, this phylum includes 3.793 algae species. [42]

These yellow-green algae mainly occur in the marine water, but few species prefer freshwater regions. They are consistent in their morphology, so they could be described as uniflagellate and spherical in shape.

In the literature no harmful effects, that were caused by algae species of this phylum, are reported. By contrast, due to their favourable cultivation conditions and their high biomass production, several algal species of the *Orchophyta* are a potential source for biofuel production. Furthermore, they were also used commercially in the pharmaceutical industry, since in some algae species one of the major accessory pigment is  $\beta$ -carotene.

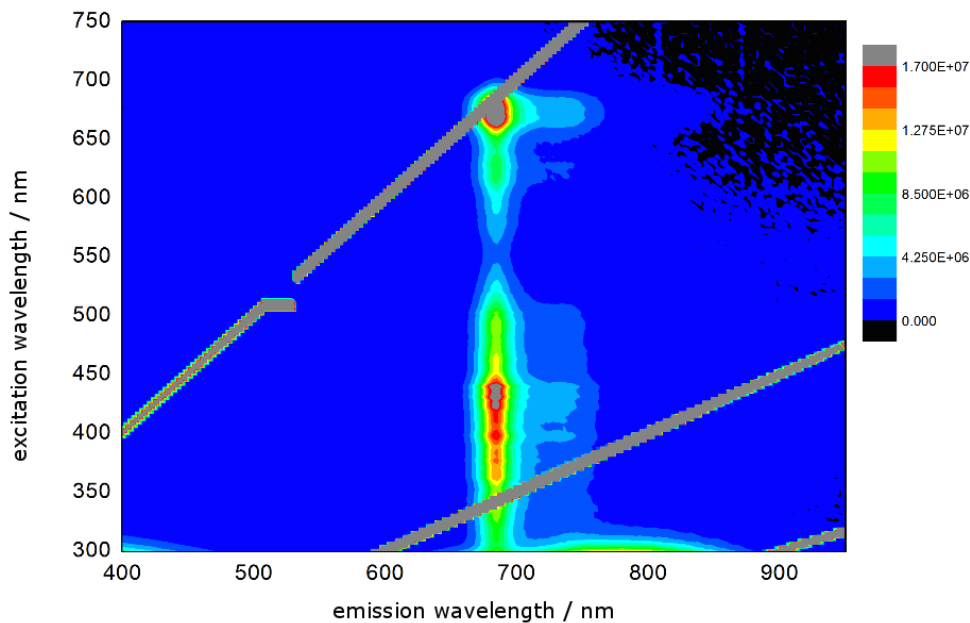


**Figure A.47.:** 3D spectrum of the algae species *Nannochloropsis salina* belonging to the phylum *Orchophyta*. Excitation between 300 - 750 nm, slitwidth = 2.5 nm; Emission between 400 - 950 nm, slitwidth = 2.5 nm.

Typical pigments, that are present in all algae species of this phylum, are  $\beta$ -carotene, *vaucheriaxanthin* and *chlorophyll a*. Due to the fact, that chlorophyll *a* is a ubiquitous photosynthetic pigment and also several carotenoids are part of different algae species of other classes, only *vaucheriaxanthin* could be used as potential "marker" pigment.

The spectral properties of algae belonging to the phylum *Orchophyta* are illustrated in Figure A.47. The significant emission band around 680 nm results from the fluorescence of chlorophyll *a*. Moreover, the intensive excitation in the range of 350 - 450 nm results from the excitation of  $\beta$ -carotene (425 nm, 449 nm, 475 nm, acetone/hexane) [17], the excitation of *vaucheriaxanthin* (418 nm, 441 nm, 470 nm, EtOH) [20] and the excitation of the Soret peak of chlorophyll *a* (432 nm) [44].

## Eustigmatos magnus – (J. B. Petersen) D. J. Hibberd

*E. magnus* is a yellow-green freshwater species that also occurs in terrestrial ecoregions. [42] An unhealthy impact of this microalga is not known in the literature, but, on the contrary, it is recognised as a source of valuable carotenoids, which have healthy and colouring properties. Besides, when the alga ages, it changes its colour from yellow-brown to yellow-orange due to an increased content of  $\beta$ -carotene. [68]

Furthermore, *E. magnus* is suggested as a potential feedstock for the biofuel production. [69]

### Characterisation

Taxonomy [42]

<b>Empire</b>	Eukaryota
<b>Kingdom</b>	Chromista
<b>Phylum</b>	Ochrophyta
<b>Class</b>	Eustigmatophyceae
<b>Order</b>	Eustigmatales
<b>Family</b>	Eustigmataceae
<b>Genus</b>	Eustigmatos

Pigments of the light-harvesting complex [68]

#### accessory pigments

major	$\beta$ -Carotene, Violaxanthin, Vaucheriaxanthin, Chlorophyll <i>a</i>
minor	Zeaxanthin, Luteoxanthin, Antheraxanthin

#### reaction centre

Chlorophyll *a*

Morphology

<b>Cell diameter</b>	15.0 $\mu\text{m}$
<b>Cell shape</b>	spherical, uniflagellate [42] eyespot at one end [70]

### Cultivation

Culture medium	MWC 0%
Light intensity	0.277 $\text{W m}^{-2}$
Light/dark cycles	10 h / 14 h
Growth temperature	19 °C



**Figure A.48.:** Cultivation of the microalga *Eustigmatos magnus*

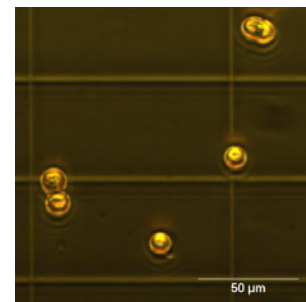


**Figure A.49.:** Spherical cells of *Eustigmatos magnus* with an eyespot under the light microscope. Lugol's solution ( $I_2/KI$ ) as fixing agent

For the description of the spectral behaviour of *E. magnus*, the algal sample was diluted in glycerine to avoid sedimentation of the cells. An excitation spectrum and an emission spectrum of the sample were recorded by using the spectrophotometer. The excitation wavelength for the emission spectrum was set to 440 nm and the emission wavelength for the excitation spectrum was set to 750 nm. The measurement for both spectra was repeated ten times and afterwards the resulting spectra were averaged and normalised as it could be seen in Figure A.50. The emission spectrum was normalised to the maximal chlorophyll fluorescence at 703 nm and the excitation spectrum was normalised to the Soret peak of chlorophyll *a* at 435 nm.

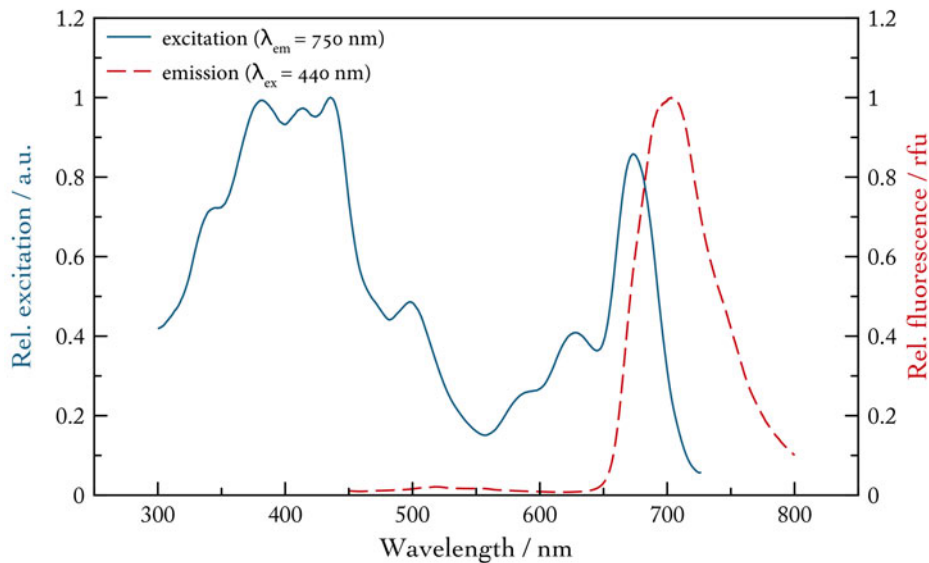


**Figure A.50.:** Normalised emission and excitation spectra of *Eustigmatos magnus*. Excitation at 440 nm, slitwidth = 5 nm, emission slitwidth = 5 nm. Emission at 750 nm, slitwidth = 20 nm, excitation slitwidth = 5 nm. Averaged spectra after 10 measurements.

## Nannochloropsis salina – D. J. Hibberd

This yellow-green marine alga is small and unicellular. Harmful effects are not known in the literature, rather it is used as a source for  $\beta$ -carotene in cosmetics or as feed in aquacultures. [42, 71]

### Characterisation

Taxonomy [42]

<b>Empire</b>	Eukaryota
<b>Kingdom</b>	Chromista
<b>Phylum</b>	Ochrophyta
<b>Class</b>	Eustigmatophyceae
<b>Order</b>	Eustigmatales
<b>Family</b>	Monodopsidaceae
<b>Genus</b>	Nannochloropsis

Pigments of the light-harvesting complex [72]

#### **accessory pigments**

major	Violaxanthin, Chlorophyll <i>a</i>
minor	Vaucheriaxanthin-(ester), Zeaxanthin, $\beta$ -Carotene

#### **reaction centre**

Chlorophyll *a*

Morphology

<b>Cell diameter</b>	6.0 $\mu\text{m}$
<b>Cell shape</b>	solitary, drop-shaped to cylindrical [73]

### Cultivation

Culture medium	special medium
Light intensity	0.13 $\text{W m}^{-2}$
Light/dark cycles	10 h / 14 h
Growth temperature	23 °C

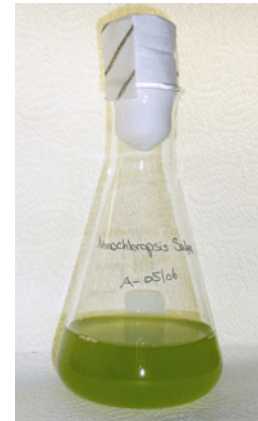


**Figure A.51.:** Cultivation of the microalga *Nannochloropsis salina*

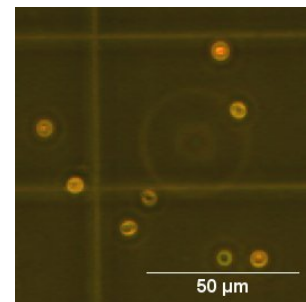


**Figure A.52.:** Microscopic photograph of *Nannochloropsis salina* with Lugol's solution ( $I_2/KI$ ) as fixing agent

An excitation and an emission spectrum of *N. salina* were measured using the spectrofluorometer for spectral characterisation. The algae sample was diluted in glycerine to avoid sedimentation of the cells. Then, an excitation wavelength of 440 nm was used for the emission spectrum. Moreover, the emission wavelength for the excitation spectrum was set to 750 nm. The measurement for each spectrum was repeated ten times and then the resulting spectra were averaged. Afterwards, both spectra were normalised separately as it is shown in Figure A.53. The excitation spectrum was normalised to the Soret band of chlorophyll *a* at 437 nm, whereas the emission spectrum was normalised to the maximal chlorophyll fluorescence at 688 nm.

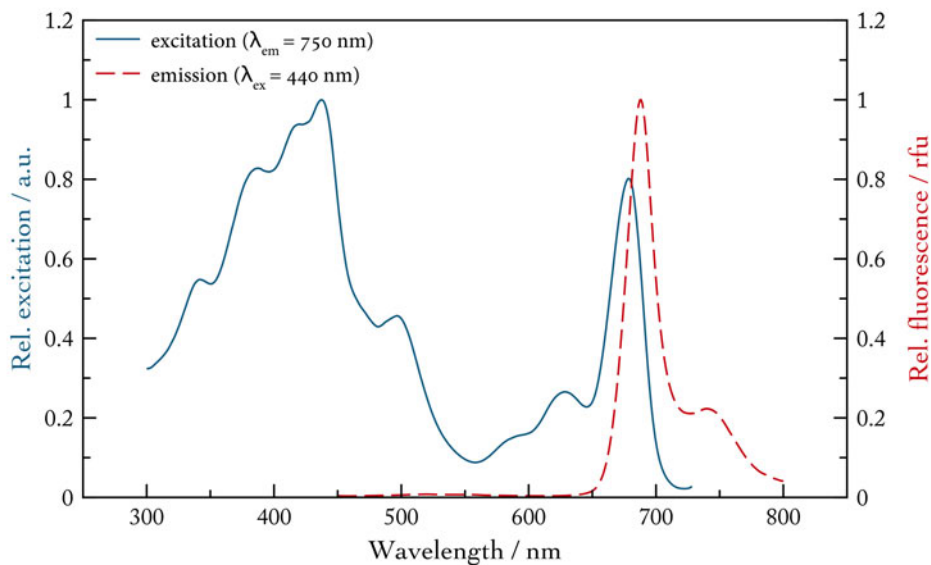


**Figure A.53.:** Normalised emission and excitation spectrum of *Nannochloropsis salina* for spectral characterisation. Excitation at 440 nm, slitwidth = 14 nm, emission slitwidth = 7 nm. Emission at 750 nm, slitwidth = 14 nm, excitation slitwidth = 7 nm. Averaged spectra after 10 measurements.

## **Chloridella neglecta – (Pascher & Geitler) Pascher**

This yellow-green marine alga is the lectotype of the genus *Chloridella*. The information in the literature and studies about this species are rare, therefore harmful effects are not noted so far. [42]

Since a detailed pigment composition of this rarely analysed algae species is not known in the literature, the description of the pigments is done by the class *xanthophyceae*.

### **Characterisation**

Taxonomy [42]

<b>Empire</b>	Eukaryota
<b>Kingdom</b>	Chromista
<b>Phylum</b>	Ochrophyta
<b>Class</b>	Xanthophyceae
<b>Order</b>	Mischococcales
<b>Family</b>	Pleurochloridaceae
<b>Genus</b>	<i>Chloridella</i>

Pigments of the light-harvesting complex [20]

#### **accessory pigments**

major	Diadinoxanthin, Diatoxanthin, Heteroxanthin, Vaucheriaxanthin, Vaucheriaxanthin-ester, Chlorophyll <i>a</i>
minor	$\beta$ -Carotene, Neoxanthin
reaction centre	Chlorophyll <i>a</i>

Morphology

<b>Cell diameter</b>	17.0 $\mu\text{m}$
<b>Cell shape</b>	spherical with an eyespot at one end [70]

### **Cultivation**

Culture medium	MWC 0%
Light intensity	0.277 $\text{W m}^{-2}$
Light/dark cycles	10 h / 14 h
Growth temperature	19 °C

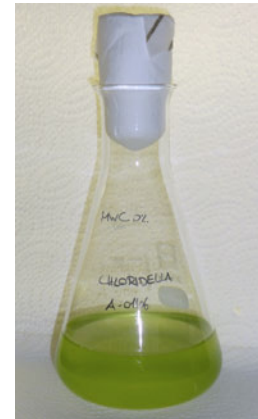


**Figure A.54.:** Cultivation of the microalga *Chloridella neglecta*

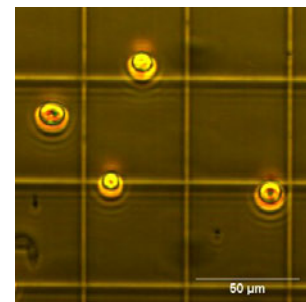


**Figure A.55.:** Spherical cells of *Chloridella neglecta* under the microscope. Lugol's solution ( $\text{I}_2/\text{KI}$ ) used as fixing agent

To describe the spectral behaviour of *Chl. neglecta*, an algal sample was first diluted in glycerine to avoid sedimentation. Then, an emission and an excitation spectrum were measured using the spectrophotometer. For the excitation spectrum an emission wavelength of 750 nm was chosen. For the emission spectrum an excitation of 440 nm was used. The measurements were repeated ten times and then, the resulting spectra were averaged and normalised. The excitation spectrum was normalised to the maximal excitation at 381 nm, whereas the emission spectrum was normalised to the maximal chlorophyll fluorescence at 707 nm. An overlaid plot of both spectra is shown in Figure A.56.

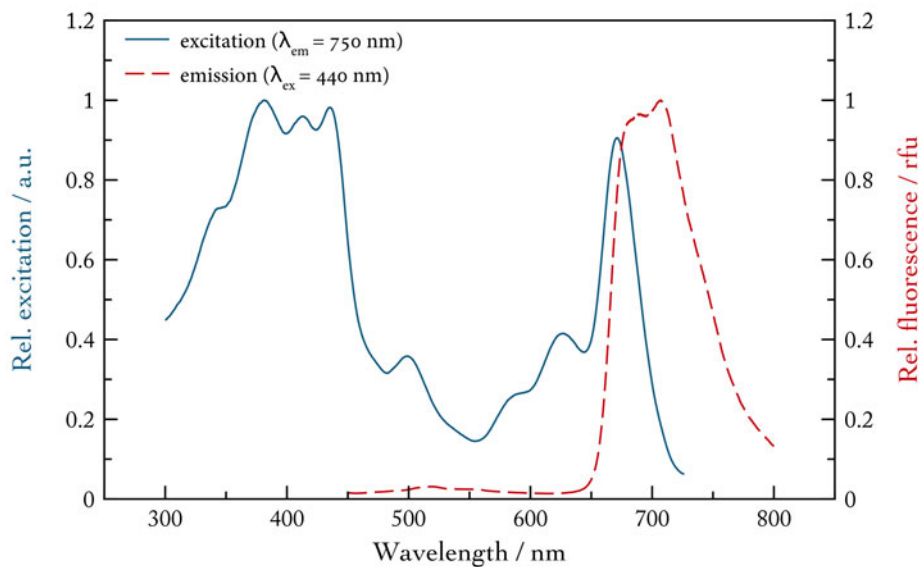


**Figure A.56.:** Normalised emission and excitation spectrum of *Chloridella neglecta* for spectral characterisation. Excitation at 440 nm, slitwidth = 5 nm, emission slitwidth = 5 nm. Emission at 750 nm, slitwidth = 20 nm, excitation slitwidth = 5 nm. Averaged spectra after 10 measurements.

## Unknown microalga

We got this microalga from our supplier under the name *Chrysochromulina chiton*. However, *Ch. chiton* is a golden-brown microalga but the grown algae is dark green. Moreover, the recorded excitation spectrum (compare Figure A.59) suggests that this microalga is more similar to a *Orchophyta* or *Chlorophyta* species than to a *Haptophyta* species.

Since the species remains unknown, a detailed pigment composition could not be researched. Therefore, the spectral characterisation is carried out by the phylum to which the alga probably belongs. The list below includes only the pigments, that are contained in all algae species belonging to the phylum *Orchophyta* and *Chlorophyta*.

### Characterisation

Taxonomy [42]

<b>Empire</b>	Eukaryota
<b>Kingdom</b>	unknown
<b>Phylum</b>	unknown
<b>Class</b>	unknown
<b>Order</b>	unknown
<b>Family</b>	unknown
<b>Genus</b>	unknown

Pigments of the light-harvesting complex [74]  
**accessory pigments**

$\beta$ -Carotene, Chlorophyll *a*

**reaction centre**

Chlorophyll *a*

Morphology

<b>Cell length</b>	20.0 $\mu\text{m}$
<b>Cell shape</b>	spherical and elongate

### Cultivation

Culture medium	F <sub>2</sub> / 30%
Light intensity	0.277 W m <sup>-2</sup>
Light/dark cycles	10 h / 14 h
Growth temperature	19 °C

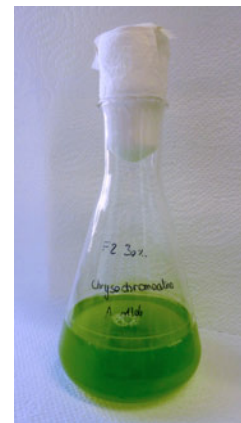


**Figure A.57.:** Cultivation of the nameless microalga

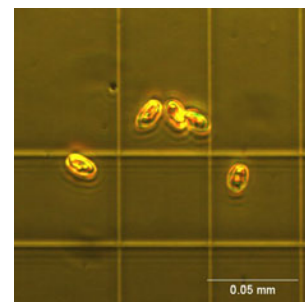


**Figure A.58.:** Elongated cells of the unknown algae under the light microscope using Lugol's solution ( $I_2/KI$ ) as fixing agent

For the spectral characterisation of this algae species, a sample was diluted in glycerine to avoid the sedimentation of the algae cells. Then, an emission spectrum as well as an excitation spectrum were measured using the spectrophotometer. The excitation wavelength for the emission spectrum was set to 440 nm, whereas the emission wavelength for the excitation spectrum was set to 750 nm. The measurement of each type of spectrum was repeated ten times and then the resulting spectra were averaged. Afterwards, the emission spectrum was normalised to the maximal chlorophyll fluorescence at 686 nm and the excitation spectrum was normalised to the excitation maximum at 376 nm. The results are given in Figure A.59.

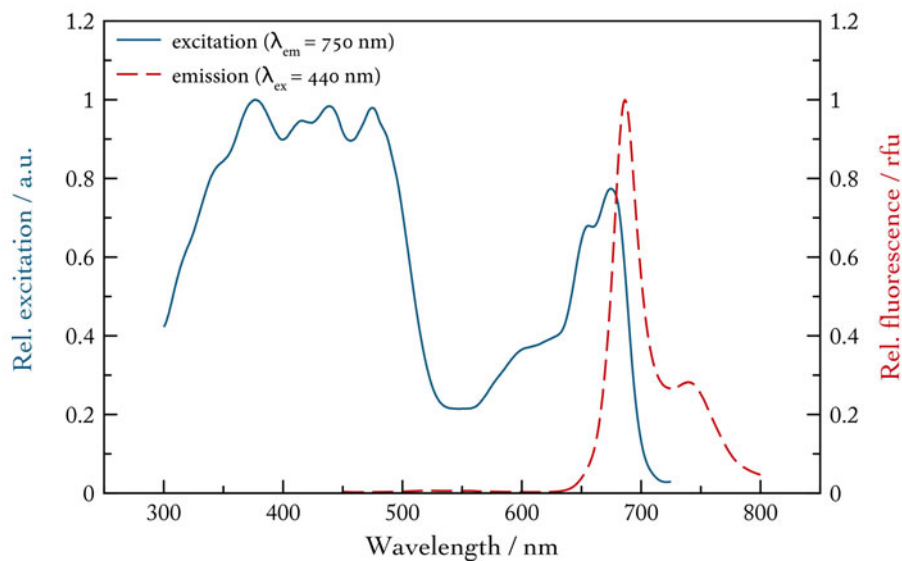


**Figure A.59.:** Normalised emission and excitation spectra of the nameless algae. Excitation at 440 nm, slitwidth = 5 nm, emission slitwidth = 5 nm. Emission at 750 nm, slitwidth = 20 nm, excitation slitwidth = 5 nm. Averaged spectra after 10 measurements.



## A.6. Chlorophyta

*Chlorophyta* are the typical and well-known "green algae" belonging to the kingdom *Plantae*. According to the algae-database AlgaeBase this phylum includes 6.032 algae species. [42]

These algae are mainly found in freshwater areas, but few of them inhabit also marine regions. Furthermore, *Chlorophyta* are bi-flagellate and ellipsoid or oval in their cell shape.

Harmful effects caused by algae species belonging to the *Chlorophyta* are not known in the literature. However, it is reported that some species are used in ecotoxicological tests. Besides, other species are a potential source for the biodiesel production or are suggested to have some healthy effects. They are able to accumulate astaxanthin or produce  $\beta$ -carotene as photosynthetic pigment, which have antioxidative properties. Therefore, these algae species are used in medical tests or as nutritional supplement.

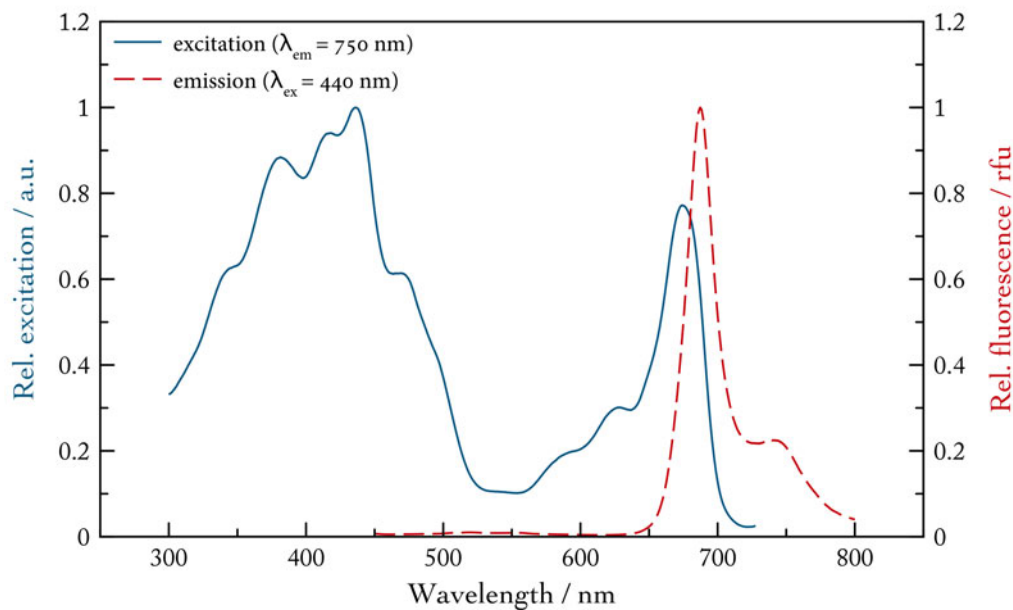


**Figure A.60.:** Averged excitation and emission spectrum of *Selenastrum capricornutum* belonging to the phylum *Chlorophyta*. Excitation at 440 nm, slitwidth = 14 nm; Emission at 750 nm, slitwidth = 7 nm. Averaged spectra after 10 measurements.

Typical pigments, that are part of the light-harvesting complex in all algae of the phylum *Chlorophyta*, are lutein,  $\beta$ -carotene and chlorophyll *a* + *b* as major pigments and violaxanthin and neoxanthin as minor pigments in the photosystems. Furthermore, chlorophyll *a* is the typical dimer in the reaction centre. The pigment that is most suitable being the "marker" pigment of the phylum *Chlorophyta*, is lutein; especially in the combination with chlorophyll *b*. Lutein is the major pigment in the light-harvesting complex and it does not appear in algae species belonging to other phyla. The absorption behaviour of these pigments leads to the overlapped excitation spectrum shown in Figure A.60. The spectral behaviour of the chlorophyta is predominantly defined by  $\beta$ -carotene (425, 449, 475 nm, acetone/hexane), lutein (445, 473 nm) and chlorophyll *a* (Soret band around 432 nm and *Q* band around 670 nm) and chlorophyll *b* (472.5, 655.5 nm, pyridinine). Moreover, violaxanthin (439, 468 nm) and neoxanthin (416, 440, 469 nm) are also typical pigments in the chlorophyta. [17, 75, 76]

## **Tetraselmis suecica – (Kylin) Butcher**

*T. suecica* is a bright-green microalga that is widely distributed in marine and brackish water. So far, unhealthy impacts are not known in the literature. [77]

On the contrary, algae species belonging to the genus *Tetraselmis* are rich in proteins and therefore might be used as nutritional supplements in human or animal feed. [71]

### **Characterisation**

Taxonomy [42]

<b>Empire</b>	Eukaryota
<b>Kingdom</b>	Plantae
<b>Phylum</b>	Chlorophyta
<b>Class</b>	Chlorodendrophyceae
<b>Order</b>	Chlorodendrales
<b>Family</b>	Chlorodendraceae
<b>Genus</b>	Tetraselmis

Pigments of the light-harvesting complex [78, 51]

#### **accessory pigments**

major	Lutein, Chlorophyll <i>a + b</i>
minor	$\beta$ -Carotene, Neoxanthin, Violaxanthin
trace	Antheraxanthin, Zeaxanthin
<b>reaction centre</b>	Chlorophyll <i>a</i>

Morphology

<b>Cell length</b>	18.0 $\mu m$
<b>Cell shape</b>	compressed, elliptical to oviform [77]

### **Cultivation**

Culture medium	MWC 0%
Light intensity	0.277 W m <sup>-2</sup>
Light/dark cycles	10 h / 14 h
Growth temperature	19 °C



**Figure A.61.:** Cultivation of the microalga *Tetraselmis suecica*

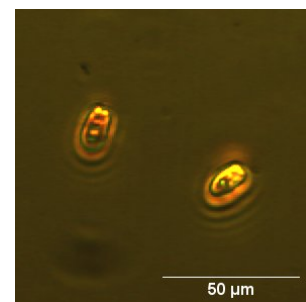


**Figure A.62.:** Solitary but compressed cells of *Tetraselmis suecica* under the microscope. Lugol's solution ( $I_2/KI$ ) used as fixing agent

As it is illustrated in Figure A.63, an emission and an excitation spectrum were measured for spectral characterisation of *T. suecica*. For this, the algal sample was diluted in glycerine to avoid sedimentation of the cells. Using the spectrofluorometer, an excitation and an emission spectrum were measured. For the emission spectrum the sample was excited at 440 nm, whereas for the excitation spectrum, the emission wavelength was set to 750 nm. The measurement was repeated ten times and then the resulting excitation and emission spectra were averaged and normalised separately as it is shown in Figure A.63. The excitation spectrum was normalised to the Soret peak of chlorophyll *a* at 434 nm and the emission spectrum was normalised to the maximal chlorophyll fluorescence at 682 nm.

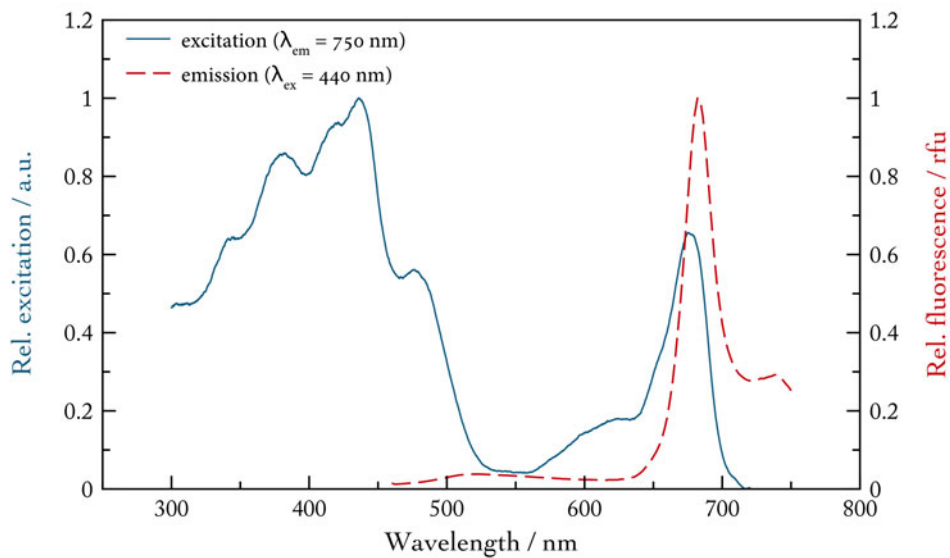


**Figure A.63.:** Normalised emission and excitation spectrum of *Tetraselmis suecica* for spectral characterisation. Excitation at 440 nm, slitwidth = 14 nm, emission slitwidth = 7 nm. Emission at 750 nm, slitwidth = 14 nm, excitation slitwidth = 7 nm. Averaged spectra after 10 measurements.

## **Chlamydomonas reinhardtii – P.A.Dangeard**

*Ch. reinhardtii* is a green microalga which is found in freshwater areas, stagnant water or on humid soil. It could also be found in marine zones or in snow. [79]

This alga is well described and analysed, hence it becomes a "model-alga", which is used for further investigations, medical or biological studies and toxicological tests. In addition, harmful effects of *Ch. reinhardtii* are not known in the literature. [80]

### **Characterisation**

Taxonomy [42]

<b>Empire</b>	Eukaryota
<b>Kingdom</b>	Plantae
<b>Phylum</b>	Chlorophyta
<b>Class</b>	Chlorophyceae
<b>Order</b>	Chlamydomonadales
<b>Family</b>	Chlamydomonadaceae
<b>Genus</b>	Chlamydomonas

Pigments of the light-harvesting complex [59]

#### **accessory pigments**

major	Lutein, Chlorophyll <i>a + b</i>
minor	Neoxanthin, Antheraxanthin, Zeaxanthin, Carotene, Violaxanthin

#### **reaction centre**

Chlorophyll *a*

Morphology

<b>Cell diameter</b>	14.0 $\mu\text{m}$
<b>Cell shape</b>	oval, bi-flagellate [81]

### **Cultivation**

Culture medium	MWC 0%
Light intensity	0.277 $\text{W m}^{-2}$
Light/dark cycles	10 h / 14 h
Growth temperature	19 °C

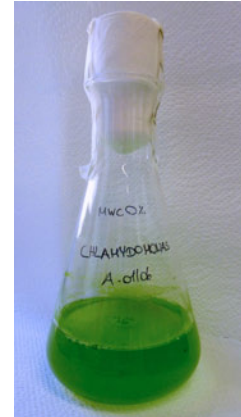


**Figure A.64.:** Cultivation of the microalga *Chlamydomonas reinhardtii*

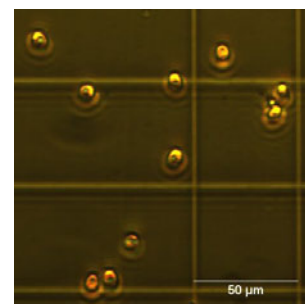


**Figure A.65.:** Microscopic photograph of *Chlamydomonas reinhardtii* with Lugol's iodine ( $I_2/KI$ ) as fixing agent

For the spectral characterisation of *Ch. reinhardtii* the algal sample was diluted in glycerine. An emission and an excitation spectrum were measured using the spectrofluorometer. For the excitation spectrum, the emission wavelength was set to 750 nm, whereas the excitation wavelength for the emission spectrum was 440 nm. The measurement for each spectrum was repeated ten times and then the resulting excitation and emission spectra were averaged. Afterwards, both spectra were normalised separately. The excitation spectrum was normalised to the Soret band of chlorophyll *a* at 436 nm. The emission spectrum, by contrast, was normalised to the maximal chlorophyll fluorescence at 684 nm. The results are given in Figure A.66.

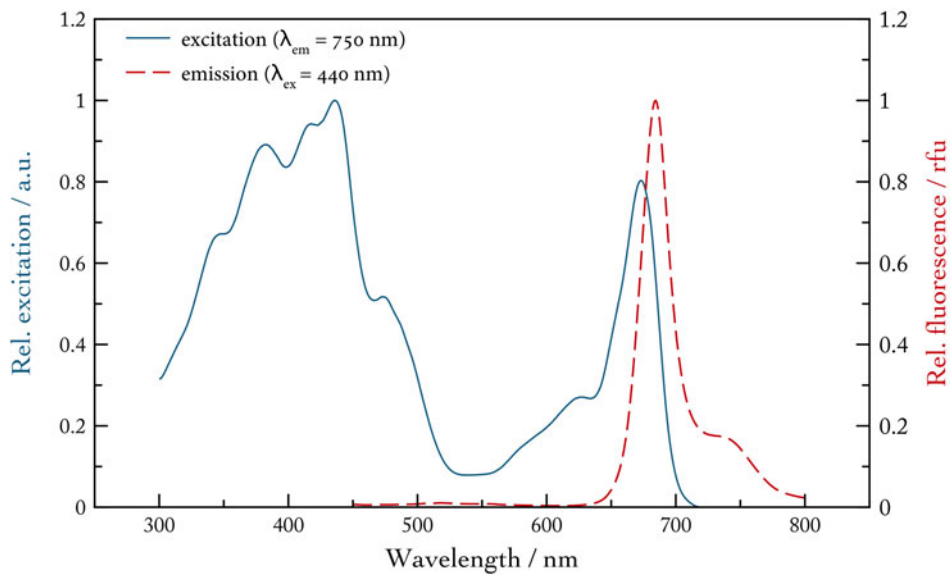


**Figure A.66.:** Normalised emission and excitation spectrum of *Chlamydomonas reinhardtii* for spectral characterisation. Excitation at 440 nm, slitwidth = 14 nm, emission slitwidth = 7 nm. Emission at 750 nm, slitwidth = 14 nm, excitation slitwidth = 7 nm. Averaged spectra after 10 measurements.

## **Choricystis minor – (Skuja) Fott**

The green microalga is a cosmopolitan alga that is found in freshwater and in nutrient-poor lakes. Unhealthy effects of this alga are not known in the literature. [82]

Moreover, it was also reported, that *Ch. minor* could be used to produce biodiesel under certain cultivation conditions. [83]

Since a detailed pigment composition of the microalga is not known in the literature, the description of the photosynthetic pigments, which are expected to be part of the light-harvesting system, is done by the phylum in general.

### **Characterisation**

Taxonomy [42]

<b>Empire</b>	Eukaryota
<b>Kingdom</b>	Plantae
<b>Phylum</b>	Chlorophyta
<b>Class</b>	Chlorophyceae
<b>Order</b>	Chlamydomonadales
<b>Family</b>	Coccomyxaceae
<b>Genus</b>	Choricystis

Pigments of the light-harvesting complex

#### **accessory pigments**

major	Lutein, $\beta$ -Carotene, Chlorophyll <i>a</i> + <i>b</i>
minor	Violaxanthin, Neoxanthin

#### **reaction centre**

Chlorophyll *a*

Morphology

<b>Cell diameter</b>	7.7 $\mu\text{m}$
<b>Cell shape</b>	ellipsoid, coccoid [84]

### **Cultivation**

Culture medium	MWC 0%
Light intensity	0.277 $\text{W m}^{-2}$
Light/dark cycles	10 h / 14 h
Growth temperature	19 °C

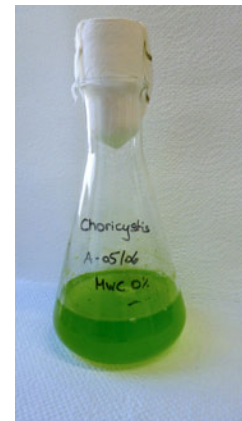


**Figure A.67.:** Cultivation of the microalga *Choricystis minor*

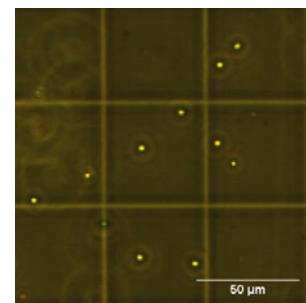


**Figure A.68.:** Coccoidal cells of *Choricystis minor* under the microscope. Lugol's solution ( $I_2/KI$ ) used as fixing agent

An emission and an excitation spectrum of *Ch. minor* were measured for spectral characterisation (compare Figure A.69). The algal sample was diluted in glycerine to avoid sedimentation of the cells and then an emission spectrum and an excitation spectrum were measured using the spectrofluorometer. The excitation wavelength for the emission spectrum was 440 nm and the emission wavelength for the excitation spectrum was 750 nm. The measurement for each spectrum was repeated ten times and then the resulting spectra were averaged and normalised separately. The excitation spectrum was normalised to the Soret peak of chlorophyll *a* at 437 nm, whereas the emission spectrum was normalised to the maximal chlorophyll fluorescence at 687 nm.

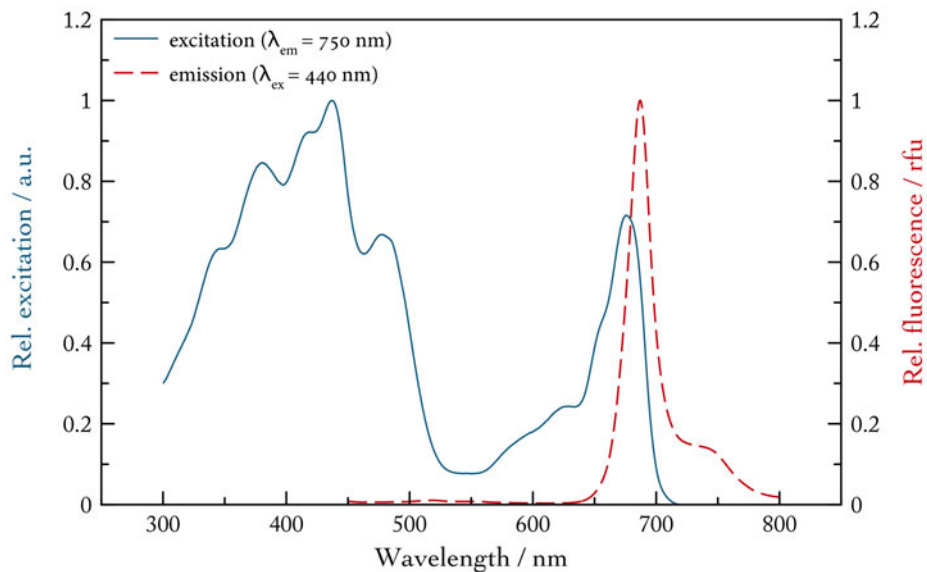


**Figure A.69.:** Normalised emission and excitation spectrum of *Choricystis minor* for spectral characterisation. Excitation at 440 nm, slitwidth = 14 nm, emission slitwidth = 7 nm. Emission at 750 nm, slitwidth = 14 nm, excitation slitwidth = 7 nm. Averaged spectra after 10 measurements.

## Dunaliella salina – (Dunal) Teodoresco

*D. salina* is a highly variable, non-toxic microalga. It mainly occurs in marine and halophilic areas, but can also be found in freshwater regions. Furthermore, this alga is very tolerant to pH-fluctuations although it prefers high pH-values. Moreover, the content of  $\beta$ -carotene in *D. salina* is high, so the alga is a well-known feedstock for the pharmaceutical and food industry. [85] Furthermore, *D. salina* is used for biodiesel production. [71]

Considering the cell shape and the algal colour, *D. salina* is a flexible alga. Depending on the season, *D. salina* changes its colour from red to green. Even the cell shape might change depending on environmental conditions – the cells could be ellipsoidal, oval, egg-shaped or spindle-shaped. [86]

### Characterisation

Taxonomy [42]

<b>Empire</b>	Eukaryota
<b>Kingdom</b>	Plantae
<b>Phylum</b>	Chlorophyta
<b>Class</b>	Chlorophyceae
<b>Order</b>	Chlamydomonadales
<b>Family</b>	Dunaliellaceae
<b>Genus</b>	Dunaliella

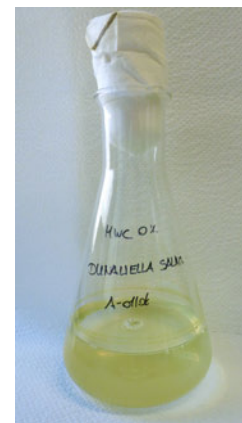


**Figure A.70.:** Cultivation of the algae species *Dunaliella salina*

Pigments of the light-harvesting complex [86]

#### **accessory pigments**

major	$\beta$ -Carotene, Chlorophyll <i>a</i> + <i>b</i>
minor	Lutein, Neoxanthin, Zeaxanthin

#### **reaction centre**

Chlorophyll *a*

Morphology

<b>Cell diameter</b>	14.0 $\mu\text{m}$
<b>Cell shape</b>	spherical to spindle-shaped, eyespot on one side, unicellular, bi-flagellate [85]

### Cultivation

Culture medium	MWC 0%
Light intensity	0.277 $\text{W m}^{-2}$
Light/dark cycles	10 h / 14 h
Growth temperature	19 °C

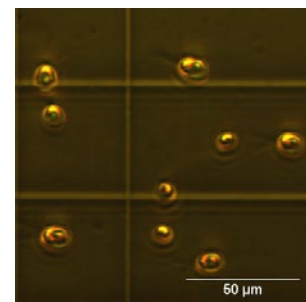


**Figure A.71.:** Spherical cells of *Dunaliella salina* under the microscope. Lugol's solution ( $\text{I}_2/\text{KI}$ ) used as fixing agent

For the spectral characterisation of *D. salina*, an algal sample was diluted in glycerine. Then an excitation and an emission spectrum were measured using the spectrofluorometer. The emission wavelength for the excitation spectrum was set to 750 nm, whereas the excitation wavelength for the emission spectrum was set to 440 nm. The measurement for each spectrum was repeated ten times and then the resulting spectra were averaged. After the measurement, both spectra were normalised as it is illustrated in Figure A.72. The emission spectrum was normalised to the maximal chlorophyll fluorescence at 684 nm and the excitation spectrum was normalised to the Soret peak of chlorophyll *a* at 436 nm.

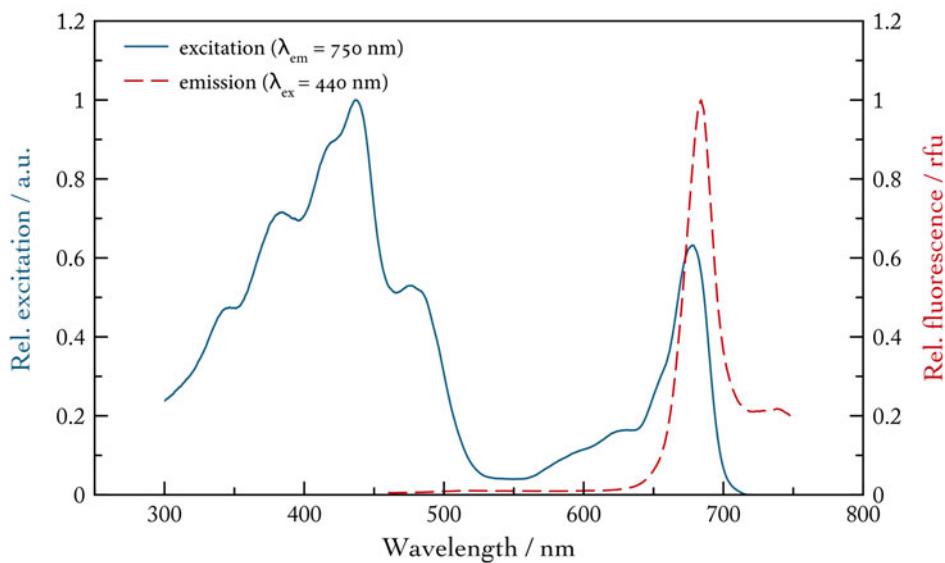


**Figure A.72.:** Normalised emission and excitation spectrum of *Dunaliella salina* for spectral characterisation. Excitation at 440 nm, slitwidth = 14 nm, emission slitwidth = 7 nm. Emission at 750 nm, slitwidth = 14 nm, excitation slitwidth = 7 nm. Averaged spectra after 10 measurements.

## **Dunaliella tertiolecta – Butcher**

The cell shape of this green marine alga can vary and may form symmetrical, oval or even pyriform cells. So far, harmful effects are not known in the literature. [42]

### **Characterisation**

Taxonomy [42]

<b>Empire</b>	Eukaryota
<b>Kingdom</b>	Plantae
<b>Phylum</b>	Chlorophyta
<b>Class</b>	Chlorophyceae
<b>Order</b>	Chlamydomonadales
<b>Family</b>	Dunaliellaceae
<b>Genus</b>	Dunaliella

Pigments of the light-harvesting complex [46]

#### **accessory pigments**

major	Lutein, Chlorophyll <i>a + b</i>
minor	Neoxanthin, Fucoxanthin, Antheraxanthin, Zeaxanthin, $\beta$ -Carotene

#### **reaction centre**

Chlorophyll *a*

Morphology

<b>Cell diameter</b>	14.0 $\mu\text{m}$
<b>Cell shape</b>	radially symmetrical, oval, bi-flagellate [42]

### **Cultivation**

Culture medium	MWC 0%
Light intensity	0.277 $\text{W m}^{-2}$
Light/dark cycles	10 h / 14 h
Growth temperature	19 °C

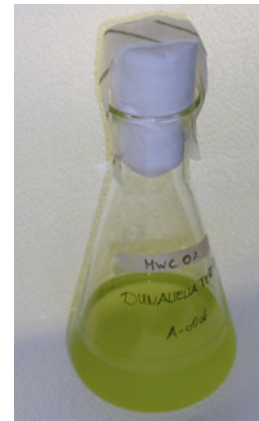


**Figure A.73.:** Cultivation of the microalga *Dunaliella tertiolecta*

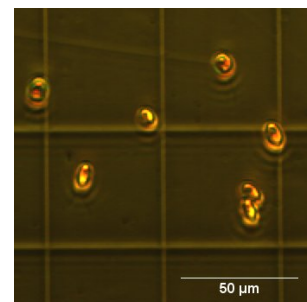


**Figure A.74.:** Oval cells of *Dunaliella tertiolecta* under the microscope. Lugol's solution ( $I_2/KI$ ) as fixing agent

For the spectral characterisation of *D. tertiolecta*, an excitation and an emission spectrum were measured using the spectrofluorometer (compare Figure A.75). The excitation wavelength for the emission spectrum was set to 440 nm and the emission wavelength for the excitation was set to 750 nm. The measurement for each spectrum was repeated ten times and the resulting spectra were averaged. Then, both spectra were normalised – the excitation spectrum was normalised to the Soret peak of chlorophyll *a* at 435 nm, whereas the emission spectrum was normalised to the maximal chlorophyll fluorescence at 681 nm. The sample was diluted in glycerine to avoid sedimentation of the algae cells.

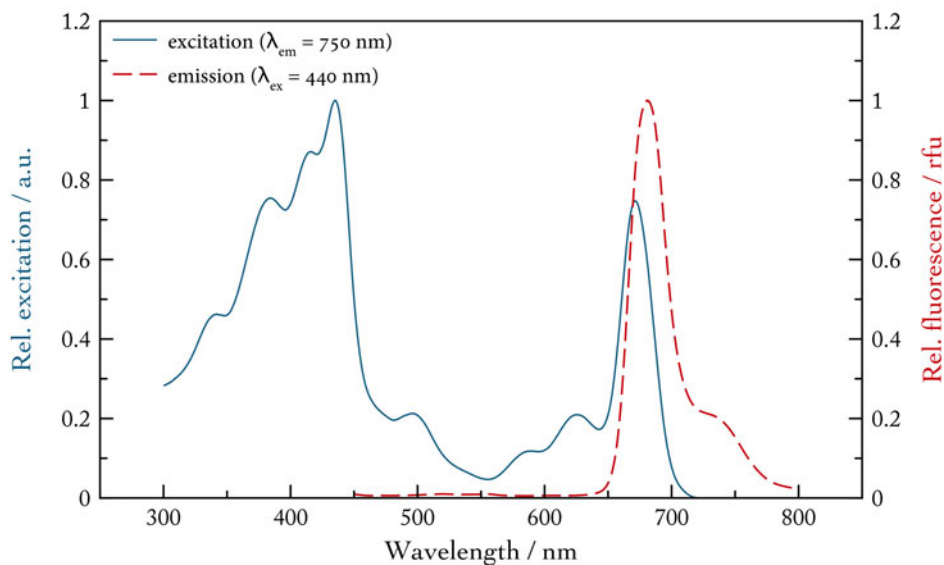


**Figure A.75.:** Normalised emission and excitation spectrum of *Dunaliella tertiolecta* for spectral characterisation. Excitation at 440 nm, slitwidth = 14 nm, emission slitwidth = 7 nm. Emission at 750 nm, slitwidth = 14 nm, excitation slitwidth = 7 nm. Averaged spectra after 10 measurements.

## Haematococcus pluvialis – Flotow

*H. pluvialis* is a freshwater species that normally appears as green and motile alga. Under unfavourable conditions, however, it becomes non-motile and red. [87] This red colour results from astaxanthin, which could be accumulated by the alga under stressful conditions. Due to the fact, that antioxidative properties are attributed to astaxanthin, the alga is of interest to the industry. [88]

Moreover until now, harmful effects of this microalga are not known in the literature. [88]

### Characterisation

Taxonomy [42]

<b>Empire</b>	Eukaryota
<b>Kingdom</b>	Plantae
<b>Phylum</b>	Chlorophyta
<b>Class</b>	Chlorophyceae
<b>Order</b>	Chlamydomonadales
<b>Family</b>	Haematococcaceae
<b>Genus</b>	Haematococcus

Pigments of the light-harvesting complex [89]

#### accessory pigments

major	$\beta$ -Carotene, Astaxanthin, Chlorophyll <i>a</i> + <i>b</i>
minor	Lutein

#### reaction centre

Chlorophyll *a*

Morphology

<b>Cell diameter</b>	26.0 $\mu\text{m}$
<b>Cell shape</b>	spherical, unicellular, bi-flagellate [87]

### Cultivation

Culture medium	MWC 0%
Light intensity	0.277 $\text{W m}^{-2}$
Light/dark cycles	10 h / 14 h
Growth temperature	19 °C

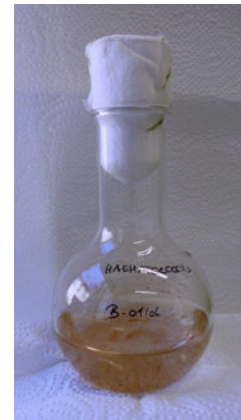


**Figure A.76.:** Cultivation of the microalga *Haematococcus pluvialis* under unfavourable conditions

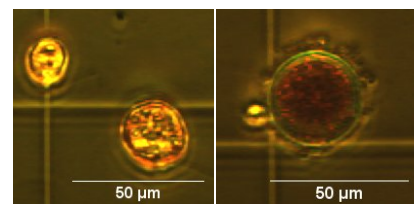


**Figure A.77.:** Microscopic photograph of green and motile (left) or red and non-motile (right) *H. pluvialis*. Lugol's solution ( $I_2/KI$ ) was used as fixing agent

An excitation spectrum as well as an emission spectrum were measured for the spectral characterisation of the red and non-motile *H. pluvialis*. First, the algal sample was diluted in glycerine and then measured using the spectrofluorometer. For the excitation spectrum, the emission wavelength was set to 750 nm and for the emission spectrum, the excitation wavelength was 440 nm. The measurement for each spectrum was repeated ten times and the resulting excitation and emission spectra were averaged. Afterwards, both spectra were normalised separately as it is shown in Figure A.78. The excitation spectrum was normalised to the Soret peak of chlorophyll *a* at 436 nm, whereas the emission spectrum was normalised to the maximal chlorophyll fluorescence at 685 nm.

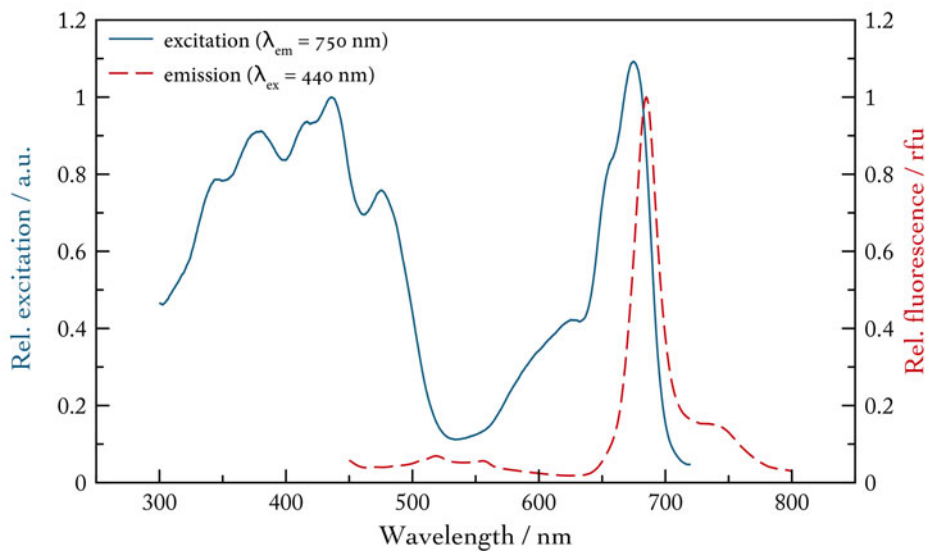


**Figure A.78.:** Normalised emission and excitation spectrum of the red and non-motile *Haematococcus pluvialis* for spectral characterisation. Excitation at 440 nm, slitwidth = 14 nm, emission slitwidth = 7 nm. Emission at 750 nm, slitwidth = 14 nm, excitation slitwidth = 7 nm. Averaged spectra after 10 measurements.

## Scenedesmus sp.

*S. sp.* is a green microalga which is found in freshwater areas. [42] Unhealthy effects of this alga are not known in the literature. On the contrary, due to the fact that it has a high lipid content and could grow under heterotrophic conditions, *S. sp.* is a potential biodiesel producer and also important as food supplements. [90]

Since a detailed pigment composition of *S. sp.* is not known in the literature, the description of the pigmentation is done by the genetically similar algae species *Scenedesmus armatus*. [91]

### Characterisation

Taxonomy [42]

<b>Empire</b>	Eukaryota
<b>Kingdom</b>	Plantae
<b>Phylum</b>	Chlorophyta
<b>Class</b>	Chlorophyceae
<b>Order</b>	Sphaeropleales
<b>Family</b>	Scenedesmaceae
<b>Genus</b>	Scenedesmus

Pigments of the light-harvesting complex [92]

#### **accessory pigments**

major	Lutein, Chlorophyll <i>a + b</i> ,
minor	$\beta$ -Carotene, Loroanthin, Violoxanthin, Neoxanthin [91]
under stress:	Astaxanthin, Canthaxanthin, Echinenone, Adonirubin

#### **reaction centre**

Chlorophyll *a*

Morphology

<b>Cell length</b>	13.0 $\mu\text{m}$
<b>Cell shape</b>	rotational ellipsoid [91]

### Cultivation

Culture medium	MWC 0%
Light intensity	0.277 $\text{W m}^{-2}$
Light/dark cycles	10 h / 14 h
Growth temperature	19 °C

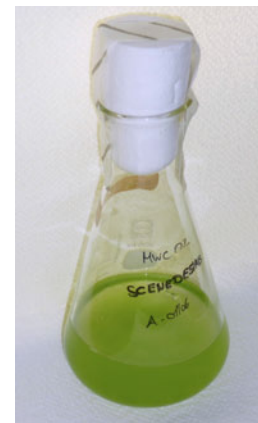


**Figure A.79.:** Cultivation of the microalga *Scenedesmus sp.*

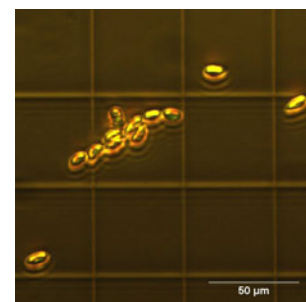


**Figure A.80.:** Ellipsoidal cells of *Scenedesmus sp.* forming long chains. Lugol's solution ( $I_2/KI$ ) used as fixing agent

To describe the spectral behaviour of *Scenedesmus sp.*, a sample of this alga was diluted in glycerine and an emission as well as an excitation spectrum were measured using the spectrophotometer. For the excitation spectrum, the emission wavelength was set to 750 nm and for the emission spectrum the alga was excited at 440 nm. The measurement for each spectrum was repeated ten times and afterwards, the resulting spectra were averaged and normalised. The emission spectrum was normalised to the maximal chlorophyll fluorescence at 688 nm, whereas the excitation spectrum was normalised to the Soret peak of chlorophyll *a* 436 nm. The results are shown in Figure A.81.

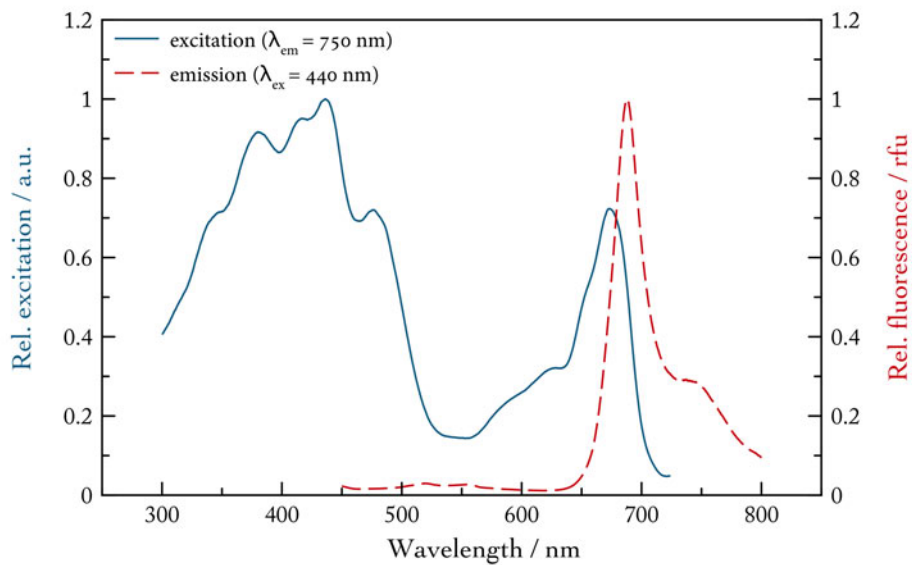


**Figure A.81.:** Normalised emission and excitation spectra of *Scenedesmus sp.*. Excitation at 440 nm, slitwidth = 5 nm, emission slitwidth = 5 nm. Emission at 750 nm, slitwidth = 20 nm, excitation slitwidth = 5 nm. Averaged spectra after 10 measurements.

## Monoraphidium

The species of this alga is unclear, but considering the genus, *Monoraphidium* is a green freshwater species which prefers slow floating, nutrient-rich regions. [58]

Harmful effects of this genus are not known in the literature, however, it contains several species that are suggested to be a potential feedstock for the biofuel production. [93]

Since the algal species is not fully defined, the description of the algal pigment composition is done by the algae species *Monoraphidium contortum*, which is a common representative of this genus.

### Characterisation

Taxonomy [42]

<b>Empire</b>	Eukaryota
<b>Kingdom</b>	Plantae
<b>Phylum</b>	Chlorophyta
<b>Class</b>	Chlorophyceae
<b>Order</b>	Sphaeropleales
<b>Family</b>	Selenastraceae
<b>Genus</b>	Monoraphidium

Pigments of the light-harvesting complex [94]

#### accessory pigments

major	Lutein, Violaxanthin Chlorophyll <i>a + b</i>
minor	Neoxanthin, $\beta$ -Carotene,
reaction centre	Chlorophyll <i>a</i>

Morphology

<b>Cell diameter</b>	18.5 $\mu\text{m}$
<b>Cell shape</b>	lean needles, curved in divers forms [95]

### Cultivation

Culture medium	MWC 0%
Light intensity	0.277 $\text{W m}^{-2}$
Light/dark cycles	10 h / 14 h
Growth temperature	19 °C

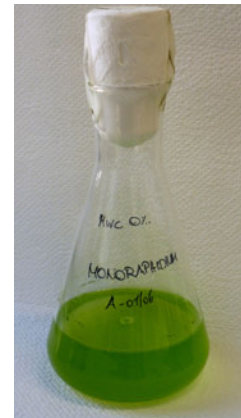


**Figure A.82.:** Cultivation of the microalga *Monoraphidium*

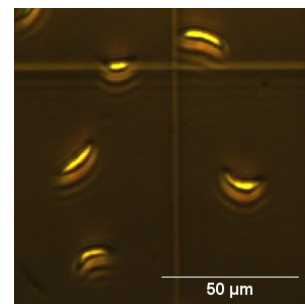


**Figure A.83.:** Curved cells of *Monoraphidium* under the light microscope. Lugol's solution ( $I_2/KI$ ) used as fixing agent

For the spectral characterisation of the alga belonging to the genus *Monoraphidium*, the algal sample was diluted in glycerine to avoid sedimentation of the cells. Then an excitation spectrum with an emission wavelength of 750 nm and an emission spectrum with an excitation wavelength of 440 nm were measured using the spectrofluorometer. The measurement of each spectrum was repeated ten times and then the spectra were averaged and normalised separately as Figure A.84 illustrates. The excitation spectrum was normalised to the Soret peak of chlorophyll *a* at 437 nm, whereas the emission spectrum was normalised to the maximal chlorophyll fluorescence at 687 nm.

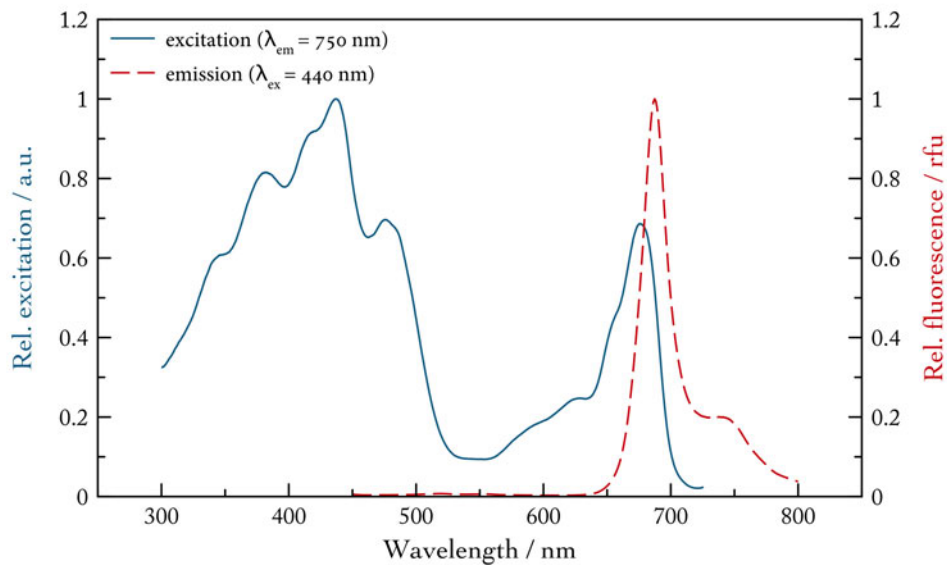


**Figure A.84.:** Normalised emission and excitation spectrum of an *Monoraphidium* algae for spectral characterisation. Species remain unknown. Excitation at 440 nm, slitwidth = 14 nm, emission slitwidth = 7 nm. Emission at 750 nm, slitwidth = 14 nm, excitation slitwidth = 7 nm. Averaged spectra after 10 measurements.

## **Pseudokirchneriella subcapitata – (Korshikov) F.Hindák**

This green microalga occurs in freshwater ponds and rivers. Due to its availability, favourable growth rates and culturing, *P. subcapitata* is often used in ecotoxicological tests. [96] Besides, unhealthy effects of this alga itself are not known in the literature.

Since a detailed pigment composition of this algal species could not be researched in the literature, the pigmentation is described by the phylum *Chlorophyta* in general. The list below contains only these pigments, that are common in all other algae species belonging to this phylum.

### **Characterisation**

Taxonomy [42]

<b>Empire</b>	Eukaryota
<b>Kingdom</b>	Plantae
<b>Phylum</b>	Chlorophyta
<b>Class</b>	Chlorophyceae
<b>Order</b>	Sphaeropleales
<b>Family</b>	Selenastraceae
<b>Genus</b>	Pseudokirchneriella

Pigments of the light-harvesting complex

#### **accessory pigments**

major	Lutein, $\beta$ -Carotene, Chlorophyll <i>a</i> + <i>b</i>
minor	Violaxanthin, Neoxanthin
<b>reaction centre</b>	Chlorophyll <i>a</i>

Morphology

<b>Cell diameter</b>	11.0 $\mu\text{m}$
<b>Cell shape</b>	semi-circularly curved, solitary [96]

### **Cultivation**

Culture medium	MWC 0%
Light intensity	0.277 $\text{W m}^{-2}$
Light/dark cycles	10 h / 14 h
Growth temperature	19 °C



**Figure A.85.:** Cultivation of the microalga *Pseudokirchneriella subcapitata*

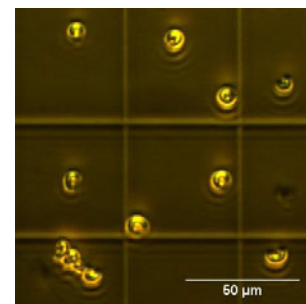


**Figure A.86.:** Solitary cells of *Pseudokirchneriella subcapitata* under the microscope using Lugol's solution ( $I_2/KI$ ) as fixing agent

For the spectral characterisation of *Pseudokirchneriella subcapitata*, the algal solution was diluted in glycerine to avoid sedimentation. Then an excitation spectrum with an emission of 750 nm and an emission spectrum with an excitation wavelength of 440 nm were recorded using the spectrofluorometer. Both spectra were normalised separately. As it is shown in Figure A.87, the excitation spectrum was normalised to the Soret band of chlorophyll *a* at 436 nm and the emission spectrum was normalised to the maximum of the chlorophyll fluorescence at 686 nm. Each spectrum was measured ten times and averaged afterwards.

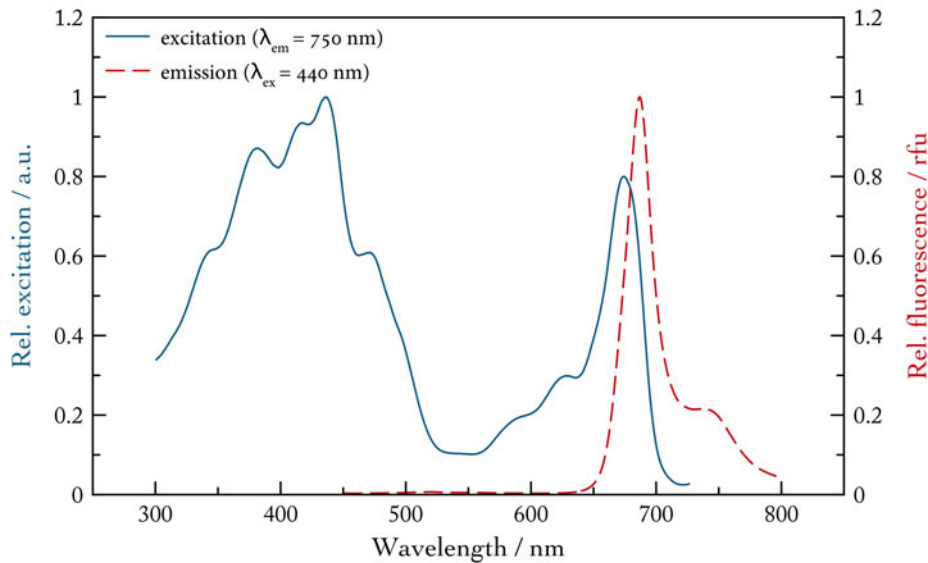


**Figure A.87.:** Normalised emission and excitation spectrum of *Pseudokirchneriella subcapitata* for spectral characterisation. Excitation at 440 nm, slitwidth = 14 nm, emission slitwidth = 7 nm. Emission at 750 nm, slitwidth = 14 nm, excitation slitwidth = 7 nm. Averaged spectra after 10 measurements.

## Selenastrum capricornutum – Printz

Formerly, *S. capricornutum* and *P. subcapitata*, a *Chlorophyta* described previously, were suggested to be of the same type, so these algae species have similar properties. It is a green microalga that is found in freshwater areas, lakes and rivers. Harmful effects of this alga are not known in the literature, but it is used in toxicity test as well as *P. subcapitata*. [96]

Since a detailed pigmentation of this alga could not be researched in the literature, the pigment composition is described by the phylum *Chlorophyta* in general. The list below contains all pigments that are common in all other algae species of the phylum *Chlorophyta*.

### Characterisation

Taxonomy [42]

<b>Empire</b>	Eukaryota
<b>Kingdom</b>	Plantae
<b>Phylum</b>	Chlorophyta
<b>Class</b>	Chlorophyceae
<b>Order</b>	Sphaeropleales
<b>Family</b>	Selenastraceae
<b>Genus</b>	Selenastrum

Pigments of the light-harvesting complex

#### accessory pigments

major	Lutein, $\beta$ -Carotene, Chlorophyll <i>a + b</i>
minor	Violaxanthin, Neoxanthin
reaction centre	Chlorophyll <i>a</i>

Morphology

<b>Cell diameter</b>	11.0 $\mu\text{m}$
<b>Cell shape</b>	semi-circularly curved solitary [96]

### Cultivation

Culture medium	MWC 0%
Light intensity	0.277 $\text{W m}^{-2}$
Light/dark cycles	10 h / 14 h
Growth temperature	19 °C

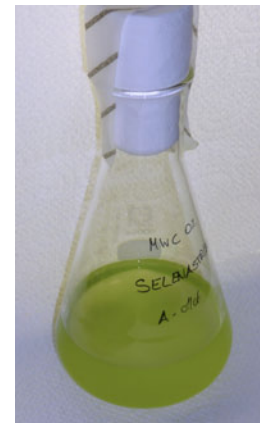


**Figure A.88.:** Cultivation of the microalga *Selenastrum capricornutum*

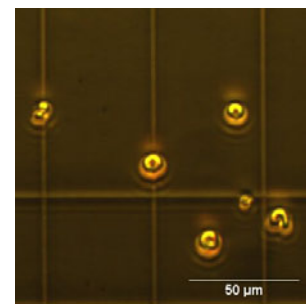


**Figure A.89.:** Microscopic photograph of *Selenastrum capricornutum* with Lugol's solution ( $I_2/KI$ ) as fixing agent

To describe the spectral behaviour of *S. capricornutum* an excitation spectrum with an emission wavelength of 750 nm as well as an emission spectrum with an excitation of 440 nm were measured using the spectrofluorometer. The measurement for each spectrum was repeated ten times and then averaged. Comparing Figure A.90, both spectra were normalised to different wavelengths. The excitation spectrum was normalised to the Soret band of chlorophyll *a* at 436 nm, whereas the emission spectrum was normalised to the maximum of the chlorophyll fluorescence at 687 nm.

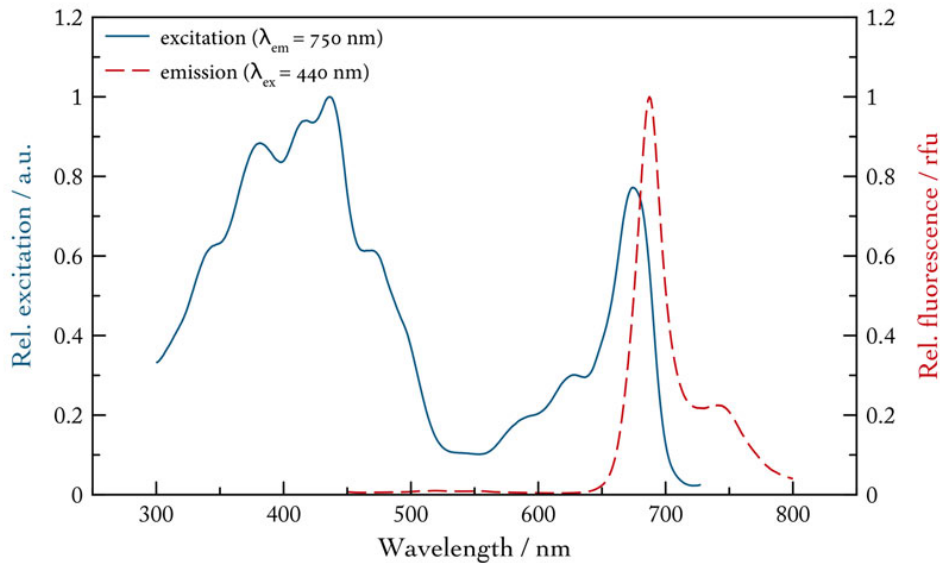


**Figure A.90.:** Normalised emission and excitation spectrum of *Selenastrum capricornutum* for spectral characterisation. Excitation at 440 nm, slitwidth = 14 nm, emission slitwidth = 7 nm. Emission at 750 nm, slitwidth = 14 nm, excitation slitwidth = 7 nm. Averaged spectra after 10 measurements.

## **Chlorella emersonii – Shihira & R.W.Krauss**

*Ch. emersonii* is a less known representative of the genus *Chlorella* than *Ch. vulgaris*, which is described later. The current accepted name of *Ch. emersonii* is *Graesiella emersonii* – (Shihara & R.W.Krauss) H.Nozaki, M.Katagiri, M.Nakagawa, K.Aizawa & M.M.Watanabe. It is a green microalga that occurs in freshwater and terrestrial zones. [58] Besides, harmful effects of this species are not known in the literature. This alga is similar to *Ch. vulgaris*, therefore, for further information see the next pages.

Since the detailed pigmentation of this algae species is not known in the literature, the general description of the pigment composition is done by the genetically similar alga *Chlorella vulgaris* and *Chlorella sp.*.

### **Characterisation**

Taxonomy [42]

<b>Empire</b>	Eukaryota
<b>Kingdom</b>	Plantae
<b>Phylum</b>	Chlorophyta
<b>Class</b>	Trebouxiophyceae
<b>Order</b>	Chlorellales
<b>Family</b>	Chlorellaceae
<b>Genus</b>	Chlorella

Pigments of the light-harvesting complex [97]

#### **accessory pigments**

major	Lutein, Violaxanthin, Chlorophyll <i>a + b</i>
minor	Zeaxanthin, Neoxanthin, Antheraxanthin

#### **reaction centre**

Chlorophyll *a*

Morphology

<b>Cell diameter</b>	11.0 $\mu m$
<b>Cell shape</b>	spherical to subspherical solitary, or grouped [58]

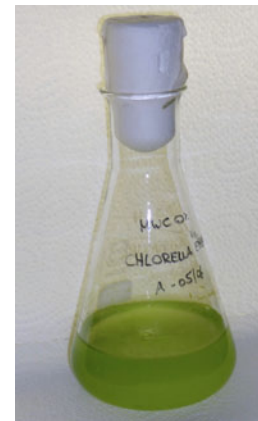


**Figure A.91.:** Cultivation of the microalga *Chlorella emersonii*

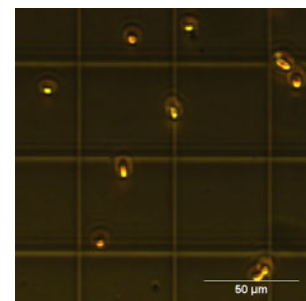


**Figure A.92.:** Subspherical cells of *Chlorella emersonii* under the microscope using Lugol's iodine ( $I_2/KI$ ) as fixing agent

**Cultivation**

Culture medium	MWC 0%
Light intensity	0.277 W m <sup>-2</sup>
Light/dark cycles	10 h / 14 h
Growth temperature	19 °C

An emission spectrum as well as an excitation spectrum were measured for the spectral characterisation of *Ch. emersonii*. First, the algal sample was diluted in glycerine to avoid sedimentation of the cells and afterwards the spectra were recorded using the spectrofluorometer. For the excitation spectrum, the emission wavelength was set to 750 nm, whereas the excitation wavelength for the emission spectrum was set to 440 nm. The measurement of each spectrum was repeated ten times and then the spectra were averaged and normalised as it is shown in Figure A.93. The excitation spectrum was normalised to the Soret peak of chlorophyll *a* at 436 nm and the emission spectrum was normalised to the chlorophyll fluorescence at 686 nm.

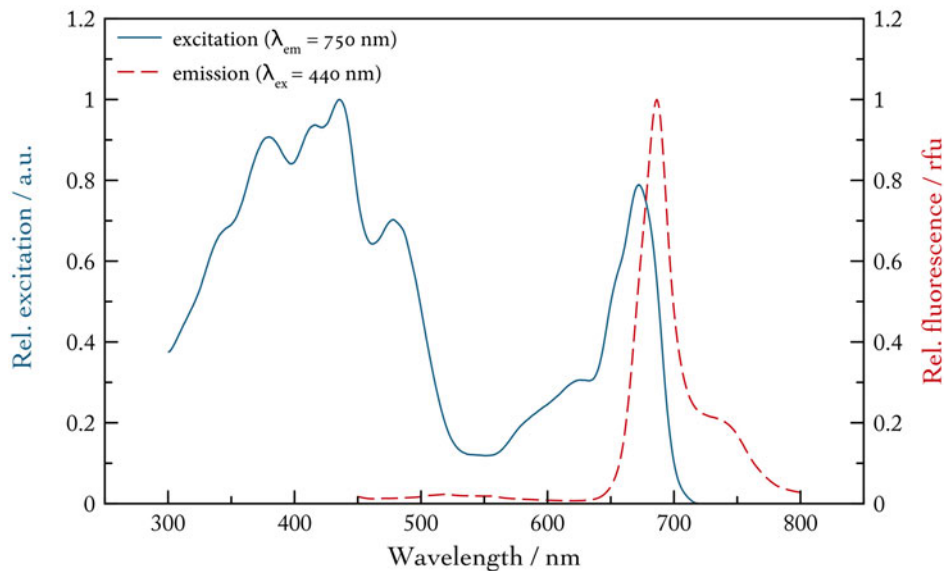


**Figure A.93.:** Normalised emission and excitation spectrum of *Chlorella emersonii* for spectral characterisation. Excitation at 440 nm, slitwidth = 14 nm, emission slitwidth = 7 nm. Emission at 750 nm, slitwidth = 14 nm, excitation slitwidth = 7 nm. Averaged spectra after 10 measurements.

## Chlorella vulgaris – Beyerinck

*Ch. vulgaris* is a cosmopolitan, green microalga that prefers stagnant water and humid soil, but might also occur in freshwater and marine regions. [42]

An unhealthy impact of this species is not known in the literature, but rather a certain health benefit. *Ch. vulgaris* is able to absorb and accumulate radionuclides and heavy metals (= bio-absorption). Therefore, this microalga could be used for wastewater treatment [98] and as food supplement, additive or colourant. Moreover, it is a potential feedstock for the biofuel production. [99]

### Characterisation

Taxonomy [42]

<b>Empire</b>	Eukaryota
<b>Kingdom</b>	Plantae
<b>Phylum</b>	Chlorophyta
<b>Class</b>	Trebouxiophyceae
<b>Order</b>	Chlorellales
<b>Family</b>	Chlorellaceae
<b>Genus</b>	Chlorella

Pigments of the light-harvesting complex [59]

#### **accessory pigments**

major	Lutein, Chlorophyll <i>a + b</i>
minor	Zeaxanthin, Antheraxanthin, $\beta$ -Carotene, Neoxanthin, Violoxanthin, Canthaxanthin Pheophytin <i>a</i> [99]

#### **reaction centre**

Chlorophyll *a*

Morphology

<b>Cell diameter</b>	10.0 $\mu m$
<b>Cell shape</b>	spherical [99]

### Cultivation

Culture medium	MWC 0%
Light intensity	0.277 $W m^{-2}$
Light/dark cycles	10 h / 14 h
Growth temperature	19 °C

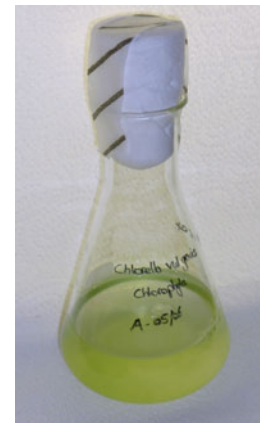


**Figure A.94.:** Cultivation of the microalga *Chlorella vulgaris*

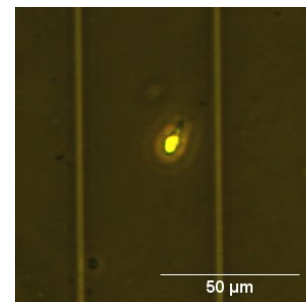


**Figure A.95.:** Microscopic photograph of *Chlorella vulgaris* with Lugol's solution ( $I_2/KI$ ) as fixing agent

For the spectral characterisation of *Ch. vulgaris*, an excitation spectrum and an emission spectrum were measured. The sample was diluted in glycerine. Then, the excitation spectrum was measured with an emission wavelength of 750 nm. Furthermore, an emission spectrum was measured by using an excitation of 440 nm. Both spectra were recorded using the spectrofluorometer. The measurements were repeated ten times and the resulting spectra were averaged and afterwards normalised. The excitation spectrum was normalised to the maximal excitation at 376 nm, whereas the emission spectrum was normalised to the maximal chlorophyll fluorescence at 686 nm. The overlaid plot of both spectra is shown in Figure A.96.

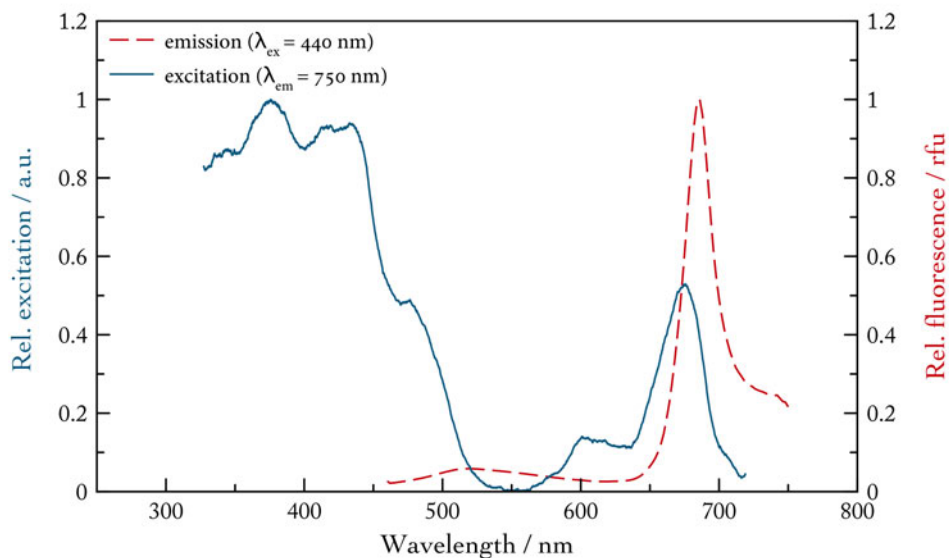


**Figure A.96.:** Normalised emission and excitation spectrum of *Chlorella vulgaris* for spectral characterisation. Excitation at 440 nm, slitwidth = 14 nm, emission slitwidth = 7 nm. Emission at 750 nm, slitwidth = 14 nm, excitation slitwidth = 7 nm. Averaged spectra after 10 measurements.

## Unknown microalga

We got this microalga from our supplier under the name *Chaetoceros peruvianus*. However, *Ch. peruvianus* is a yellow-brown diatom and the grown alga is bright green. Furthermore, the recorded excitation spectrum (compare Figure A.99) suggests that the alga is more similar to the *Chlorophyta* species than to the *Diatoms*.

Since the species remains unknown, a detailed pigment composition could not be researched. Therefore, the spectral characterisation is carried out by the phylum to which the alga belongs. The list below includes only the pigments, that are contained in all algae species belonging to the phylum *Chlorophyta*.

### Characterisation

Taxonomy [42]

<b>Empire</b>	Eukaryota
<b>Kingdom</b>	Plantae
<b>Phylum</b>	Chlorophyta
<b>Class</b>	unknown
<b>Order</b>	unknown
<b>Family</b>	unknown
<b>Genus</b>	unknown

Pigments of the light-harvesting complex

#### accessory pigments

major	Lutein, $\beta$ -Carotene Chlorophyll <i>a + b</i>
minor	Violaxanthin, Neoxanthin

#### reaction centre

Chlorophyll *a*

Morphology

<b>Cell diameter</b>	7.6 $\mu\text{m}$
<b>Cell shape</b>	coccoid, spherical

### Cultivation

Culture medium	F <sub>2</sub> / 30%
Light intensity	0.277 W m <sup>-2</sup>
Light/dark cycles	10 h / 14 h
Growth temperature	19 °C

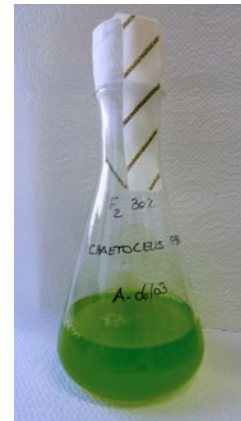


Figure A.97.: Cultivation of the unknown microalgae

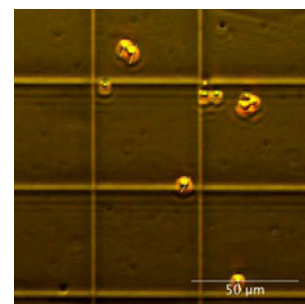
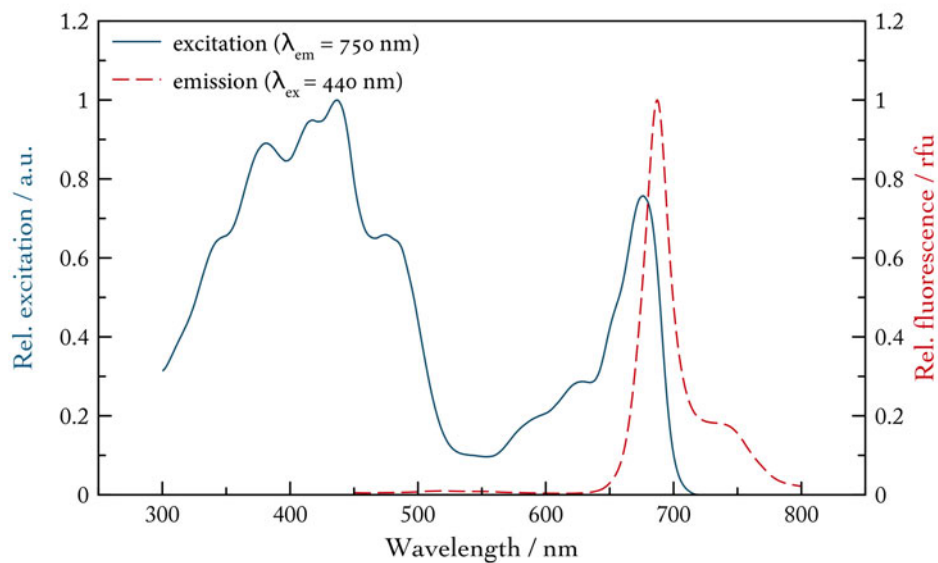


Figure A.98.: Microscopic image of the nameless algae. Lugol's solution (I<sub>2</sub>/KI) use as fixing agent

For the spectral characterisation of the unknown microalga as it is illustrated in Figure A.99, the algal sample was diluted in glycerine to avoid sedimentation effects of the cells. An emission spectrum with an excitation at 440 nm and an excitation spectrum with an emission wavelength of 750 nm were measured using the spectrofluorometer. Each measurement was repeated ten times and then the excitation and emission spectra were averaged. After the measurement, the emission spectrum was normalised to the maximal chlorophyll fluorescence (687 nm), whereas the excitation spectrum was normalised to the Soret peak of chlorophyll *a* (437 nm).



**Figure A.99.:** Normalised emission and excitation spectrum of the unknown *Chlorophyta* as spectral characterisation. Excitation at 440 nm, slitwidth = 14 nm, emission slitwidth = 7 nm. Emission at 750 nm, slitwidth = 14 nm, excitation slitwidth = 7 nm. Averaged spectra of 10 measurements.



## A.7. Cyanophyta

*Cyanophyta* are also known under the name *Cyanobacteria*. Previously, they were classified as *blue-green algae* to the empire of the algae. By contrast today, the *Cyanophyta* are classified to the prokaryotic bacteria, since they have no nucleus. Nevertheless, they share some properties with the algae. According to the algae-database, there are 4.483 photosynthetic cyanobacteria listed in the literature. [42]

Cyanobacteria mainly occur in freshwater regions and form filamentous organisms that might be curved and coiled or linear. Furthermore, they are dominant bloom-forming organisms and some of the cyanobacteria might create hypoxic conditions or produce toxins, known as cyanotoxins. Since the cyanotoxins can lead to skin disorders (= *dermatotoxins*), liver diseases (= *hepatotoxins*) or even neurological diseases (= *neurotoxins*), the harmful bacteria should be recognised at an early stage. [100, 101]

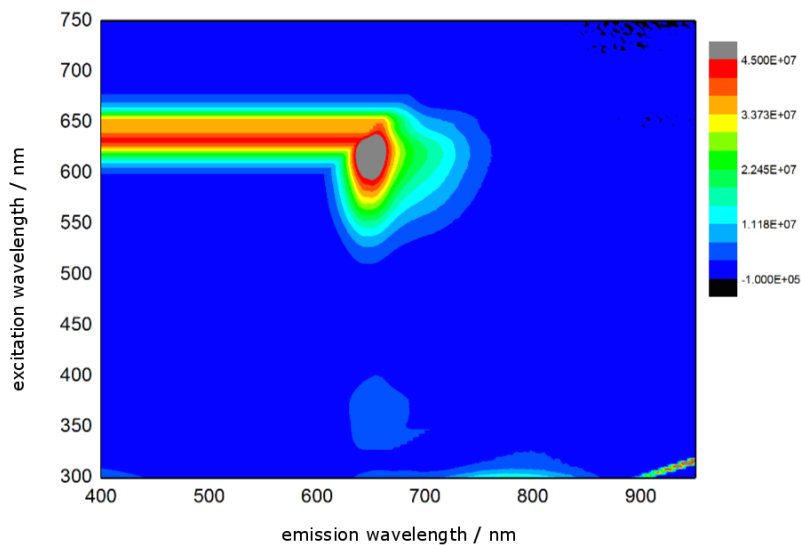


**Figure A.100.:** 3D spectrum of an *blue-green cyanobacteria* belonging to the phylum *Cyanobacteria*. The exact species is unknown. Excitation between 300 - 750 nm, slitwidth = 2.5 nm; Emission between 400 - 950 nm, slitwidth = 2.5 nm.

In addition to the light-harvesting complex, the cyanobacteria have another peripheral antenna complex, which is called phycobilisome. Within this complex phycocyanin (excitation at 621 nm, emission at 634 nm), allophycocyanin (655 nm, solvent unknown), and phycoerythrin (excitation at 566 nm, emission at 574 nm) are the accessory pigments. Due to this, cyanobacteria can use a wider range of the incident light in order to close the green gap, where chlorophyll and other pigments do not absorb. [18, 22, 102] They predominantly define the spectral behaviour of the blue-green algae. Besides these phycobilisomes, cyanobacteria contain common light-harvesting pigments as other algae. Typical pigments are  $\beta$ -carotene (425, 449, 475 nm, acetone/hexane), zeaxanthin (425, 450, 475 nm, acetone/hexane), echinenone (460 nm, acetone/hexane), myxoxanthophyll (449, 474, 505 nm, ethanol) and chlorophyll *a*, whereby zeaxanthin is most suitable as "marker" pigment. [18, 17, 103, 104]

Figure A.100 illustrates a 3D spectrum of a blue-green cyanobacteria. The absorbance behaviour is clearly different to other algal phyla, since the excitation spectrum is predominantly defined by the absorption of the phycobilisomes.

## Blue-green cyanobacteria

The species of this bacteria is unknown, therefore a general description of the cyanobacteria, its habitat and pigment composition is not possible. Moreover, it is not clear if this species has harmful effects, however, cyanobacteria are associated with cyanotoxins and Saxitoxin which cause serious damages to health or even lead to death.

Besides, during the cultivation process, it was observed that these cyanobacteria are capable of switching their photosynthesis process between an anoxygenic form of photosynthesis to an oxygenic form. In accordance to Garlick, Oren, and Padan, there are eleven different cyanobacteria which are capable of using a facilitative anoxygenic photosynthesis. [13]

Since the right species is unknown, the pigment composition of this alga could not be researched in the literature.

### Characterisation

Taxonomy [42]

<b>Empire</b>	Prokaryota
<b>Kingdom</b>	Eubacteria
<b>Phylum</b>	Cyanobacteria
<b>Class</b>	Cyanophyceae
<b>Order</b>	unknown
<b>Family</b>	unknown
<b>Genus</b>	unknown

Pigments of the light-harvesting complex [105]

#### **accessory pigments**

major	Phycobilins, Chlorophyll <i>a</i>
minor	unknown

#### **reaction centre**

Chlorophyll *a*

Morphology

<b>Cell length</b>	68.0 $\mu\text{m}$
<b>Cell shape</b>	long, filamentous chains without nucleus

### Cultivation

Culture medium	special medium
Light intensity	1 $\text{W m}^{-2}$
Light/dark cycles	4 h / 20 h
Growth temperature	26 °C



**Figure A.101.:** Cultivation of the *cyanobacteria* at different stages

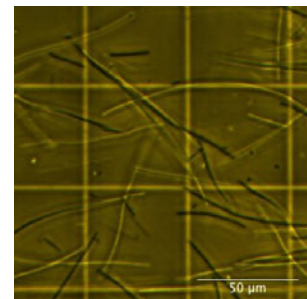


**Figure A.102.:** Microscopic photograph of the *cyanobacteria* with Lugol's iodine ( $I_2/KI$ ) as fixing agent

For spectral characterisation of this *cyanobacteria*, an emission as well as an excitation spectrum were measured using the spectrofluorometer. The bacterial sample was diluted in glycerine to avoid sedimentation. For the excitation spectrum, the emission wavelength was set to 750 nm and for the emission spectrum the excitation was 595 nm. The measurement was repeated ten times and then the resulting spectra were averaged. Afterwards, the excitation and the emission spectra were normalised separately. The excitation spectrum was normalised to the maximal excitation at 630 nm and the emission spectrum was normalised to the maximal fluorescence of the phycobilines at 663 nm.

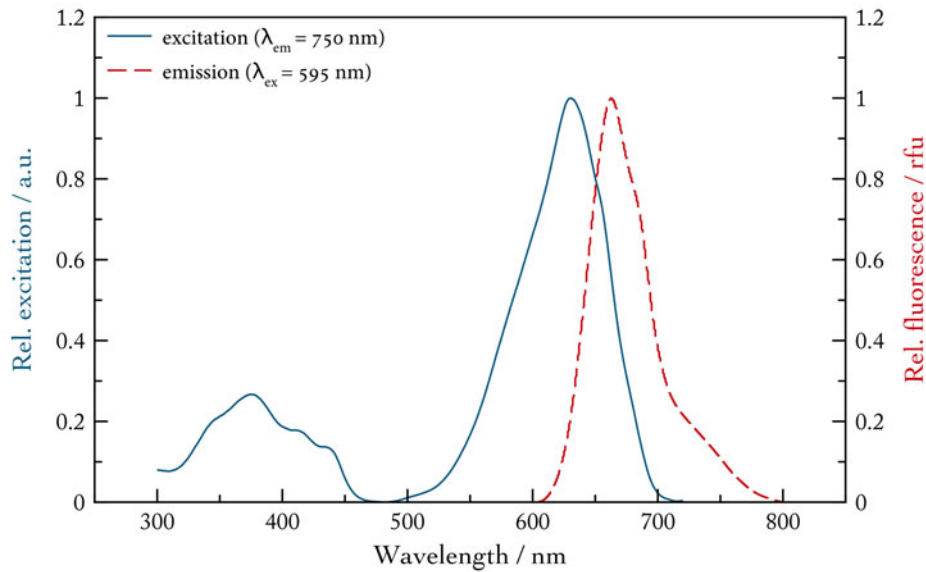


**Figure A.103.:** Normalised emission and excitation spectra of a *blue-green cyanobacteria*. Excitation at 595 nm, slitwidth = 14 nm, emission slitwidth = 7 nm. Emission at 750 nm, slitwidth = 14 nm, excitation slitwidth = 7 nm. Averaged spectra after 10 measurements.

## Anabaenopsis elenkinii – V.V.Miller

*A. elenkinii* is a cyanobacteria that lives in freshwater areas. [42] Under normal conditions, this bacteria occurs as mossy green culture, but under unfavourable conditions the colour turns to yellow. At the moment the toxicity of *A. elenkinii* is not yet officially accepted, nevertheless, in accordance to Maršálek, Bláha, and Hindák, it is suggested to produce hepatotoxic and neurotoxic alkaloids, especially when it blooms. Besides, *A. elenkinii* is a strong bloom-forming species. [100]

### Characterisation

Taxonomy [42]

<b>Empire</b>	Prokaryota
<b>Kingdom</b>	Eubacteria
<b>Phylum</b>	Cyanobacteria
<b>Class</b>	Cyanophyceae
<b>Order</b>	Nostocales
<b>Family</b>	Aphanizomenonaceae
<b>Genus</b>	Anabaenopsis

Pigments of the light-harvesting complex [103, 105]

#### accessory pigments

major	Phycobilins, $\beta$ -Carotene, Echinenone, Chlorophyll <i>a</i>
minor	Myxoxanthin, Zeaxanthin
<b>reaction centre</b>	Chlorophyll <i>a</i>

Morphology

<b>Cell length</b>	61.0 $\mu\text{m}$
<b>Cell shape</b>	coiled filament, terminal heterocytes and akinetes [106]

### Cultivation

Culture medium	MWC 0%
Light intensity	0.13 $\text{W m}^{-2}$
Light/dark cycles	10 h / 14 h
Growth temperature	23 °C

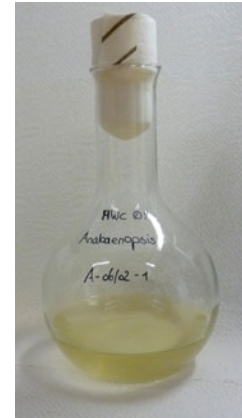


**Figure A.104.:** Cultivation of the microalga *Anabaenopsis elenkinii* under unfavourable conditions.

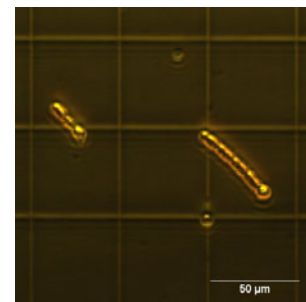


**Figure A.105.:** Slightly curved filament of *Anabaenopsis elenkinii* under the microscope. Lugol's solution ( $I_2/KI$ ) as fixing agent

To describe the spectral behaviour of *A. elenkinii* an excitation and an emission spectrum were measured using the spectrofluorometer. The sample was diluted in glycerine to avoid sedimentation. The emission wavelength for the excitation spectrum was set to 750 nm, whereas the excitation for the emission spectrum was set to 595 nm. The measurement was repeated ten times and then the spectra were averaged and normalised as it is shown in Figure A.106. The excitation spectrum was normalised to the maximal excitation peak at 656 nm and the emission spectrum, by contrast, was normalised to the maximal fluorescence of the phycobilines at 664 nm.

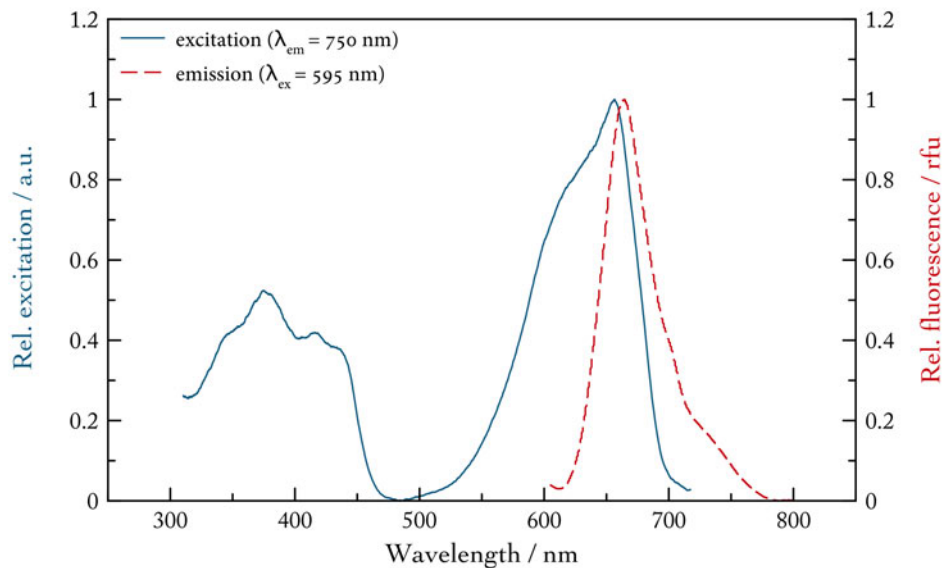


**Figure A.106.:** Overlaid emission and excitation spectra of *Anabaenopsis elenkinii*. Excitation at 595 nm, slitwidth = 14 nm, emission slitwidth = 7 nm. Emission at 750 nm slitwidth = 14 nm, excitation slitwidth = 7 nm. Averaged spectra after 10 measurements.

## Synechocystis sp. PCC 6803

This yellow-green cyanobacteria is unicellular with cryptic plasmids. *Synechocystis sp.* inhabits freshwater areas and it is used as a source for biofuel production. Furthermore, *Synechocystis sp.* is a model organism, so it is a well described and analysed cyanobacteria. [107, 108, 109] Harmful effects of this bacterial species are not known in the literature.

### Characterisation

Taxonomy [42]

<b>Empire</b>	Prokaryota
<b>Kingdom</b>	Eubacteria
<b>Phylum</b>	Cyanobacteria
<b>Class</b>	Cyanophyceae
<b>Order</b>	Synechococcales
<b>Family</b>	Merismopediaceae
<b>Genus</b>	<i>Synechocystis</i>

Pigments of the light-harvesting complex [59, 105]

#### **accessory pigments**

major	Phycobilins, Carotene, Zeaxanthin, Chlorophyll <i>a</i>
minor	Myxoxanthophyll, Echinenone
<b>reaction centre</b>	Chlorophyll <i>a</i>

Morphology

<b>Cell diameter</b>	7.0 $\mu\text{m}$
<b>Cell shape</b>	cryptic plasmids with up to four plasmids forming bands [108]

### Cultivation

Culture medium	F <sub>2</sub> / 18%
Light intensity	0.13 W m <sup>-2</sup>
Light/dark cycles	10 h / 14 h
Growth temperature	23 °C



**Figure A.107.:** Cultivation of the microalga *Synechocystis sp.*

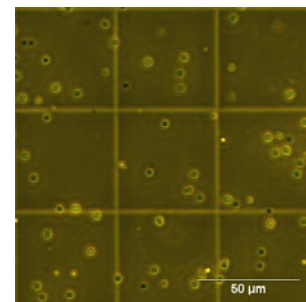


**Figure A.108.:** Plasmid-band of *Synechocystis sp.* under the light microscope; downloaded from

An emission and an excitation spectrum of *S. sp.* were recorded using the spectrofluorometer for spectral characterisation. First the bacterial sample was diluted in glycerine. Then, the excitation spectrum was measured with an emission wavelength of 750 nm. For the emission spectrum, an excitation of 595 nm was used. The measurement was repeated ten times and the resulting spectra were averaged afterwards. At least, both spectra were normalised separately. The excitation spectrum was normalised to the maximal excitation at 656 nm, whereas the emission spectrum was normalised to the maximal phycobilin fluorescence at 664 nm.

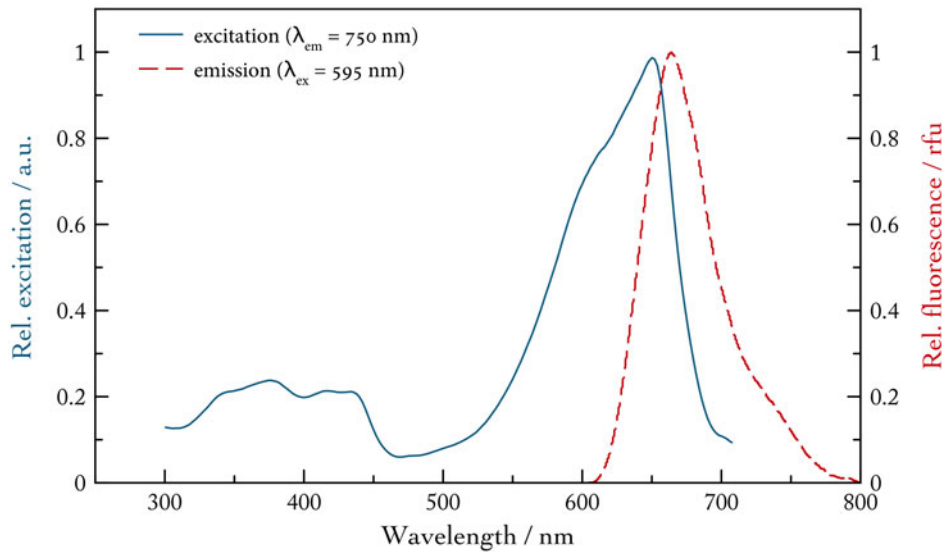


**Figure A.109.:** Overlaid emission and excitation spectra of *Synechocystis sp.*. Excitation at 595 nm, slitwidth = 14 nm, emission slitwidth = 7 nm. Emission at 750 nm, slitwidth = 14 nm, excitation slitwidth = 7 nm. Averaged spectra after 10 measurements.



## B. List of Equipment

**Table B.1.:** All instruments and components used for the algae detection module

instrument name	manufacturer	description
ThomaNeu	CarlRoth	hemocytometer, 0.05 x 0.05 x 0.1 mm <sup>3</sup> volume of least squares
Axiovert 25 Fluorolog <sup>®</sup> Fluorometer	Carl Zeiss Horiba HITACHI	inverted transmitted light microscope steady state spectrofluorometer fluorescence spectrophotometer F-7000
Aluminium Acetal Copolymer (POM-C) PIC32-PINGUINO-MICRO	protolabs protolabs OLIMEX	CNC machined optics block, grey CNC machined optics block, black printed-circuit-board with 80 MHz microcontroller and SD-card
ADC	MAZeT	analog-digital-converter
LED375-06 + BG25/39, 2 mm	Roithner LaserTechnik	LED1a1- LED/filter combination, (380 nm)
LED405-06V + BG25/39, 2 mm	Roithner LaserTechnik	LED1a2- LED/filter combination, (401 nm)
LED430-06 + BG25/39, 2 mm	Roithner LaserTechnik	LED1a3- LED/filter combination, (428 nm)
LED450-06 + BG25/39, 2 mm	Roithner LaserTechnik	LED1a4- LED/filter combination, (448 nm)
B56L5111P + BG25/39, 2 mm	Roithner LaserTechnik	LED2a1- LED/filter combination, (470 nm)
B5B-433-B505 + F39-558 550/88, 2 mm	Roithner LaserTechnik	LED2b1- LED/filter combination, (502 nm)
B5B-433-B525 + F39-558 550/88, 2 mm	Roithner LaserTechnik	LED2b2- LED/filter combination, (516 nm)
LED545-06 + F39-558 550/88, 2 mm	Roithner LaserTechnik	LED1b1- LED/filter combination, (539 nm)
B5B-433-20 + F39-558 550/88, 2 mm	Roithner LaserTechnik	LED2b3- LED/filter combination, (572 nm)
Y5CA5111P + F39-558 550/88, 2 mm	Roithner LaserTechnik	LED2b4- LED/filter combination, (595 nm)
B5B-435-TL + F49-645 645/30, 1.12 mm	Roithner LaserTechnik	LED2c1- LED/filter combination, (640 nm)
B5B-436-30 + F49-645 645/30, 1.12 mm	Roithner LaserTechnik	LED3c2- LED/filter combination, (653 nm)

continuation on next page

*B. List of Equipment*

---

instrument name	manufacturer	description
RG9	Schott	longpass / bandpass filter, $\tau_i$ (720 nm) $\leq$ 0.45
RG665	Schott	longpass filter, $\tau_i$ (665 nm) = 0.5
BPW34 photodiode	Vishay	silicon pin photodiode
Capillary	Hilgenberg	quartz, ID = 1.94 mm, OD = 3 mm

---





---

## C. List of Figures

2.1.	<i>Example of different cell shapes to demonstrate the diversity of algae. . . . .</i>	8
2.2.	<i>Example of an algal bloom caused by cyanobacteria leading to a discolouration of the water surface. [6] . . . . .</i>	9
2.3.	<i>TriLux Fluorimeter from Chelsea Technologies as low-cost digital fluorometer for phycoerythrin, phycocyanin and chlorophyll a detection. [10] . . . . .</i>	11
2.4.	<i>Comparison of a bench-top flow cytometer which is placed into a buoy and a microflow cytometer that exhibits a smaller footprint requiring only low power. Both systems can be used for marine monitoring . . . . .</i>	11
2.5.	<i>Scheme of the photosynthesis. It consists of two partial reactions – the light reaction and the dark reaction, also called Calvin cycle. During the light reaction the energy of the sun is converted into chemical energy to synthesise organic compounds. . . . .</i>	12
2.6.	<i>Scheme of the electron transfer in the light reaction, when oxygen is evolved, based on the publication of Govindjee. The electrons are transported over several complex reaction cascades to the coenzyme II which is used during the Calvin cycle to synthesise carbohydrates. The redox potential is indicated on the left. [1] . . . . .</i>	13
2.7.	<i>Simplified model of the light-harvesting complex and its energy transport cascade, based on Schopfer, Brennicke, and Mohr. A part of the incident light is absorbed by the antenna pigments to increase the efficiency of light absorption. [14] . . . . .</i>	14
2.8.	<i>A Jablonski diagram demonstrating the excitation of a pigment D to its excited states <math>S_1</math> or <math>S_2</math> followed by possible relaxation processes to reach the energetically favourable ground state <math>S_0</math>. . . . .</i>	16
2.9.	<i>A Jablonski diagram to describe the Förster resonance energy transfer (FRET). A pigment D is excited and besides the common relaxation processes of radiationless deactivation, phosphorescence or fluorescence, the pigment can transfer its excitation energy to an acceptor molecule A. The donor goes back radiationless to the ground state. . . . .</i>	18
2.10.	<i>A Jablonski diagram to give an overview of the energy trapping. All energy absorbed by the accessory pigments is transmitted to the chlorophyll-dimer in the reaction centre. The overall efficiency of the energy trapping exceeds 90%. . . . .</i>	19
2.11.	<i>Structures of chlorophyll a (left) and b (right), which differ only in one substituent. . . . .</i>	20
2.12.	<i>Spectral characterisation of chlorophyll a and b based on [24]. The pigments were dissolved in diethylether. The excitation wavelength for the chlorophyll a emission was 614 nm and for chlorophyll b 435 nm. . . . .</i>	21
2.13.	<i>Left: Structure of <math>\beta</math>-carotene as an example for the carotenoids. Right: Spectral characterisation of the pigment, which was dissolved in toluene; based on [25]. The excitation wavelength for the emission spectrum was 475 nm. . . . .</i>	21
2.14.	<i>Left: Structure of phycoerythrobilin, the chromophoric group of phycoerythrin, which is part of the peripheral antenna complexes in cyanobacteria and red algae. Right: Spectral characterisation of the phycobilin in sodium phosphate / EDTA / sodium azide; based on [23]. . . . .</i>	22

2.15.	<i>Left: Structure of phycocyanobilin, the chromophoric group of phycocyanin, which is part of the peripheral antenna complex in cyanobacteria. Right: Spectral characterisation of the phycobilin in sodium phosphate / EDTA / sodium azide; based on [23]. . . . .</i>	23
2.16.	<i>Comparison of the absorption behaviour of different pigments. Phycobilins close the green gap where chlorophyll can not absorb light and enable a algal growth in the depth of the oceans. [26] . . . . .</i>	23
2.17.	<i>A characteristic chlorophyll fluorescence induction curve of dark-adapted needles of Pinus sylvestris based on Bolhar-Nordenkamp, Long, and Lechner. The curve which can divided into a fast phase (A) and a slow phase (B), was measured on a fluorometer with a photon flux of <math>100 \mu\text{mol m}^{-2} \text{s}^{-1}</math> at <math>20^\circ\text{C}</math>. The characteristic measurement points are marked. [27] . . . . .</i>	24
3.1.	<i>Example of the algal cultivation in sterile Erlenmeyer flasks with cellulose plug (left). Right: Final storage of the algae species under the timer controlled lighting installation in a dark and temperature-controlled laboratory. . . . .</i>	34
3.2.	<i>Algae cultivation tubes with a timer controlled illumination. Each tube fits 3 litres of algae culture and the aeration can be adjusted for each tube. . . . .</i>	35
3.3.	<i>ThomaNeu counting chamber for microscopic investigations. The picture on the right shows one group square divided into 16 least squares. . . . .</i>	37
3.4.	<i>Picture of Horiba's Fluorolog<sup>®</sup> - Spectrofluorometer on the left. Examples of 3D spectra of different phyla to demonstrate the spectral differences. The spectra are shown for cyanobacteria and brown algae (right). . . . .</i>	38
3.5.	<i>Left: Picture of Hitachi's fluorescence spectrophotometer. The excitation spectra illustrate different absorption behaviour due to a different pigmentation in algae belonging to different phyla (middle). By contrast, the emission spectra on the right is quite similar as chlorophyll a is the principal molecule in the reaction centre. . . .</i>	39
3.6.	<i>Principle of PCA – Original data set were the data points of one species, which should be separated are marked in red. Blue marked is the distance between the data centre and a single data point, whereas the euclidean distance which is the distance between an assumed straight line (<math>PC_1</math>) and the data point, is marked in orange. The best approximation is achieved, when the euclidean distance is minimal. . . . .</i>	41
3.7.	<i>Histogram showing the proportion of the total data variance for different principal components as an example. The number of components used for the data analysis depends on the desired content of information of the original data. . . . .</i>	42
3.8.	<i>A: Original data set where the red marked data point represent the sample that should be separated. B: Principle of the PCA and data after coordinate transformation and projection onto a specific principal component (C). D: Score plot with two PCs to visualise the resulting separation of the original data set. . . . .</i>	44
4.1.	<i>1<sup>st</sup> generation prototype. Adapted optical oxygen meter from PyroScience with one exchangeable LED. . . . .</i>	48
4.2.	<i>The time drive shows that by using the modified fluorometer a signal change could be recorded down to a concentration of approximately 2 cells in <math>10 \mu\text{l}</math> – the measurement volume of the flow channel. . . . .</i>	49
4.3.	<i>2<sup>nd</sup> generation prototype with electronics which enables high speed sampling and a smaller footprint. . . . .</i>	49

4.4.	<i>The intensity vs. time data recorded with the 2<sup>nd</sup> generation prototype show that the sharp spikes shown in the first plot is in fact not an electronic spike but a real particles luminescing while passing the measurement volume. Consequently a higher time resolution is needed to identify these signal peaks as sample peaks rather than random electronic noise. The duration of one peak corresponds to the residence time of a particle in the measurement chamber calculated from the diameter of the capillary and the pump speed. . . . .</i>	50
4.5.	<i>3<sup>rd</sup> generation prototype. 4 LEDs can be used together with a sampling frequency of 460 Hz per channel. . . . .</i>	50
4.6.	<i>Example of the time data recorded with the 3<sup>rd</sup> generation prototype. The differences in the signal intensity result from the different spectral behaviour of the emission filter and also from the different excitation potential of the chosen LED. . . . .</i>	51
4.7.	<i>Rendered picture of our low-cost prototype featuring 8 channels in an optics block with minimized dimensions. The upper three figures show rendered representations of the assembled device without the electronics. The lower 2 figures show photographs of the machined optics block with standard barbed fluidic connectors. . . . .</i>	52
4.8.	<i>Emission/Transmission spectra of the LED and filters, used for the algae detection module. . . . .</i>	54
4.9.	<i>LED module showing the composition above and a cross section through the module below. This housing for the LEDs allows an easy replacement of the light source on demand. . . . .</i>	55
5.1.	<i>Time drive of amphora samples with different cell densities: The average signal level depends on the average biomass within the optical path. The higher the biomass, the higher and more compressed are the fluorescence signals emitted from the algal sample.</i>	58
5.2.	<i>Comparison between the different signal levels for seawater (left) and air (right). The signal level for air is twice higher than for water due to the better refraction conditions within the capillary. . . . .</i>	59
5.3.	<i>Device made out of POM-C installed on a cardboard to store it in the metal box during the measurements. Besides, the device is grounded on the metal box. . . . .</i>	61
5.4.	<i>Left: Example of the standard solutions enclosed in capillaries for an easy replacement. Right: Spectral behaviour of Sulforhodamine 101. The excitation and emission wavelengths used for the linearity test are marked. The molar attenuation coefficient is 139.000 L cm<sup>-1</sup> mol<sup>-1</sup>. . . . .</i>	62
5.5.	<i>Linearity test with Sulforhodamine 101. The coefficient of determination (<math>R^2</math>) is lower when the bicycle tube is used as optical isolator in the system (left). When the isolator is removed, the linearity increase (right). The scaling of the y-axis is varying due to a better presentation of the linearity. . . . .</i>	63
5.6.	<i>Linearity test with Sulforhodamine 101 showing the same results as above but with the focus on the lower concentrations. The bicycle tube leads to a loss of the sensitivity (left), whereas after removing the tube, all channels exhibit a good sensitivity (right). The scaling of the y-axis is varying due to a better presentation of the linearity. . . . .</i>	63
5.7.	<i>Average noise level of four different channels when the capillary is filled with air. The device is connected with the peristaltic pump over PCV tubes. The average noise level is 700 - 1400 pW and the deviation of the noise amplitude is 13 pW. . . . .</i>	64

5.8.	<i>Average noise level of four different channels, when the capillary is filled with water. The sinusoidal signal results from the surrounding electro-magnetic irradiation. The average background level is 300 - 825 pW and the deviation of the noise is 300 pW. .</i>	65
5.9.	<i>One end of a PVC tube that connects the peristaltic pump with the detection module; coated with steel to prevent electro-magnetic interferences. . . . .</i>	65
5.10.	<i>Average noise level of four different channels, when the capillary is filled with water and the PVC tubes are shielded. The average noise level is more statistical than before and furthermore reduced by half compared to the previous measurement. The baseline is here 225 - 420 pW and the deviation of the noise is now 5 pW. . . . .</i>	66
5.11.	<i>Average noise level of four different channels, when the capillary is filled with air and the PVC tubes are shielded. The noise level and also the deviation of the noise amplitude is reduced by 1.6. Now the average background level is 490 - 850 pW and the noise is approximately 8 pW. . . . .</i>	66
5.12.	<i>Left: Rendered picture of the detection module to demonstrate the direction of the flow. Right: The high resolution of the aluminium device enables the capturing of cells passing through the system. The experiment was done with Amphora algae at a cell density of 3 cells / measurement volume (5.91 µL). . . . .</i>	68
5.13.	<i>The <b>measured</b> residence time of a particular algae cell matches well with the <b>calculated</b> time (right). Furthermore, the signal-to-noise-ratio can be calculated in this case to <math>SNR \approx 10.3</math>. The microscopic image on the left illustrates the average cell length of the Amphora cells. . . . .</i>	69
5.14.	<i>Linearity test for the whole POM-C device by using Sulforhodamine 101 as standard solution. The signals are blank corrected. All channels behave linearly. . . . .</i>	70
5.15.	<i>Sensitivity test with Sulforhodamine 101 for the whole detection module. All eight channels exhibit a high sensitivity, since they are able to detect the lowest concentrated standard on an average light intensity of 270 pW. The signals are blank corrected. . . . .</i>	71
5.16.	<i>Example of the spectral differences between a diatom and a bacterial species. While the emission spectra seem to be quite similar, the excitation spectra are clearly different. Therefore the excitation of the samples has to be done in these spectral ranges that lead to a maximal variance in the excitation intensities. . . . .</i>	72
5.17.	<i>Example of the pigment patterns of four different algae species and two bacterial species (marked with *). These patterns exhibit the efficiency of excitation and illustrate therefore the actual pigment composition how it could be measured on the detection module. The LEDs and emission filters used in this experiment are listed on the right. . . . .</i>	73
5.18.	<i>Resulting score plot after analysing the data by the means of the principal component analysis. Both cyanobacteria – the unknown bacteria and the anabaenopsis species were separated clearly from the rest. . . . .</i>	74
A.1.	<i>3D spectrum of <i>Skeletonema Costatum</i> (Bacillariophyta / Diatomee) . . . . .</i>	83
A.2.	<i>Cultivation of the alga belonging to the genus <i>Amphora</i> . . . . .</i>	84
A.3.	<i>Cell shape of an Amphora algae under the light microscope . . . . .</i>	84
A.4.	<i>Spectral characterisation of an Amphora species . . . . .</i>	85
A.5.	<i>Cultivation of the microalga <i>Phaeodactylum tricornutum</i> . . . . .</i>	86
A.6.	<i>Cell shape of <i>Phaeodactylum tricornutum</i> under the light microscope . . . . .</i>	86
A.7.	<i>Spectral characterisation of <i>Phaeodactylum tricornutum</i> . . . . .</i>	87
A.8.	<i>Cultivation of the microalga <i>Ditylum brightwellii</i> . . . . .</i>	88

A.9.	Cell shape of <i>Ditylum brightwellii</i> under the light microscope . . . . .	88
A.10.	Spectral characterisation of <i>Ditylum brightwellii</i> . . . . .	89
A.11.	Cultivation of the microalga <i>Skeletonema Costatum</i> . . . . .	90
A.12.	Cell shape of <i>Skeletonema costatum</i> under the light microscope . . . . .	90
A.13.	Spectral characterisation of <i>Skeletonema costatum</i> . . . . .	91
A.14.	Cultivation of the microalga <i>Cyclotella meneghiniana</i> . . . . .	92
A.15.	Cell shape of <i>Cyclotella meneghiniana</i> under the light microscope . . . . .	92
A.16.	Spectral characterisation of <i>Cyclotella meneghiniana</i> . . . . .	93
A.17.	3D spectrum of <i>Rhodomonas minuta</i> (Cryptophyta) . . . . .	95
A.18.	Clear to bluish culture of the microalga <i>Hemiselmis sp.</i> . . . . .	96
A.19.	Cell shape of <i>Hemiselmis sp.</i> under the light microscope . . . . .	96
A.20.	Spectral characterisation of <i>Hemiselmis sp.</i> . . . . .	97
A.21.	Cultivation of the microalga <i>Rhodomonas minuta</i> . . . . .	98
A.22.	Cell shape of <i>Rhodomonas minuta</i> under the light microscope . . . . .	98
A.23.	Spectral characterisation of <i>Rhodomonas minuta</i> . . . . .	99
A.24.	Cultivation of the microalga <i>Rhodomonas salina</i> . . . . .	100
A.25.	Cell shape of <i>Rhodomonas salina</i> under the light microscope . . . . .	100
A.26.	Spectral characterisation of <i>Rhodomonas salina</i> . . . . .	101
A.27.	3D spectrum of <i>Alexandrium minutum</i> (Dinophyta) . . . . .	103
A.28.	Cultivation of the microalga <i>Alexandrium minutum</i> . . . . .	104
A.29.	Cell shape of <i>Alexandrium minutum</i> under the light microscope . . . . .	104
A.30.	Spectral characterisation of <i>Alexandrium minutum</i> . . . . .	105
A.31.	Cultivation of the microalga <i>Heterocapsa triquetra</i> . . . . .	106
A.32.	Cell shape of <i>Heterocapsa triquetra</i> under the light microscope . . . . .	106
A.33.	Spectral characterisation of <i>Heterocapsa triquetra</i> . . . . .	107
A.34.	3D spectrum of <i>Pleurochrysis elongata</i> (Haptophyta) . . . . .	109
A.35.	Cultivation of the microalga <i>Pleurochrysis elongata</i> . . . . .	110
A.36.	Cell shape of <i>Pleurochrysis elongata</i> under the light microscope . . . . .	110
A.37.	Spectral characterisation of <i>Pleurochrysis elongata</i> . . . . .	111
A.38.	Cultivation of the microalga <i>Isochrysis galbana</i> . . . . .	112
A.39.	Cell shape of <i>Isochrysis galbana</i> under the light microscope . . . . .	112
A.40.	Spectral characterisation of <i>Isochrysis galbana</i> . . . . .	113
A.41.	Cultivation of the microalga <i>Ruttnera spectabilis</i> . . . . .	114
A.42.	Cell shape of <i>Ruttnera spectabilis</i> under the light microscope . . . . .	114
A.43.	Spectral characterisation of <i>Ruttnera spectabilis</i> . . . . .	115
A.44.	Cultivation of the microalga <i>Prymnesium saltans</i> . . . . .	116
A.45.	Cell shape of <i>Prymnesium saltans</i> under the light microscope . . . . .	116
A.46.	Spectral characterisation of <i>Prymnesium saltans</i> . . . . .	117
A.47.	3D spectrum of <i>Nannochloropsis salina</i> (Orchophyta) . . . . .	119
A.48.	Cultivation of the microalga <i>Eustigmatos magnus</i> . . . . .	120
A.49.	Cell shape of <i>Eustigmatos magnus</i> under the light microscope . . . . .	120
A.50.	Spectral characterisation of <i>Eustigmatos magnus</i> . . . . .	121
A.51.	Cultivation of the microalga <i>Nannochloropsis saina</i> . . . . .	122
A.52.	Cell shape of <i>Nannochloropsis salina</i> under the light microscope . . . . .	122
A.53.	Spectral characterisation of <i>Nannochloropsis salina</i> . . . . .	123
A.54.	Cultivation of the microalga <i>Chloridella neglecta</i> . . . . .	124
A.55.	Cell shape of <i>Chloridella neglecta</i> under the light microscope . . . . .	124
A.56.	Spectral characterisation of <i>Chloridella neglecta</i> . . . . .	125

A.57.	Cultivation of the nameless microalga . . . . .	126
A.58.	Cell shape of the nameless microalgae under the light microscope . . . . .	126
A.59.	Spectral characterisation of the unknown microalgae . . . . .	127
A.60.	Excitation and emission spectrum of <i>Selenastrum</i> (Chlorophyta) . . . . .	129
A.61.	Cultivation of the microalga <i>Tetraselmis suecica</i> . . . . .	130
A.62.	Cell shape of <i>Tetraselmis suecica</i> under the light microscope . . . . .	130
A.63.	Spectral characterisation of <i>Tetraselmis suecica</i> . . . . .	131
A.64.	Cultivation of the microalga <i>Chlamydomonas reinhardtii</i> . . . . .	132
A.65.	Cell shape of <i>Chlamydomonas reinhardtii</i> under the light microscope . . . . .	132
A.66.	Spectral characterisation of <i>Chlamydomonas reinhardtii</i> . . . . .	133
A.67.	Cultivation of the microalga <i>Choricystis minor</i> . . . . .	134
A.68.	Cell shape of <i>Choricystis minor</i> under the light microscope . . . . .	134
A.69.	Spectral characterisation of <i>Choricystis minor</i> . . . . .	135
A.70.	Cultivation of the algae species <i>Dunaliella salina</i> . . . . .	136
A.71.	Cell shape of <i>Dunaliella salina</i> under the light microscope . . . . .	136
A.72.	Spectral characterisation of <i>Dunaliella salina</i> . . . . .	137
A.73.	Cultivation of the microalga <i>Dunaliella tertiolecta</i> . . . . .	138
A.74.	Cell shape of <i>Dunaliella tertiolecta</i> under the light microscope . . . . .	138
A.75.	Spectral characterisation of <i>Dunaliella tertiolecta</i> . . . . .	139
A.76.	Cultivation of the microalga <i>Haematococcus pluvialis</i> under unfavourable conditions . . . . .	140
A.77.	Cell shape of <i>Haematococcus pluvialis</i> under the light microscope . . . . .	140
A.78.	Spectral characterisation of <i>Haematococcus pluvialis</i> . . . . .	141
A.79.	Cultivation of the microalga <i>Scenedesmus sp.</i> . . . . .	142
A.80.	Cell shape of <i>Scenedesmus sp.</i> under the light microscope . . . . .	142
A.81.	Spectral characterisation of <i>Scenedesmus sp.</i> . . . . .	143
A.82.	Cultivation of the microalga <i>Monoraphidium</i> . . . . .	144
A.83.	Cell shape of <i>Monoraphidium</i> under the light microscope . . . . .	144
A.84.	Spectral characterisation of <i>Monoraphidium</i> . . . . .	145
A.85.	Cultivation of the microalga <i>Pseudokirchneriella subcapitata</i> . . . . .	146
A.86.	Cell shape of <i>Pseudokirchneriella subcapitata</i> under the light microscope . . . . .	146
A.87.	Spectral characterisation of <i>Pseudokirchneriella subcapitata</i> . . . . .	147
A.88.	Cultivation of the microalga <i>Selenastrum capricornutum</i> . . . . .	148
A.89.	Cell shape of <i>Selenastrum capricornutum</i> under the light microscope . . . . .	148
A.90.	Spectral characterisation of <i>Selenastrum capricornutum</i> . . . . .	149
A.91.	Cultivation of the microalga <i>Chlorella emersonii</i> . . . . .	150
A.92.	Cell shape of <i>Chlorella emersonii</i> under the light microscope . . . . .	150
A.93.	Spectral characterisation of <i>Chlorella emersonii</i> . . . . .	151
A.94.	Cultivation of the microalga <i>Chlorella vulgaris</i> . . . . .	152
A.95.	Cell shape of <i>Chlorella vulgaris</i> under the light microscope . . . . .	152
A.96.	Spectral characterisation of <i>Chlorella vulgaris</i> . . . . .	153
A.97.	Cultivation of the unknown microalgae . . . . .	154
A.98.	Cell shape of the unknown algae under the light microscope . . . . .	154
A.99.	Spectral characterisation of the unknown <i>Chlorophyta</i> . . . . .	155
A.100.	3D spectrum of a <i>blue-green cyanobacteria</i> (Cyanophyta) . . . . .	157
A.101.	Cultivation of the <i>cyanobacteria</i> at different stages . . . . .	158
A.102.	Cell shape of the unknown cyanobacteria under the light microscope . . . . .	158
A.103.	Spectral characterisation of a blue-green algae . . . . .	159

A.104. Cultivation of the microalga *Anabaenopsis elenkinii* under unfavourable conditions. . . . . 160

A.105. Cell shape of *Anabaenopsis elenkinii* under the light microscope . . . . . 160

A.106. Spectral characterisation of *Anabaenopsis elenkinii* . . . . . 161

A.107. Cultivation of the microalga *Synechocystis sp.* . . . . . 162

A.108. Plasmid-band of *Synechocystis sp.* under the light microscope; downloaded from 162

A.109. Spectral characterisation of *Synechocystis sp.* . . . . . 163

---

## D. References

- [1] Govindjee. *LIGHT EMISSION BY PLANTS AND BACTERIA*. Ed. by Jan Ames and David Charles Fork. Cell biology - A series of monographs. Academic Press, Inc., 1986. 638 pp. ISBN: 978-0-12-412462-2.
- [2] Jens Boenigk and Sabina Wodniok. *Biodiversität und Erdgeschichte*. Berlin: Springer-Spektrum, 2014. 401 pp. ISBN: 978-3-642-55389-9 978-3-642-55388-2.
- [3] F. v. Rheinbaben. "Algen und ihre Bedeutung für die Humanhygiene". In: *Krankenhaus-Hygiene + Infektionsverhütung* 37.3 (June 2015), pp. 103–108. ISSN: 07203373. DOI: 10.1016/j.khin.2015.02.012. URL: <http://linkinghub.elsevier.com/retrieve/pii/S0720337315000522> (visited on 10/20/2015).
- [4] C.F.C. Araújo and L.P. Souza-Santos. "Use of the microalgae *Thalassiosira weissflogii* to assess water toxicity in the Suape industrial-port complex of Pernambuco, Brazil". In: *Ecotoxicology and Environmental Safety* 89 (2013), pp. 212–221. ISSN: 01476513. DOI: 10.1016/j.ecoenv.2012.11.032. URL: <http://linkinghub.elsevier.com/retrieve/pii/S0147651312004526> (visited on 08/04/2015).
- [5] D.M. Anderson et al. *Monitoring and Management Strategies for Harmful Algal Blooms in Coastal Waters*. #201-MR-01.1 59. Paris: APEC - Asia Pacific Economic Program, Singapore, and Intergovernmental Oceanographic Commission, 2001. URL: <https://www.whoi.edu/files/server.do?id=24193&pt=10&p=19155>.
- [6] Florida Department of Environmental Protection. *Blue-green Algae*. 2015. URL: <http://www.dep.state.fl.us/water/bgalgae/>.
- [7] Samantha Faber. "Saxitoxin and the induction of paralytic shellfish poisoning". In: *Journal of Young Investigators* 23.1 (2012). URL: [http://www.jyi.org/wp-content/uploads/JYI-Volume-23-Issue-2-Faber-Samantha\\_Saxitoxin-and-the-induction-of-paralytic-shellfish-poisoning4.pdf](http://www.jyi.org/wp-content/uploads/JYI-Volume-23-Issue-2-Faber-Samantha_Saxitoxin-and-the-induction-of-paralytic-shellfish-poisoning4.pdf).
- [8] Luděk Bláha, Pavel Babica, and Blahoslav Maršálek. "Toxins produced in cyanobacterial water blooms - toxicity and risks". In: *Interdisciplinary Toxicology* 2.2 (Jan. 1, 2009), pp. 36–41. ISSN: 1337-9569, 1337-6853. DOI: 10.2478/v10102-009-0006-2. URL: <http://www.degruyter.com/view/j/intox.2009.2.issue-2/v10102-009-0006-2/v10102-009-0006-2.xml> (visited on 07/21/2015).
- [9] *Harmful Algal Blooms*. National Ocean Service. United States Department of commerce: National Oceanic and Atmospheric Administration (NOAA), Aug. 11, 2014. URL: <http://oceanservice.noaa.gov/hazards/hab/welcome.html>.
- [10] Chelsea Technologis Group Ltd. *TriLux Fluorometer (for Chlorophyll, Phycoerythrin, Phycocyanin & Turbidity monitoring)*. URL: <http://www.chelsea.co.uk/allproduct/marine/fluorometers/unilux-fluorometer>.
- [11] CytoBuoye b.v. *Flow Cytometry and Imaging*. URL: <http://www.cytobuoy.com>.

- 
- [12] Nastaran Hashemi et al. "Optofluidic characterization of marine algae using a microflow cytometer". In: *Biomicrofluidics* 5.3 (Sept. 20, 2011), pp. 032009–032009–9. ISSN: 1932-1058. DOI: 10.1063/1.3608136. URL: <http://www.ncbi.nlm.nih.gov/pmc/articles/PMC3364819/> (visited on 06/13/2015).
- [13] S. Garlick, A. Oren, and E. Padan. "Occurrence of facultative anoxygenic photosynthesis among filamentous and unicellular cyanobacteria." In: *Journal of Bacteriology* 129.2 (Feb. 1977), pp. 623–629. ISSN: 0021-9193 / 1098-5530. URL: <http://jb.asm.org/content/129/2/623.short> (visited on 11/10/2015).
- [14] Peter Schopfer, Axel Brennicke, and Hans Mohr. *Pflanzenphysiologie*. 7. Aufl. Heidelberg: Spektrum, Akad. Verl, 2010. 702 pp. ISBN: 978-3-8274-2351-1.
- [15] Gerhart Drews. *Mikrobiologie: die Entdeckung der unsichtbaren Welt*. Heidelberg: Springer, 2010. 245 pp. ISBN: 978-3-642-10756-6 978-3-642-10757-3.
- [16] René Schödel. "Zur Kinetik von Singulett- und Triplett-Anregungen im Lichtsammelkomplex des Photosystems II höherer Pflanzen (LHCII)". PhD thesis. Humboldt-Universität Berlin, 1999. URL: <http://edoc.hu-berlin.de/dissertationen/physik/schoedel-rene/PDF/Schoedel.pdf>.
- [17] Takashi Maoka, Takashi Kuwahara, and Masanao Narita. "Carotenoids of Sea Angels *Cliene limacina* and *Paedocliene doliiformis* from the Perspective of the Food Chain". In: *Marine Drugs* 12.3 (Mar. 13, 2014), pp. 1460–1470. ISSN: 1660-3397. DOI: 10.3390/md12031460. URL: <http://www.mdpi.com/1660-3397/12/3/1460/> (visited on 08/10/2015).
- [18] Maximiliano Figueroa et al. "In silico model of an antenna of a phycobilisome and energy transfer rates determination by theoretical Förster approach". In: *The Protein Society* 45.10-11 (Oct. 9, 2012), pp. 1921–1928. DOI: 10.1002/pro.2176. URL: <http://onlinelibrary.wiley.com/doi/10.1002/pro.2176/epdf> (visited on 08/11/2015).
- [19] Takayuki Kajikawa et al. "Syntheses of ylidenbutenolide-modified derivatives of peridinin and their stereochemical and spectral characteristics". In: *Organic & Biomolecular Chemistry* 8.11 (2010), pp. 2513–2516. ISSN: 1477-0520, 1477-0539. DOI: 10.1039/c002006k. URL: <http://xlink.rsc.org/?DOI=c002006k> (visited on 07/09/2015).
- [20] S.J. Whittle and P.J. Casselton. "The chloroplast pigments of the algal classes Eustigmatophyceae and Xanthophyceae. I. Eustigmatophyceae". In: *British Phycological Journal* 10.2 (June 11, 1975), pp. 179–191. ISSN: 0007-1617. DOI: 10.1080/00071617500650171. URL: <http://www.tandfonline.com/doi/abs/10.1080/00071617500650171> (visited on 07/21/2015).
- [21] Paavo H. Hynninen, Jari S. Kavakka, and Markku Mesilaakso. "Electronic structure of the enolate anion of chlorophyll b". In: *Tetrahedron Letters* 46.7 (Feb. 2005), pp. 1145–1147. ISSN: 00404039. DOI: 10.1016/j.tetlet.2004.12.075. URL: <http://linkinghub.elsevier.com/retrieve/pii/S0040403904027789> (visited on 08/13/2015).
- [22] Roberta Croce and Herbert van Amerongen. "Natural strategies for photosynthetic light harvesting". In: *Nature Chemical Biology* 10.7 (June 17, 2014), pp. 492–501. ISSN: 1552-4450, 1552-4469. DOI: 10.1038/nchembio.1555. URL: <http://www.nature.com/doi/finder/10.1038/nchembio.1555> (visited on 10/06/2015).

- [23] Torsten Mayr. *Fluorophores.org - Database of Fluorescent Dyes, Properties and Applications*. URL: <http://www.fluorophores.tugraz.at/>.
- [24] Scott Prahl and Steven L. Jacques. *Biomedical Optics in Portland*. URL: <http://omlc.org> (visited on 2014).
- [25] B. Schmidt et al. "A broadband Kerr shutter for femtosecond fluorescence spectroscopy". In: *Applied Physics B: Lasers and Optics* 76.8 (July 1, 2003), pp. 809–814. ISSN: 0946-2171, 1432-0649. DOI: 10.1007/s00340-003-1230-7. URL: <http://link.springer.com/10.1007/s00340-003-1230-7> (visited on 11/10/2015).
- [26] *Photosynthesis Lab Manual*. York University, 2013. URL: [http://biologywiki.apps01.yorku.ca/images/e/e9/Pigment\\_spectra.png](http://biologywiki.apps01.yorku.ca/images/e/e9/Pigment_spectra.png).
- [27] H. R. Bolhar-Nordenkamp, S. P. Long, and E. G. Lechner. "Die Bestimmung der Photosynthesekapazität über die Chlorophyllfluoreszenz als Maß für die Streßbelastung von Bäumen". In: *Phyton (Austria)* 29.1 (1989), pp. 119–135. URL: [http://www.landesmuseum.at/pdf\\_frei\\_remote/PHY\\_29\\_1\\_0119-0135.pdf](http://www.landesmuseum.at/pdf_frei_remote/PHY_29_1_0119-0135.pdf).
- [28] Robert R. L. Guillard. *Culture of phytoplankton for feeding marine invertebrates*. Ed. by Smith W.L. and Chanley M.H. Plenum Press. New York, USA: Culture of Marine Invertebrate Animals, 1975.
- [29] Robert R. L. Guillard and John H. Ryther. "STUDIES OF MARINE PLANKTONIC DIATOMS: I. CYCLOTELLA NANA HUSTEDT, AND DETONULA CONFERVACEA (CLEVE) GRAN." In: *Canadian Journal of Microbiology* 8.2 (Apr. 1962), pp. 229–239. ISSN: 0008-4166, 1480-3275. DOI: 10.1139/m62-029. URL: <http://www.nrcresearchpress.com/doi/abs/10.1139/m62-029> (visited on 09/29/2015).
- [30] R. R. L. Guillard and P. E. Hargraves. "Stichochrysis immobilis is a diatom, not a chrysophyte". In: *Phycologia* 32.3 (May 1993), pp. 234–236. ISSN: 0031-8884. DOI: 10.2216/i0031-8884-32-3-234.1. URL: <http://www.phycologia.org/doi/abs/10.2216/i0031-8884-32-3-234.1> (visited on 09/30/2015).
- [31] Maureen D. Keller et al. "MEDIA FOR THE CULTURE OF OCEANIC ULTRAPHYTOPLANKTON1,2". In: *Journal of Phycology* 23.4 (Apr. 30, 2007), pp. 633–638. ISSN: 00223646. DOI: 10.1111/j.1529-8817.1987.tb04217.x. URL: <http://doi.wiley.com/10.1111/j.1529-8817.1987.tb04217.x> (visited on 09/30/2015).
- [32] Robert R. L. Guillard and Carl J. Lorenzen. "YELLOW-GREEN ALGAE WITH CHLOROPHYLLIDE C<sup>2</sup>". In: *Journal of Phycology* 8.1 (Mar. 1972), pp. 10–14. ISSN: 0022-3646, 1529-8817. DOI: 10.1111/j.1529-8817.1972.tb03995.x. URL: <http://doi.wiley.com/10.1111/j.1529-8817.1972.tb03995.x> (visited on 09/29/2015).
- [33] Robert A. Andersen, ed. *Algal culturing techniques*. Burlington, Mass: Elsevier/Academic Press, 2005. 578 pp. ISBN: 9780120884261.
- [34] Patrick Lavens and Patrick Sorgeloos, eds. *Manual on the Production and Use of Live Food for Aquaculture*. FAO Fisheries Technical Paper. 361. Rome: Food and Agriculture Organization of the United Nations, 1996. URL: <http://www.fao.org/docrep/003/w3732e/w3732e00.htm#Contents>.
- [35] *Axiovert 25 / 25 C / 25 CFL Inverted Microscope (Manual)*. Carl Zeiss. Jena, Aug. 1999. URL: [http://loci.wisc.edu/files/loci/axiovert25\\_manual.pdf](http://loci.wisc.edu/files/loci/axiovert25_manual.pdf) (visited on 07/22/2015).

- 
- [36] U. Jütting et al. *(Teil-)Automatisierte Analyse der Phytoplanktonzusammensetzung nach der Utermöhl-Methode*. Tagungsbericht der Deutschen Gesellschaft für Limnologie (DGL). Institut für Pathologie, 2003. URL: [http://karo03.bplaced.net/karsten.rodenacker/Me/Misc\\_WWW/pdf/DGL03.pdf](http://karo03.bplaced.net/karsten.rodenacker/Me/Misc_WWW/pdf/DGL03.pdf) (visited on 07/22/2015).
- [37] K. Danzer et al. *Chemometrik — Grundlagen und Anwendungen*. Springer Berlin Heidelberg, 2001.
- [38] James N. Miller and Jane C. Miller. *Statistics and Chemometrics for Analytical Chemistry — fifth edition*. Pearson, 2005.
- [39] Roithner Laser Technik GmbH. *Diverse LEDs*. URL: <http://www.roithner-laser.com/>.
- [40] M. A. M. J. van Zandvoort et al. "CHLOROPHYLLS IN POLYMERS. I. STATE OF CHLOROPHYLL a IN UNSTRETCHED POLYMER SYSTEMS". In: *Photochemistry and Photobiology* 62.2 (Aug. 1995), pp. 279–289. ISSN: 0031-8655, 1751-1097. DOI: 10.1111/j.1751-1097.1995.tb05270.x. URL: <http://doi.wiley.com/10.1111/j.1751-1097.1995.tb05270.x> (visited on 10/11/2015).
- [41] *Datasheet — Silicon PIN Photodiode BPW34, BPW34S*. Rev. 2.1. Vishay Semiconductors, 2011. URL: <http://www.vishay.com/docs/81521/bpw34.pdf>.
- [42] M.D. Guiry and G.M. Guiry. *AlgaeBase. World-wide electronic publication*. URL: <http://www.algaebase.org/>; (visited on 01/14/2015).
- [43] Bidhan Dhar et al. "Molecular Detection of a Potentially Toxic Diatom Species". In: *International Journal of Environmental Research and Public Health* 12.5 (May 6, 2015), pp. 4921–4941. ISSN: 1660-4601. DOI: 10.3390/ijerph120504921. URL: <http://www.mdpi.com/1660-4601/12/5/4921/> (visited on 07/30/2015).
- [44] Robert R. Bidigare, Michael E. Ondrusek, and John H. Morrow. "In-vivo absorption properties of algal pigments". In: *Proceedings of SPIE - The International Society for Optical Engineering*. Ed. by Dale A. Spinrad. Vol. 1302. Ocean Optics X. Society of Photo/Optical Instrumentation Engineers, 1990, pp. 290–302. URL: <http://proceedings.spiedigitallibrary.org/proceeding.aspx?articleid=944075>.
- [45] Alessandra De Martino et al. "Physiological and Molecular Evidence that Environmental Changes Elicit Morphological Interconversion in the Model Diatom *Phaeodactylum tricorutum*". In: *Protist* 162.3 (July 2011), pp. 462–481. ISSN: 14344610. DOI: 10.1016/j.protis.2011.02.002. URL: <http://linkinghub.elsevier.com/retrieve/pii/S143446101100006X> (visited on 07/25/2015).
- [46] J.L. Pinckney et al. "Flow scintillation counting of <sup>14</sup>C-labeled microalgal photosynthetic pigments". In: *Journal of Plankton Research* 18.10 (1996), pp. 1867–1880. ISSN: 0142-7873, 1464-3774. DOI: 10.1093/plankt/18.10.1867. URL: <http://plankt.oxfordjournals.org/cgi/doi/10.1093/plankt/18.10.1867> (visited on 07/23/2015).
- [47] Dr. T. Ivanochko et al. *EOS - The Phytoplankton Encyclopedia Project*. 2012. URL: [http://www.eos.ubc.ca/research/phytoplankton/diatoms/centric/coscino/discus/c\\_granii.html](http://www.eos.ubc.ca/research/phytoplankton/diatoms/centric/coscino/discus/c_granii.html) (visited on 07/13/2015).
- [48] P. Henriksen. "Effects of nutrient-limitation and irradiance on marine phytoplankton pigments". In: *Journal of Plankton Research* 24.9 (Sept. 1, 2002), pp. 835–858. ISSN: 14643774. DOI: 10.1093/plankt/24.9.835. URL: <http://www.plankt.oupjournals.org/cgi/doi/10.1093/plankt/24.9.835> (visited on 07/23/2015).

- [49] M Laviale and J Neveux. "Relationships between pigment ratios and growth irradiance in 11 marine phytoplankton species". In: *Marine Ecology Progress Series* 425 (Mar. 14, 2011), pp. 63–77. ISSN: 0171-8630, 1616-1599. DOI: 10.3354/meps09013. URL: <http://www.int-res.com/abstracts/meps/v425/p63-77/> (visited on 07/21/2015).
- [50] Bánk Beszteri. "Morphometric and molecular investigations of species limits in *Cycleotella meneghiniana* (Bacillariophyceae) and closely related species *Cycleotella meneghiniana* (Bacillariophyceae) and closely related species". PhD thesis. Bremerhaven: Universität Bermen, 2005.
- [51] A. Laza-Martinez et al. "Phytoplankton pigment patterns in a temperate estuary: from unialgal cultures to natural assemblages". In: *Journal of Plankton Research* 29.11 (Sept. 17, 2007), pp. 913–929. ISSN: 0142-7873, 1464-3774. DOI: 10.1093/plankt/fbm069. URL: <http://www.plankt.oxfordjournals.org/cgi/doi/10.1093/plankt/fbm069> (visited on 07/23/2015).
- [52] K. Hoef-Emden and M. A. John. *Cryptomonads / Cryptophyta*. The Tree of Life Web Project. documentation. Apr. 2, 2010. URL: <http://tolweb.org/Cryptomonads> (visited on 08/10/2015).
- [53] Alexander B. Doust et al. "The photophysics of cryptophyte light-harvesting". In: *Journal of Photochemistry and Photobiology A: Chemistry* 184.1-2 (Nov. 2006), pp. 1–17. ISSN: 10106030. DOI: 10.1016/j.jphotochem.2006.06.006. URL: <http://linkinghub.elsevier.com/retrieve/pii/S1010603006003224> (visited on 08/10/2015).
- [54] E. Gantt, M. R. Edwards, and L. Provasoli. "Chloroplast structure of cryptophyceae — Evidence for Phycobiliproteins within intrathylakoidal spaces". In: *The Journal of Cell Biology* 48.2 (1971), pp. 280–290. URL: <http://www.ncbi.nlm.nih.gov/pmc/articles/PMC2108187/pdf/280.pdf>.
- [55] Christopher E. Lane and John M. Archibald. "New Marine members of the genus *HEMISELMIS* (CRYPTOMONADALES, CRYPTOPHYCEAE)". In: *Journal of Phycology* 44.2 (Apr. 2008), pp. 439–450. ISSN: 00223646, 15298817. DOI: 10.1111/j.1529-8817.2008.00486.x. URL: <http://doi.wiley.com/10.1111/j.1529-8817.2008.00486.x> (visited on 07/23/2015).
- [56] I. Olenina et al. *Biovolumes and size-classes of phytoplankton in the Baltic Sea*. 106. HELCOM Balt.Sea Environ. Proc., 2006, 144pp. URL: <http://epic.awi.de/30141/1/bsep106.pdf> (visited on 07/22/2015).
- [57] K. Hoef-Emden and M. A. John. *Rhodomonas | Rhinomonas | Storeatula*. The Tree of Life Web Project. documentation. Apr. 2, 2010. URL: [http://tolweb.org/Rhodomonas\\_%7C\\_Rhinomonas\\_%7C\\_Storeatula/128540](http://tolweb.org/Rhodomonas_%7C_Rhinomonas_%7C_Storeatula/128540) (visited on 07/23/2015).
- [58] D. M. John, B. A. Whitton, and A. J. Brook. *The Freshwater Algal Flora of the British Isles: An Identification Guide to Freshwater and Terrestrial Algae, Band 1*. Vol. 1. Cambridge University Press, Apr. 25, 2002. 702 pp. ISBN: 0521770513, 9780521770514. URL: [https://books.google.at/books?id=Sc4897dfM\\_MC&pg=PA185&lpg=PA185&dq=Rhodomonas+minuta+habitat&source=bl&ots=n4cHwdFNOP&sig=UBB4MR6JCddNq-ciN1kils37XIk&hl=de&sa=X&ved=0CCoQ6AEwAWoVChMIoLDxw83wxgIVxjgUCh1peQCv#v=onepage&q=Rhodomonas%20minuta%20habitat&f=false](https://books.google.at/books?id=Sc4897dfM_MC&pg=PA185&lpg=PA185&dq=Rhodomonas+minuta+habitat&source=bl&ots=n4cHwdFNOP&sig=UBB4MR6JCddNq-ciN1kils37XIk&hl=de&sa=X&ved=0CCoQ6AEwAWoVChMIoLDxw83wxgIVxjgUCh1peQCv#v=onepage&q=Rhodomonas%20minuta%20habitat&f=false) (visited on 07/23/2015).

- 
- [59] Lauridsen T. L. Krogh G. Jørgensen T. Schlüter L. "Identification and quantification of phytoplankton groups in lakes using new pigment ratios – a comparison between pigment analysis by HPLC and microscopy". In: *Freshwater Biology* 51.8 (2006), pp. 1474–1485. DOI: 10.1111/j.1365-2427.2006.01582.x. URL: <http://onlinelibrary.wiley.com/doi/10.1111/j.1365-2427.2006.01582.x/full>.
- [60] A Barreiro et al. "Relative importance of the different negative effects of the toxic haptophyte *Prymnesium parvum* on *Rhodomonas salina* and *Brachionus plicatilis*". In: *Aquatic Microbial Ecology* 38 (2005), pp. 259–267. ISSN: 0948-3055, 1616-1564. DOI: 10.3354/ame038259. URL: <http://www.int-res.com/abstracts/ame/v38/n3/p259-267/> (visited on 07/23/2015).
- [61] M. A. Faust and R. A. Gulledge. *Identifying Harmful Marine Dinoflagellates - Alexandrium minutum*. Identifying Harmful Marine Dinoflagellates. Ed. by Smithsonian Institution / National Museum of Natural History. Vol. 42. Washington, D.C.: Contributions from the United States National Herbarium, 2002. URL: <http://botany.si.edu/references/dinoflag/Taxa/Aminutum.htm> (visited on 07/02/2015).
- [62] Intergovernmental Oceanographic Commission of UNESCO. *Harmful Algal Bloom Programme*. URL: [http://hab.ioc-unesco.org/index.php?option=com\\_content&view=article&id=5&Itemid=16](http://hab.ioc-unesco.org/index.php?option=com_content&view=article&id=5&Itemid=16) (visited on 08/10/2015).
- [63] Lydia Ignatiades, Olympia Gotsis-Skretas, and Angelina Metaxatos. "Field and culture studies on the ecophysiology of the toxic dinoflagellate *Alexandrium minutum* (Halim) present in Greek coastal waters". In: *Harmful Algae* 6.2 (Feb. 2007), pp. 153–165. ISSN: 15689883. DOI: 10.1016/j.hal.2006.04.002. URL: <http://linkinghub.elsevier.com/retrieve/pii/S1568988306000400> (visited on 07/21/2015).
- [64] A. Houdan et al. "Toxicity of coastal coccolithophores (Prymnesiophyceae, Haptophyta)". In: *Journal of Plankton Research* 26.8 (Apr. 21, 2004), pp. 875–883. ISSN: 1464-3774. DOI: 10.1093/plankt/fbh079. URL: <http://www.plankt.oupjournals.org/cgi/doi/10.1093/plankt/fbh079> (visited on 07/23/2015).
- [65] M Zapata et al. "Photosynthetic pigments in 37 species (65 strains) of Haptophyta: implications for oceanography and chemotaxonomy". In: *Marine Ecology Progress Series* 270 (2004), pp. 83–102. ISSN: 0171-8630, 1616-1599. DOI: 10.3354/meps270083. URL: <http://www.int-res.com/abstracts/meps/v270/p83-102/> (visited on 07/23/2015).
- [66] Yen-Hui Lin et al. "Influence of growth phase and nutrient source on fatty acid composition of *Isochrysis galbana* CCMP 1324 in a batch photoreactor". In: *Biochemical Engineering Journal* 37.2 (Nov. 2007), pp. 166–176. ISSN: 1369703X. DOI: 10.1016/j.bej.2007.04.014. URL: <http://linkinghub.elsevier.com/retrieve/pii/S1369703X07001751> (visited on 07/22/2015).
- [67] Edna Granéli et al. "The ecophysiology and bloom dynamics of *Prymnesium* spp." In: *Harmful Algae* 14 (Feb. 2012), pp. 260–270. ISSN: 15689883. DOI: 10.1016/j.hal.2011.10.024. URL: <http://linkinghub.elsevier.com/retrieve/pii/S1568988311001521> (visited on 07/22/2015).

- [68] Zhen Li et al. "Profiling of carotenoids in six microalgae (Eustigmatophyceae) and assessment of their  $\beta$ -carotene productions in bubble column photobioreactor". In: *Biotechnology Letters* 34.11 (Nov. 2012), pp. 2049–2053. ISSN: 0141-5492, 1573-6776. DOI: 10.1007/s10529-012-0996-2. URL: <http://link.springer.com/10.1007/s10529-012-0996-2> (visited on 07/22/2015).
- [69] G. Markou and E. Neratzis. "Microalgae for high-value compounds and biofuels production: A review with focus on cultivation under stress conditions". In: *Biotechnology Advances* 31.8 (2013), pp. 1532–1542. URL: [http://ac.els-cdn.com/S0734975013001250/1-s2.0-S0734975013001250-main.pdf?\\_tid=b2324742-3c05-11e5-83a1-00000aacb360&acdnat=1438843266\\_2b8a239be2bbfb7b04bc8d3a0a7380cb](http://ac.els-cdn.com/S0734975013001250/1-s2.0-S0734975013001250-main.pdf?_tid=b2324742-3c05-11e5-83a1-00000aacb360&acdnat=1438843266_2b8a239be2bbfb7b04bc8d3a0a7380cb).
- [70] D.J. Hibberd and G.F. Leedale. "Cytology and ultrastructure of the Xanthophyceae. II. The zoospore and vegetative cell of coccoid forms, with special reference to *Ophioctyum majus* Naegeli". In: *British Phycological Journal* 6.1 (Apr. 30, 1971), pp. 1–23. ISSN: 0007-1617. DOI: 10.1080/00071617100650011. URL: <http://www.tandfonline.com/doi/pdf/10.1080/00071617100650011> (visited on 07/28/2015).
- [71] Indira Priyadarshani and Biswajit Rath. "Commercial and industrial applications of micro algae – A review". In: *Journal of Algal Biomass Utilization* 3.4 (2012), pp. 89–100. ISSN: 2229-6905. URL: <http://jalgalbiomass.com/paper14vol13no4.pdf> (visited on 08/06/2015).
- [72] J. S. Brown. "Functional Organization of Chlorophyll a and Carotenoids in the Alga, *Nannochloropsis salina*". In: *Plant Physiology* 83.2 (Feb. 1, 1987), pp. 434–437. ISSN: 0032-0889, 1532-2548. DOI: 10.1104/pp.83.2.434. URL: <http://www.plantphysiol.org/cgi/doi/10.1104/pp.83.2.434> (visited on 07/22/2015).
- [73] Karen P. Fawley and Marvin W. Fawley. "Observations on the Diversity and Ecology of Freshwater *Nannochloropsis* (Eustigmatophyceae), with Descriptions of New Taxa". In: *Protist* 158.3 (July 2007), pp. 325–336. ISSN: 14344610. DOI: 10.1016/j.protis.2007.03.003. URL: <http://linkinghub.elsevier.com/retrieve/pii/S1434461007000235> (visited on 07/22/2015).
- [74] Robert A. Andersen. "Biology and systematics of heterokont and haptophyte algae". In: *American Journal of Botany* 91.10 (June 22, 2004), pp. 1508–1522. URL: <http://www.amjbot.org/content/91/10/1508.full.pdf+html>.
- [75] Chunhua Zhou et al. "Carotenoids in Fruits of Different Persimmon Cultivars". In: *Molecules* 16.1 (Jan. 17, 2011), pp. 624–636. ISSN: 1420-3049. DOI: 10.3390/molecules16010624. URL: <http://www.mdpi.com/1420-3049/16/1/624> (visited on 08/11/2015).
- [76] Yumiko Sakuragi et al. "Association of bacteriochlorophyll a with the CsmA protein in chlorosomes of the photosynthetic green filamentous bacterium *Chloroflexus aurantiacus*". In: *Biochimica et Biophysica Acta (BBA) - Bioenergetics* 1413.3 (Nov. 1999), pp. 172–180. ISSN: 00052728. DOI: 10.1016/S0005-2728(99)00092-4. URL: <http://linkinghub.elsevier.com/retrieve/pii/S0005272899000924> (visited on 09/26/2015).

- [77] Mani Arora et al. "Tetrasselmis indica (Chlorodendrophyceae, Chlorophyta), a new species isolated from salt pans in Goa, India". In: *European Journal of Phycology* 48.1 (Feb. 2013), pp. 61–78. ISSN: 0967-0262, 1469-4433. DOI: 10.1080/09670262.2013.768357. URL: <http://www.tandfonline.com/doi/abs/10.1080/09670262.2013.768357> (visited on 07/21/2015).
- [78] Manuel Zapatal, Francisco Rodriguezl, and José L. Garrido. "Separation of chlorophylls and carotenoids from marine phytoplankton: a new HPLC method using a reversed phase C8 column and pyridine- containing mobile phases". In: *Mar Ecol Prog Ser* 195 (Mar. 31, 2000). Ed. by Inter-Research, pp. 29–45. ISSN: 1616-1599. URL: <http://www.int-res.com/articles/meps/195/m195p029.pdf> (visited on 07/21/2015).
- [79] M. D. Guiry. *The Seaweed Site : Information on marine algae*. URL: <http://www.seaweed.ie/algae/chlamydomonas.php> (visited on 07/23/2015).
- [80] Pr. Dr. M. Mittag and PD Dr. B. Becker, eds. *Alge des Jahres 2014: Chlamydomonas reinhardtii - schneller Schwimmer steht Modell*. Sektion Phykologie der Deutschen Botanischen Gesellschaft (DBG) e.V., 2014. URL: <http://www.dbg-phykologie.de/pages/22PressemitteilungAlgeJahr2014.html>.
- [81] Jean-David Rochaix. "Assembly, Function, and Dynamics of the Photosynthetic Machinery in *Chlamydomonas reinhardtii*". In: *Plant Physiology* 127.4 (2001), pp. 1394–1398.
- [82] T. Mazzuca Sobczuk and Chisti Yusuf. "Potential fuel oils from the microalga *Choricystis minor*". In: *Journal of Chemical Technology & Biotechnology* 85.1 (Oct. 7, 2009), pp. 100–108. ISSN: 02682575, 10974660. DOI: 10.1002/jctb.2272. URL: <http://doi.wiley.com/10.1002/jctb.2272> (visited on 07/09/2015).
- [83] R. S. Menezes et al. "Evaluation of fatty acid composition of the microalgae *Choricystis minor* var. *minor* according to two different nutrient feeding strategies". In: *Journal of Renewable and Sustainable Energy* 7.4 (July 2015), pp. 043117–1–043117–7. ISSN: 1941-7012. DOI: 10.1063/1.4926908. URL: <http://scitation.aip.org/content/aip/journal/jrse/7/4/10.1063/1.4926908> (visited on 08/06/2015).
- [84] Ralitsa Zidarova, Dobrina Temniskova, and Balik Dzhabazov. "Karyological and endosymbiotic notes on two *Choricystis* species (Trebouxiophyceae, Chlorophyta)". In: *Biologia* 64.1 (Jan. 1, 2009), pp. 43–47. ISSN: 1336-9563, 0006-3088. DOI: 10.2478/s11756-009-0009-7. URL: <http://www.degruyter.com/view/j/biolog.2009.64.issue-1/s11756-009-0009-7/s11756-009-0009-7.xml> (visited on 07/23/2015).
- [85] M. A. Borowitzka. "The mass culture of *dunaliella salina*". In: *Technical resource papers regional workshop on the culture and utilization of seaweeds volume II*. Australia: Food and Agriculture Organization of the United Nations (FAO), 1990. URL: <http://www.fao.org/docrep/field/003/ab728e/ab728e06.htm> (visited on 07/21/2015).
- [86] R. H. Al-Hasan et al. "Correlative Changes of Growth, Pigmentation and Lipid Composition of *Dunaliella salina* in Response to Halostress". In: *Microbiology* 133.9 (Sept. 1, 1987), pp. 2607–2616. ISSN: 1350-0872, 1465-2080. DOI: 10.1099/00221287-133-9-2607. URL: <http://mic.sgmjournals.org/content/journal/micro/10.1099/00221287-133-9-2607> (visited on 07/21/2015).

- [87] Aaron M. Collins et al. "Carotenoid Distribution in Living Cells of *Haematococcus pluvialis* (Chlorophyceae)". In: *PLoS ONE* 6.9 (Sept. 6, 2011). Ed. by Terence Evens, e24302. ISSN: 1932-6203. DOI: 10.1371/journal.pone.0024302. URL: <http://dx.plos.org/10.1371/journal.pone.0024302> (visited on 07/23/2015).
- [88] Akira Satoh et al. "Preliminary Clinical Evaluation of Toxicity and Efficacy of A New Astaxanthin-rich *Haematococcus pluvialis* Extract". In: *Journal of Clinical Biochemistry and Nutrition* 44.3 (2009), pp. 280–284. ISSN: 1880-5086, 0912-0009. DOI: 10.3164/jcbn.08-238. URL: <http://joi.jlc.jst.go.jp/JST.JSTAGE/jcbn/44.280?from=CrossRef> (visited on 07/23/2015).
- [89] Judith R Denery et al. "Pressurized fluid extraction of carotenoids from *Haematococcus pluvialis* and *Dunaliella salina* and kavalactones from *Piper methysticum*". In: *Analytica Chimica Acta* 501.2 (Jan. 2004), pp. 175–181. ISSN: 00032670. DOI: 10.1016/j.aca.2003.09.026. URL: <http://linkinghub.elsevier.com/retrieve/pii/S0003267003012339> (visited on 07/23/2015).
- [90] Hong-Yu Ren et al. "A new lipid-rich microalga *Scenedesmus* sp. strain R-16 isolated using Nile red staining: effects of carbon and nitrogen sources and initial pH on the biomass and lipid production". In: *Biotechnology for Biofuels* 6.143 (2013), p. 10.
- [91] Zbigniew Tukaj et al. "Changes in the pigment patterns and the photosynthetic activity during a light-induced cell cycle of the green alga *Scenedesmus armatus*". In: *Plant Physiology and Biochemistry* 41.4 (Apr. 2003), pp. 337–344. ISSN: 09819428. DOI: 10.1016/S0981-9428(03)00028-7. URL: <http://linkinghub.elsevier.com/retrieve/pii/S0981942803000287> (visited on 07/23/2015).
- [92] Fong Lam Chu et al. "Carotenogenesis Up-regulation in *Scenedesmus* sp. Using a Targeted Metabolomics Approach by Liquid Chromatography-High-Resolution Mass Spectrometry". In: *Journal of Agricultural and Food Chemistry* 59.7 (Apr. 13, 2011), pp. 3004–3013. ISSN: 0021-8561, 1520-5118. DOI: 10.1021/jf105005q. URL: <http://pubs.acs.org/doi/abs/10.1021/jf105005q> (visited on 07/23/2015).
- [93] Christian Bogen et al. "Identification of *Monoraphidium contortum* as a promising species for liquid biofuel production". In: *Bioresource Technology* 133 (Apr. 2013), pp. 622–626. ISSN: 09608524. DOI: 10.1016/j.biortech.2013.01.164. URL: <http://linkinghub.elsevier.com/retrieve/pii/S096085241300196X> (visited on 08/07/2015).
- [94] G. Kowalewska. "Identification of Phytoplankton Pigments by RP-HPLC with Diode-Array Type Detector". In: *Chem. Anal (Warsaw)* 38.711 (1993), pp. 711–718. URL: <http://www.chem.uw.edu.pl/chemanal/PDFs/1993/CHAN1993V0038P00711.pdf>.
- [95] L. Krienitz, G. Klein, and H. Böhm. "Morphologie und Ultrastruktur einiger Arten der Gattung *Monoraphidium* (Chlorellales) II." In: *Algological Studies/Archiv für Hydrobiologie, Supplement* 44 (1986). Ed. by Stuttgart Schweizerbart Science Publishers, pp. 331–350. URL: [http://www.researchgate.net/profile/Lothar\\_Krienitz/publication/272324709\\_Morphologie\\_und\\_Ultrastruktur\\_einiger\\_Arten\\_der\\_Gattung\\_Mnoraphidium\\_\(Chlorellales\)\\_II/links/54e1b9c90cf296663792d9a0.pdf](http://www.researchgate.net/profile/Lothar_Krienitz/publication/272324709_Morphologie_und_Ultrastruktur_einiger_Arten_der_Gattung_Mnoraphidium_(Chlorellales)_II/links/54e1b9c90cf296663792d9a0.pdf).

- 
- [96] Villem Aruoja. "Algae Pseudokirchneriella subcapitata in environmental hazard evaluation of chemicals and synthetic nanoparticles". ISBN: 978-9949-484-11-9. PhD thesis. Tartu: Estonian University of Life Sciences, Dec. 2011. 114 pp. URL: [VillemiPhD2011final.pdf](#) (visited on 07/24/2015).
- [97] Rachael M. Morgan-Kiss et al. "Identity and physiology of a new psychrophilic eukaryotic green alga, *Chlorella* sp., strain BI, isolated from a transitory pond near Bratina Island, Antarctica". In: *Extremophiles* 12.5 (Sept. 2008), pp. 701–711. ISSN: 1431-0651, 1433-4909. DOI: 10.1007/s00792-008-0176-4. URL: <http://link.springer.com/10.1007/s00792-008-0176-4> (visited on 07/23/2015).
- [98] Zümriye Aksu and Sevilay Tezer. "Biosorption of reactive dyes on the green alga *Chlorella vulgaris*". In: *Process Biochemistry* 40.3-4 (Mar. 2005), pp. 1347–1361. ISSN: 13595113. DOI: 10.1016/j.procbio.2004.06.007. URL: <http://linkinghub.elsevier.com/retrieve/pii/S0032959204002195> (visited on 07/23/2015).
- [99] Carl Safi et al. "Morphology, composition, production, processing and applications of *Chlorella vulgaris*: A review". In: *Renewable and Sustainable Energy Reviews* 35 (July 2014), pp. 265–278. ISSN: 13640321. DOI: 10.1016/j.rser.2014.04.007. URL: <http://linkinghub.elsevier.com/retrieve/pii/S1364032114002342> (visited on 07/23/2015).
- [100] B. Maršálek, L. Bláha, and F. Hindák. "Review of toxicity of cyanobacteria in Slovakia". In: *Biologia (Bratislava)* 55.6 (2000), pp. 645–652. ISSN: 0006-3088. URL: [http://ecotox.ibot.cas.cz/en/publications/2000\\_marsalek+etal\\_biologia\\_55\\_645.pdf](http://ecotox.ibot.cas.cz/en/publications/2000_marsalek+etal_biologia_55_645.pdf) (visited on 07/21/2015).
- [101] United States Environmental Protection Agency Office of Water. *Cyanobacteria and Cyanotoxins: Information for Drinking Water Systems*. EPA-810F11001. 2012. URL: [http://water.epa.gov/scitech/swguidance/standards/criteria/nutrients/upload/cyanobacteria\\_factsheet.pdf](http://water.epa.gov/scitech/swguidance/standards/criteria/nutrients/upload/cyanobacteria_factsheet.pdf).
- [102] Satya Shila Singh et al. "Diversity and distribution pattern analysis of cyanobacteria isolated from paddy fields of Chhattisgarh, India". In: *Journal of Aisa-Pacific Biodiversity* 7.4 (Dec. 30, 2014), pp. 462–470. DOI: 10.1016/j.japb.2014.10.009. URL: [http://ac.els-cdn.com/S2287884X14000703/1-s2.0-S2287884X14000703-main.pdf?\\_tid=129d324a-402f-11e5-a68c-00000aacb35d&acdnat=1439300842\\_c7eaffbc53535fec44e12bfa0f888347](http://ac.els-cdn.com/S2287884X14000703/1-s2.0-S2287884X14000703-main.pdf?_tid=129d324a-402f-11e5-a68c-00000aacb35d&acdnat=1439300842_c7eaffbc53535fec44e12bfa0f888347) (visited on 08/11/2015).
- [103] Michael Schagerl and Brigitte Müller. "Acclimation of chlorophyll a and carotenoid levels to different irradiances in four freshwater cyanobacteria". In: *Deep Sea Research Part II: Topical Studies in Oceanography* 163.7 (May 2006), pp. 709–716. ISSN: 01761617. DOI: 10.1016/j.jplph.2005.09.015. URL: <http://linkinghub.elsevier.com/retrieve/pii/S0176161705004207> (visited on 07/21/2015).
- [104] Peter M. Bramley and Gerhard Sandmann. "In vitro and in vivo biosynthesis of xanthophylls by the cyanobacterium *aphanocapsa*". In: *Phytochemistry* 24.12 (Mar. 18, 1985), pp. 2919–2922. URL: [http://ac.els-cdn.com/0031942285800273/1-s2.0-0031942285800273-main.pdf?\\_tid=3b02be4e-4034-11e5-acd4-00000aacb35d&acdnat=1439303057\\_3052ed366f7b2ba52667eeef39d3390](http://ac.els-cdn.com/0031942285800273/1-s2.0-0031942285800273-main.pdf?_tid=3b02be4e-4034-11e5-acd4-00000aacb35d&acdnat=1439303057_3052ed366f7b2ba52667eeef39d3390) (visited on 08/11/2015).

- [105] M. Schagerl and Karl Donabaum. "Patterns of major photosynthetic pigments in freshwater algae. 1. Cyanoprokaryota, Rhodophyta and Cryptophyta". In: *Annales de Limnologie - International Journal of Limnology* 39.1 (Mar. 2003), pp. 35–47. ISSN: 0003-4088. DOI: 10.1051/limn/2003003. URL: <http://www.limnology-journal.org/10.1051/limn/2003003> (visited on 10/11/2015).
- [106] Andreas Ballot et al. "Morphological and Phylogenetic Analysis of *Anabaenopsis abijatae* and *Anabaenopsis elenkinii* (Nostocales, Cyanobacteria) from Tropical Inland Water Bodies". In: *Microbial Ecology* 55.4 (May 2008), pp. 608–618. ISSN: 0095-3628, 1432-184X. DOI: 10.1007/s00248-007-9304-4. URL: <http://link.springer.com/10.1007/s00248-007-9304-4> (visited on 07/21/2015).
- [107] Arul M. Varman et al. "Metabolic Engineering of *Synechocystis* sp. Strain PCC 6803 for Isobutanol Production". In: *Applied and Environmental Microbiology* 79.3 (Feb. 2013), pp. 908–914. DOI: 10.1128/AEM.02827-12. URL: <http://aem.asm.org/content/79/3/908.full#cite-as> (visited on 08/12/2015).
- [108] Kazusa DNA Research Institute. *CyanoBase*. URL: <http://genome.microbedb.jp/CyanoBase#about>.
- [109] Bongani Kaiser Ndimba et al. "Biofuels as a sustainable energy source: An update of the applications of proteomics in bioenergy crops and algae". In: *Journal of Proteomics* 93 (Nov. 2013), pp. 234–244. ISSN: 18743919. DOI: 10.1016/j.jprot.2013.05.041. URL: <http://linkinghub.elsevier.com/retrieve/pii/S1874391913003321> (visited on 09/29/2015).